

**PATTERNS AND DRIVERS OF TETRAPOD
DIVERSITY AND BIOGEOGRAPHY IN THE
LATE PALAEOZOIC AND EARLY MESOZOIC**

EMMA M. DUNNE

A thesis submitted to the University of Birmingham
for the degree of DOCTOR OF PHILOSOPHY

School of Geography, Earth and Environmental Sciences
College of Life and Environmental Sciences
University of Birmingham

September 2019

UNIVERSITY OF
BIRMINGHAM

University of Birmingham Research Archive

e-theses repository

This unpublished thesis/dissertation is copyright of the author and/or third parties. The intellectual property rights of the author or third parties in respect of this work are as defined by The Copyright Designs and Patents Act 1988 or as modified by any successor legislation.

Any use made of information contained in this thesis/dissertation must be in accordance with that legislation and must be properly acknowledged. Further distribution or reproduction in any format is prohibited without the permission of the copyright holder.

Abstract

Tetrapods (four-limbed vertebrates) invaded the land more than 370 million years ago and began to diversify into a spectacular range of morphologies and life modes, rapidly achieving a global distribution. However, due to the inherent temporal and spatial bias of the fossil record, global patterns of tetrapod diversity and biogeography during critical intervals of the group's evolution remain unresolved. This thesis focuses on examining the patterns and drivers of tetrapod diversity during two of these key intervals. Firstly, advanced statistical, phylogenetic, and modelling approaches were used to examine the impact of major environmental change on the first tetrapods to emerge onto land during the late Palaeozoic (358–272 million years ago). Next, these approaches were combined with palaeoclimatic reconstructions to examine the influence of climate on tetrapod diversity during the early Mesozoic (237–174 million years ago), when modern vertebrate groups, including the dinosaurs, were originating. Together, the results provide a comprehensive assessment of the impact of sampling biases on estimates of past diversity, as well as providing greater insights into the role of environmental and climate change on tetrapod diversity and biogeography.

Acknowledgements

None of the work contained in this thesis would have been remotely possible without the help and support of so many wonderful people. My sincerest thanks to my supervisor Richard Butler, who has been a constant source of support, insight, and guidance throughout my PhD. I am extremely grateful to Richard for this opportunity and could not have imagined a better or more inspiring mentor. An enormous thank you to the most recent member of my supervisory team, Sarah Greene, whom I am not quite sure how I survived without for so long. I also thank my co-supervisors, Roger Close and Roger Benson for their invaluable discussions and assistance on many parts of this thesis.

This research was built on foundations laid by all those who contributed data to the Paleobiology Database, so my utmost gratitude is extended to everyone who dedicated their energy to help create this extraordinary resource. I have had the absolute pleasure of working with and learning from many incredible people who helped me immeasurably, even in the smallest of ways. For sharing their data, code, resources, and knowledge, thank you to Gemma Benevento, Neil Brocklehurst, David Button, Dan Cashmore, Ale Chiarenza, Natalie Cooper, Christopher Dean, Kirsty Edgar, Alex Farnsworth, Pedro Godoy, Lydia Greene, Jason Hilton, Gene Hunt, Andy Jones, Lewis Jones, Graeme Lloyd, Andy Rees, James Rosindell, and Sam Thompson.

I am very grateful to my wonderful colleagues at the University of Birmingham who saw me through the last four years. My deepest thanks to The Butler Babes, Dan, Pedro, Andy, and Juan, as well as The Pembs 2K16 Crew, Ben, Dan, and Davey, for their unwavering friendship and consistent availability for chats over a cup of tea (or WhatsApp). Thanks also to my fabulous Analytical Paleobiology Workshop 2019 course mates who reignited my passion at just the right time. Very special thanks to Holly, Nikki, Laura, Vicki, and Emma for keeping me (in)sane when I needed it most.

To Finn, Scout, and Hugo: the cuddles and impeccable schedule-keeping were very much appreciated. And to my very bestest friend, Thomas, it was this work caused us to meet, and it wouldn't have been completed without your incredible support - go raibh míle maith agat.

Finally, my greatest thanks go to my family, especially my parents, Mary and Pat, for without their immense, relentless and unending support none of this would have been possible.

Contents

1	INTRODUCTION	1
1.1	The first studies of palaeodiversity	2
1.2	Sampling biases	3
1.3	Modern studies of palaeodiversity	9
1.4	Sampling standardisation	10
1.5	Objectives and outline	12
2	DIVERSITY CHANGE DURING THE RISE OF TETRAPODS AND THE IMPACT OF THE 'CARBONIFEROUS RAINFOREST COLLAPSE'	17
2.1	Introduction	18
2.2	Methods	20
2.2.1	Fossil occurrence data	20
2.2.2	Raw patterns of diversity and sampling	20
2.2.3	Sampling standardised richness	21
2.2.4	Phylogenetic Biogeographic Connectedness (pBC)	23
2.3	Results & Discussion	24
2.3.1	Patterns of diversity and sampling	24
2.3.2	Patterns of biogeography	28
2.4	Conclusions	32
2.4.1	Post-publication review of current literature	32
3	TETRAPOD DIVERSIFICATION AND THE 'CARBONIFEROUS RAINFOREST COLLAPSE' UNDER NEUTRAL THEORY	35
3.1	Introduction	35
3.2	Methods	37
3.2.1	Fossil occurrence data	37
3.2.2	Neutral models	38
3.2.3	Model parameterisation	40
3.2.4	Habitat fragmentation	41
3.3	Results	41

3.3.1	Baseline models	41
3.3.2	Models incorporating habitat fragmentation and loss	43
3.3.3	Models exploring the effect of sampling biases	45
3.4	Discussion	48
4	LATITUDINAL PATTERNS OF LATE TRIASSIC TETRAPOD DIVERSITY AND CLIMATE	53
4.1	Introduction	53
4.2	Methods	55
4.2.1	Fossil occurrence data	55
4.2.2	Latitudinal sampling and species diversity	56
4.2.3	Palaeoclimate reconstructions	58
4.2.4	Testing potential drivers of diversity	60
4.3	Results	61
4.3.1	Diversity and sampling	61
4.3.2	Potential drivers of diversity	65
4.4	Discussion	71
5	THE ROLE OF CLIMATE IN THE EARLY EVOLUTION OF DINOSAURS	77
5.1	Introduction	77
5.2	Methods	81
5.2.1	Fossil occurrence data	81
5.2.2	Supertree and time calibration	81
5.2.3	Palaeoclimate reconstructions	82
5.2.4	Palaeoclimatic niche space	83
5.2.5	Temporal variation in palaeoclimatic niche evolution	84
5.2.6	Macroevolutionary models	85
5.2.7	Sauropodomorph biology and palaeoclimate	87
5.3	Results	88
5.3.1	Palaeoclimatic niche space	88
5.3.2	Temporal variation in palaeoclimatic niche evolution	91
5.3.3	Spatial and temporal patterns in sampling and palaeoclimate	93
5.3.4	Macroevolutionary models	97
5.3.5	Sauropodomorph biology and palaeoclimate	99
5.4	Discussion	101
6	CONCLUSIONS AND PERSPECTIVES	106
6.1	General conclusions and summary	106

6.2 Future work and prospects	109
References	112
Appendices	146
A Early tetrapod diversity	147
A.1 Implementing SQS through iNEXT	147
A.2 Carboniferous and early Permian sampling	148
A.3 Phylogenetic Biogeographic Connectedness	151
A.3.1 Palaeogeographical regions	152
A.3.2 Early tetrapod supertree	152
B Early tetrapods & neutral theory	156
C Late Triassic latitudinal diversity	159
D Early dinosaur evolution & climate I	163
E Early dinosaur evolution & climate II	176
F Early dinosaur evolution & climate III	182
G Early dinosaur evolution & climate IV	198

List of Figures

1.1	First estimate of Phanerozoic diversity using British fossil data (Phillips, 1860)	2
1.2	Diversity curve showing the Big Five mass extinctions (Raup and Sepkoski, 1981)	3
1.3	The Paleobiology Database Navigator webpage showing occurrences of Mesozoic dinosaur fossils	11
1.4	Simplified timeline of the key intervals studied in this thesis.	14
2.1	Raw (=uncorrected) species richness and local richness (alpha diversity) from the Carboniferous to early Permian	25
2.2	Patterns of sampling in the Carboniferous and early Permian	27
2.3	Estimates of diversity of Carboniferous–early Permian tetrapods using coverage-based subsampling	29
2.4	Phylogenetic Biogeographic Connectedness (pBC) during the Carboniferous and early Permian	30
3.1	Simulated tetrapod biodiversity patterns over time compared against the fossil record, where the habitat fragmentation is not included	43
3.2	Simulated tetrapod biodiversity patterns over time compared against the fossil record, where the habitat fragmentation is included	44
3.3	Random habitat loss: Simulated tetrapod biodiversity patterns over time compared against the fossil record.	45
3.4	Clustered habitat scenario: Simulated tetrapod diversity over time from neutral models incorporating habitat loss from the CRC following the clustered habitat scenario.	46
3.5	Upscaled biodiversity from the fossil record using neutral models	47
3.6	Simulated tetrapod diversity from neutral models where temporal sampling biases are removed.	48

4.1	Simplified cladogram showing the phylogenetic relationships between the Archosauromorpha, Pseudosuchia, Avemetatarsalia, and Synapsida	57
4.2	Patterns of species richness and sampling during the Late Triassic . . .	62
4.3	Local richness (alpha diversity) during the Late Triassic	64
4.4	Coverage-rarified species richness during the Late Triassic	65
4.5	Palaeolatitude plotted against palaeoclimate variables from the palaeoclimate model HadCM3L	66
4.6	Climatic variables from the palaeoclimate model HadCM3L at each locality in the Late Triassic occurrence dataset	67
4.7	Tetrapod palaeoclimatic ranges (<i>cont. on next page</i>)	68
5.1	Temporal sampling patterns during the Late Triassic and Early Jurassic	80
5.2	Palaeoclimatic niche space during the Late Triassic and Early Jurassic .	89
5.3	Visualisation of the palaeoclimatic conditions occupied by the three tetrapod/dinosaur groups in the Late Triassic and Early Jurassic	90
5.4	PC1 mapped onto dinosaur phylogeny	92
5.5	Palaeoclimatic niche disparity-through-time for all dinosaur species using three subsampling approaches	94
5.6	Palaeoclimatic niche disparity-through-time for sauropodomorph and non-sauropodomorph dinosaurs	95
5.7	Variation in each palaeoclimatic variables across the Late Triassic and Early Jurassic	96
5.8	AICc scores of the evolutionary models fitted to the dinosaur phylogeny and palaeoclimate data	97
5.9	Sauropodomorph morphological disparity though time	98
A.1	Correlation between species richness and sampling in the Carboniferous and early Permian	150
A.2	Schematic illustration of network biogeography methods	151
A.3	Palaeomaps illustrating the locations of the geographic regions defined by cluster analysis	154
B.1	Predictions of tetrapod diversity from a neutral model parameterised for Carboniferous diversity.	157
B.2	Palaeogeographic maps showing tetrapod occurrences during each interval of the late Carboniferous and early Permian	158
C.1	Devonian–present tetrapod sampling across latitudes	159

C.2	Patterns of raw species richness and sampling during the early Late Triassic and late Late Triassic.	160
C.3	Local richness (alpha diversity) across latitudes throughout the Late Triassic	161
D.1	Scatterplot displaying PC1 values from the ordination analysis of palaeoclimatic niche space	168
D.2	Temporal sampling patterns during the Late Triassic and Early Jurassic	169
D.3	Correlation between each palaeoclimatic variable and palaeolatitude in the Late Triassic and Early Jurassic	170
D.4	Dinosaur body mass estimates through time	173
D.5	Modelled surface air temperature (°C) during the Late Triassic and Early Jurassic from the model HadCM3L	174
E.1	PC2 mapped onto dinosaur phylogeny	177
E.2	MAT mapped onto dinosaur phylogeny	178
E.3	MAP mapped onto dinosaur phylogeny	179
E.4	SVT mapped onto dinosaur phylogeny	180
E.5	SVP mapped onto dinosaur phylogeny	181
F.1	Dinosaur palaeoclimatic niche disparity-through-time (time binning method) - trees 2–9	183
F.2	Dinosaur palaeoclimatic niche disparity-through-time (time binning method) - trees 10–17	184
F.3	Dinosaur palaeoclimatic niche disparity-through-time (time binning method)- trees 18–25	185
F.4	Dinosaur palaeoclimatic niche disparity-through-time (time binning method with ancestral state reconstruction) - trees 2–9	186
F.5	Dinosaur palaeoclimatic niche disparity-through-time (time binning method with ancestral state reconstruction) - trees 10–17	187
F.6	Dinosaur palaeoclimatic niche disparity-through-time (time binning method with ancestral state reconstruction) - trees 18–25	188
F.7	Dinosaur palaeoclimatic niche disparity-through-time (time binning method with ancestral state reconstruction) - trees 2–9	189
F.8	Dinosaur palaeoclimatic niche disparity-through-time (time binning method with ancestral state reconstruction) - trees 10–17	190
F.9	Dinosaur palaeoclimatic niche disparity-through-time (time binning method with ancestral state reconstruction) - trees 18–25	191

F.10	Non-sauropodomorph dinosaur palaeoclimatic niche disparity-through-time - trees 2–9	192
F.11	Non-sauropodomorph dinosaur palaeoclimatic niche disparity-through-time - trees 10–17	193
F.12	Non-sauropodomorph dinosaur palaeoclimatic niche disparity-through-time - trees 18–25	194
F.13	Sauropodomorph palaeoclimatic niche disparity-through-time - trees 2–9	195
F.14	Sauropodomorph palaeoclimatic niche disparity-through-time - trees 10–17	196
F.15	Sauropodomorph palaeoclimatic niche disparity-through-time - trees 18–25	197
G.1	Sauropodomorph morphological disparity-through-time - trees 2–9 . . .	199
G.2	Sauropodomorph morphological disparity-through-time - trees 10–17 . .	200
G.3	Sauropodomorph morphological disparity-through-time - trees 18–25 . .	201

List of Tables

2.1	Counts of species, collections (=fossil localities), formations, and equal area grid cells as proxies for sampling in each interval of the Carboniferous and early Permian	26
4.1	Summary of model fits to Late Triassic latitudinal species richness	70
4.2	Summary of explanatory variables within the GLS multiple regression models for Late Triassic latitudinal species richness	70
4.3	Summary of model fits to Late Triassic equal-area grid cell species richness	70
4.4	Summary of explanatory variables within the GLS multiple regression models for Late Triassic equal-area grid cell species richness	71
5.1	Summary of GLS model fits to sauropodomorph body mass	100
5.2	Summary of explanatory variables within the PGLS multiple regression models for sauropodomorph body mass	100
A.1	Details of the most speciose collections (=fossil localities) in the Paleobiology Database during the Carboniferous and early Permian	149
A.2	Pearson's product moment correlation co-efficient showing the strength and direction of association between raw species richness and proxies for sampling	149
A.3	Geographic clusters for analyses of Phylogenetic Biogeographic Connectedness as defined by k-means clustering of palaeocoordinates	153
C.1	Details of the occurrences contained within each of the richest collections (=fossil localities) during the Late Triassic	162
C.2	Correlation between palaeolatititude and four variables from the palaeoclimate model HadCM3L during the Late Triassic	162
C.3	Likelihood ratio test results for the two best models of the GLS analysis	162
D.1	List of species and specimens in the informal dinosauromorph supertree	164

D.2	Recently-described dinosaur species added to the Button <i>et al.</i> (2017) supertree of amniote species.	167
D.3	Pairwise comparisons (Mann–Whitney–Wilcoxon) of values for each climatic variable between the three tetrapod/dinosaur groups in both the Late Triassic and Early Jurassic.	171
D.4	Correlation between palaeolatitude and four variables from the palaeoclimate model HadCM3L for both the Late Triassic and Early Jurassic.	171
D.5	Theta values from the non-uniform OU model for the first 10 time-calibrated dinosauromorph trees	172

1 | INTRODUCTION

The fossil record is central to our understanding of the history of life on Earth. Our concerted efforts to document and assess changes in the fossil record are not only driven by the desire to unravel the mysteries of past biodiversity, but also by the possibility of using these insights to better understand and predict future changes in our planet's biodiversity. Reconstructing and analysing changes in biodiversity across geological time depends almost exclusively on data from the fossil record, either directly in the form of counts of fossil taxa through time, or indirectly as a way to time-calibrate phylogenies. However, it is universally acknowledged that the fossil record is incomplete; fossils have not been uniformly sampled across time and space. The impact of uneven temporal and spatial sampling on estimates of palaeodiversity has been noted in the literature for almost half a century (Raup, 1972, 1976; Sepkoski *et al.*, 1981), yet debate continues over the extent to which this incompleteness and unevenness in fossil sampling affects estimates of palaeodiversity (Smith and McGowan, 2007; Alroy *et al.*, 2008; Benson *et al.*, 2009; Benton *et al.*, 2011; Mannion *et al.*, 2011; Vilhena and Smith, 2013; Close *et al.*, 2017).

In recent years, a confluence of factors has led to immense progress in the measurement and interpretation of past diversity, not least the construction of large fossil occurrence databases such as the Paleobiology Database, and the development of quantitative methods of sampling standardisation. This chapter provides an overview of previous investigations of palaeodiversity, as well as an outline of the biases that underpin the fossil record and the key innovations that have been developed to examine

patterns of diversity in light of these biases.

1.1 The first studies of palaeodiversity

The first estimate of Phanerozoic biodiversity was produced in 1860, almost a century before the first computers (Phillips, 1860). This 'diversity curve' was constructed based upon the British fossil record and showed the gradual rise and fall in the number of taxa across the last 542 million years (Figure 1.1). But it was not until more than a century later that using fossil occurrence data to examine the patterns and drivers of past biodiversity really came to prominence. Like many other scientific fields in the late twentieth century, the emergence of quantitative palaeobiology was propelled primarily by advances in technology. Computers permitted large quantities of fossil data to be stored and analysed efficiently, enabling a plethora of studies on the history of life on Earth, such as the rate at which species appeared and disappeared, timing and extent of extinction events, and how environmental and climatic conditions affected diversity, at both local and global scales.

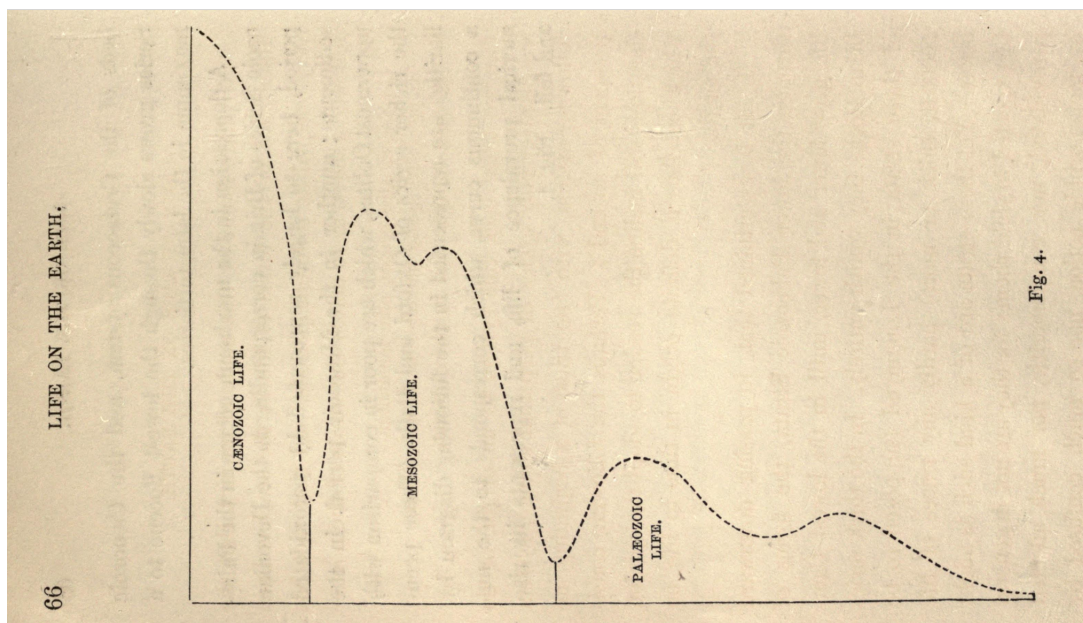


Figure 1.1: First estimate of Phanerozoic diversity using British fossil data (Phillips, 1860)

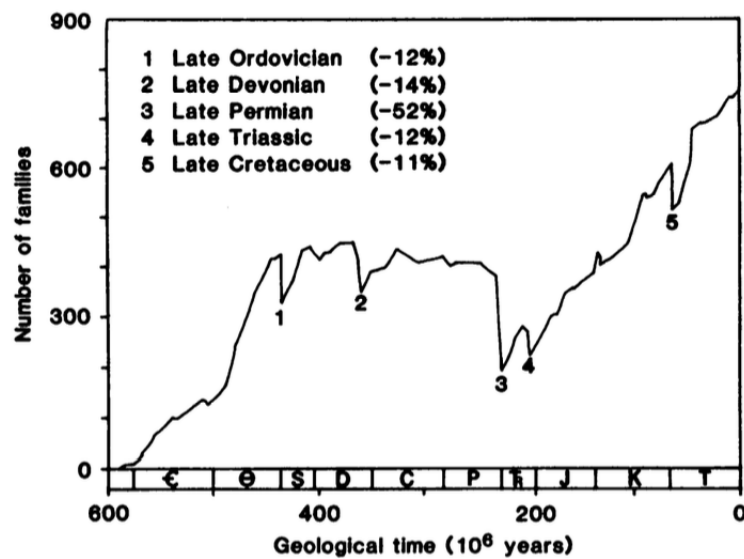


Figure 1.2: Diversity curve showing the Big Five mass extinctions (Raup and Sepkoski, 1981)

During the 1970s and 1980s, John ‘Jack’ Sepkoski and David Raup were among the first palaeontologists to use digital databases of fossil occurrences to investigate how marine invertebrate diversity has changed over the course of the Phanerozoic. Their work, alongside that of colleagues Richard Bambach and James Valentine, led to a series of seminal papers that formed the basis of this new field of quantitative palaeobiology, including their publication that identified the ‘Big Five’ mass extinctions (Raup and Sepkoski, 1982) (Figure 1.2). Early studies of diversity through deep time (e.g. Valentine, 1969; Sepkoski *et al.*, 1981; Benton, 1985) generally interpreted the fossil record literally, using face-value (‘raw’ or ‘observed’) counts of taxa. While this work was a critical first step in studying changes in taxonomic richness through time, this approach is no longer appropriate given the pervasive sampling biases documented in the fossil record.

1.2 Sampling biases

Even early pioneers of palaeodiversity studies recognised the quantity of sedimentary rock available as a bias on estimates of diversity (Phillips, 1860). Charles Darwin, too,

noted that “our palaeontological collections are very imperfect” (Darwin, 1859). Soon after the first large-scale quantitative studies of diversity of the 1970s, serious concerns about the impact of incomplete and uneven sampling of the fossil record on estimates of diversity began to arise (Raup 1972, 1976). In the first of these papers, Raup (1972) outlined seven “sources of error” within the fossil record that may influence estimates of taxic richness through time, which are outlined below (as in Brocklehurst, 2015). These “sources of error”, or sampling biases, still remain central to investigations of past diversity in the fossil record and many are pertinent directly to the work conducted in this thesis.

Early estimates of diversity were based exclusively on range charts, compendia that recorded the first to last occurrence dates of each taxon. With this counting method, the range of a taxon occurring in, for example, the Carnian and Rhaetian stages of the Late Triassic would pass through the Norian, even if no fossils of that taxon had been recorded from that stage. More modern studies of diversity, especially those concerning vertebrates, also typically use range-through counts (e.g. Dunne *et al.*, 2018; Cleary *et al.*, 2018). However, this can inflate the number of taxa in certain time bins and can result in increases or decreases in diversity being interpreted as being greater than is actually the case. These range-through counts can also lead to phenomena known as ‘edge effects’; since the first and last appearances of a fossil are unlikely to be true first and last appearances of that taxon, the ranges will be truncated at either end. This has been dubbed the Signor-Lipps effect in cases where the youngest fossil is unlikely to represent the last appearance of an organism (Signor and Lipps, 1982). This truncation leads to diversity being artificially lowered in earlier (i.e. stratigraphically older) time bins as taxon ranges do not extend back to them, resulting in diversity data being biased towards an increase in observed diversity through time (Raup, 1972).

The Pull of the Recent (Raup, 1972), is a specific edge effect that describes how estimates of diversity during the Mesozoic and Cenozoic will be inflated relative

to older intervals, due to a higher number of taxa in these intervals having living relatives. Since our knowledge of extant taxa is greater than that of fossil taxa, those with living representatives are likely to have their ranges extended to the recent (Cutbill and Funnel, 1967). For example, an extant taxon with a single fossil occurrence in the Jurassic would be given the range Jurassic–Recent. Studies have suggested that The Pull of the Recent only accounts for a small portion of inflated diversity towards the present day (e.g. Jablonski *et al.*, 2003; Sahney and Benton, 2017), but as biases in the fossil record are rarely mutually exclusive, it is difficult to eliminate all factors that may exaggerate diversity increases through the Cenozoic, such as rock age and outcrop area. While this thesis does not concern Cenozoic diversity, there is a noticeable difference between the quantity of data available for the late Palaeozoic and that of the early Mesozoic.

Time bins used in studies of diversity are typically based on geological time units, such as periods or stages, which may be problematic, given that longer geological time bins would theoretically contain more diversity (Raup, 1972; Foote, 1994). Additionally, longer time bins may also have greater amounts of sedimentation, leading to a higher probability of preservation (Miller and Foote, 1996). To overcome this issue, some workers have preferred to use equal-length time bins (e.g. 10 million years). But, in practice the time bin length may not influence diversity estimates, as in their study of dinosaur diversity, Fastovsky *et al.* (2004) did not find a correlation between richness and the length of the time bins based on the geological time units. It is important to note that geological time units are not independent of species turnover, as many units are defined based on biostratigraphy. Furthermore, the ages of geological units are subject to change when more evidence becomes available (e.g. Langer *et al.*, 2018).

Raup (1972) suggested that diversity estimates could also be affected by the level of interest in a certain group, as well as the quality and quantity of research into a group's taxonomy. Amongst palaeontologists, there are clear preferences for certain taxonomic groups, for reasons such as their general popularity as fossil organisms

(e.g. dinosaurs, Quaternary mammals, trilobites) or their purported ‘usefulness’ (e.g. ammonites and graptolites in biostratigraphy). Moreover, there is a widely documented bias in the literature towards particular geographic areas, with taxa from northern landmasses, such as North America, Europe, and Asia, amassing considerably more attention (Fastovsky *et al.*, 2004; Upchurch *et al.*, 2011; Brocklehurst *et al.*, 2012; Cleary *et al.*, 2018; Dunne *et al.*, 2018). These “monographic effects” may be negligible when they are randomly distributed amongst major clades and throughout the stratigraphic column, but they can make studies of more restricted intervals and taxonomic groups more difficult (Raup, 1972).

Exceptionally fossiliferous sites, termed Lagerstätten, preserve organic remains that would normally be lost to taphonomic processes, and therefore allow extraordinary insights into ancient life that would otherwise not have been possible. Many of these sites are also known for the exceptional preservation of soft-tissues (i.e. Konservat-Lagerstätten), such as the Cambrian Burgess Shale in Canada, the late Carboniferous Mazon Creek in Illinois, USA, and the Solnhofen Limestone from the Jurassic of Germany. Examples of Lagerstätten from this thesis, which are more accurately termed Konzentrat Lagerstätten due to the extraordinary concentration of fossils, include the Linton Diamond Coal Mine in Ohio that preserves an abundance of Carboniferous tetrapods, and Ghost Ranch in New Mexico, which is known primarily for its Triassic dinosaurs, most notably the theropod *Coelophysis*. Lagerstätten can have a significant effect on diversity curves, and many studies have noted a correlation between peaks in diversity and the presence of areas with exceptional concentrations of fossils (e.g. Benson *et al.*, 2009; Brocklehurst *et al.*, 2012; Friedman and Sallan, 2012; Butler *et al.*, 2013; Cleary *et al.*, 2015; Dean *et al.*, 2016; Dunne *et al.*, 2018; Driscoll *et al.*, 2019). However, Raup (1972) noted that as Lagerstätten appear to be more common in younger rocks, their greatest impact is to add noise to the data in a similar fashion to the monographic effect discussed above.

When a new geographic area is opened up to exploration, it is inevitable that

new taxa will be discovered, as organisms are geographically restricted to certain areas by factors such as climate. Therefore, the diversity of a fossil group is constrained by the amount of area available for sampling (Raup, 1972). This variation in the geographic spread of fossiliferous sites can strongly impact estimates of diversity due to the ubiquitous scaling of species richness with area i.e. the species-area relationship (Preston, 1962; Rosenzweig, 1995; Barnosky *et al.*, 2005; Close *et al.*, 2017). This means that the number of taxa sampled is not only dependant on outcrop area, but also on the size of the geographic area (Barnosky *et al.*, 2005). Raup (1972) suggested that this issue is more pronounced in the marine realm, as only a small portion of the total ocean area at any point in geological time is available for study. Geographic biases are prolific in all time intervals studied as part of this thesis, as discussed in individual chapters. The vast majority of fossil tetrapods have been sampled from areas in North America and Europe, as well as parts of South America, southern Africa, and Asia (see Figure 1.3, illustrating how researcher preference clearly plays a role the geographic extent of sampling).

Raup (1972) was the first to note a correlation between sediment volume and estimates of diversity. Subsequently, numerous studies have also observed this correlation, or a correlation between diversity and a similar proxy for sediment volume such as outcrop area or number of formations (e.g. Smith, 2001; Crampton *et al.*, 2003; Smith and McGowan, 2007; Fröbisch, 2008, 2013; Benson and Upchurch, 2013). Three hypotheses have been proposed to explain this pattern; 1) the rock record bias hypothesis places sampling as the primary driver of observed diversity i.e. the more rock area sampled, the higher the observed diversity (Raup, 1972, 1976; Smith, 2001; Smith *et al.*, 2012), 2) the common-cause hypothesis states that sampling and diversity are driven by some common factor, such as fluctuations in sea level or tectonic activity (Peters, 2005; Peters and Heim, 2010, 2011; Hannisdal and Peters, 2011), and 3) the redundancy hypothesis states that sampling and diversity are entirely or partially redundant with each other (Benton *et al.*, 2011; Dunhill *et al.*, 2014; Walker *et al.*, 2017;

Dunhill *et al.*, 2018).

Since the publication of Raup's paper, almost half a century ago, many more processes and factors that remove information from the fossil record, and thus impact diversity estimates, have been documented. While this thesis focuses broadly on the seven biases discussed above, it is nonetheless critical to consider other biological and taphonomic biases that influence the completeness of the fossil record. The environmental setting in which an organism lived would certainly have affected its probability of preservation, as well as the completeness of the fossil specimen (Benson and Butler, 2011; Brocklehurst *et al.*, 2012; Cleary *et al.*, 2015; Purnell *et al.*, 2018). The size of an organism may also impact its probability of preservation, as smaller organisms may be more easily destroyed by taphonomic processes. While this has been demonstrated in specific fossil beds, i.e. Dinosaur Park Formation, late Campanian (Brown *et al.*, 2013), it is not a universal rule (Fara and Benton, 2000; Cleary *et al.*, 2015; Bath Enright *et al.*, 2017). Furthermore, taphonomic processes, such as decay, diagenesis, and erosion, immediately post-mortem, as well as during and after fossilisation, can result in the loss of information from the fossil record (Briggs, 2003; Allison and Bottjer, 2011; Muscente *et al.*, 2017). Human biases, such as historical and societal factors are also important to consider. Historical changes in database compilation have the potential to substantially influence interpretations of diversity patterns, as more occurrences of fossil taxa are recorded with time (Tennant *et al.*, 2018). This is closely linked to practices of fossil collection, where preference is typically given to better preserved specimens, leaving behind others that may have potentially important information but be less aesthetically pleasing to the researcher or collector. This was particularly pertinent during the early days of palaeontological collection, when a desire for large articulated specimens for museum display influenced collecting practices (Brown *et al.*, 2013).

With all of these factors impacting the completeness and evenness of the fossil record, often simultaneously, it is unsurprising that debate exists over whether the patterns of diversity we observed in the fossil record are genuine or an artefact of

biases. Amongst his colleagues, Raup was considerably more active in issuing words of caution regarding the influences of biases in the fossil record. In particular, he was concerned that the apparent continuous rise in marine invertebrate diversity across the Phanerozoic could be primarily attributed to the concurrent increase in exposed marine sediments (Raup, 1976). However, in a paper dubbed the “kiss and makeup paper”, Raup joined his colleagues in arguing for a real if somewhat more limited increase in biodiversity through time, in what could be seen as an attempt to ease concerns about biases (Sepkoski *et al.*, 1981). I believe it is important that we do not regard acknowledgements of the incompleteness of the fossil record as pessimism. Indeed, there are many things that we might never know about extinct species, such as their true geographic range or abundances. But, for now, we should view our knowledge of the history of life on Earth as a work in progress (Benson, 2018).

1.3 Modern studies of palaeodiversity

In the late 1990s a second wave of research into patterns of palaeodiversity appeared (Miller, 2000; Wall *et al.*, 2009). Studies during this time began to demonstrate that sampling biases have the potential to profoundly alter our view of past diversity patterns (e.g. Miller and Foote, 1996; Alroy *et al.*, 2001). However, debate continued over the extent to which these biases impact diversity patterns; is there still a trace of a genuine pattern detectible from the raw data? This renewed interest in palaeodiversity studies also turned the spotlight away from the marine realm and onto other groups, including terrestrial vertebrates. Until this time, the majority of studies on patterns of palaeodiversity and sampling biases in the fossil record had been based on marine invertebrates (e.g. Sepkoski *et al.*, 1981; Crampton *et al.*, 2003; Smith and McGowan, 2007; Alroy *et al.*, 2008), in part due to the greater abundance of marine fossil data when compared with terrestrial data. A major exception to this trend was the work of Michael Benton, who led the publication of *The Fossil Record*, a collection of data on the ranges and localities of fossil algae, fungi, protists, plants and animals (Benton,

1993). Vertebrate data included within this compilation paved the way for a plethora of studies on tetrapod diversity through time (e.g. Benton, 1995, 2001, 2010; Sahney and Benton, 2008). However, this compendium not only relied on taxon ranges, like those from early palaeodiversity studies, which, as previously mentioned, has several limitations when compared to occurrence data, but also used family-level taxonomic assignments rather than genera or species.

Today, there are several large occurrence databases in existence, but none is used more widely than the Paleobiology Database, (PBDB, <https://paleobiodb.org>). Since its founding in 1998 by John Alroy and Charles Marshall, the database has grown immensely to contain, at the time of writing, over 1.42 million occurrences of fossil organisms, including plants, invertebrates and vertebrates, which have been collected from the published literature by over 400 researchers (Figure 1.3). The data collected include information on the location, stratigraphy, geology, and taxonomy associated with each individual fossil (see Peters and McClennen, 2015). Compelled by this increased availability of comprehensive occurrence data and the emergence of palaeodiversity as a central theme of investigation, the last two decades have seen a surge in the number of studies of patterns of past diversity, especially those of terrestrial vertebrates. But perhaps most importantly, these studies have attempted to account for and subsequently correct for the pervasive sampling biases present amongst the data using recently developed methods of sampling standardisation.

1.4 Sampling standardisation

In addition to the debate surrounding the extent of the impact of sampling biases on observed patterns of diversity, there is also ongoing discussion on how best to estimate taxic richness and ‘correct for’ these sampling biases. Several methods have been developed to estimate diversity from incomplete and uneven data, using a variety of approaches, that can be placed into three broad categories:

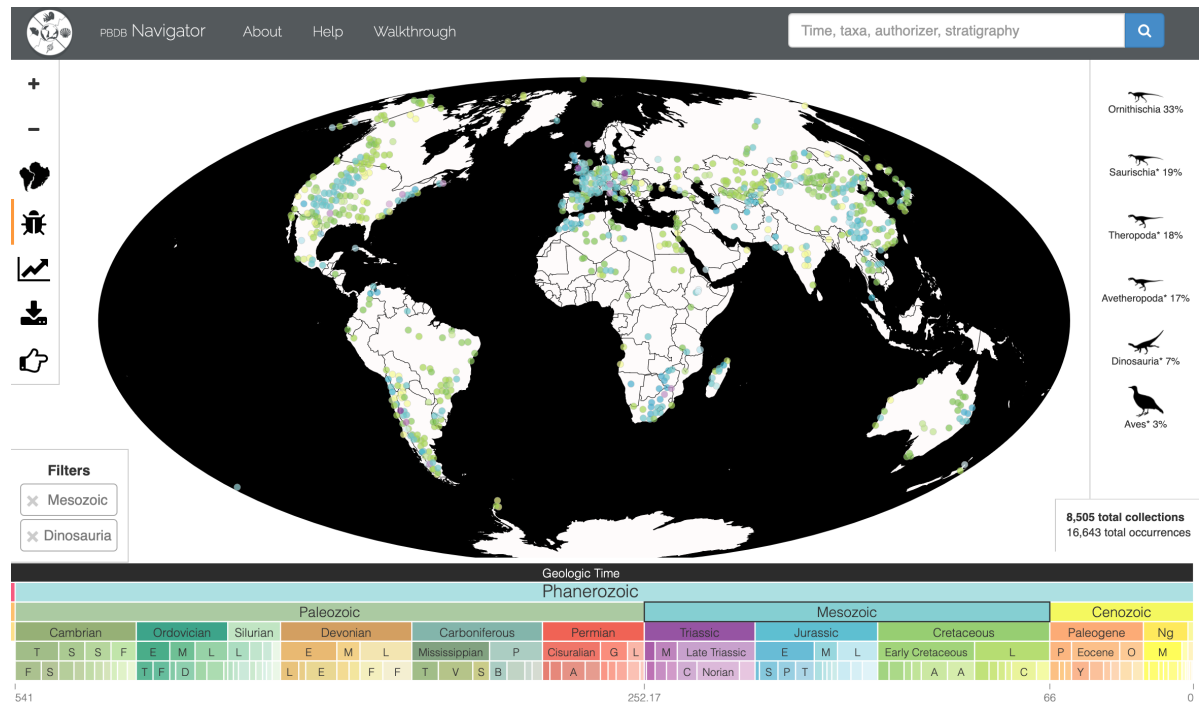


Figure 1.3: The Paleobiology Database Navigator webpage, accessed through <https://paleobiodb.org/navigator>, showing occurrences of Mesozoic dinosaur fossils

1. **Phylogenetic corrections**, more frequently used in studies of modern or genetic diversity where phylogenetic trees are more readily available, use phylogenetic trees to infer ghost lineages (gaps in a group's evolutionary history) that are the result of incomplete sampling (Norell and Novacek, 1992; Lane *et al.*, 2005).
2. The **residual approach** (or 'residual diversity method') uses residuals from a modelled relationship between palaeodiversity and a proxy for sampling in an attempt to remove the signal of sampling (Smith and McGowan, 2007; Lloyd, 2012). Deviations from the model are suggested to reveal troughs and peaks in taxic richness. This method, and modifications of it, has been applied in some pivotal studies on the palaeodiversity of terrestrial tetrapods (e.g. Barrett *et al.*, 2009). However, the approach has recently come under scrutiny for apparent statistical errors in the generation of the model results (Brocklehurst, 2015; Sakamoto *et al.*, 2016).
3. **Subsampling (and rarefaction) approaches**, in the broadest sense, attempt to

standardise unequally sized samples to allow direct comparison of diversity between samples, or assemblages, that have been sampled to different levels of intensity (Bush *et al.*, 2004; Alroy *et al.*, 2008; Benson *et al.*, 2016; Close *et al.*, 2018). The most popular and widely used subsampling approach is Shareholder Quorum Subsampling (SQS), first introduced to the field of palaeontology by John Alroy (Alroy *et al.*, 2008; Alroy, 2010b, 2010a, 2010c) and known in ecology/neontology as coverage-based rarefaction (Chao and Jost, 2012). This method standardizes samples to equal levels of ‘completeness’, as opposed to sample size in classical rarefaction (Sanders, 1968). Another, more recently proposed, method of subsampling is the extrapolation method TRiPS (true richness estimation using Poisson sampling) (Starrfelt and Liow, 2016). Although a recent study (Close *et al.*, 2018) has criticised TRiPS for tracking un-standardised (i.e. raw) richness curves.

No method of sampling standardisation is without shortcomings, and some methods will be more appropriate for certain datasets and for answering certain questions than others. In this thesis, I exclusively present sampling-standardised diversity (richness) estimates obtained through the subsampling method SQS, which was implemented through an approach more widely used in neontological/ecological studies (see Chapter 2 for full description of this approach). Richness estimators that standardise by coverage, such as SQS, are among the best currently available methods for reconstructing deep-time biodiversity patterns (Close *et al.*, 2018). SQS was also chosen due to its relative ease of use, but also to allow direct comparison between my estimates and previous studies of related groups and time intervals that also used SQS.

1.5 Objectives and outline

Despite the recent renewed interest in examining past diversity in light of sampling biases, to date, these kinds of studies have focused on particular taxonomic groups

or restricted intervals of geological time (e.g. Butler *et al.*, 2011a; Mannion *et al.*, 2012; Butler *et al.*, 2013; Cleary *et al.*, 2018). Moreover, studies of tetrapod (four-limbed terrestrial vertebrate) diversity patterns during the late Palaeozoic and early Mesozoic have tended to focus on the end-Permian mass extinction (e.g. Fröbisch, 2008, 2013; Sahney and Benton, 2008). The aim of this thesis is to quantitatively assess the temporal and spatial patterns of global terrestrial tetrapod diversity during key intervals in the early evolutionary history of tetrapods (Figure 1.4). Underpinning this work is the exploration of the impact of sampling biases on observed patterns of diversity and the use of sampling standardisation to mitigate their effects.

Sampling biases can mask key drivers of observed diversity patterns, making it difficult to ascertain how environmental and climate changes impacted global diversity through time. Furthermore, previous studies investigating the relationship between diversity and climate have been hampered by the absence of appropriate global palaeoclimate reconstructions that can be compared across long intervals of geological time. Instead, previous work has relied on gross oversimplifications of global palaeoclimatic conditions, such as a single global mean value for temperature (e.g. Cleary *et al.*, 2018).

Through a combination of comprehensive species occurrence datasets compiled within the Paleobiology Database, methods of sampling standardisation, advanced statistical approaches, and the integration of phylogenetic information and palaeoclimate reconstructions from a palaeoclimate model, I examine the drivers behind patterns of global tetrapod diversity and biogeography across two key intervals: 1) the Carboniferous to early Permian, during the diversification of the first vertebrates to emerge on land, and 2) the Late Triassic to Early Jurassic, when many modern vertebrate groups originated and began to diversify (Figure 1.4).

Chapter 2 explores the patterns of tetrapod diversity and biogeography during the Carboniferous and early Permian (272 million years ago) and assesses the impact of the 'Carboniferous rainforest collapse' using sampling standardisation and a

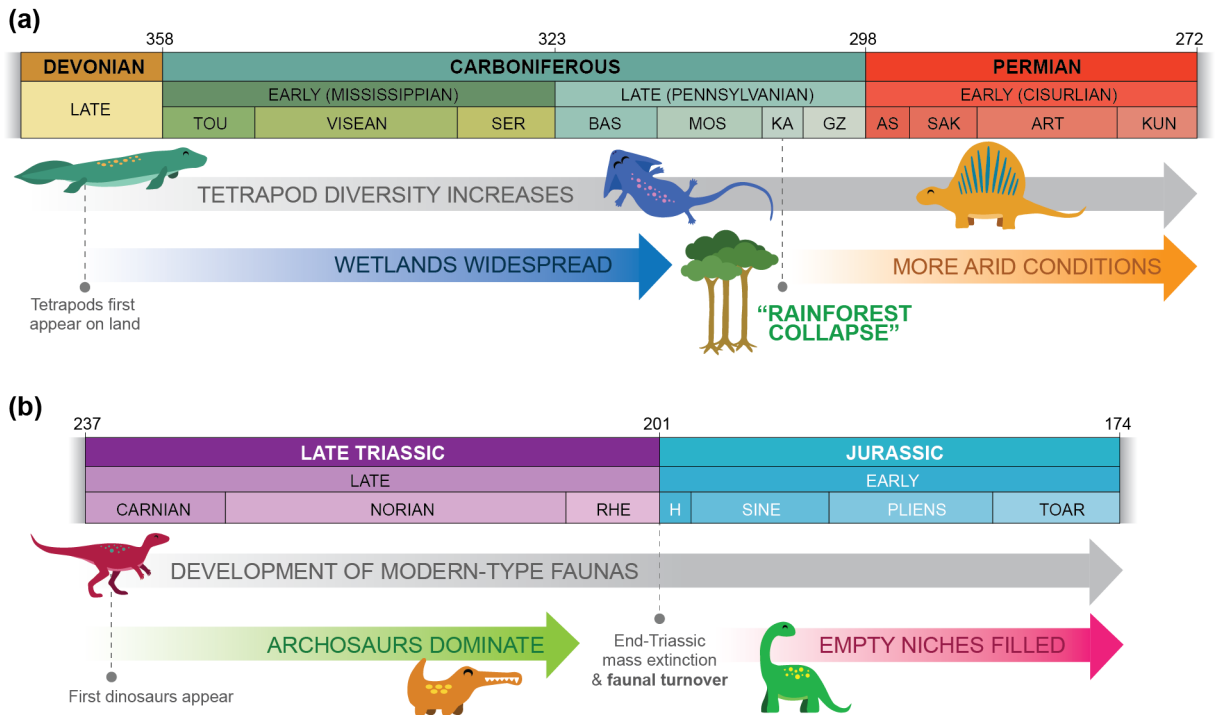


Figure 1.4: Simplified timeline of the key intervals studied in (a) Chapters 2 and 3, and (b) Chapters 4 and 5.

phylogenetic network biogeography approach.

Chapter 3 expands on this work, through a collaboration with Sam Thompson at Imperial College London. For this, we used a mechanistic ecological model, based on neutral theory, to test current hypotheses of diversity change during the late Carboniferous and early Permian, as well as evaluate how the sampling regime during this interval influenced observed patterns of diversity.

Chapter 4 focuses on patterns of latitudinal diversity during the Late Triassic, a time when many modern tetrapod groups such as mammals, reptiles, and dinosaurs were beginning to diversify. Using palaeoclimatic reconstructions from a spatially explicit general circulation palaeoclimate model, HadCM3L, I examined the relationship between palaeolatitude, and palaeoclimate to assess the drivers of tetrapod diversity during this interval.

Finally, Chapter 5 investigates the impact of climate on the diversity and evolutionary patterns of early dinosaurs during the Late Triassic and Early Jurassic. Using

evolutionary model fitting and analyses of both climate niche and morphological disparity through time, I examined the climatic niches occupied by early dinosaurs and their changes across the Triassic–Jurassic boundary, focusing on testing previous hypotheses that specifically link early sauropodomorph dinosaur global distribution to changes in palaeoclimate.

2 | DIVERSITY CHANGE DURING THE RISE OF TETRAPODS AND THE IMPACT OF THE 'CARBONIFEROUS RAINFOREST COLLAPSE'

This chapter is a lightly modified version of the following publication as it appeared in print at Proceedings of the Royal Society: Biological Sciences.

Dunne EM, Close RA, Button DJ, Brocklehurst N, Cashmore DD, Lloyd GT, and Butler RJ. (2018) Diversity change during the rise of tetrapods and the impact of the 'Carboniferous Rainforest Collapse'. *Proceedings of the Royal Society: B*, 285: 20172730.

The full text and supplementary files of this publication can be found at: <https://royalsocietypublishing.org/doi/full/10.1098/rspb.2017.2730>

My contribution to this work involved conducting all parts of the research, including collecting and collating the data, co-designing the methodology, analysing the data, and interpreting the results, as well as writing the manuscript. My co-authors collaborated by co-designing the research, sharing phylogenetic data, providing feedback on the interpretations of the results, and giving important comments on earlier versions of the manuscript. The editorial 'we' is used here to reflect these contributions. The formatting used here remains relatively unchanged from that used in the version published online at the link above.

2.1 Introduction

Tetrapods (four-limbed vertebrates) first appeared on land in the late Devonian (Ahlberg, 1995; Clack *et al.*, 2016), and during the Carboniferous and early Permian established the first terrestrial vertebrate communities. In the early Carboniferous, these amphibian-like early tetrapods radiated rapidly and diversified into a wide variety of morphologies and sizes (Clack *et al.*, 2016). Later in the Carboniferous, crown amniotes appeared (Coates *et al.*, 2008) and by the early Permian the terrestrial vertebrate fauna was dominated by synapsids (the mammalian stem-group), such as edaphosaurids and sphenacodontids, alongside a diverse array of basal reptiles (e.g. captorhinids) and amphibians (Brocklehurst *et al.*, 2013; Ruta *et al.*, 2008).

This diversification occurred as the surrounding environment was transitioning from wetlands in the Carboniferous to more arid conditions in the Permian. During the late Carboniferous, Euramerica (Europe and North America) lay at the equator and was predominantly covered by tropical rainforests, commonly referred to as the 'Coal Forests' (Cleal *et al.*, 2009a). During the Kasimovian (approximately 303–307 Ma) these rainforests began to disappear from large parts of the globe, and by the early Permian had been replaced in many regions by dryland vegetation as a more arid climate developed (Cleal *et al.*, 2009b; Cleal *et al.*, 2012). This 'rainforest collapse' culminated in what is considered one of two mass extinction events evident in the plant fossil record (Cascales-Miñana and Cleal, 2014).

Despite this interval being a crucial time for tetrapod evolution and the establishment of terrestrial ecosystems, few studies have focused on Carboniferous–early Permian tetrapod diversity patterns or have attempted to quantify the impact of the 'Carboniferous rainforest collapse' (CRC) on the terrestrial vertebrate fauna. Instead, most work has been focused on the later end-Permian mass extinction (Sahney and Benton, 2008; Fröbisch, 2013) and more recently on the early and mid-Permian extinction events (e.g.: Day *et al.*, 2015; Brocklehurst *et al.*, 2017). A previous study

that attempted to assess the impact of the CRC suggested that the newly-fragmented habitats following the collapse drove the development of endemism among tetrapod communities (Sahney *et al.*, 2010). This is proposed to have led to reduced local richness (alpha diversity) but higher global diversity (gamma diversity) following the CRC. However, this study failed to adequately account for how sampling of the fossil record varies in both time and space, largely accepting raw diversity patterns at face value. Moreover, the analysis was conducted using a family-level dataset, rather than one at species-level, and some of the data used in this study are no longer accessible.

The impact of uneven sampling on estimates of diversity has been appreciated for almost half a century (Raup, 1972; Raup, 1976; Sepkoski *et al.*, 1981), and in recent years there have been an increasing number of studies investigating the influences of sampling biases on palaeodiversity (Peters and Foote, 2001; Smith and McGowan, 2007; Alroy *et al.*, 2008). The correlation between palaeodiversity and sampling has been repeatedly demonstrated in many fossil groups including terrestrial vertebrates (Barrett *et al.*, 2009; Butler *et al.*, 2011a; Benson *et al.*, 2016; Close *et al.*, 2017), marine vertebrates (Benson *et al.*, 2009), insects (Clapham *et al.*, 2016), marine invertebrates (Vilhena and Smith, 2012), and plants (Cascales-Miñana *et al.*, 2013, 2016). Sampling intensity is influenced by several factors including geographical location, volume and variety of preserved sedimentary environments, collection methods, and academic interest. Substantial efforts have been made recently to develop statistical methods which can mitigate these biases allowing diversity to be estimated from an incomplete fossil record.

Here, using a newly-compiled global species-level dataset alongside sampling standardisation and network biogeography methods, we investigate patterns of early tetrapod diversity and biogeography from the Carboniferous to early Permian to answer the following questions: (i) What are the major patterns of tetrapod diversity during this interval? (ii) How do sampling biases impact estimates of diversity, and how can we best account for them? (iii) Did the 'Carboniferous rainforest collapse' drive the

development of endemism among tetrapod communities?

2.2 Methods

2.2.1 *Fossil occurrence data*

Newly-compiled data detailing the global occurrences of early tetrapod species from the beginning of the Carboniferous (Tournaisian) to the end of the Cisuralian epoch (Kungurian), informally referred to as the ‘early Permian’, were downloaded from the Paleobiology Database (paleobiodb.org, accessed September 19th, 2017). These data result from a concerted effort to document the Palaeozoic terrestrial tetrapod fossil record, led by the lead author of this study. The data represent the current published knowledge on the global occurrences and taxonomic opinions of early tetrapods. Data preparation and analyses were conducted within R 3.4.1 (R Core Team, 2017). All marine taxa and ichnotaxa were discarded from the dataset, and the final cleaned dataset comprises 476 tetrapod species from 385 collections (=fossil localities), totalling 1,047 unique global occurrences.

2.2.2 *Raw patterns of diversity and sampling*

To enable direct comparison with earlier studies, we present raw (=uncorrected or observed) diversity patterns at global and local spatial scales. However, we do so with the proviso that raw diversity counts may be highly misleading, and focus on our interpretation of the diversity patterns produced using coverage-based sampling standardisation. Global (=gamma scale) raw diversity curves were computed using sampled-in-bin counts of specifically determinate occurrences using the function within the SQS Perl script provided by John Alroy (in order to count all taxa with ranges spanning one bin or more, the “deorphan” option was set to ‘yes’, meaning that collections spanning multiple bins were assigned to bins including more than half of their age estimate limits). Separate curves were computed for 1) all tetrapod species; 2) non-amniotes (early

tetrapodomorphs and amphibians); and 3) amniotes (including Reptiliomorpha). We also plotted raw family diversity to allow direct comparison with the dataset of previous analyses (Sahney *et al.*, 2010). Family-level assignments were based upon those recorded in the dynamic taxonomy of the Paleobiology Database.

We estimated local richness (=alpha diversity) by counting species per collection (=fossil locality). These counts included not only occurrences determinate at species level but also those indeterminate at species level that must logically represent distinct species according to the taxonomic hierarchy of the Paleobiology Database. This allowed a more accurate picture of local diversity, using all of the available data. We present raw estimates of local richness because sampling-standardised estimates would require abundance data, which is not consistently available in the literature. Although recent work by our group has argued that ‘global’ diversity curves are problematic due to substantial changes in the palaeogeographic spread of localities through time (e.g. Close *et al.*, 2017), we argue that this is less of a concern for the Carboniferous–early Permian because the great majority of sampling of the tetrapod record is from a relatively small palaeogeographic area (palaeoequatorial regions of Laurasia). Although increases in palaeogeographic sampling do occur through time (Figure 2), they are small.

Additionally, we quantify patterns of sampling using counts of total collections, fossiliferous formations, and occupied equal-area grid cells (50 km spacing) (Barnes *et al.*, 2017) in each interval (recorded in the Paleobiology Database dataset), and also show how sample-based coverage varies through time using Good’s u (Good, 1953; Chao and Jost, 2012).

2.2.3 *Sampling standardised richness*

We focus our interpretation of gamma-scale (global) diversity patterns on coverage-standardised estimates. Coverage-based sampling standardisation uses the concept of frequency-distribution coverage (a measure of sample completeness that can be

accurately and precisely estimated using Good's u (Good, 1953) to make fair comparisons of diversity between assemblages that may be sampled to very different levels of intensity). Sample coverage is simply the fraction of individuals in the original population that belong to the sampled species (i.e. the degree to which the sampled species 'cover' the entire frequency distribution). Alroy (2010a; 2010b; 2010c; 2014) introduced this method under the name Shareholder Quorum Subsampling (SQS), using an algorithmic approach.

We implemented SQS (also known as 'coverage-based rarefaction') using the analytical equations described by Chao and Jost (2012) via the R package iNEXT (iNterpolation/EXTrapolation) (Hsieh *et al.*, 2016). The analytical implementation of SQS in iNEXT yields confidence intervals and allows coverage-based extrapolation (using the Chao1 estimator), in addition to interpolation (=subsampling). The data were rarefied by collection, by analysing incidence-frequency matrices of the occurrence data. Extrapolated estimates were limited to no more than twice the observed sample size (as recommended by Hsieh *et al.*, 2016). We elected not to use the optional three-collections-per-reference protocol advocated by Alroy (2014), because 1) unlike marine invertebrate datasets, Carboniferous–early Permian tetrapods do not suffer from over-reporting of common taxa, and 2) sample coverage in some intervals is so low that limiting the amount of data drawn (to no more than three collection per reference per trial) prohibited us from obtaining diversity estimates at meaningful quorum levels (i.e. target levels of standardised coverage). We computed coverage-standardised diversity estimates at both species and genus level. Both ranked and relative richness among assemblages may change depending on quorum level if there are differences in evenness or the shape of the abundance distribution (Chao and Jost, 2012); therefore, in addition to presenting diversity-through-time curves, we also present coverage-based rarefaction curves to show how coverage-standardised diversity estimates for different time intervals vary with coverage.

2.2.4 *Phylogenetic Biogeographic Connectedness (pBC)*

Sidor *et al.* (2013) developed a network model of biogeography to assess regional biogeographic changes by quantifying biogeographic connectedness (BC) between regions containing tetrapod fauna. This general approach can be used to test the biogeographic hypothesis proposed by Sahney *et al.* (2010) that global tetrapod faunas became increasingly endemic after the CRC (i.e. less well-connected). The Sidor *et al.* approach may be of limited utility when analysing a fossil record dominated by 'singletons' (taxa occurring at a single locality or within a single geographic area), as is the case for the Carboniferous–early Permian. Instead, we utilised a modification of the Sidor *et al.* network model presented by Button *et al.* (2017), where phylogenetic information is incorporated into the calculation of BC (see Figure A2), thus addressing issues arising from using only binary presence-absence data. This method inversely weights links between taxa in different geographic regions in proportion to the phylogenetic distance between them, and these links are used to calculate phylogenetic biogeographic connectedness (pBC). Values of pBC range between 0 and 1, with higher values equating to more cosmopolitan faunas, whereas lower values indicate greater endemism and phylogenetic distinction between geographic regions.

To analyse phylogenetic biogeographic connectedness, we first defined geographical input areas for the analysis through a k-means clustering of palaeocoordinate data for all 1,047 tetrapod occurrences in the occurrence dataset described above. This approach to defining geographic areas uses only the palaeocoordinate data to identify geographically discrete clusters of fossil localities and does not take into account species relationship or taxonomy. k-means clustering was performed within R for each interval separately, varying the value of *k* from 3–10. Ten-thousand replicates were performed for each analysis, with ten random starts. The performance of each iteration (3–10) was compared based upon the percentage of variance explained by the resolved clusters (the ratio of the between clusters sum of squares: total sum of squares). The best performing iteration for each value of *k* was retained for further

comparison. Comparison between the results of different values of k was principally performed on the basis of variance explained by each, with those scoring <90% being omitted from consideration. Further comparison was performed by considering following criteria: the consistency of the clusters through the time interval in question and their consistency with previously recognised biogeographic provinces. This resulted in the designation of seven discrete geographic regions each for the Carboniferous and early Permian (Appendix A, Table 3 and Figure 1.2). Species were assigned to one or more of the regions as appropriate, creating a taxon-region matrix for each time interval.

We assembled an informal species-level supertree of early tetrapods, consisting of 325 species based upon the most recent phylogenetic analyses and formal supertrees available for the major clades of Carboniferous–early Permian tetrapods (see Appendix). As in the diversity analyses, marine taxa were excluded. Phylogenetic biogeographic connectedness (pBC) was then calculated for each time interval using the appropriate taxon-region matrix. The constant μ was set at 15 million years following Button *et al.* (2017). Jackknifing, with 10,000 replicates, was used to calculate 95% confidence intervals. We performed this analysis first for all tetrapod species in the Carboniferous (Tournaisian–Gzhelian) and early Permian (Asselian–Kungurian), then separately for amphibians and amniotes in the same two intervals, and finally for all tetrapod species in three shorter intervals (pre-CRC, Bashkirian–Kasimovian; immediately post-CRC, Gzhelian–Sakmarian; post-CRC, Artinskian–Kungurian).

2.3 Results & Discussion

2.3.1 *Patterns of diversity and sampling*

Raw global tetrapod species richness (= uncorrected or observed species counts) generally rose from the Carboniferous to early Permian, but this rise was not steady (Figure 2.1a). The greatest increases in raw species richness occur during the late

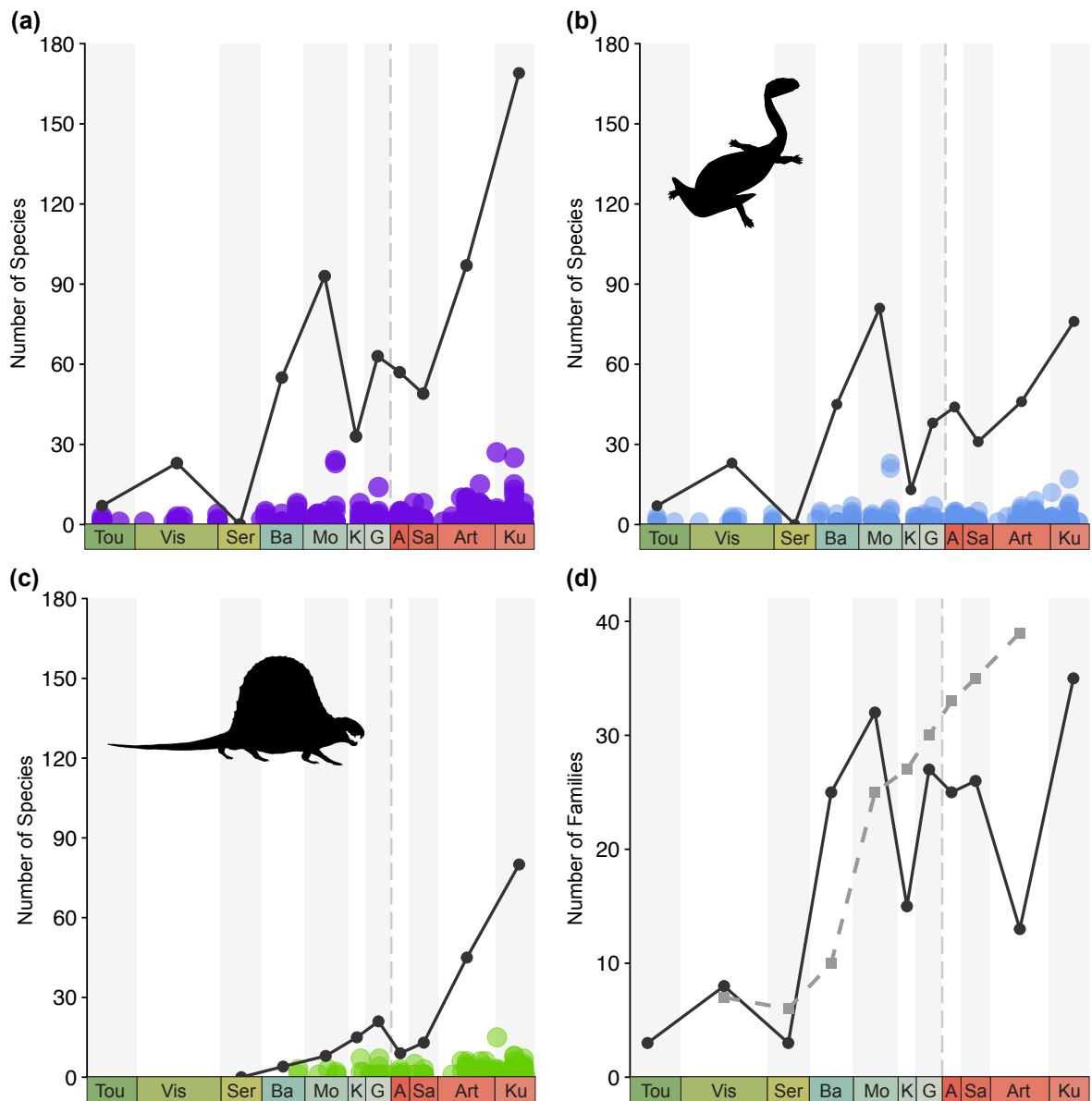


Figure 2.1: Raw (=uncorrected) richness and local richness (alpha diversity) from the Carboniferous to early Permian. Local richness here is the number of species per collection (=fossil locality). (a)-(c) Species richness (solid line) and alpha diversity (circles) for all tetrapod species, non-amniote species, and amniote species respectively. (d) comparison between family diversity estimated by Sahney et al. (2010) (dashed line) and this study (solid line). Abbreviations of interval names: Tou = Tournaisian, Vis = Visean, Ser = Serpukhovian, Ba = Bashkirian, Mo = Moscovian, K = Kasimovian, G = Gzhelian, A = Asselian, Sa = Sakmarian, Art = Artinskian, Ku = Kungurian.

Carboniferous (Serpukhovian–Moscovian) and in the final stages of the early Permian (Sakmarian–Kungurian). Carboniferous diversity is dominated by non-amniote taxa (tetrapodomorphs and amphibians), with a marked rise in richness from the Serpukho-

vian to Moscovian (Figure 2.1b). This increase is followed by a substantial decrease in the Kasimovian before richness begins to generally increase again during the early Permian. Amniotes first appeared in the late Carboniferous and from then richness rose into the early Permian, disrupted only by a decrease across the Carboniferous/Permian boundary (Gzhelian–Asselian) (Figure 2.1c). By the end of the early Permian, both non-amniotes and amniotes had reached similar levels of species richness. Raw family richness also increased across the interval, as reported by Sahney *et al.* (2010). Directly comparing our estimates of family richness with those of Sahney *et al.* (2010) reveals the differences between both datasets (Figure 2.1d), which may result in part from the different approach to taxon counting: range-through in Sahney *et al.* (2010) (which has the effect of smoothing the diversity curve) and sampled-in-bin counting here.

Raw species richness estimates are heavily influenced by temporal and spatial sampling biases. From the Carboniferous to early Permian, the numbers of fossiliferous formations, collections (=fossil localities), and occupied equal-area grid cells fluctuate, indicating a high degree of variation in temporal sampling (Figure 2.2, Table 2.1). Visual inspection shows that raw species richness in the Carboniferous closely tracks patterns of sampling; intervals with high richness also have high counts of sampled formations, collections, and grid cells (Figure 2.2). In the early Permian, this pattern is less evident, and higher values for Good's u in the Asselian, Artinskian, and Kungurian indicate that the early Permian is comparatively better sampled than all stages of the

Table 2.1: Counts of species, collections (=fossil localities), formations, and equal area grid cells as proxies for sampling in each interval of the Carboniferous and early Permian. Abbreviations of interval names are as given in Figure 2.1

Count	Tou	Vis	Ser	Ba	Mo	K	G	A	Sa	Art	Ku
Species	7	23	0	55	93	33	63	57	49	97	169
Collections	5	17	2	24	21	11	41	63	61	64	75
Formations	2	6	2	12	9	9	24	26	18	24	10
Grid cells	4	11	2	21	20	9	36	27	31	28	22
Good's u	0.28	0.17	-	0.24	0.33	0.19	0.29	0.64	0.39	0.47	0.72

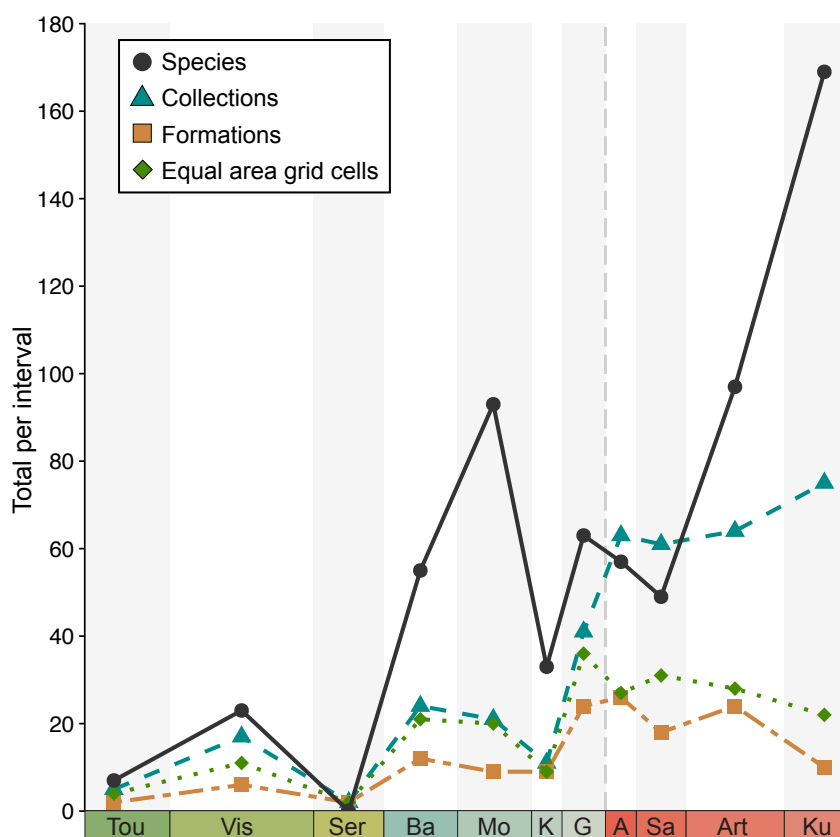


Figure 2.2: Sampling in the Carboniferous and early Permian. Tetrapod species richness (solid grey line) closely tracks total number of formations, collections, and equal area grid cells in the Carboniferous, but then begins to deviate from this trend in the early Permian. Abbreviations of interval names are as given in figure 2.1

Carboniferous (Table 2.1).

Local richness, or alpha diversity, potentially provides important insights into patterns of early tetrapod diversification, as alpha diversity estimates may be less strongly affected by biases in sampling that can confound global diversity compilations (Bambach, 1977). We found that local richness for both non-amniotes and amniotes increased across the interval (Figure 2.1a-c), contrary to the pattern recovered in previous analyses (Sahney *et al.*, 2010). Local richness rose slowly through the Carboniferous, with most collections (=fossil localities) containing fewer than ten species. At the end of the early Permian, this increase accelerates as the number of species per collection increases. Exceptionally well-sampled sites can be clearly seen to be isolated from the general pattern (Figure 2.1a-c), further exemplifying uneven sampling during

this interval. For example, exceptional sites occur in the Moscovian (Linton Diamond coal mine, Ohio and Nyraňy coal mine, Czech Republic), and Artinskian/Kungurian (Coffee Creek locality, Texas and Richard's Spur quarry site, Oklahoma) (see Table A1).

Coverage-standardised richness estimates of diversity across the Carboniferous/ Permian boundary suggest that diversity increased into the late Carboniferous, but fell substantially across the boundary (with the decline beginning in the Gzhelian) and subsequently began to increase again, albeit slowly, through the early Permian (Figure 2.3a). However, it is important to recognise that both relative and rank-order richness can change depending on quorum level, and at higher quorum levels the relative drop in diversity from the Carboniferous to the Permian becomes less pronounced (Figure 2.3b). These estimates stand in stark contrast to the patterns of raw diversity. The marked decrease in standardised diversity across the Carboniferous/Permian boundary correlates closely with the time of the 'rainforest collapse', suggesting a close link between gamma diversity and floral composition. The apparent conflict between heightened local richness (alpha diversity) but lower gamma diversity in the earliest Permian relative to the late Carboniferous is explicable if beta diversity decreased i.e. faunas became less biogeographically distinct (more cosmopolitan) – as discussed below.

2.3.2 *Patterns of biogeography*

Previous investigations of early tetrapod biogeography patterns suggest that habitat fragmentation following the CRC (Kasimovian, 305 Ma) drove the development of increased endemism for the first time amongst tetrapod faunas in the early Permian (Sahney *et al.*, 2010). Our analyses do not support this hypothesis; instead we recover a significant increase in global phylogenetic biogeographic connectedness (pBC) from before the CRC (Carboniferous) to after (early Permian) (Figure 2.4a). Instead of endemism developing, communities appear to have become better connected following

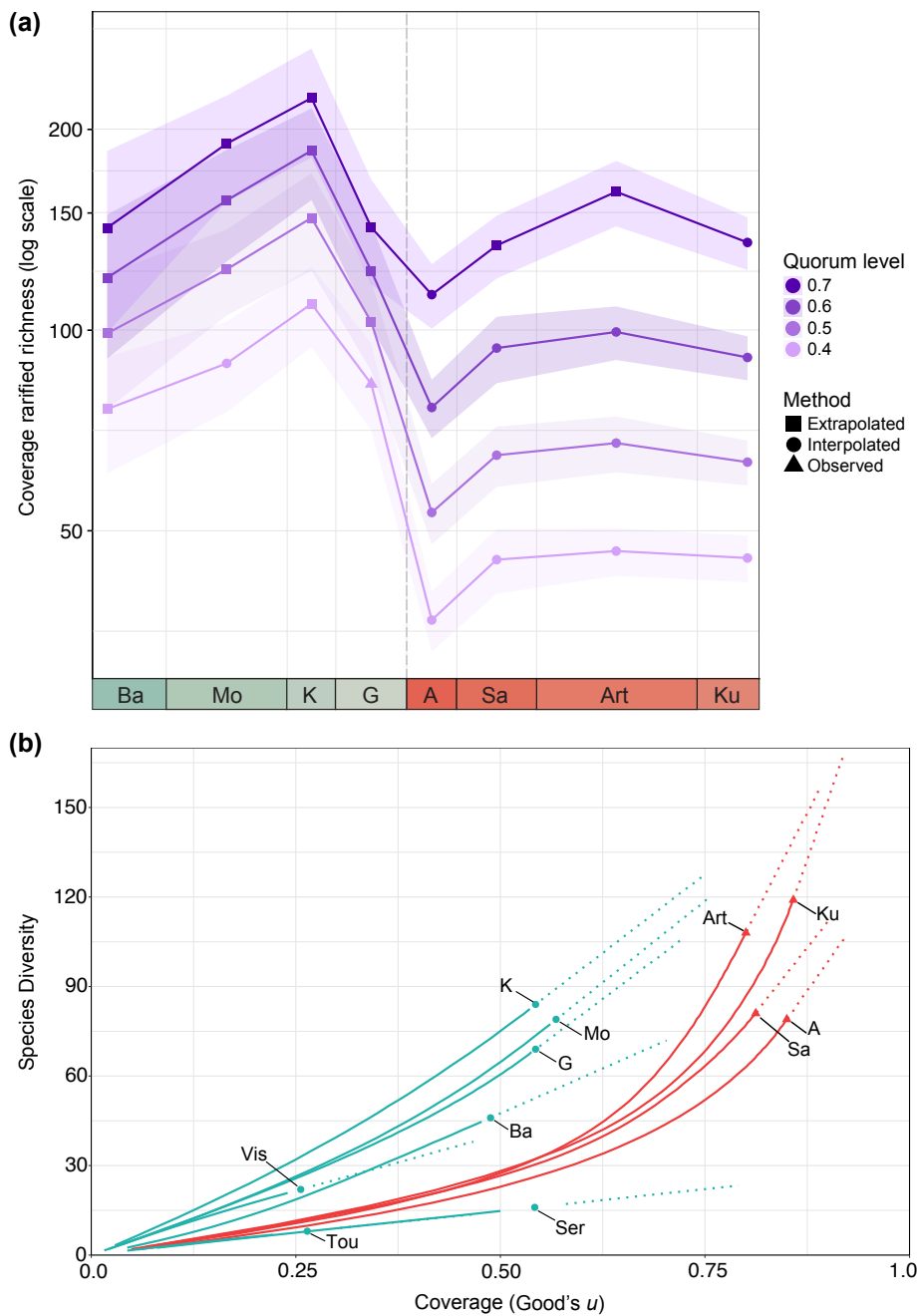


Figure 2.3: Estimates of diversity of Carboniferous–early Permian tetrapods using coverage-based subsampling. (a) Coverage-standardised diversity curve for intervals across the Carboniferous/Permian boundary showing estimates at different quorum levels. Abbreviations of interval names are as given in Figure 2.1. (b) Coverage-based rarefaction curve for all intervals of the Carboniferous (green/blue) and early Permian (red). Extrapolated portions of lines represent analytical solutions for the Chao1 extrapolator at specific levels of coverage. Diversity was extrapolated at up to twice the reference sample size as recommended by Hsieh *et al.* (2016).

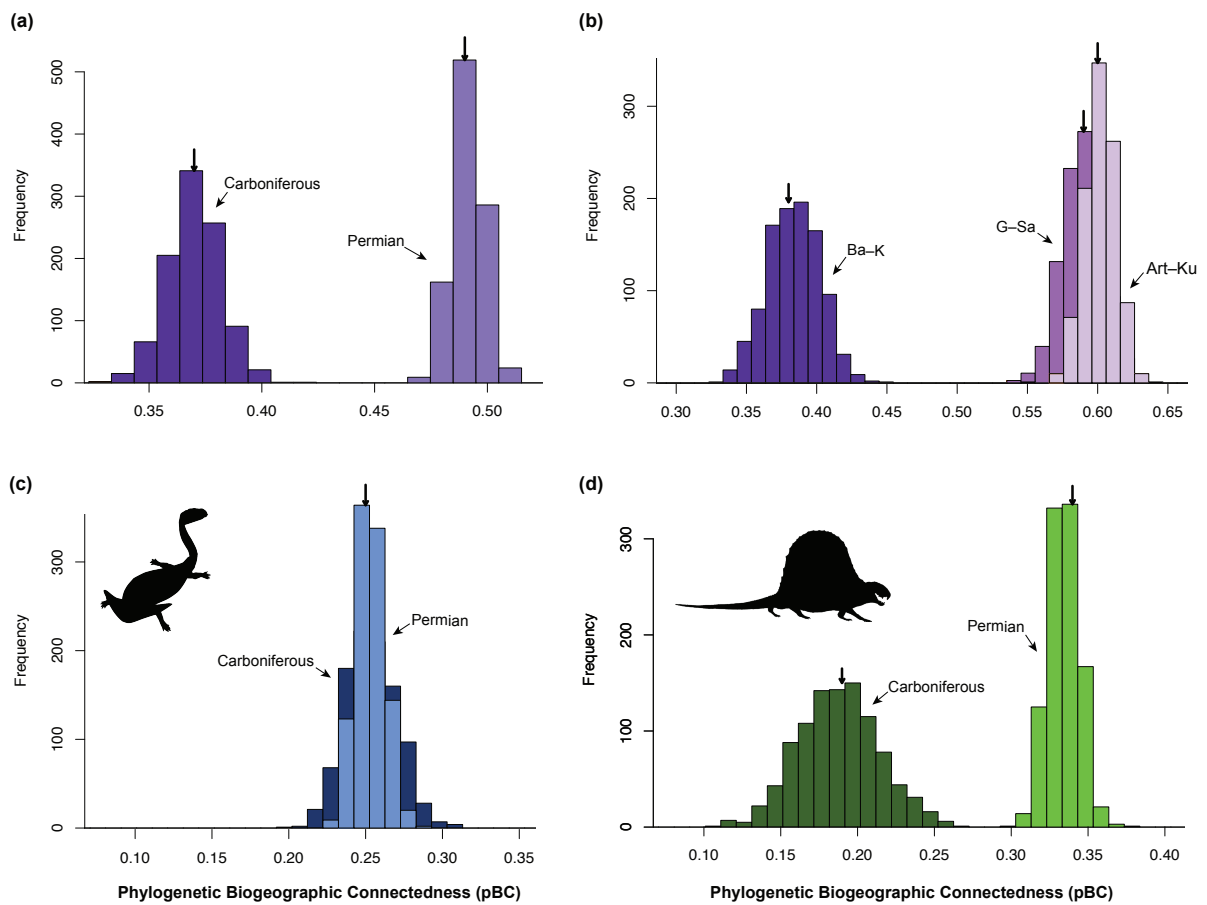


Figure 2.4: Histograms showing the distribution of bootstrap analyses of phylogenetic Biogeographic Connectedness (pBC). (a) Carboniferous and early Permian for all tetrapod species; (b) Bashkirian–Kasimovian (pre-CRC), Gzhelian–Sakmarian (post-CRC), and Artinskian–Kungurian (post-CRC) intervals, again for all tetrapod species; (c) Carboniferous and early Permian for non-amniote species; (d) Carboniferous and early Permian for amniote species. Higher pBC values indicate increasing connectivity between regions, and arrows indicate the mean pBC value for each interval (e.g. in (a) Carboniferous = 0.37, early Permian = 0.49)

the ‘rainforest collapse’. This same pattern is seen when three shorter intervals, instead of only two, are analysed (Figure 2.4b).

Sahney *et al.* (2010) formed their hypothesis of endemism based on a simple calculation of dividing global tetrapod family diversity by mean alpha diversity for each time bin. However, given the strong sampling biases present in the data, we argue that more sophisticated methods are necessary to decipher the responses of tetrapod faunas to the rainforest collapse. To explain their finding of enhanced endemism, Sahney

et al. (2010) invoked the theory of island biogeography (MacArthur and Wilson, 1967) which suggests that habitat fragmentation can drastically affect diversity. However, this conclusion may stem from an oversimplification of the floral changes that happened at the end of the Carboniferous. Instead of the rainforests “collapsing”, the floral composition of the landscape at the equator transitioned gradually from wetlands to drylands (Cleal *et al.*, 2009b). The main areas of rainforests in Euramerica disappeared at the end of the Moscovian, however areas of swamps persisted in Variscan intramontane basins in Europe and some lowland areas of central North America through the late Pennsylvanian (Cleal and Thomas, 1999; 2005). Furthermore, in China, these wetland swamps did not fully develop until the late Pennsylvanian and continued to expand in the early Permian, indicating that the coal forest biome was migrating gradually eastwards during much of the late Carboniferous (Cleal and Thomas, 2005). This change in floral composition at the end of the Carboniferous, while recorded as a mass extinction event in the plant fossil record (Cascales-Miñana *et al.*, 2016), may not have resulted in tetrapod communities being isolated from one another by new, unsuitable landscape as suggested by Sahney *et al.* (2010).

Instead, more open landscapes could conceivably have favoured dispersal, leading to increased connectivity between previously separate faunal communities. Amphibians do not show any significant change in biogeographic connectedness from the Carboniferous–early Permian (Figure 2.4c), suggesting that dispersal rates did not increase following the disappearance of the rainforests, and that the pattern of increased connectedness in tetrapod faunas in the early Permian is driven primarily by amniotes (Figure 2.4d). Amniotes, such as edaphosaurids and sphenacodontids, with their generally larger body size relative to earlier tetrapods, began to appear at the end of the Carboniferous and in the early Permian. Unlike amphibians, which dominated earlier faunas, these taxa were not confined to wetland environments and could freely disperse across the new landscape.

2.4 Conclusions

Despite recent concerted attempts to close the gaps in our knowledge of early tetrapod diversity (Clack *et al.*, 2016; Anderson *et al.*, 2015), tetrapod data for the Carboniferous and early Permian is still lacking. Nevertheless, using a newly-complied species-level dataset and a range of quantitative approaches for estimating patterns of diversity and biogeography, we have been able to comprehensively test the major patterns of diversity change during this interval. Species diversity increased towards the end of the Carboniferous, before decreasing across the Carboniferous/Permian boundary and subsequently remaining lower in the early Permian. Our analyses of early tetrapod biogeography do not support the previous hypothesis that habitat fragmentation following the end-Carboniferous rainforest Collapse drove the development of endemism, resulting in tetrapod communities diversifying in isolation in the early Permian. Instead, we found that tetrapod communities were increasingly well-connected following the ‘rainforest collapse’, which may have led to lower gamma diversity. This ‘collapse’ of the rainforests is better represented as a gradual transition between wetlands and drylands, and resulted in a more open landscape which favoured dispersal, particularly among amniote faunas.

2.4.1 *Post-publication review of current literature*

Since this work was published in February 2018, two other papers examining patterns of early tetrapod diversity and biogeography have been published. Brocklehurst *et al.*, (2018) (a study in which I was involved) focused on the patterns of tetrapod dispersal and vicariance using a likelihood approach to infer ancestral areas alongside stochastic mapping. Across the Carboniferous-Permian boundary, Brocklehurst *et al.* identified a decrease in dispersal and a peak in vicariance in both amphibians and amniotes. This result appears to be in conflict with our finding that biogeographic connectedness increased across the same interval (suggesting an increase in dispersal). Brocklehurst

et al. attribute the conflict to the manner in which each study's data were clustered geographically; ours uses different clusters in the late Carboniferous and early Permian (Figure A3), while the Brocklehurst *et al.* clusters do not change between intervals. Repeating their analysis using our clusters, Brocklehurst *et al.* found results more consistent with ours, leading to the suggestion that in the late Carboniferous, dispersal between larger regions was more difficult than between smaller-scale regions. This supports the inference that the primary barriers to dispersal in the late Carboniferous were physical barriers between continental-scale regions (e.g. mountains), rather than environmental barriers (Brocklehurst *et al.*, 2018). Our findings, therefore, reflect an increase in local-scale dispersal between tetrapod communities. Crucially, Brocklehurst *et al.* (2018) also firmly rejected the island-biogeography effect posited by Sahney *et al.* (2010).

Pardo *et al.* (2019) examined the effects of climate change across the Carboniferous–Permian boundary on the early radiation of terrestrial tetrapods using ecological ordination analyses combined with a phylogenetic approach and a comprehensive dataset based on early tetrapod occurrence data from the Paleobiology Database. Their results demonstrated that the reduction of tropical wetlands (rainforests) accommodated emerging dryland-adapted amniote faunas, beginning in western Pangaea and moving eastward (the 'Vaughn-Olson model'), similar to the inference presented in our discussion above. Pardo *et al.* also found that the strongest palaeoecological signal across the Carboniferous-Permian boundary is heterogeneous sampling of faunal assemblages.

These three studies together have further enhanced our understanding of early tetrapod diversity by revealing patterns otherwise obscured by global time-series diversity curves calculated across broad intervals, as well as further illuminating the strong phylogenetic signals underpinning the faunal composition of terrestrial assemblages.

3 | TETRAPOD DIVERSIFICATION AND THE 'CARBONIFEROUS RAINFOREST COLLAPSE' UNDER NEUTRAL THEORY

This work was written in direct collaboration with Sam Thompson (Imperial College London) and also features in their PhD thesis (Thompson, 2019, Chapter 6). I collated the data, based on the dataset used in Chapter 2, from the Paleobiology Database, and Sam led the neutral theory simulations and plotting of these results. We both contributed equally to the interpretation of the results and wrote the manuscript, of which this chapter is a lightly modified version. Our co-authors R. Close, J. Rosindell, and R. Butler provided feedback on the methodology and interpretation of the results, as well as feedback on earlier versions of the manuscript. As in the previous chapter, the editorial 'we' is used here to reflect these contributions.

3.1 Introduction

As outlined in the previous chapter, past assessments of early tetrapod diversity and biogeography during the late Carboniferous and early Permian (323–252 million years ago) have all used statistical or phylogenetic methods alongside literature-based occurrence datasets. Yet, statistical methods of inferring past diversity change are inevitably limited at some level by the available data. An alternative approach is to use a mechanistic model to produce simulated communities in which diversity is an emergent feature and can be sampled. These simulated communities provide a way of testing how

the real sampling regime affects the face-value diversity patterns. As mechanistic models can be scaled up beyond empirical sample sizes, such models can predict wider biodiversity patterns, as well as providing estimations of detectability levels within the currently available fossil data (Brocklehurst, 2015). Studies involving mechanistic models can even be used to test theories of biodiversity generation at global scales, much larger than could ever be directly perceived in the fossil record (Holland and Sclafani, 2015; Jordan *et al.*, 2016; Holland, 2018).

Assessments of spatial and temporal biases using a mechanistic basis by definition require a model which is spatially and temporally explicit. In addition, to study the impact of habitat loss and fragmentation on biodiversity requires a model which can directly incorporate these dynamics within the biodiversity-generating process. Neutral models fulfil all these requirements. Neutral theory (Hubbell, 2001) assumes that the properties of an individual are independent of its species identity and that all species within a community have equivalent demographic rates. The dynamics of neutral models are dictated by some combination of dispersal, ecological drift and speciation. The output of neutral models is a simulated ecological community, where each individual has an assigned species identity. The communities provide a baseline for expected biodiversity under “idealised” conditions (Alonso *et al.*, 2006) against which the biodiversity from real communities can be compared. However, neutral theory has rarely been applied in analyses of fossil data. Only a few palaeoecological studies have used spatially implicit neutral theory (Holland and Sclafani 2015; Jordan *et al.* 2016; Holland 2018) where populations (e.g. within separate continents) are divided to roughly represent spatial barriers. In this study, however, we use a spatially explicit variant of neutral theory that can simulate each individual from the fossil record at a precise position and time, allowing us to fully incorporate information about the geographic structure of the fossil record.

Our spatially explicit neutral models test the hypothesis that habitat fragmentation following the CRC resulted in increased global diversity by promoting endemism,

first proposed by Sahney *et al.* (2010). In addition, we examine to what extent the current fossil record can detect first order (global) patterns of diversity, thus investigating how sampling biases can mislead analyses of global diversity and biogeography. We test if our neutral models reproduce the face-value diversity patterns (i.e. 'raw', or uncorrected taxon counts) observed in the fossil record, both with and without habitat fragmentation driven by the CRC. By "up-sampling" our simulated communities (i.e. sampling more individuals than noted by the face-value fossil record), we explore how these face-value diversity patterns change with more complete sampling. In doing so, we highlight the problems that can arise from inferring large-scale diversity changes from very limited samples and demonstrate the potential that mechanistic models, such as those founded on neutral theory, have for testing hypotheses of diversity change.

3.2 Methods

3.2.1 *Fossil occurrence data*

Data detailing the global occurrences of early tetrapod species from the late Carboniferous (Bashkirian) to early Permian (Kungurian) were downloaded from the Paleobiology Database (www.paleobiodb.org, accessed 26th April 2018). These data represent the current published knowledge on the global occurrences and taxonomic opinions of early tetrapod species, and the dataset is the result of a concerted effort to document the Palaeozoic terrestrial tetrapod fossil record (see Chapter 2). The dataset was cleaned by removing marine taxa, ichnotaxa, and taxa with uncertain taxonomic identifications. The total number of amniote (including Reptiliomorpha) and amphibian (non-amniotes and early tetrapodomorphs) species per site was ascertained and recorded. The resulting dataset details the number of amniote and amphibian species found at each site (i.e. collection) during each interval from the Bashkirian to the Kungurian.

3.2.2 *Neutral models*

Neutral models ignore demographic differences between individuals and species, with simulations typically involving ecological drift, speciation and some form of dispersal (either as immigration from a metacommunity, or movement from other parts of the landscape). The classic, spatially implicit model (Hubbell 2001) conceives of a local community connected to a metacommunity by immigration, described by an immigration rate parameter. As it is based on biological mechanisms, neutral theory has high utility for identifying important dynamics (Vergnon *et al.* , 2009), acting as a null or “ideal” model (Alonso *et al.* 2006) or making predictions at broader spatial or temporal scales than possible with field experiments (Rahbek *et al.*, 2007). However, integrating spatial biases requires, by definition, a spatially explicit model. As such, our neutral model extends the original spatially implicit concept, incorporating the locations of each individual in space and relying on a dispersal kernel to represent the distance moved by offspring from their parents. The metacommunity from the spatially implicit version is replaced in our model by a broad spatially explicit landscape.

In the model, an individual is first chosen to die. To find the species identity of the replacement, we choose a parent from nearby individuals according to our dispersal kernel; we use a two-dimensional normal distribution to provide the probability of an individual moving a given distance from its parent. Occasionally, with rate ν , instead of selecting from any existing species, a new species identity is introduced as a speciation event. Over many iterations, nearby individuals are more likely to be the same species, whereas distant populations will have higher beta diversity, with fewer shared species. We use these models to generate communities of species across the landscape.

A major development for neutral theory was backwards-time coalescence methods (Rosindell *et al.*, 2008), which produce equivalent results to traditional forwards-time models but are vastly superior in computational performance. As well as the expanded spatial scales made available through coalescence, many scenarios are made possible that are not possible in the forwards-time approach, such as infinite

landscapes (Rosindell and Cornell, 2007) sampling a subset of individuals from the landscape. The latter feature means that our models can simulate just the locations from the fossil record, but account for the full spatial structure of the continents from the relevant periods. An equivalent model using forwards-time techniques would require simulating every tetrapod that existed across the entire time frame, a feat not feasible with current computational power. We use the `pycoalescence` package available for Python (available at: bitbucket.org/thompsonsens/pycoalescence), which uses coalescence methods implemented in C++ for high performance spatially explicit neutral simulations. All simulations were performed on high-throughput computing systems at Imperial College London.

We grouped fossils into one of eight stratigraphical intervals: Bashkirian, Moscovian, Kasimovian, Gzhelian, Asselian, Sakmarian, Artinskian or Kungurian. Our density maps of individuals across the globe were determined for each interval from the continental boundaries of the time. (The definition of ‘density’ here is the number of individuals of a given species that occur within a given area.) Global rasterised maps were produced at 0.01 degree resolution latitude and longitude (around 1 km² - this represents a single cell for our model), using the continental extents provided by the Paleobiology Database based on GPlates palaeogeographical reconstructions (Seton *et al.*, 2012). The palaeocoordinates of each fossil site were calculated and aggregated within each 1 km² cell. This generates a map defining the number of individuals to be sampled at each position in space. As we are not sampling from the majority of the globe, most cells in this sample map will be 0. The density and the sample map together contain the spatial information of the entire global community of tetrapods for the simulation and define which individuals from this global community are simulated. We split the tetrapods into two groups, amphibians and amniotes, to reflect their differing physiologies and environmental preferences. Every fossil identified to the species level was simulated as a separate individual, and multiple specimens of the same species within the same site were ignored to resolve uncertainties regarding numbers of indi-

viduals from within a single record. The intervals are sufficiently far apart in time that we reasonably assumed no shared species between the intervals within the model. Consequently, we ran intervals as separate neutral models in parallel, and aggregated the communities post-simulation.

We performed simulations with parameters encompassing a broad range of biologically-feasible values: density values ranged from 25–1000 individuals per km, the parameter of dispersal (σ) varied to give mean distances of 0.1–14km, and speciation rates varied from 10^{-9} – 10^{-1} . We explored 25 combinations of the density and dispersal parameters using Latin hypercube sampling (McKay *et al.*, 1979) to evenly sample from parameter space. Under coalescence methods, higher speciation rates can be applied post-simulation for generating communities (Rosindell *et al.* 2008). We performed simulations using a minimum speciation rate of 10^{-8} and applied all other speciation rates afterwards to generate additional communities.

3.2.3 Model parameterisation

In order to determine how well the simulations fit patterns in the fossil record, four biodiversity metrics were used for each interval: the alpha diversity for each site (the local species richness), the mean alpha diversity, the mean beta diversity (calculated as $\beta = \gamma/\alpha$) and the total species richness across all sites. The mean actual percentage error was calculated for each metric between the real and simulated fossil records. Averaging the mean actual percentage errors for the four metrics gives an indication of the goodness of fit for one simulation - we refer to this percentage as the accuracy of a single simulation.

As each interval was run as a separate neutral simulation, the parameters of speciation rate, density and dispersal could be allowed to vary over time. However, as combinations of parameters can be aggregated in any number of ways, we considered just two possibilities that reflected our assumptions of ecological changes over time: either there was no change in these parameters (i.e. we use a single parameter set for

all intervals), or the parameters could change at the time of the CRC (i.e. we use two parameter sets - one for pre-CRC [323–307 Ma] and one for post-CRC [307–372 Ma]). The first scenario represents a neutral ecosystem with no changes in fundamental ecological dynamics. The second presents a neutral scenario that assumes ecological changes were generated by the CRC and may be reflected in neutral dynamics.

Our initial model contains no habitat loss (i.e., pristine habitat covers everywhere) and individuals were restricted in their movement only by continental boundaries. Either a single set of parameters (speciation rate, dispersal and density) is used for all intervals, or this requirement is relaxed for investigating how the parameters themselves change over time.

3.2.4 *Habitat fragmentation*

We tested two scenarios of habitat loss and fragmentation: first, habitat was lost at the time of the CRC in a random pattern (our “random” habitat scenario) where the landscape is fragmented according to a random spatial pattern, so that land areas contained habitat on a percentage of their area (either 20%, 40% or 80% of habitat remaining); second, habitat was lost in a clustered pattern (our “clustered” habitat scenario), leaving just circular clusters of habitat of 100 km radius at each fossil site. The random habitat scenario maintains connectivity across the landscape but can still contain considerable habitat loss. The clustered habitat scenario leaves isolated islands of habitat that will promote endemism within each island over geological timescales, thus directly testing the theory of Sahney *et al.* (2010).

3.3 Results

3.3.1 *Baseline models*

Tetrapod diversity was simulated on a pristine (i.e. uniform, with no habitat fragmentation) global landscape restricted only by continental boundaries and mimicking the

exact spatial and temporal distribution of fossils within the fossil record. From the best-fitting models and without allowing parameters to vary over time, the simulations produced 89–92% mean accuracy with the empirical fossil record. Even from this baseline neutral model, the simulations successfully reproduce a considerable amount of the temporal variation in biodiversity patterns seen in the empirical data, yet certain elements of the entire biodiversity trends were less well-captured (Figure 3.1). In particular, both beta diversity and species richness for each interval were over-estimated by neutral simulations in the early Permian (Figure 3.1), with the effect being more noticeable for amniotes. This effect is highlighted if the models are parameterised using only data from the late Carboniferous (Figure B1) and then run across all times with those fixed parameters; under these conditions, the neutral simulations more closely match the fossil record from the Carboniferous, but diverge even further from fossil data in the early Permian. Taken together, these results indicate that while there is an increase in face-value global species richness and beta diversity into the early Permian, the neutral baseline expectation is for that increase to be much larger.

We explored two explanations for why these baseline neutral models failed to capture the entire face-value diversity trend seen in the fossil record: (1) that the changes in diversity were caused by ecological dynamics changing over time, or (2) that the pattern was caused by habitat loss and fragmentation. To test whether changes in diversity were caused by ecological dynamics, the parameters for the neutral model were split so that the late Carboniferous (pre-CRC) and early Permian (post-CRC) were parameterised separately. Whilst there is still a slight overestimation for global species richness and beta diversity, the simulated estimates appear to be better matched to face-value estimates (Figure 3.2). This suggests that there is a change in ecological dynamics across the interval, which could be represented in the neutral model through a decrease in density and/or dispersal.

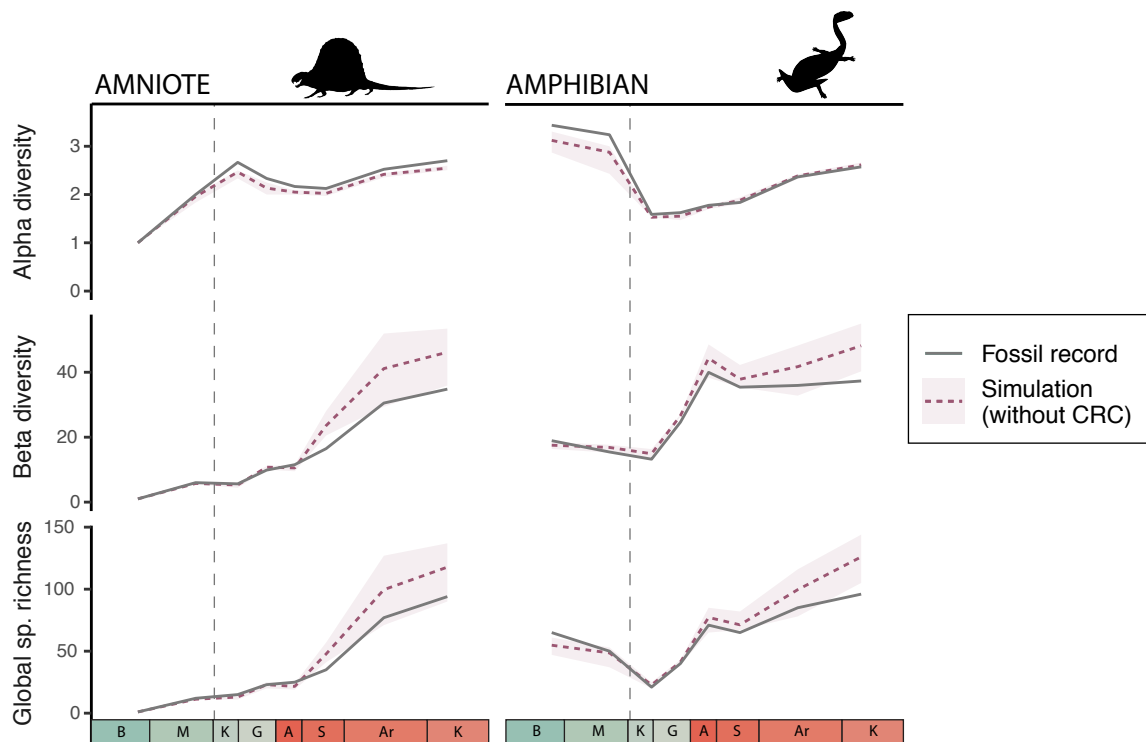


Figure 3.1: Simulated tetrapod biodiversity patterns over time compared against the fossil record. Here, the impact of the CRC is not accounted for. Three metrics of biodiversity are shown for both amphibians and amniotes from the Bashkirian to Kungurian from either simulated communities (purple dashed line) or from empirical data (solid green line). The shaded area represents the variation in the five best fitting simulations. The following abbreviations are used for intervals: "B" = Bashkirian, "M" = Moscowian, "K" = Kasimovian, "G" = Gzhelian, "A" = Asselian, "S" = Sakmarian, "Ar" = Artinskian and "K" = Kungurian.

3.3.2 Models incorporating habitat fragmentation and loss

The best-fitting habitat fragmentation and loss scenario had 20% of habitat remaining (i.e. 80% habitat loss) and produced mean percentage errors of 92–95% (as shown in Figure 3.3). The neutral models demonstrate that random habitat fragmentation, accompanied by habitat loss, reduces simulated diversity both locally and globally, in addition to aligning more closely with the face-value diversity patterns (Figure 3). This is in contrast with the hypothesis that habitat loss and fragmentation from the CRC promoted endemism and increased global diversity (Sahney *et al.* 2010).

Our clustered habitat scenario tested whether habitat loss resulting in highly

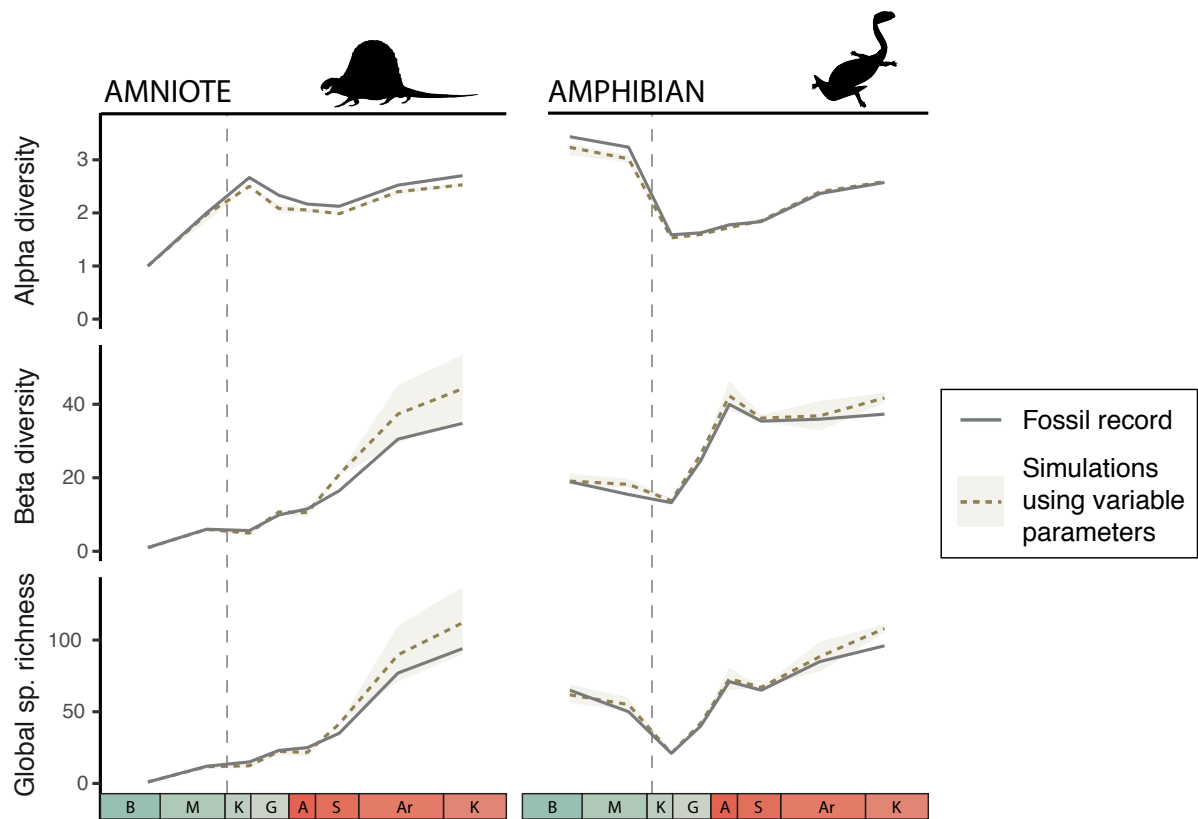


Figure 3.2: Simulated tetrapod biodiversity patterns over time compared against the fossil record. Here, the impact of the CRC is represented by differing sets of parameters between the late Carboniferous and early Permian. As in Figure 1, three metrics of biodiversity are shown across the interval and the shaded area represents the variation in the five best fitting simulations. The dashed line at 307 Ma indicates the timing of the CRC. Interval abbreviations are as in Figure 3.1

disconnected habitat islands, promoting endemism between islands, was supported by neutral theory. Under these circumstances, unless the fossil sites were close, dispersal between distinct fossil sites would have been almost entirely restricted, meaning that the number of shared species between sites is likely to be very low. The neutral simulations of the clustered habitat scenario generated diversity patterns that did not align well with the face-value diversity patterns (Figure 3.4). After the CRC, the simulations generally underestimated all metrics of diversity apart from during the Kungurian, where diversity was overestimated. The best-fitting simulations of the clustered habitat scenario occupy a relatively narrow band of possible values, which indicates that the simulation results are more constrained by the landscape structure – which is

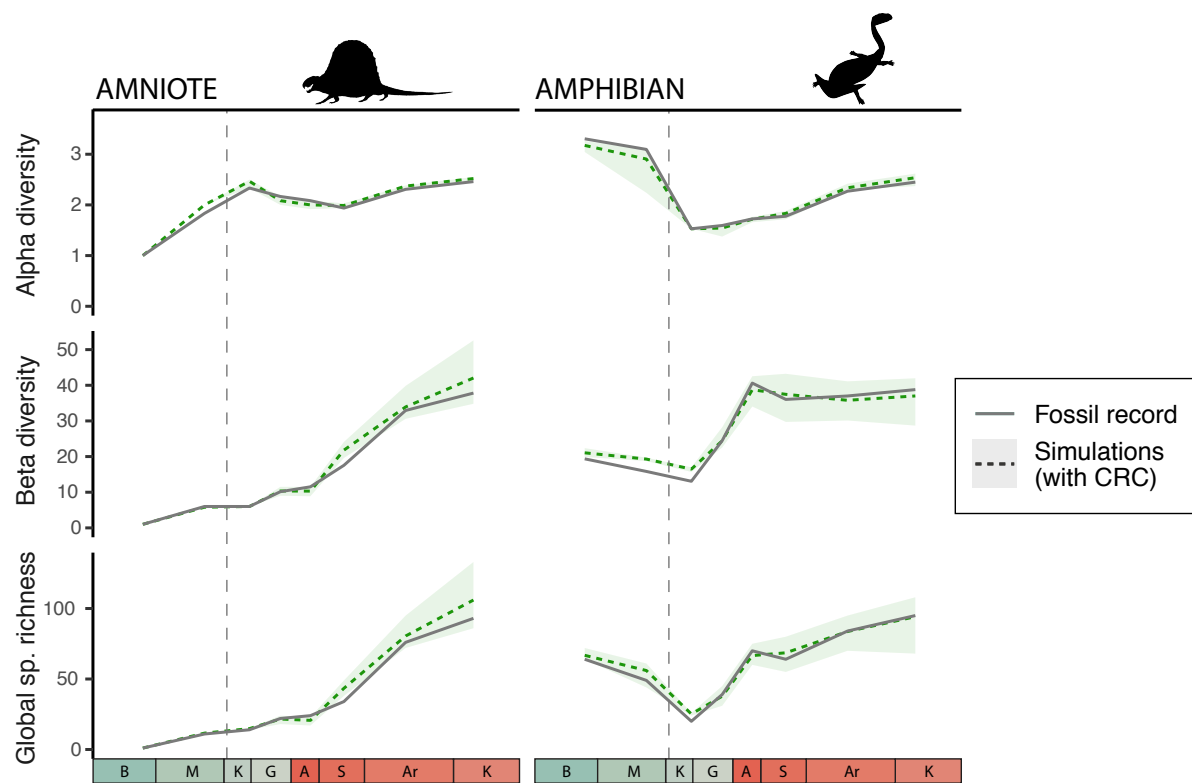


Figure 3.3: Random habitat loss: Simulated tetrapod biodiversity patterns over time compared against the fossil record. Here, the impact of the CRC is represented by habitat loss occurring in a random fashion at 307 Ma (dashed line). The scenario here represents 80% habitat loss, meaning 20% of habitat remains following the CRC. The dashed line at 307 Ma indicates the timing of the CRC. Interval abbreviations are as in Figure 3.1

consistent between simulations – than the parameter choice – which varies between simulations. The exception to this agreement in simulated biodiversity outcomes is the final interval, the Kungurian, during which the diversity estimates from the neutral models are relatively broad (Figure 3.4). The dynamic driving this divergence may be the increased number of localities found during the Kungurian when compared with other intervals (Figure B2), i.e. there were more ‘habitat island’ supporting tetrapods during the Kungurian.

3.3.3 Models exploring the effect of sampling biases

By simulating this same best-fitting habitat loss scenario (i.e. 80% random habitat loss) but sampling more individuals at each site (“upscaling”), it is possible to observe

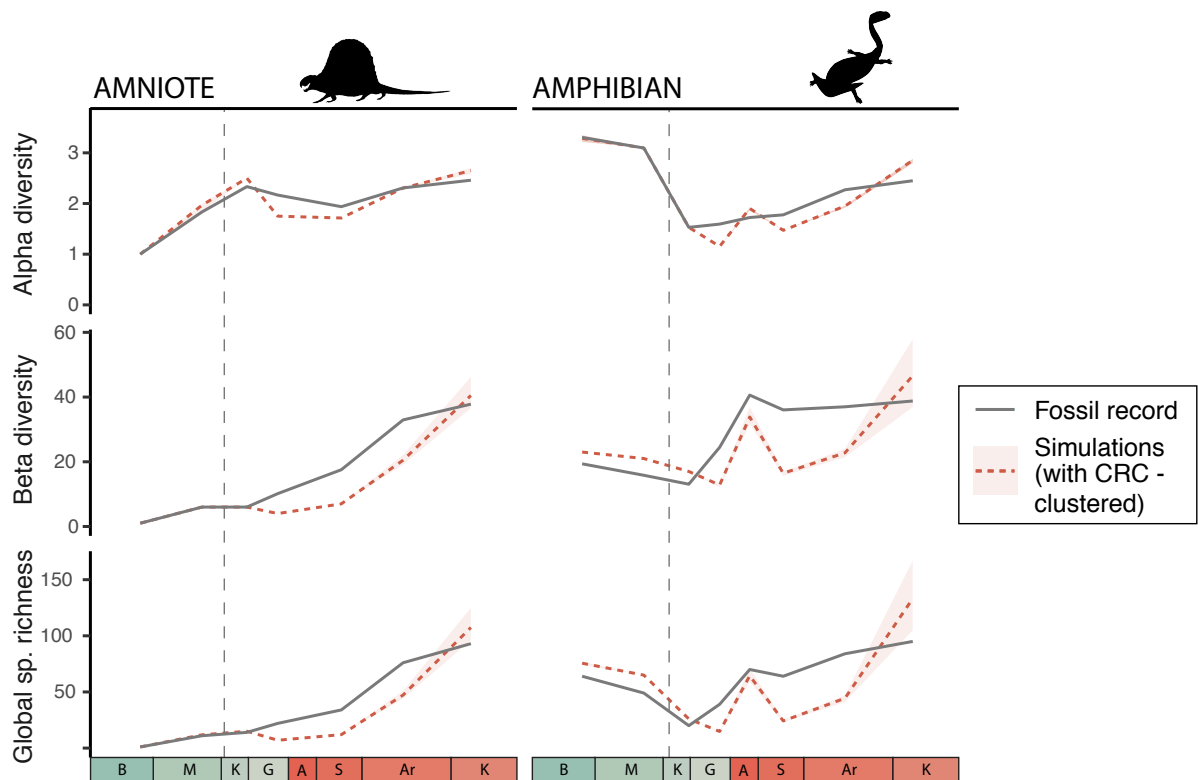


Figure 3.4: Clustered habitat scenario: Simulated tetrapod diversity over time from neutral models incorporating habitat loss from the CRC following the clustered habitat scenario. The remaining habitat following the CRC is associated into habitat islands 100 km diameter at the locations of each fossil site. The dashed line at 307 Ma indicates the timing of the CRC. Interval abbreviations are as in Figure 3.1

what the broader biodiversity changes might look like under the assumptions of the neutral model. When ten times more individuals are sampled from each fossil site (Figure 3.5), differences emerge when compared with simulations where the face-value diversity patterns are exactly matched (Figure 3.3). The general trend in simulated global species richness and alpha diversity over time for both amniotes and amphibians is roughly similar to the trends in the face-value patterns, but beta diversity no longer sees a large and rapid increase post-CRC, especially for amphibians (Figure 3.5). This might suggest that the temporal changes in beta diversity found in the fossil record may disappear as more fossils are sampled, in turn indicating that current face-value patterns are the product of sampling biases.

To remove variation in temporal sampling, but retain some element of variation

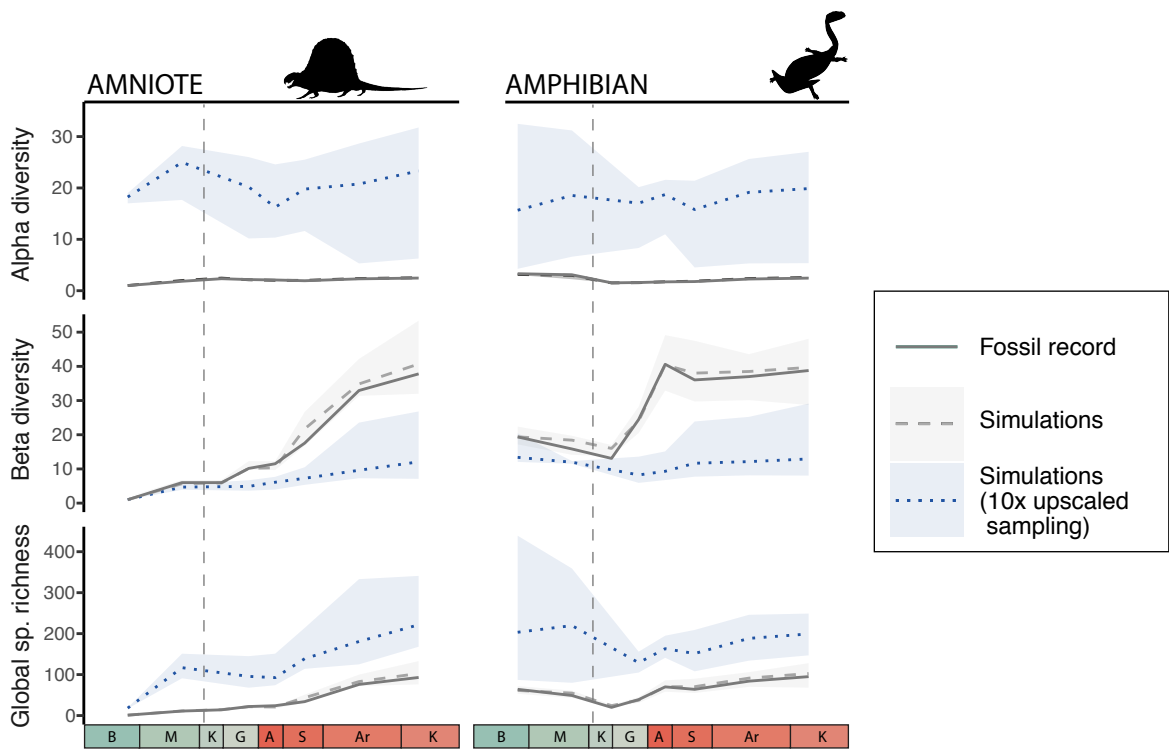


Figure 3.5: Upscaled biodiversity from the fossil record using neutral models. Grey dashed lines represent the mean values from simulations of the five best-fitting parameters from the scenario with 80% habitat loss (20% remaining) under random clearing (as per Figure 3.3). The blue dotted lines represent the same simulations, but sampling ten times more individuals than is present in the fossil record. The shaded areas represent the variation in the five best fitting simulations. The dashed line at 307 Ma indicates the timing of the CRC. Interval abbreviations are as in Figure 3.1

in spatial sampling, a scenario was simulated where the sampling effort was constant in each time interval. When 100 individuals are randomly selected from each time interval, the simulated patterns in diversity bear only slight resemblance to the face-value patterns; only the general trend for beta diversity is captured (Figure 3.6). As the same number of individuals are selected within each interval, this suggests that the face-value patterns in beta diversity may be an artefact of spatial sampling biases, specifically, variation in the number of locations sampled within each interval. Given the only minor changes in global species richness, this again implies that the face-value changes in species richness through time may be a result of temporal sampling biases.

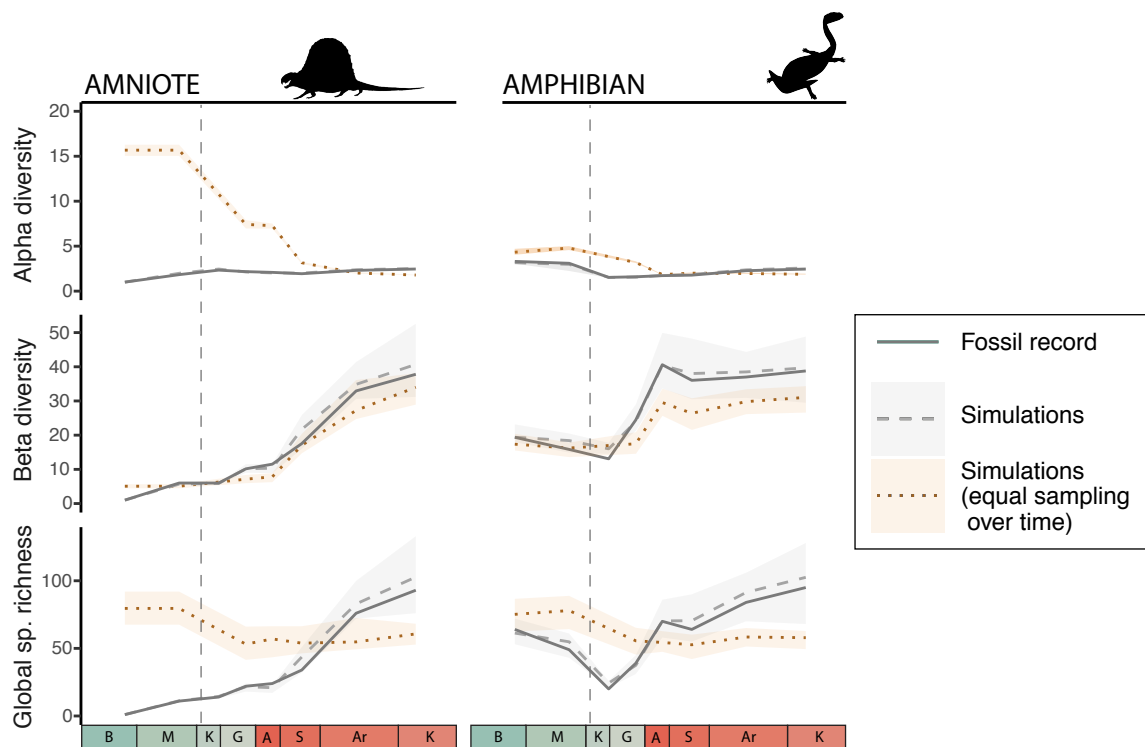


Figure 3.6: Simulated tetrapod diversity from neutral models where temporal sampling biases are removed. Grey dashed lines represent the mean values from simulations of the five best-fitting parameters from the scenario with 80% habitat loss (20% remaining) under random clearing (as per Figure 3.3). The grey short-dashed lines represent the same simulations, but randomly sampling 100 individuals for each interval and the species richness of the sample is calculated. These simulations are without any temporal bias in sampling frequency. The shaded areas represent the variation in the five best fitting simulations. The dashed line at 307 Ma indicates the timing of the CRC. Interval abbreviations are as in Figure 3.1

3.4 Discussion

Although statistical approaches to estimating patterns of past diversity can provide important insights not documented by face-value estimates (e.g. Butler *et al.*, 2011a; Lloyd, 2012; Mannion *et al.*, 2012; Dunne *et al.*, 2018), they are generally still limited by the scale of available data. In this study, spatially explicit neutral models have proven to be a useful tool for directly testing hypotheses of palaeodiversity and illuminating the effects of sampling biases.

Based on our neutral models, there is evidence that face-value (raw or ‘un-corrected’) patterns of species diversity are heavily influenced by sampling biases.

Neutral simulations of a uniform landscape (i.e. no habitat fragmentation) fail to capture the trends in face-value diversity (Figure 3.1), indicating that apparent increases in face-value diversity can be explained by a simple mechanistic model that accounts for spatial and temporal biases in sampling. However, there does appear to be a small but observable change in the characteristics of tetrapods around 307 Ma, the date inferred for the CRC in our analysis. This can either be explained by changes in dispersal, changes in tetrapod density, or fragmentation of the habitat (which is roughly equivalent in a theoretical sense to a reduction in tetrapod diversity). This outcome corroborates the previous assessment of diversity patterns across the CRC, which found evidence of increasing connectedness (i.e. dispersal) between tetrapod communities following the CRC (Dunne *et al.*, 2018; Chapter 2).

Our results suggest that endemism did not produce the diversity patterns detected in the fossil record. This is in contrast with previous hypotheses (Sahney *et al.* 2010), but consistent with the most recent studies, which did not find evidence of endemism (Dunne *et al.*, 2018; Brocklehurst *et al.*, 2018). Instead, our findings suggest that face-value diversity patterns reveal limited changes to global tetrapod richness, and may be primarily driven by changes in global tetrapod density, which is also in line with the expected ecological impact of the collapse of the rainforests and drying of the climate. The scenario that aligns best with the real data is provided by random habitat loss of roughly 80%, a scenario that is dynamically identical under neutral theory to an equivalent reduction in density (Thompson, 2019).

Neutral simulations suggest that the habitat-loss scenario that is most consistent with the face-value patterns is one where there are disconnected islands of habitat i.e. the clustered habitat scenario. When sampling the simulations in a realistic manner (based on the fossil record), this results in a decrease in global species richness and beta diversity (Figure 3.4). Under this scenario, global diversity losses are even greater than observed in the fossil record (after accounting for the changes in sampling effort over time). The development of endemism is not enough to offset the diversity

decrease from habitat loss, as proposed by Sahney *et al.* (2010). A more realistic potential driver of endemism would be disparate habitat types generated by fragmentation causing differentiation between tetrapod populations. The testing of this niche-based hypothesis falls outside the scope of this current study (in part because it cannot yet be tested by standard neutral models), but provides a stimulating line of future work for resolving ecological mechanisms driving early tetrapod diversification.

To better inform neutral models, it would be useful to ascertain more realistic patterns of Carboniferous rainforest habitat loss, based on either palaeoclimate reconstructions or occurrence data for fossil plants. Integrating more accurate maps of tropical rainforest coverage over time with the mechanistic basis of neutral theory would be much more informative for exploring theories of diversity generation following the CRC. This is not currently possible due to the absence of readily available palaeoclimate reconstructions for this time interval (in particular, the Carboniferous) and the lack of a comprehensive, spatially explicit, occurrence-based database for fossil plants, similar in structure and content to the Paleobiology Database. It is also not immediately clear how one would relate forest patterns to the dynamics of tetrapod diversity, as tetrapods (both modern and ancient) exhibit broad ranges in their dependency on forest cover. An example of an 'immediate pattern' of rainforest loss and habitat fragmentation that may have been possible to incorporate into our neutral models had empirical data been available is the hypothesis that the disappearance of the Carboniferous rainforest began in western Pangaea before moving eastwards across the continents (Cleal and Thomas, 1999, 2005).

The neutral models explored here assume that densities were consistent over time, except in the case of habitat loss. The density of early tetrapod species would have affected the number of specimens preserved, for example more abundant species would be better represented in the fossil record. Lower numbers of fossil specimens sampled per site could be indicative of smaller populations and lower species richness, but this is more likely to be a consequence of taphonomic effects and sampling

effort. Across our dataset of late Carboniferous and early Permian tetrapods, the number of specimens sampled per site varies substantially (see Figure B2 and discussion in Chapter 2). In the late Carboniferous, there are sites such as the coal deposits of Nyraňy in the Czech Republic and Linton Diamond Mine in Ohio, USA, that have yielded a high number of specimens, many of which are exceptionally well preserved. In the early Permian, due to the combination of orogenic activity and drier climatic conditions, the fossils of this age are much less likely to be preserved in coal deposits. Instead, many richly diverse localities in the early Permian are located in sandstone quarries that have been extensively excavated over many decades (e.g. various localities in the 'Red Beds' of Texas and Oklahoma, USA). Due to these temporal changes in preservation it is basically impossible to infer the true abundances and population densities of early tetrapods during this interval (and indeed any interval in the geological past). This limitation motivated keeping density as a free parameter but precludes understanding of how both tetrapod densities and preservation rates varied. The resolution to this problem requires a more intimate understanding of both the true densities of tetrapods over time and changes to the preservation rates over time (one of the measures that is possible to estimate for species within assemblages). But this, again, lies outside the scope of this study.

Our approach using mechanistic models based on neutral theory to test hypotheses of diversity in the fossil record represents a novel direction for integrating modern ecological theory with palaeontological data. Such inter-disciplinary studies have been identified as crucial for informing predictions for future diversity (Barnosky *et al.*, 2017) as well as more accurately understanding past biodiversity patterns (Willis and Birks, 2006; Bonuso, 2007; Mayhew, Jenkins and Benton, 2008). Our results demonstrate how even simple models of biodiversity based on modern ecological theory can provide a deeper understanding of palaeoecological theories and offer insights not previously possible through traditional macroevolutionary methods.

4 | LATITUDINAL PATTERNS OF LATE TRIASSIC TETRAPOD DIVERSITY AND CLIMATE

My contribution to this work involved conducting all parts of the research, including collecting and collating the data, co-designing the methodology, analysing the data, and interpreting the results, as well as writing the text. A. Farnsworth provided the palaeoclimate reconstructions, and S. Greene and R. Butler both provided feedback on the methodology and research design and interpretations of the results. The editorial 'we' is used here, as in previous chapters, to represent our collective viewpoint, but fully reflects the above share in contributions.

4.1 Introduction

The latitudinal biodiversity gradient (LBG), characterised by an increase in species richness towards the equator, is one of the most widely recognised global patterns in macroecology (Willig *et al.*, 2003; Hillebrand, 2004). Though the LBG has been extensively documented in modern terrestrial vertebrate faunas, its evolution and drivers through deep time remain uncertain. The fossil record offers an exceptional deep-time perspective on the LBG, and previous work suggests that a modern-type gradient has not been persistent in terrestrial tetrapods throughout the Phanerozoic, instead varying widely across time and taxonomic groups (e.g. Rose *et al.*, 2011; Mannion *et al.*, 2012, 2014; Marcot *et al.*, 2016; Brocklehurst *et al.*, 2017).

Whilst numerous hypotheses relating to the age and areal extent of modern-day tropical regions have been proposed to explain the LBG (Chown and Gaston, 2000; Mittelbach *et al.*, 2007), climate is often regarded as the primary driver of latitudinal variation in diversity through time (Powell, 2007; Erwin, 2009; Archibald *et al.*, 2010; Rose *et al.*, 2011; Marcot *et al.*, 2016; Kröger, 2017). However, few studies have been able to directly test the relationship between climate and patterns of diversity through time. Instead, temporal trends in latitudinal diversity are indirectly compared with trends in palaeoclimate, or palaeolatitude is used as a proxy for climate conditions (e.g. Powell, 2007; Marcot *et al.*, 2016). Even in studies of the modern-day LBG, latitude is often used as a proxy for numerous interacting environmental variables, such as temperature and seasonality (Willig *et al.*, 2003; Hillebrand, 2004).

Further difficulty arises when examining the LBG through time, as variation in spatial and temporal sampling strongly influence the fossil data; the presence or absence of a latitudinal gradient in certain time intervals or in selected fossil groups cannot be confidently attributed to any abiotic or biotic factor without considering biases in sampling. Debate continues over whether it is possible to decipher genuine latitudinal gradients in diversity from the fossil record, or whether the apparent patterns in latitudinal species richness are artefacts of geographical shifts in sampling efforts through time (Close *et al.*, 2017; Fraser, 2017).

The Late Triassic (235–201 million years ago) is likely the best pre-Cenozoic interval for exploring latitudinal gradients in terrestrial diversity. During the Late Triassic, both the climate and continental configuration were very different to the present day, with generally much warmer temperatures, an absence of ice at the poles, and the configuration of the continents into the supercontinent Pangaea. When compared with neighbouring intervals, the Late Triassic has been extensively spatially sampled (Figure C.1). This is particularly true for sites at low-palaeolatitudes, for example in the southwestern USA (e.g. Long and Murry, 1995), but also at mid-palaeolatitudes (e.g. Germany), as well as at high-palaeolatitudes, such as in Argentina's Ischigualasto For-

mation (e.g. Martínez *et al.*, 2012), and the Elliot Formation in South Africa (e.g. Knoll, 2005).

The Late Triassic was also a key interval in the evolutionary history of tetrapods, as by this time the early radiations of several major modern lineages such as mammaliamorphs (Ruta *et al.*, 2013), crocodylomorphs (Butler *et al.*, 2011b), and dinosaurs (Benton, 1983; Brusatte *et al.*, 2008) were underway. Previous studies have recognised palaeolatitudinal variation in Late Triassic tetrapod faunas (Tucker and Benton, 1982; Shubin and Sues, 1991; Irmis *et al.*, 2007; Ezcurra, 2016). However, the link between this palaeolatitudinal structuring and climate has not been extensively explored across all tetrapods, largely due to the absence of a comprehensive dataset of global tetrapod occurrences and palaeoclimate reconstructions with sufficient temporal and spatial coverage to examine and compare patterns across large time intervals.

Here, we explore the latitudinal variation in Late Triassic tetrapod diversity, using fossil occurrence data from the Paleobiology Database and sampling standardisation to mitigate the effects of heterogeneous spatial sampling. Then, combining this occurrence data with palaeoclimate reconstructions from the spatially-explicit general circulation climate model, HadCM3L (Valdes *et al.*, 2017), we assess the potential drivers of the Late Triassic tetrapod latitudinal diversity gradient by directly testing, for the first time, the relationships between species richness, sampling, and palaeoclimate.

4.2 Methods

4.2.1 Fossil occurrence data

Global occurrences of tetrapod species from all stages of the Late Triassic (Carnian–Rhaetian; 237–201.3 Ma) were downloaded from the Paleobiology Database (paleobiodb.org, accessed February 3rd, 2019). Before download, the data were checked against the current published literature for completeness and any missing occurrences were added. All data preparation and analyses were conducted within R 3.5.2 (R Core

Team, 2018). The dataset was filtered following download to remove trace fossils, marine and flying taxa, as well as occurrences that could not confidently be attributed to a valid taxon, as outlined in Chapter 2 (Section 2.2.1). The final cleaned dataset comprises 1,401 tetrapod occurrences, representing 413 species, from 676 collections (=fossil localities).

4.2.2 *Latitudinal sampling and species diversity*

For the following analyses of sampling and diversity patterns, the data were placed in palaeolatitudinal bins, which were set at 10-degree intervals (with the exception of the most poleward bin in each hemisphere, which was set at $\pm 50\text{--}90^\circ$). We first present face-value (=raw, uncorrected or observed) diversity patterns at global and local spatial scales; however, we do so with the proviso that face-value diversity counts may be highly misleading, and instead focus our interpretation on diversity patterns produced using coverage-based sampling standardisation. Global (gamma scale) face-value diversity curves were computed using sampled-in-bin counts of specifically determinate occurrences. Collection (=fossil locality) and formation counts, as well as occupied equal-area grid cells, were used as proxies for sampling effort. To look at temporal changes in diversity, the data were further sub-divided into datasets for the 'early Late Triassic' (approximately Carnian–early Norian) and 'late Late Triassic' (approximately late Norian–Rhaetian) based on the stratigraphic ages of individual formations, as outlined in Button *et al.* (2017).

We estimated local richness (alpha diversity) by counting the total number of species per collection for 1) all tetrapods; 2) Archosauromorpha, 3) Pseudosuchia (*sensu* Ezcurra, 2016), 4) Avemetatarsalia (*sensu* Nesbitt *et al.*, 2017), and 5) Synapsida (Figure 4.1). These counts included not only occurrences determinate at species level but also those indeterminate at species level that must logically represent distinct species according to the taxonomic hierarchy of the Paleobiology Database (Close *et al.* 2019). Prior to the interpretation of these results, we tested for, and found no, in-

fluence of well-sampled sites on estimates of local richness by removing collections with greater than ten distinct occurrences (see Table C1). Additionally, we tested and found no effect of literature biases by removing occurrences originating in the large monograph publication by Long and Murry (1995).

Following the procedure outlined in Dunne *et al.* (2018) (Chapter 2), we used coverage-based sampling standardisation to estimate global latitudinal diversity patterns, via the R package iNEXT (Hsieh *et al.*, 2016). We computed coverage-standardised richness at both species and genus level for each of the five aforementioned groups using varying sizes of latitudinal bin (10° and 15°) to assess any variations in resulting patterns that may be a consequence of taxonomic level and bin size.

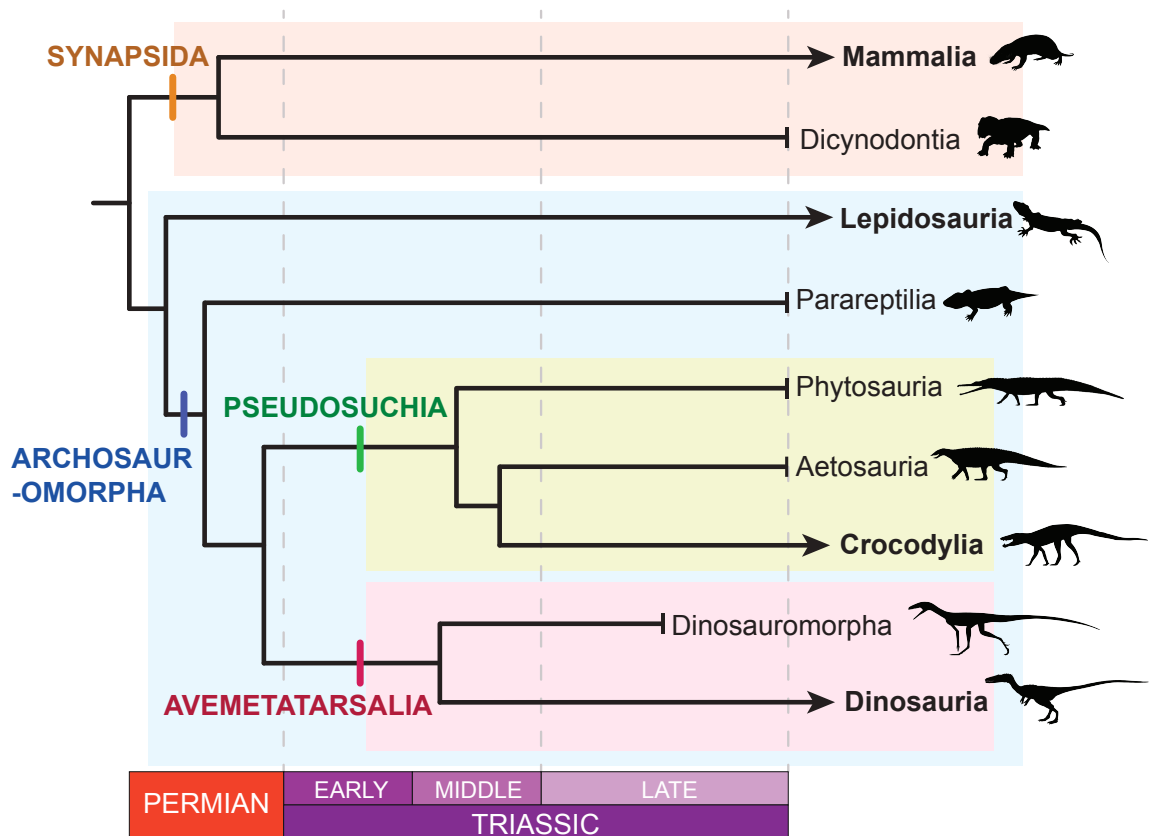


Figure 4.1: Simplified cladogram showing the phylogenetic relationships between the four tetrapod subgroups studied in this chapter. Representative clades of each subgroup are shown, with the lineages that lead to modern tetrapod groups denoted with an arrow and bold text, i.e. modern mammals (Mammalia), modern reptiles (Lepidosauria), crocodiles (Crocodylia), and dinosaurs (Dinosauria). Silhouettes from phylopic.org, with thanks to Nobu Tamura and Scott Hartman.

4.2.3 *Palaeoclimate reconstructions*

One of the major factors limiting examination of specific hypotheses linking palaeodiversity and palaeoclimate is the lack of readily comparable climatic reconstructions across geological time. For our investigations of the relationship between palaeolatitudinal diversity and palaeoclimate, we used a set of readily comparable model runs comparable across geologic time that have become available for the first time. The fully coupled Atmospheric–Ocean General Circulation Model HadCM3L (version 4.5) *sensu* Lunt *et al.* (2015) features a standardised experimental methodology including an internally consistent set of palaeogeographic reconstructions, making model simulations readily comparable across geologic time. The palaeo-digital elevation models (topography, bathymetry, ice sheets) used as HadCM3L boundary conditions are derived from palaeogeographic reconstructions created by Getech Plc using an extensive geologic database of tectonics, structures, and depositional environments (Lunt *et al.*, 2015). HadCM3L has demonstrated good skill in predicting global and regional scale climate patterns not only in the present (Valdes *et al.*, 2017), but crucially in the past as well (Farnsworth *et al.* 2019). In addition, the model has been successfully used in several high profile deep time niche modelling studies (Fenton *et al.*, 2016; Saupe *et al.*, 2019) and demonstrated good ability in predicting species distributions (Chiarenza *et al.*, 2019).

It is important to note here that the palaeoclimate model simulations are single realisations of potential late Triassic and early Jurassic palaeoclimate states, and have not yet been thoroughly “ground-truthed” against independent palaeoclimate proxy evidence for these intervals. Although they are likely robust in providing the broad patterns of spatial variability in climate (arid/wet; continental/maritime; latitudinal gradients), the “absolute” values of any simulated climate parameter are subject to considerable uncertainty. In this sense, comparisons of climate variables between spatial distributed sites (“wetter than...”, “hotter than...”, “drier than...”) will be more robust than an assertion of what the late Triassic and early Jurassic climate was actually like.

One simulation was run per each geological stage (Carnian, Norian, and Rhaetian), using stage-specific palaeogeography (consisting of Getech palaeogeographic Digital Elevation Models [DEMs]), a stage-appropriate reduced solar constant (Gough, 1981) and an atmospheric CO₂ concentration of 1120 ppmv (or 4x pre-industrial CO₂, representing a generic 'greenhouse world'), which is within the range of uncertainty provided by the latest proxy pCO₂ reconstructions of Foster *et al.* (2017). These simulations were run for $\sim \geq 9000$ model years to ensure the climate system had reached full equilibrium in the atmosphere and ocean.

To obtain palaeoclimatic reconstructions for the collections (=fossil localities) in the occurrence dataset detailed above, each collection's modern-day coordinates were rotated back to the stage-appropriate palaeocoordinates in the Getech palaeogeography. From the model output, we extracted four of the most commonly used palaeoclimatic variables in studies of the links between palaeodiversity and palaeoclimate: mean annual surface temperature (MAT), mean annual precipitation (MAP), and seasonal variations of both measures derived from the difference between the mean warmest month and the mean coldest month and the mean wettest month and the mean driest month, respectively. These extracted variables are the average value of the rotated model grid cell plus all adjacent 'land' grid cells, as opposed to single values for individual model grid cells (subject to some degree of numerical 'noise'). Furthermore, the model runs use a modern orbital configuration, which approximates a mean palaeo-orbital configuration. If a collection occurred in more than a single time interval (due to stratigraphic uncertainty), the mean value for each climatic variable was computed and collections spanning more than two intervals were discarded from the dataset.

We visually and statistically examined the correlation between palaeolatitude and each individual palaeoclimate variable to assess if palaeolatitude is a fair proxy for climatic conditions. Finally, we constructed boxplots to illustrate and explore the range of palaeoclimatic conditions occupied by each tetrapod group.

4.2.4 *Testing potential drivers of diversity*

Generalised least-squares (GLS) is a multiple regression technique that does not assume independence of data series (or points within a data series), which has previously been utilised in palaeontological studies to examine relationships between multiple time series variables simultaneously (e.g. Hunt *et al.*, 2005; Benson and Butler, 2011; Mannion *et al.*, 2012; Cleary *et al.*, 2018; De Celis *et al.*, 2019). Following the approach of Benson and Butler (2011) and Benson *et al.* (2015), we used GLS to examine the relationship between face-value global species richness, sampling (tetrapod-bearing collections), and palaeoclimate (mean annual temperature and precipitation). The best models (i.e. combinations of explanatory variables) were identified using the AIC for small sample sizes (AICc; Hurvich and Tsai, 1989) which selects the model(s) that explain the highest proportion of variation in global species richness with the fewest explanatory variables. All GLS and associated tests were performed in R 3.2.5 (R Core Team, 2017) with the package nlme (Pinheiro *et al.*, 2019).

We first examined the relationship between latitudinal species richness, sampling, and palaeoclimate across all palaeolatitudes, by assembling total species counts, counts of tetrapod-bearing collections, and mean annual temperature (MAT) and precipitation (MAP) measures into 10° palaeolatitudinal bins. The mean MAT and MAP were calculated for each palaeolatitudinal bin using the values assigned from the palaeoclimate reconstructions to the collections (localities) within each of those bins. Autoregressive models of order zero, one or two were fit to combinations of explanatory variables used to predict latitudinal species richness, and the best order determined by likelihood ratio tests, implemented using the *gls* function of nlme. Species richness, sampling proxies and climatic variables were log-transformed prior to analysis to ensure normality and homoskedasticity of residuals. Likelihood-ratio based pseudo-R₂ values were calculated separately using the *r.squaredLR* function of the R package MuMIn (Barton, 2019).

To examine the global geographic relationship between species richness and

possible drivers, we incorporated palaeolongitude into our GLS analyses by dividing the global dataset into equal-area grid cells (using the R package *dggridR*; Barnes, 2018) and applied GLS using a correction for spatial autocorrelation. The spacing of the grid cells was set to 1,000 km, resulting in a total of 40 occupied grid cells. As for the latitudinal GLS, we calculated the total number of species and tetrapod-bearing collections (TBCs) per grid cell, along with the mean value for MAT and MAP. To inform the spatial autocorrelation structure in the GLS models, the midpoint between all localities present in each grid cell was ascertained. Spatial autocorrelation of the data was verified using Moran's I and the rational quadratic autoregressive model (determined by AIC values against other autocorrelation structures prior to this GLS) was implemented to account for this autocorrelation. Again, species richness, sampling proxies and climatic variables were log-transformed prior to analysis to ensure normality and homoskedasticity of residuals, and likelihood-ratio based pseudo- R_2 values were calculated separately using the *r.squaredLR* function of the R package *MuMIn*.

4.3 Results

4.3.1 *Diversity and sampling*

Sampling of Late Triassic tetrapods varies across palaeolatitudes (Figure 4.2a), with sampling greatest in the northern palaeo-hemisphere at low- and mid-palaeolatitudes (0–40°). There is a complete absence of sampling between 0–30° in the southern palaeo-hemisphere, an area of land that is today covered in part by the Sahara Desert in Africa and Amazon rainforest in South America (Figure 4.2b). However, in the southern palaeo-hemisphere there is a level of sampling at mid-palaeolatitudes (30–40°) that is analogous to the corresponding palaeolatitudes in the northern palaeo-hemisphere. Visual inspection finds that face-value species richness closely tracks proxies for sampling effort (counts of collections, formations, and occupied equal-area grid cells) across most palaeolatitudinal bins, except in the 10–20° North bin where collection count far

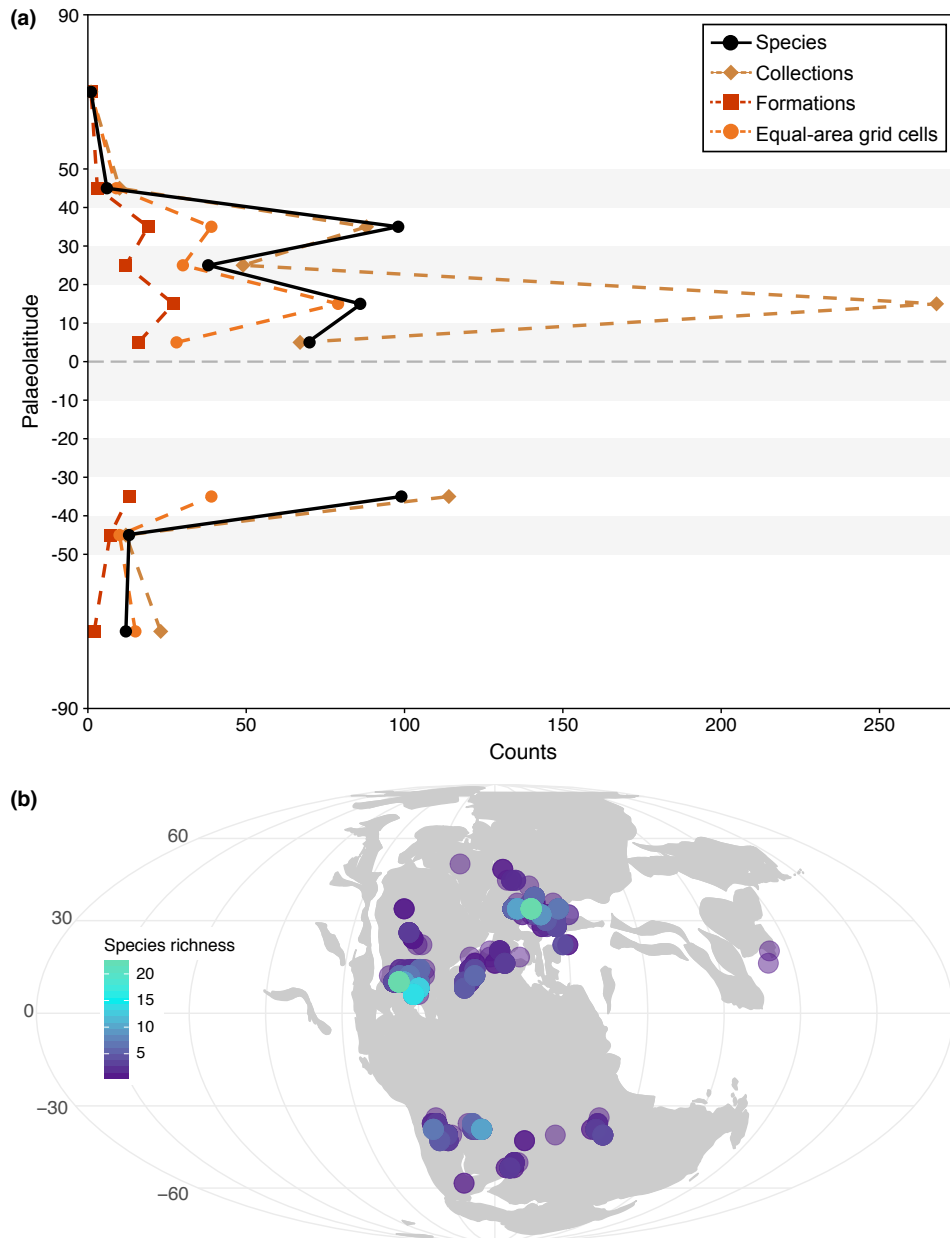


Figure 4.2: Patterns of species richness and sampling: (a) Latitudinal species richness and sampling in the Late Triassic. Species richness is highest between 30–40° palaeolatitude, both north and south of the palaeoequator. (b) Palaeogeographical map of fossil localities during the Late Triassic, where colour corresponds to total number of species at each site.

exceeds total species, indicating extensive sampling within this region. Temporal variation in sampling is also evident between the early Late Triassic and late Late Triassic (Figure C.2a–b) but continues to be high during both sub-intervals in the 10–20° North bin. Values of Good’s u (an indication of ‘coverage’, or how well-sampled a bin is) are

more or less consistent across all sampled palaeolatitudinal bins, both when the Late Triassic is treated as a single interval and when it is divided, and generally remains within the range of 0.5–0.8 (Figure C.2c–e).

Local richness, or alpha diversity, potentially provides important insights into latitudinal patterns of diversity, as alpha diversity estimates may be less strongly affected by biases in sampling that can confound global diversity compilations (Close *et al.*, 2019). Across the entire Late Triassic, tetrapod local richness is highest at low palaeolatitudes, mostly in the northern palaeo-hemisphere (Figure 4.3a). Most of the localities with the highest species richness lie in the northern palaeo-hemisphere (between 5–35°) and correspond to well-sampled localities in Texas and the Southwest USA (Figure 4.3a, Table C1). The richest southern palaeo-hemisphere locality lies in Brazil but contains less than half the richness of the richest localities in the northern palaeo-hemisphere (Figure 4.3a, Table C1). For both Archosauromorpha and Pseudosuchia, local richness is highest at low palaeolatitudes, between 0–15° in the northern palaeo-hemisphere (Figure 4.3b–c). There is no clear latitudinal signal in the local richness of Avemetatarsalia (Figure 4.3d), with richness being equally high at both mid (30–40° North and South) and low (0–15° North) palaeolatitudes. Synapsid local richness is highest at mid-palaeolatitudes (30–40°) in both palaeo-hemispheres (Figure 4.3e). One locality, Saint Nicholas de Port, France, contains notably higher richness than any other locality (Figure 4.3e, Table C1). Many of the specimens recovered from this site are mammal teeth (Debuyschere *et al.*, 2015), and this difference in specimen sampling compared with other tetrapod groups may be the reason for its conspicuously high richness. Tetrapod local richness is highest during the Norian for all taxonomic groups, except for Synapsida where it was highest during the Rhaetian (Figure C.3). However, during the Rhaetian, there are no sampled localities in the southern palaeo-hemisphere.

Coverage-standardised richness estimates of diversity across palaeolatitudes for the entire Late Triassic suggest that diversity was highest at mid-palaeolatitudes

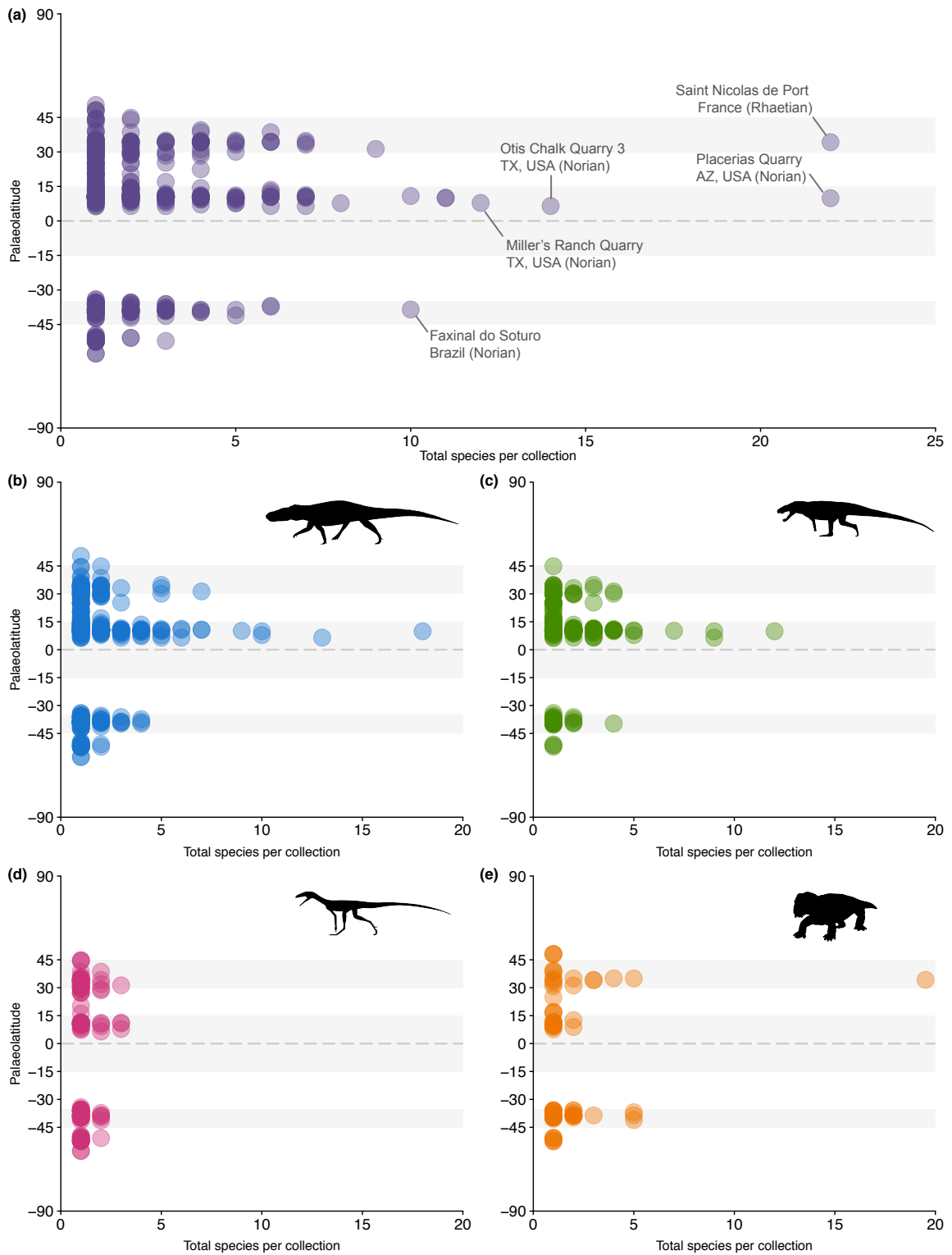


Figure 4.3: Local richness (alpha diversity) during the Late Triassic for (a) all tetrapods, (b) Archosauromorpha, (c) Pseudosuchia, (d) Avemetatarsalia, and (e) Synapsida. Local richness across palaeolatitudes through time can be seen in Figure C.3. Silhouettes: phylopic.org.

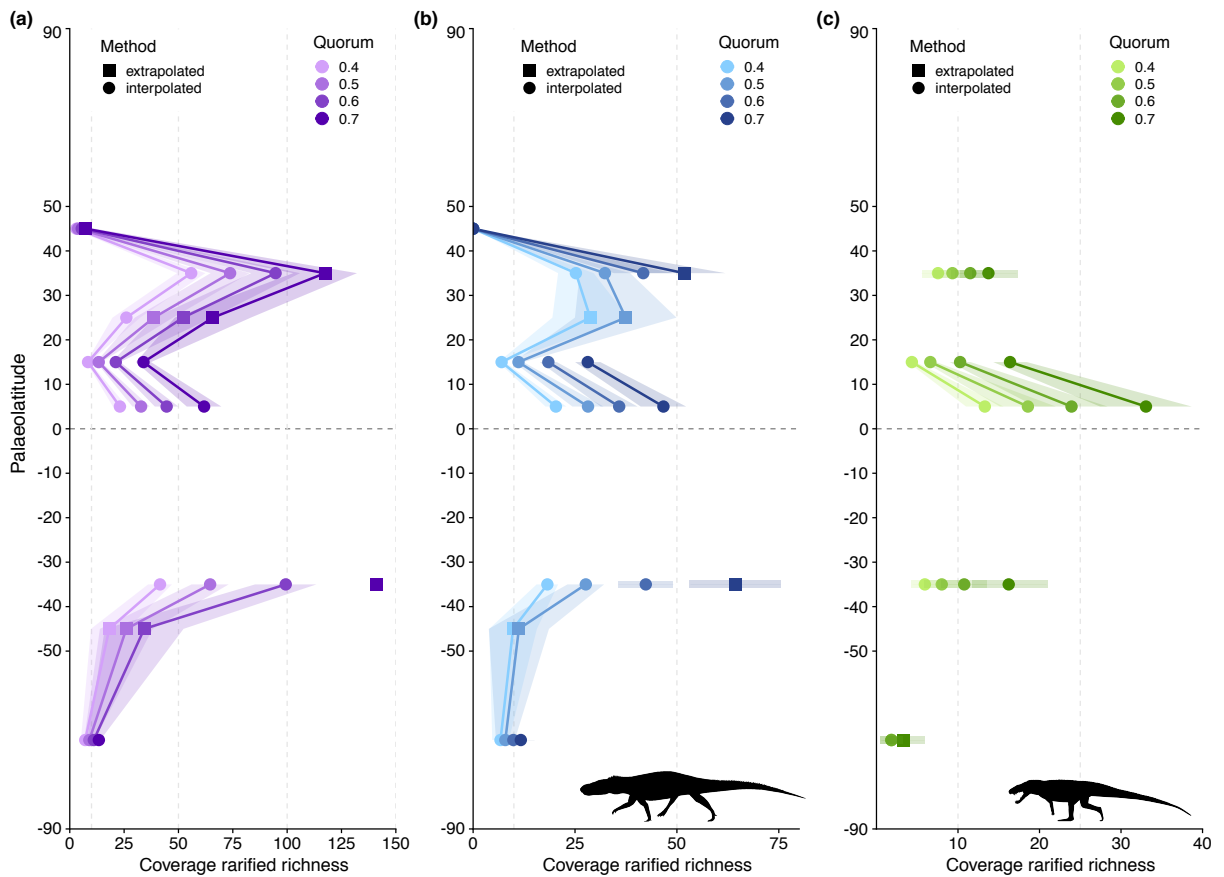


Figure 4.4: Coverage-rarified species richness for (a) Tetrapoda, (b) Archosauromorpha and (c) Pseudosuchia across all latitudes (using 10° latitudinal bins), showing estimates at different levels of quorum (0.4–0.7). Silhouettes: phylopic.org.

for all tetrapods (Figure 4.3a). This pattern is also evident for archosauromorphs (Figure 4.4b), but pseudosuchian richness was highest at lower latitudes (Figure 4.4c). Coverage was too low for both avemetarsalians and synspsids to obtain estimates of coverage-standardised richness. However, from estimates of archosauromorph and pseudosuchian coverage-standardised richness, it is possible to visually infer that the pattern of high richness at mid-palaeolatitudes is mostly driven by non-pseudosuchian taxa i.e. avemetatarsalians.

4.3.2 Potential drivers of diversity

Examining the correlation between the values extracted from the palaeoclimate model for each locality (collection) and the palaeolatitude of each locality, we find that palaeo-

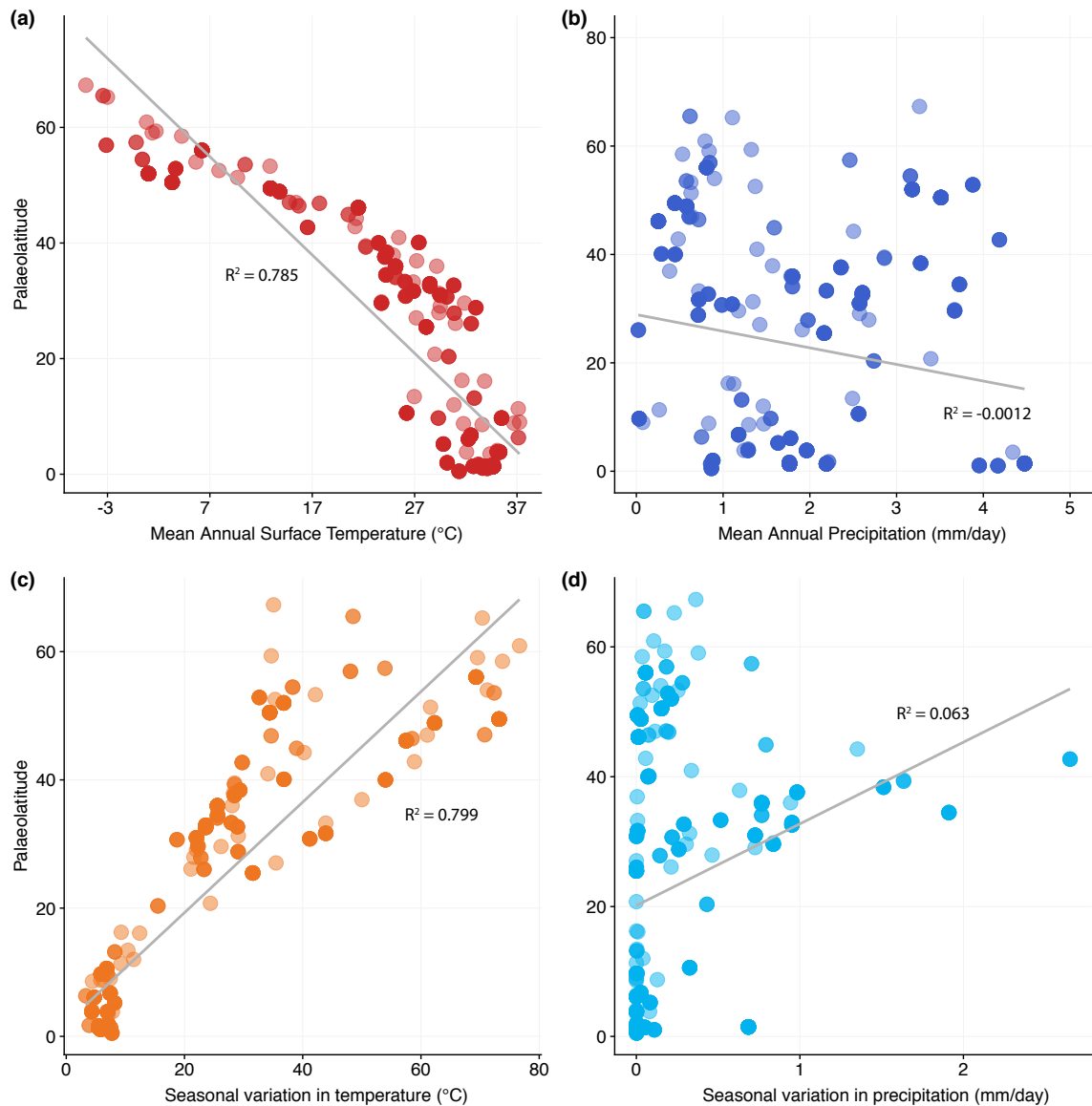


Figure 4.5: Palaeolatitude plotted against palaeoclimate variables from the palaeoclimate model HadCM3L: (a) mean annual surface temperature, (b) mean annual precipitation, (c) seasonal variation in temperature, (d) seasonal variation in precipitation.

latitude strongly correlates with mean annual temperature ($R_2 = 0.785$, $p = <0.001$) and seasonal variation in temperature ($R_2 = 0.799$, $p = <0.001$) (Figure 4.5, Table C2). MAT generally increases towards lower (equatorial) palaeolatitudes, and greater seasonal variation in MAT is seen at higher palaeolatitudes (Figure 4.6). But palaeolatitude explains very little of the variation in mean annual precipitation ($R_2 = 0.028$, $p = <0.001$) or seasonal variation in precipitation ($R_2 = 0.064$, $p = <0.001$) (Figure 4.5, Table C2).

The mean palaeoclimate values for all tetrapods across the Late Triassic indi-

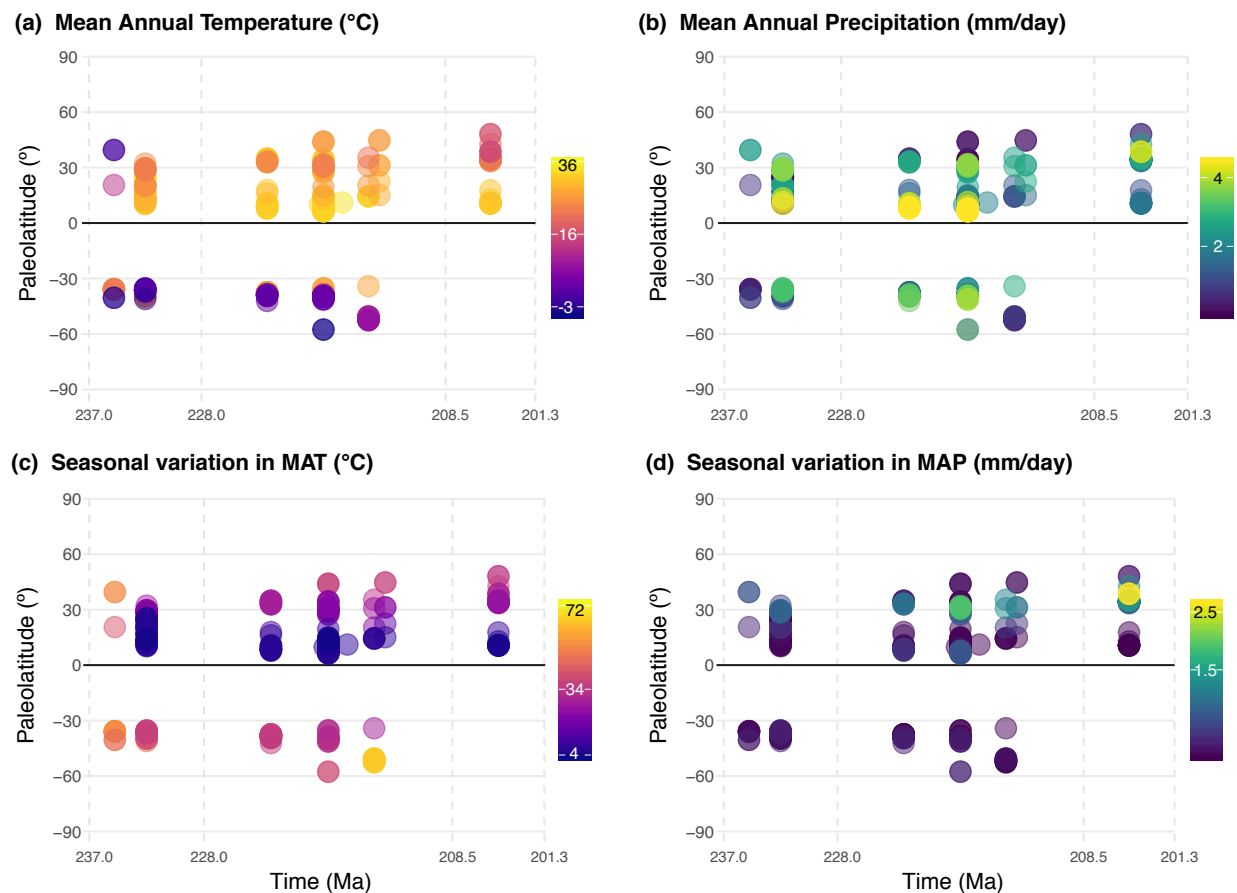


Figure 4.6: Climatic variables from the palaeoclimate model HadCM3L at each locality in the Late Triassic occurrence dataset: (a) mean annual temperature, (b) mean annual precipitation, (c) seasonal variation in temperature, and (d) seasonal variation in precipitation.

cate that the majority occupy areas that are warm (mean = 27°C) and have low seasonal variation in both temperature and precipitation (Figure 4.7). Archosauromorpha, as the largest tetrapod clade that contains both the Pseudosuchia and Avemetatarsalia, predictably occupies almost identical climatic ranges to all tetrapods (Figure 4.7a–d). The majority of pseudosuchians occupy hotter areas (a mean MAT of 31°C, compared with a tetrapod mean of 27°C), with the least seasonal variation in both temperature and precipitation with respect to other groups. However, the mean annual precipitation of areas occupied by pseudosuchians falls within the general range of other non-pseudosuchian archosauromorphs (Figure 4.7b). Avemetatarsalians and synapsids occupy areas with lower mean annual temperatures than other tetrapods (Figure

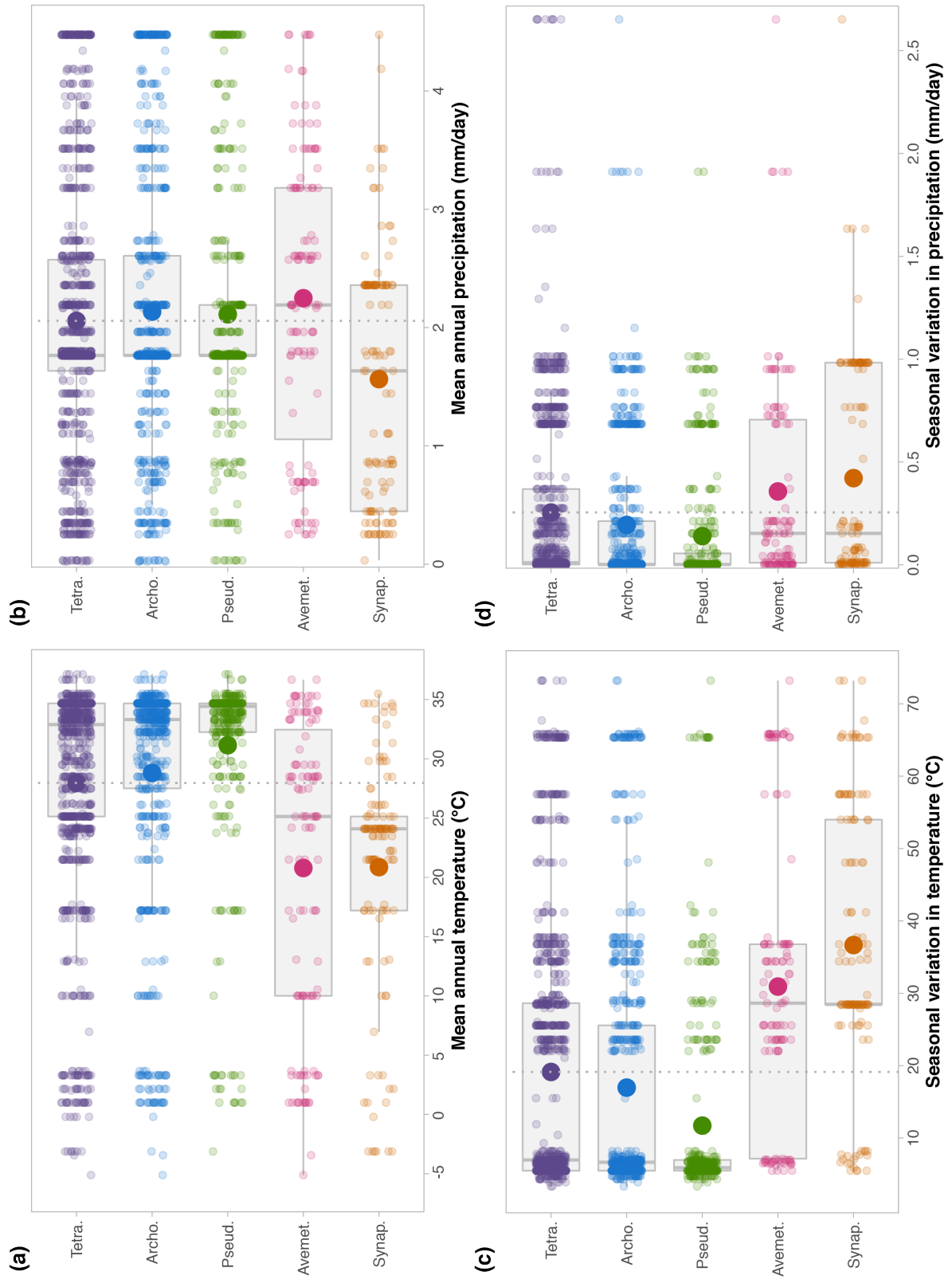


Figure 4.7: Tetrapod palaeoclimatic ranges (*cont. on next page*)

Figure 4.7: Visualisation of the palaeoclimatic conditions occupied by each tetrapod subgroup. Each dot represents a single occurrence of a species (note, the vertical spacing of dots is random). A single larger point for each subgroup represents the mean value for each variable, and a vertical dotted line indicates the mean value for all tetrapods. Climate variables: (a) mean annual surface temperature, (b) mean annual precipitation, (c) seasonal variation in temperature, (d) seasonal variation in precipitation. Abbreviations: Tetra. = All Tetrapoda, Archo. = Archosauromorpha, Pseud. = Pseudosuchia, Avemet. = Avemetatarsalia, Synap. = Synapsida.

4.7a). These two groups also occupy areas with more seasonal variation in both temperature and precipitation (Figure 4.7c–d). Synapsids generally occupy drier areas (those with the lower MAP) than other tetrapods.

Late Triassic latitudinal face-value species richness is best explained by a regression model solely featuring tetrapod-bearing collections (TBCs), a proxy for sampling (Table 4.1). This model accounts for 99% AICw, indicating overwhelming support for this over the other models featuring palaeoclimate. Global species richness, where the data are assembled in global equal-area grid cells, is best explained by a regression model including tetrapod-bearing collections (TBCs) and mean annual surface temperature (MAT) (Table 4.3). It is not possible to clearly distinguish the four best models based on AIC scores, and each of these models contains sampling as an explanatory variable. Likelihood ratio tests between the best two models (Table C3) suggest that adding MAT results in only trivial gains to the explanatory power of the model, and species richness may be best explained by the model containing only TBCs.

Table 4.1: Summary of model fits to Late Triassic latitudinal species richness, where the data was assembled into 10° palaeolatitudinal bins, in order of AICc value. N = 8 palaeolatitudinal bins; ‘TBCs’, tetrapod-bearing collections; ‘MAT’, mean annual surface temperature from the climate model HadCM3L; ‘MAP’, mean annual precipitation, also from the climate model.

Regression model	R ₂	Log likelihood	AICc	AIC weight
TBCs	0.932	-3.09	24.179	0.990
TBCs + MAP	0.941	-2.457	34.915	0.005
TBCs + MAT	0.940	-2.519	35.038	0.004
MAT	0.63	-10.718	39.437	0.000
null model	0.165	-14.376	39.551	0.000
MAP	0.502	-12.048	42.096	0.000
MAT + MAP	0.833	-7.145	44.290	0.000
TBCs + MAT + MAP	0.954	-1.336	56.671	0.000

Table 4.2: Summary of explanatory variables within the GLS multiple regression models for Late Triassic latitudinal species richness (indicated in Table 1). Abbreviations as in Table 4.1.

Regression model	Sampling (TBCs)			MAT			MAP		
	slope	SE	p	slope	SE	p	slope	SE	p
TBCs	0.916	0.083	<0.001***	–	–	–	–	–	–
TBCs + MAP	0.853	0.107	<0.01**	–	–	–	-0.780	0.820	0.378
TBCs + MAT	0.802	0.143	<0.01**	0.283	0.295	0.376	–	–	–
MAT	1.626	0.402	0.005**	–	–	–	–	–	–
null model	–	–	–	–	–	–	–	–	–
MAP	-4.676	2.053	0.057	–	–	–	–	–	–
MAT + MAP	–	–	–	1.474	0.266	0.002**	-2.829	0.956	0.025*
TBCs + MAT + MAP	0.689	0.171	0.010*	0.356	0.299	0.287	-1.042	0.829	0.264

*p = <0.05, **p=<0.01, ***p=0.001

Table 4.3: Summary of model fits to species richness where the data was assembled into equal-area grid cells, in order of AICc value. N = 40 equal-area grid cells. Abbreviations as in Table 4.1.

Regression model	R ₂	Log likelihood	AICc	AIC weight
TBCs + MAT	0.848	-22.280	56.325	0.317
TBCs	0.849	-23.793	56.730	0.259
TBCs + MAT + MAP	0.864	-21.202	56.950	0.232
TBCs + MAP	0.864	-22.779	57.322	0.192
MAT + MAP	0.112	-54.019	119.804	0.000
MAT	0.038	-55.346	119.835	0.000
null model	0.023	-58.154	122.974	0.000
MAP	0.079	-57.129	123.401	0.000

Table 4.4: Summary of explanatory variables within the GLS multiple regression models for grid-cell species richness (indicated in Table 4.3). Abbreviations as in Table 4.1.

Regression model	Sampling (TBCs)			MAT			MAP		
	slope	SE	p	slope	SE	p	slope	SE	p
TBCs + MAT	0.916	0.065	<0.001***	-0.056	1.836	0.976	–	–	–
TBCs	0.917	0.063	<0.001***	–	–	–	–	–	–
TBCs + MAT + MAP	0.891	0.063	<0.001***	0.700	1.823	0.703	0.309	0.149	0.046*
TBCs + MAP	0.897	0.061	<0.001***	–	–	–	0.294	0.143	0.047*
MAT + MAP	–	–	–	5.326	4.608	0.255	0.660	0.377	0.088
MAT	–	–	–	3.805	4.890	0.441	–	–	–
null model	–	–	–	–	–	–	–	–	–
MAP	–	–	–	–	–	–	0.580	0.376	0.131

*p = <0.05, **p=<0.01, ***p=0.001

4.4 Discussion

Despite the Late Triassic interval being relatively well-sampled across palaeolatitudes (Figure 4.2, Figure C.2), sampling still has a strong influence over the diversity patterns recovered. This is exhibited by face-value species richness closely tracking the number of tetrapod-bearing collections and formations across all palaeolatitudes (Figure 4.2a). The amount of sampling varies markedly, both spatially across palaeolatitudes (Figure 4.2a), and also temporally between the early and late Late Triassic (Figure C.1a–b). These peaks in sampling correspond closely with present-day geographic regions that contain important, extensively-studied fossil localities, for example, localities in the Chinle Formation in southwestern USA (low-palaeolatitudes) and in the Caturrita and Santa Maria Formations of southern Brazil (mid-palaeolatitudes), which have yielded important fossil specimens that have contributed significantly to the understanding of early dinosaur evolution (Irmis *et al.*, 2011; Müller *et al.*, 2015; Langer *et al.*, 2018). Investigations of local richness (alpha diversity) offer a way to at least partially circumvent many sampling biases that confound regional and global palaeo-diversity curves (Close *et al.*, 2019). Late Triassic tetrapod local richness is greatest at low- and mid-palaeolatitudes, a pattern driven primarily by well-sampled sites (Table C1), but nonetheless affording an insight into the potential level of richness at regional

scales (Figure 4.3a, Figure C.2). The only group of tetrapods to have high local richness exclusively at mid-palaeolatitudes is Synapsida (Figure 4.3), which potentially indicates a difference in the environmental or climatic constraints on the distribution of archosauromorph and synapsid species.

While the above measures of face-value species richness indicate that tetrapod diversity was highest at low palaeolatitudes, sampling-standardised estimates reveal a more nuanced story and suggest that tetrapod species richness was highest at mid-palaeolatitudes, unlike the modern latitudinal biodiversity gradient (Figure 4.4). This pattern is evident in both palaeo-hemispheres, despite relatively poor sampling in the southern palaeo-hemisphere (although with the caveat that there is no sampling at all in low-palaeolatitudes (0–30°) of the southern palaeo-hemisphere). The overall latitudinal pattern for tetrapods appears to be driven by non-pseudosuchian taxa, namely non-pseudosuchian (basal) archosauromorphs, avemetatarsalians (including dinosaurs), and synapsids (including mammals). This suggests that the modern-type LBG did not exist at the beginning of the evolutionary histories of these major animal groups. Previous work found a palaeotemperature peak in dinosaur diversity throughout the group's entire evolutionary history (Mannion *et al.*, 2012). Conversely, pseudosuchians (crocodylians and their relatives) exhibit a modern-type gradient in diversity, and this pattern has been found to have been retained throughout the evolutionary history of the group (Mannion *et al.*, 2015).

Our finding that only mean annual temperature (MAT) and seasonal variation in temperature from the palaeoclimate model data correlate strongly with palaeolatitude (Figure 4.5, Table C2) suggests that palaeolatitude, used widely as an approximation for palaeoclimate, is a fair proxy for temperature, but does not capture all aspects of palaeoclimatic conditions (e.g. precipitation) and should be used with caution.

Using the output from the palaeoclimate model, HadCM3L, we, for the first time, were able to explore the ranges of climatic conditions from the areas occupied by major tetrapod groups. Generally, each tetrapod group occupies the complete range of

each climatic variable (Figure 4.7), demonstrating an overlap in realised niches. The majority of species in each group occupy generally warm conditions with low seasonal variability, which is consistent with the conditions found at mid-palaeolatitudes (Figure 4.7). Pseudosuchia were visually the most constrained in the range of climatic conditions occupied by the group (Figure 4.7), preferring warmer and less seasonally variable temperatures than other tetrapod groups. Previous studies have linked pseudosuchian diversity with palaeoclimate (Markwick, 1998; Carvalho *et al.*, 2010; Martin *et al.*, 2014; Shirley and Austin, 2017; De Celis *et al.*, 2019). Even today, modern crocodylomorphs exhibit relatively narrow temperature ranges and temperature greatly affects their feeding and reproductive strategies (Grigg and Kirshner, 2015). Avemetatarsalia, the archosaur group containing dinosaurs, has the largest range in both mean annual temperature and precipitation compared with the other groups, and it does appear that the group occupies distinct climatic ranges when compared to other archosauromorphs, particularly with regard to mean annual temperature and seasonality (Figure 4.7). Dinosaur diversity has also been linked to climate (e.g. Benson *et al.*, 2012; Mannion *et al.*, 2012; Whiteside *et al.*, 2015; Bernardi *et al.*, 2018), but the development of this link at the very beginning of dinosaur evolution has not yet been rigorously tested (see Chapter 5).

The differences in palaeoclimatic conditions occupied by pseudosuchians and avemetatarsalians may be indicative of differences in thermal physiology. Pseudosuchians generally have restricted climatic ranges (Figure 4.7), which is analogous to modern day reptilian ectotherms ('cold-blooded' organisms) that rely on their environment for temperature regulation. Conversely, avemetatarsalians exhibit comparatively wider ranges in occupied palaeoclimatic conditions (Figure 4.7), which is more similar to endotherms ('warm-blooded' animals), such as birds and mammals. This pattern exhibited by avemetatarsalians is also more comparable to synapsids than to any other archosaur group within our dataset (Figure 4.7). Thermal physiology is a central, and yet unresolved, issue in dinosaur biology (Benson, 2018). Many hypotheses have been

proposed, but the current consensus, obtained primarily through osteohistological observations, is that dinosaurs were mesothermic, an intermediate physiology where their metabolic rates were elevated when compared with other reptiles but did not match those of extant mammals and birds (Grady *et al.*, 2014; Eagle *et al.*, 2015). Our data suggests that avemetarsalians (including early dinosaurs) were not constrained by climatic conditions, as would be expected by an ectothermic condition. Furthermore, there is evidence for an endothermic ancestral condition at the archosaur node, and a later reversal to an ectothermic state in modern crocodylians (e.g. Seymour *et al.*, 2004; Legendre *et al.*, 2016). While it is beyond the scope of this investigation to confirm this, the overall range of palaeoclimatic conditions occupied by Late Triassic archosauromorphs does not suggest that species were constrained by climate.

Our GLS did not capture a clear relationship between face-value species richness and palaeoclimate. Instead, the best models from both the latitudinal and global GLS analyses all featured the sampling proxy (TBCs) as an explanatory variable, indicating that sampling is the major determinant of observed patterns of spatial species richness during the Late Triassic. This finding is unsurprising and consistent with the same analysis performed for lepidosaurs (Cleary *et al.*, 2018), marine reptiles (Benson and Butler, 2011), dinosaurs (Benson and Mannion, 2012; Mannion *et al.*, 2012), and pterosaurs (Butler *et al.*, 2013), which also found the number of tetrapod-bearing collections as either the best explanatory variable, or the best in conjunction with non-marine area and/or the presence of Lagerstätten (another proxy for sampling). These previous studies were conducted on time series data (exploring the relationship between explanatory variables and taxic richness through time) and the novelty in our approach lies in the use of a spatial dimension, more commonly used in modern ecology. The best model in our spatial GLS featured mean annual temperature in addition to sampling, and both the third and fourth best models featured either MAT or MAP, suggesting that climate may also have some role in driving diversity that was not fully captured in our analyses. However, our analyses serve as a clear indication that future

GLS analyses of this kind should be conducted using sampling standardised estimates of species richness instead of face-value counts, as face-value counts are heavily influenced by spatial and temporal sampling biases.

Nevertheless, exploring the climatic ranges of tetrapod groups using high resolution palaeoclimate data has allowed us to gain a much greater insight into the spatial distribution of these animals. Sampling heterogeneity will continue to impede studies of taxic palaeodiversity, therefore approaches that can more appropriately utilise palaeoclimate reconstructions instead of reducing the output down to single values for coarse spatial bins should be favoured. Such approaches as ecological niche modelling (Chiarenza *et al.*, 2019; Jones *et al.*, 2019; Saupe *et al.*, 2019), or those that incorporate palaeoclimate with phylogenetic relationships (Pie *et al.*, 2017; Chapter 5), with their ability to circumvent many issues associated with uneven and incomplete sampling, are much more promising avenues for investigations of the link between climate and palaeodiversity. This work in particular could be expanded by using the approach of Saupe *et al.* (2019), where suitable habitat is modelled via ecological niche modelling using palaeoclimate reconstructions from the HadCM3L model, ultimately allowing the role of climate in driving changes in the geographical distribution of species to be ascertained while reducing the dependence on raw occurrence data.

5 | THE ROLE OF CLIMATE IN THE EARLY EVOLUTION OF DINOSAURS

My contribution to this work involved conducting all parts of the research, including collecting and collating the data, co-designing the methodology, analysing the data, and interpreting the results, as well as writing the text and creating the figures. A. Farnsworth provided the palaeoclimate reconstructions. R. Benson and P. Godoy provided advice on the methodology along with R code for parts of the analyses. S. Greene and R. Butler provided feedback on the methodology, research design and interpretations of the results. As in previous chapters, the editorial ‘we’ is used to reflect these proportional contributions.

5.1 Introduction

Dinosaurs are one of the most recognisable and widely studied groups of fossil vertebrates but, despite a long history of study and increasing research interest in recent decades, many aspects of their macroevolutionary patterns remain contentious (Brusatte *et al.*, 2008a; Brusatte *et al.*, 2010; Langer *et al.*, 2010; Benson, 2018). In particular, not much is known about how climatic conditions impacted dinosaurs during their rise to ecological dominance in the Late Triassic and Early Jurassic.

Climate is a fundamental control on species diversity and distributions; many of the large-scale ecological patterns on Earth today, such as the latitudinal biodiversity gradient (Willig *et al.*, 2003; Hillebrand, 2004; Chapter 4), are structured by global

variation in climate. Climate has also been hypothesised to underpin many large-scale ecological and evolutionary patterns observed in the fossil record, including changes in global biodiversity through time (Mayhew *et al.*, 2008), shifting latitudinal biodiversity gradients (Mannion *et al.*, 2014), and the evolution of body size (Smith *et al.*, 2010). Several studies have indicated that climate played a profound role in many aspects of dinosaur ecology and evolution, including their biodiversity and biogeography (Rees *et al.*, 2004; Noto and Grossman, 2010; Mannion *et al.*, 2012) and survivorship during mass extinction events (Bernardi *et al.*, 2018), as well as the origins of gigantism (Sander *et al.*, 2011).

Dinosaurs are inferred to have originated by the Middle Triassic (Langer *et al.*, 2010; Brusatte *et al.*, 2011; Nesbitt *et al.*, 2013), and their rapid diversification during the Late Triassic and Early Jurassic is often referred to as a classic example of an adaptive radiation. During this time, dinosaurs diversified into many dozens of lineages and body types (Benton, 2004), setting the stage for over 100 million years of subsequent dominance in terrestrial ecosystems. However, many aspects of the macroevolutionary pattern and drivers of this radiation are poorly known (Brusatte *et al.*, 2008a; 2008b; Irmis, 2011). Most previous studies have treated the rise of dinosaurs as a single event driven by either successful competition with other vertebrates owing to their advanced metabolism and superior locomotory adaptations such as an erect stance (Bakker, 1972; Bonaparte, 1982), or opportunistic expansion after the extinction of other competing large-bodied terrestrial vertebrates, such as rhy-chosaurs, at the proposed Carnian–Norian extinction event (Tucker and Benton, 1982; Benton, 1983; Benton *et al.*, 2018; Bernardi *et al.*, 2018). However, more recent work suggests that this was a diachronous process, with the diversification of herbivorous sauropodomorphs in the Norian followed by larger theropods and armoured herbivorous groups in the Early Jurassic (Irmis *et al.*, 2007, 2011; Nesbitt *et al.*, 2009; Irmis, 2011). This two-step model is supported by studies of theropods which became larger and more common after the Triassic–Jurassic boundary (Olsen *et al.*, 2002)

Some authors have suggested that the early diversification of dinosaurs might have been driven by the Carnian Pluvial Event, a period of increased rainfall that led to increased humidity compared to the generally arid conditions of the Late Triassic, and which is a proposed driver for the Carnian–Norian extinction event (Benton *et al.*, 2018; Bernardi *et al.*, 2018; Dal Corso *et al.*, 2018). Another hypothesis concerning the influence of climate on early dinosaur diversity is the proposal that the absence of larger herbivorous dinosaurs (i.e. sauropodomorphs) at low palaeolatitudes in the Late Triassic was due to ‘unstable’ climatic conditions in equatorial regions (Whiteside *et al.*, 2015; Lindström *et al.*, 2016). By contrast, in the Early Jurassic, sauropodomorphs appear to have been more common in low latitude regions, such as southwestern parts of the USA (Sertich and Loewen, 2010; Rowe *et al.*, 2011) (Figure 5.1). These biogeographic patterns have been hypothesised to track zonal climatic conditions across Pangaea (Irmis *et al.*, 2007; Nesbitt *et al.*, 2009; Whiteside *et al.*, 2011). However, these hypotheses linking early dinosaur diversity and evolution with climatic conditions in the Late Triassic and Early Jurassic have not yet been rigorously tested, in part due to the absence of palaeoclimate data with sufficient temporal and spatial coverage to draw comparisons with patterns of diversity and biogeography across large intervals of deep time.

To test the influence of climate on early dinosaur diversity and distribution during the Late Triassic and Early Jurassic, we used, for the first time, the results of a spatially explicit general circulation palaeoclimate model (HadCM3L), combined with a comprehensive dataset of global dinosaur occurrences from the Paleobiology Database and a supertree of early dinosaur species. We explored the climatic conditions occupied by early dinosaurs and used a selection of macroevolutionary approaches to answer the following questions: (i) Did early dinosaurs occupy the same climatic niches as other terrestrial vertebrates during the Late Triassic and Early Jurassic? (ii) Was there a change in the climatic niche space occupied by dinosaurs across the Triassic–Jurassic (T/J) boundary? (iii) What evolutionary model best explains the

mode of climatic evolution for dinosaurs across this interval? and (iv) Did any shift in climatic conditions across the T/J boundary correspond with biological changes in sauropodomorphs? We explore questions (i)–(iii) for all early dinosaur species, focusing particular attention on sauropodomorph dinosaurs to examine previous hypotheses about their global distribution (Whiteside *et al.*, 2015; Lindström *et al.*, 2016).

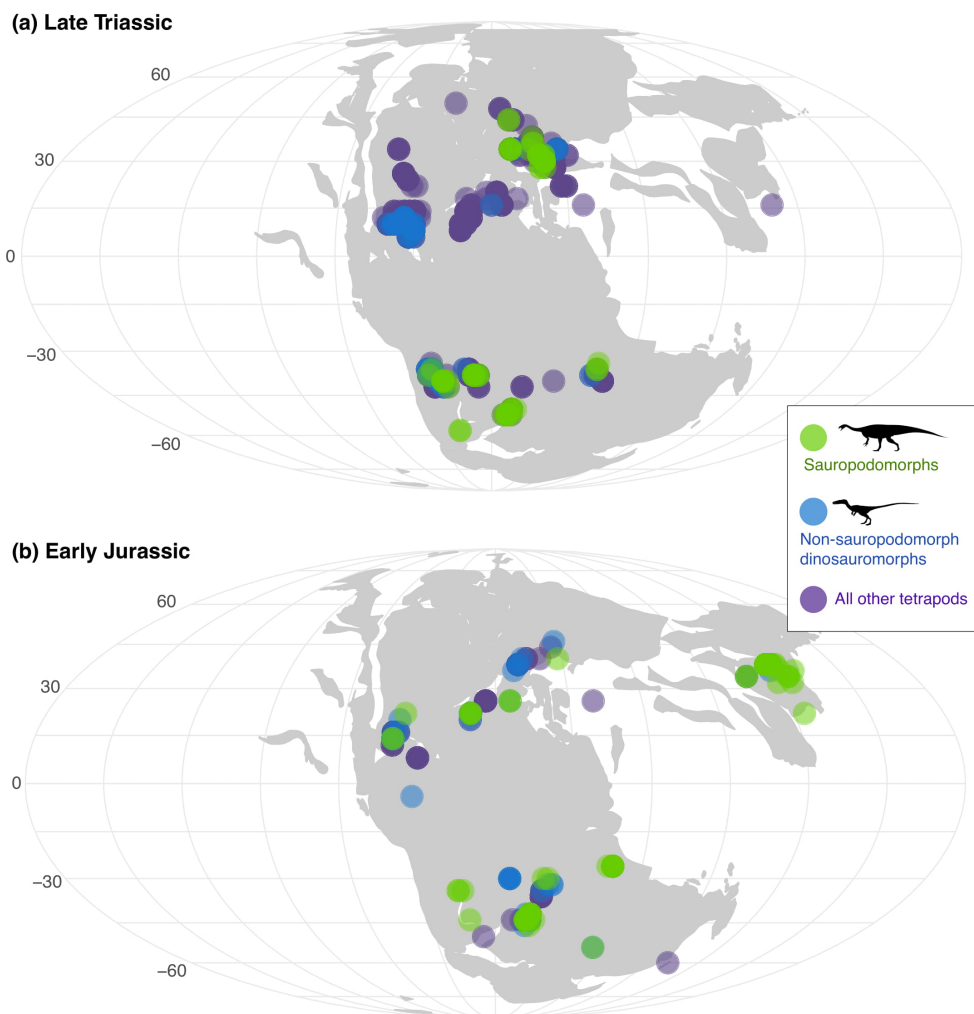


Figure 5.1: Temporal sampling patterns during the Late Triassic and Early Jurassic for (a) all tetrapods, including dinosaurs, and (b) dinosaurs. Each dot represents a single species occurrence and the colour indicates which major group the species belongs to (see legend). Silhouettes from phylopic.org.

5.2 Methods

5.2.1 *Fossil occurrence data*

Global occurrences of all tetrapod species, including early dinosaurs, from the beginning of the Late Triassic to the end of the Early Jurassic (Carnian–Toarcian; 237–174 Ma) were downloaded from the Paleobiology Database (paleobiodb.org, accessed April 24th, 2019). Before download, the data were checked against the current published literature for completeness and any missing occurrences were added. Data preparation and analyses were conducted within R 3.5.2 (R Core Team, 2018). The dataset was filtered following download to remove trace fossils, marine and flying taxa, and taxonomically indeterminate occurrences, as in Chapter 2 (Section 2.2.1).

5.2.2 *Supertree and time calibration*

An informal species-level supertree for early dinosaurs, comprising 121 taxa, was constructed by hand based on the most up-to-date phylogenetic analyses available for Late Triassic–Early Jurassic dinosaurs and dinosauiromorphs (Table D1). The basis of this tree was the informal supertree of amniotes constructed by Button *et al.* (2017). Several informally named specimens are retained in the supertree to provide additional geographic information (see Table D2).

Prior to performing comparative analyses of trait evolution, the supertree was time calibrated. This step is critical, as the use of different methods may impact upon the inference of evolutionary models and the interpretation of results (Bapst, 2013, 2014). As such, we decided to use a tip-dating approach, using the fossilised birth-death (FBD) model (Stadler, 2010). The FBD method is a Bayesian total-evidence dating approach, which uses a birth-death process that includes the probability of fossilisation and sampling to model the occurrence of fossil species in the phylogeny and estimate divergence times (=node ages) (Ronquist *et al.*, 2012a; Matzke and Wright, 2016; Zhang *et al.*, 2016; Wright, 2017). Information on occurrence times for species

in the supertree (i.e. tip ages) were initially obtained from the Paleobiology Database but were then checked against the current literature and updated if more precise information was available. Following the method outlined in Godoy *et al.* (2019), Bayesian Markov chain Monte Carlo (MCMC) analyses were performed in MrBayes 3.2.6 (Ronquist *et al.*, 2012b) using the protocol within the R package paleotree (Bapst, 2012). The supertree was used as a topological constraint and uniform priors were set on the age of tips based on the occurrence dates information. A uniform prior was used for the root of the tree, constrained between 250 and 265 Ma. 50,000,000 generations were used, after which the parameters indicated that both MCMC runs seemed to converge (i.e., the Potential Scale Reduction Factor approached 1.0 and average standard deviation of split frequencies was below 0.01). 25 trees were randomly sampled from the posterior distribution after a burn-in of 25%. Analyses run across all 25 trees allowed us to characterise the influence of topological and time-scale uncertainties on the results of palaeoclimatic disparity-through-time analyses and macroevolutionary model comparisons.

5.2.3 *Palaeoclimate reconstructions*

As discussed in Chapter 4, one of the major factors limiting examination of specific hypotheses linking palaeodiversity and palaeoclimate is the lack of readily comparable climatic reconstructions across geologic time. To overcome this limitation, we again used HadCM3L (version 4.5), a fully coupled Atmospheric–Ocean General Circulation Model sensu Lunt *et al.* (2015), which comprises a set of readily comparable model runs comparable across geologic time. Details of this model, its caveats, and the variables extracted are outlined in Chapter 4, Section 4.2.3.

We used two approaches for assigning palaeoclimatic variables to individual species. For each dinosaur species within the supertree we used a ‘randomised-averaging’ process, where species that spanned two time intervals were randomly assigned to a single interval, and then if the species occurred in more than one collection

within that interval, the average value of each palaeoclimatic variable was calculated. This was done primarily to ensure that results from phylogeny-based analyses were consistent with all other analyses. For species not in the supertree i.e. all other non-dinosauromorph tetrapods that are not included in phylogeny-based analyses, values for each palaeoclimatic variable were obtained simply by averaging across all intervals and collections that a species occurred in. Occurrences of species that spanned more than two intervals (due to stratigraphic uncertainty) were discarded from the dataset. The mean values for each palaeoclimatic variable did not change substantially between iterations of this assignment process, but to ensure consistency across the results, analyses were run using 10 various iterations of the 'randomised averaging process' and the output examined before presentation.

Prior to analyses of palaeoclimatic niche space, the underlying spatial and temporal sampling patterns for both tetrapod and dinosaur species across the Late Triassic and Early Jurassic were examined. Additionally, the spatial and temporal variation in each palaeoclimatic variable, and how they correlated with palaeolatitude was assessed.

5.2.4 *Palaeoclimatic niche space*

Obtaining information on species fundamental niches from the fossil record is challenging; therefore, the term 'palaeoclimatic niche' used hereafter refers to an approximation of the realised climatic niche of the fossil taxa. To explore the palaeoclimatic niche space occupied by early dinosaurs and other tetrapods, we performed a principle component analysis (PCA) using the *prcomp* function in R, which included the scaling argument so that variables were scaled to have unit variance before the analysis took place. Despite recent suggestions that using PC scores from standard PCA could bias the fit of alternative models of evolution (Uyeda *et al.*, 2015), we chose not to implement a phylogenetic PCA (pPCA) approach as including only species for which phylogenetic information was available would considerably diminish the amount of data for analy-

sis. Separate PCA plots were constructed for the Late Triassic and Early Jurassic to explore changes across the Triassic–Jurassic (T/J) boundary. We also constructed boxplots to illustrate and explore the range of palaeoclimatic conditions occupied by each tetrapod group, again separated into the Late Triassic and Early Jurassic. Additionally, pairwise comparisons of the palaeoclimatic variables were performed using non-parametric Mann–Whitney–Wilcoxon tests, which compare the standard deviation and median of datasets.

5.2.5 *Temporal variation in palaeoclimatic niche evolution*

General patterns of temporal variation in early dinosaur climatic niche evolution were studied using complementary methods. First we used the continuous character mapping function *contMap* in phytools (Revell, 2012), in which mapping is accomplished by estimating the states at internal nodes of the tree using maximum likelihood (ML) with the function *fastAnc* (a fast estimation of the ML ancestral states for a continuous trait) and interpolating the states along each edge using equation [2] of Felsenstein (1985). Next, we calculated dinosaur palaeoclimatic niche disparity-through-time with the R package *dispRity* (Guillerme, 2018), using PC scores from a PCA performed for dinosaur species in the supertree only (where the palaeoclimate variables were assigned as described in section 5.3.4). The sum of variances was selected as the disparity metric, because variance-based metrics are more robust to sample size variation than other commonly used metrics for measuring disparity-through-time (Butler *et al.*, 2012; Guillerme and Cooper, 2018).

Different subsampling approaches can have important impacts on the results of disparity-through-time analyses (Guillerme and Cooper, 2018). For example, a widely used approach is to use stratigraphic intervals as stages (e.g. Stubbs *et al.* 2013; Benton *et al.* 2014), but this can introduce sampling biases, since shorter time bins can include few taxa, leading to large confidence intervals (Guillerme and Cooper, 2018). Another approach is to set time bins to represent equal length intervals

(e.g., Butler *et al.* 2012), which can diminish the issues of uneven temporal sampling (Guillerme and Cooper, 2018). As an alternative to this time-binning method, Guillerme and Cooper (2018) recently proposed the “time-slicing” method, a phylogeny-based method that takes into consideration those taxa contemporaneous at specific equidistant points in time (instead of taxa that were present between two points in time), resulting in even sampling. Furthermore, this method allows *a priori* definition of the evolutionary model underlying the changes in disparity.

Therefore, to more rigorously assess the patterns of dinosaur palaeoclimatic niche disparity-through-time, we used both subsampling procedures: time-binning and time-slicing. For both procedures, the number of sub-samples (time bins or time slices) was set to 5, 10, and 20 (i.e., equal-length time bins in the time-binning method, and equally distant specific points in time in the time-slicing method) to assess the impact of the number of time intervals on the results. Taxa were allowed to occur in multiple time intervals, using first and last occurrence data for each taxon. PC scores of taxa in each were subjected to bootstrapping (1,000 iterations) to calculate confidence intervals. The time-binning method was implemented both without and with estimates of ancestral states, which were obtained using the *fastAnc* function in phytools. Finally, for the time-slicing method, we chose to calculate disparity assuming punctuated models of evolution (i.e., the “proximity” model; Guillerme and Cooper 2018), where selection of values of ancestors or descendants was based on the position of the time slice along the branch, using the score of the ancestor if it is located in the first half of the branch, and the score of the descendant if it is in the second half.

5.2.6 *Macroevolutionary models*

To characterise the evolutionary mode of early dinosaur palaeoclimatic evolution, we applied a model-fitting approach using a set of uniform and non-uniform evolutionary models. This was carried out using the R package mvMORPH (Clavel *et al.*, 2015), which allows fitting of multivariate evolutionary models and can be used with

any dataset of one or multiple covarying continuous traits. In this instance, the traits are PC scores from a PCA of palaeoclimate variables for species in the supertree.

Uniform models apply a single set of model parameters across all branches of a phylogeny. We fitted four uniform models: (1) A uniform Brownian motion (BM model), which describes diffusive, unconstrained evolution via random walks along independent phylogenetic lineages, resulting in no directional trend in trait mean, but with increasing trait variance (=disparity) through time (Felsenstein, 1985; Hunt and Carrano, 2010; Slater, 2013). (2) The “early burst” (EB model; a special case of the ACDC model [Blomberg *et al.*, 2003]), in which the lineages experience an initial maximum in evolutionary rate of change, that decreases exponentially through time according to the parameter r (Harmon *et al.*, 2010). This results in a rapid early increase in trait variance followed by deceleration. EB models have been used to study adaptive radiations (e.g. Cooper and Purvis, 2010). (3) A uniform “trend” model, in which the parameter μ is incorporated into the BM model to describe directional multi-lineage increase or decrease in trait values through time in the entire clade (Hunt and Carrano, 2010; Hunt, 2012). (4) The Ornstein-Uhlenbeck (OU) model, which describes processes where a trait’s variance is constrained around one or several optima often referred as ‘selective regime’ or ‘adaptive zone’ optima at the macroevolutionary scale (Butler and King, 2004; Slater, 2013; Benson *et al.*, 2018).

While uniform models are important for describing many aspects of trait evolution and are often the null hypothesis in such investigations, they may not be sufficient to characterise the complex variation in the dynamics of evolutionary changes through time and space as well as among clades and environments. In addition to these four uniform models (BM, EB, trend, and OU), we also fitted six non-uniform, or multi-regime, models. For each of these models a regime shift at the Triassic–Jurassic boundary (201.3 Ma) was ‘mapped’ onto each of the time calibrated trees using the *make.era.map* function in phytools (Revell, 2012). First, we fitted a non-uniform BM model (BMM; BM with two selective regimes, one before and one after the bound-

ary) and a non-uniform OU model (OUM; OU process with two adaptive optima per trait, one before and one after the boundary) (Clavel *et al.*, 2015). We also fitted four non-uniform ‘shift’ models, available in the mvMORPH package and first introduced by Slater (2013): (1) shift from an OU to a BM process at 201.3 Ma (OUBM); (2) shift from BM to an OU process at 201.3 Ma (BMOU); (3) “constrained ecology” (EC), which is a model of where traits are constrained in an OU process after a fixed point in time (e.g., after invasion of a competitive species in a given ecosystem); (4) “ecological release and radiate” (RR), which combines an OU process with a BM process, but allows the Brownian rate to vary relative to the OU rate (see equation [4] of Slater, 2013). Model support was compared using Akaike weights computed from small-sample-corrected AIC scores (AICc) (Hurvich and Tsai, 1989; Burnham and Anderson, 2002), where lower AICc scores correspond to better fitting models.

5.2.7 *Sauropodomorph biology and palaeoclimate*

Finally, we explored if there was an association between dinosaur biology and palaeoclimate. We assembled body mass data for Late Triassic and Early Jurassic dinosaur species from Benson *et al.* (2018), which was updated with unpublished sauropodomorph body mass data from D. Cashmore. Values for palaeoclimatic variables were assigned to each species through the same randomised averaging procedure as described in section 5.2.3. The following analyses were first performed on all dinosaur species, and then for only sauropodomorph species. First, we tested for phylogenetic signal of body mass and each palaeoclimate variable using Pagel’s λ in the R package caper (Orme *et al.*, 2018). We then tested for a relationship between palaeoclimate and body mass using a phylogenetic generalised least squares (PGLS) regression analysis to account for phylogenetic non-independence amongst the data. The PGLS incorporated a correlation structure that follows an OU evolutionary model and was performed over each of the 10 iterations of palaeoclimate value assignment, as well as over 3 different time-calibrated trees, to ensure the results were generally consistent each time. The best

models (i.e. combinations of explanatory variables) were identified using the AIC for small sample sizes (AICc; Hurvich and Tsai, 1989) which selects the model(s) that explain the highest proportion of variation in global species richness with the fewest explanatory variables. All PGLS and associated tests were performed in R with the packages nlme (Pinheiro *et al.*, 2019), ape and geiger. Likelihood-ratio based pseudo- R_2 values were calculated separately using the function *r.squaredLR* of the R package MuMIn (Barton, 2019).

We also inspected the pattern of sauropodomorph morphological disparity-through-time using dispRity (Guillerme, 2018) and a morphological character matrix from Marsh and Rowe (2018), which is an update on the matrix from McPhee and Choiniere (2018). Prior to analysis, the character matrix was converted to a distance matrix using the *MorphDistMatrix* function in the R package Claddis (Lloyd, 2016) and ordinated using the *cmdscale* function in base R. Additionally, the strict consensus tree of Marsh and Rowe (2018) was time-calibrated using the *timePaleoPhy* function with minimum branch lengths in paleotree (Bapst, 2012), which produced 25 time-calibrated trees in line with previous analyses. Taxon occurrence dates were obtained from the Paleobiology Database. For this disparity-through-time analysis, we used only the time-binning subsampling approach (without ancestral state reconstructions), as detailed in section 5.2.5, to allow direct comparison between this and the palaeoclimatic niche disparity analyses.

5.3 Results

5.3.1 Palaeoclimatic niche space

PCA plots allowed an exploration of palaeoclimatic niche space for dinosaurs and other tetrapods during the Late Triassic and Early Jurassic (Figure 5.2). Together PC1 and PC2 account for over 80% of the variation in both intervals, so we focus our interpretations on these two PC axes. In both intervals (Late Triassic and Early Jurassic), the

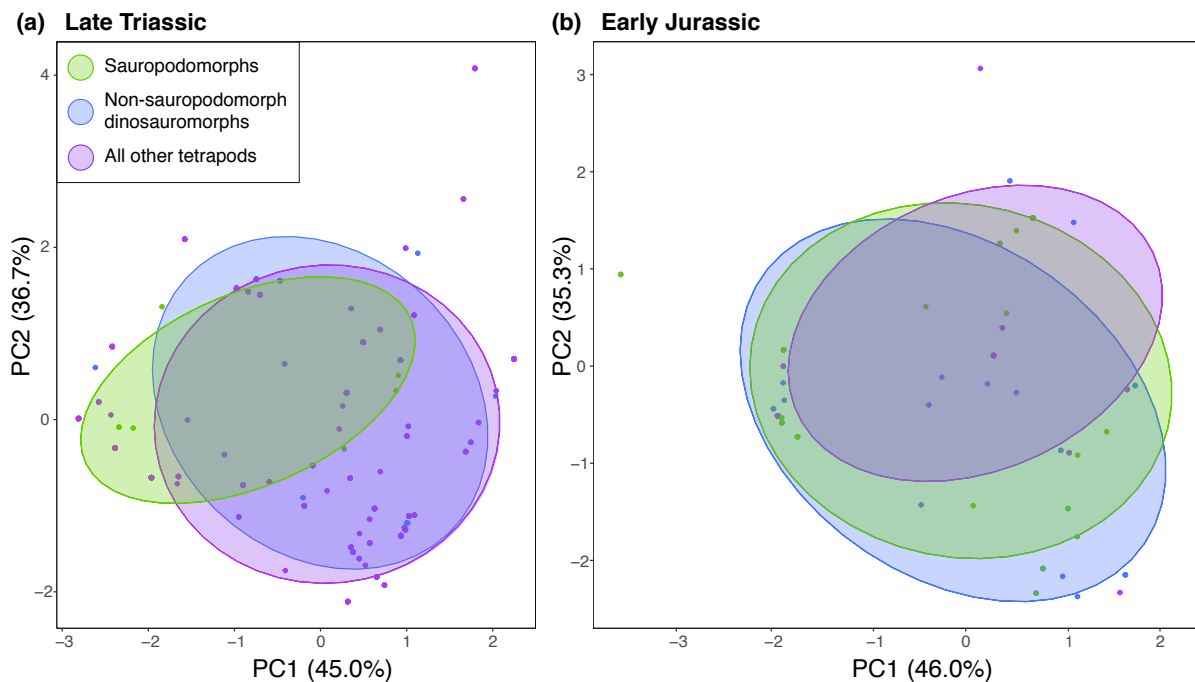


Figure 5.2: Palaeoclimatic niche space represented by the scores of the first two PC axes for (a) Late Triassic and (b) Early Jurassic, sauropodomorphs (green), non-sauropodomorph dinosaurs and dinosauriforms (blue), and all other tetrapods (purple). The ellipses represent 68% confidence intervals. Lower (i.e. more negative) scores of PC1 indicate conditions with more seasonal variation in temperature, whereas higher (i.e. more positive) values indicate increasing mean annual temperature values. Higher values of PC2 indicate increasing mean annual precipitation and greater seasonal variation in precipitation.

first PC corresponded to variation in temperature, both mean annual temperature and seasonal variation in temperature: lower (i.e. more negative) scores of PC1 on the PCA ordination plot indicate conditions with more seasonal variation in temperature, whereas higher (i.e. more positive) values indicate increasing mean annual temperature values (Figure 5.2). The second PC reflected variation in precipitation (both mean annual precipitation and seasonal variation in precipitation) and seasonal variation in temperature: higher values of PC2 indicate increasing mean annual precipitation and greater seasonal variation in precipitation, while lower values correspond to increasing seasonal variation in temperature (Figure 5.2).

The distribution of species on the PCA ordination plot during the Late Triassic indicates that sauropodomorph dinosaurs had a more restricted palaeoclimatic niche

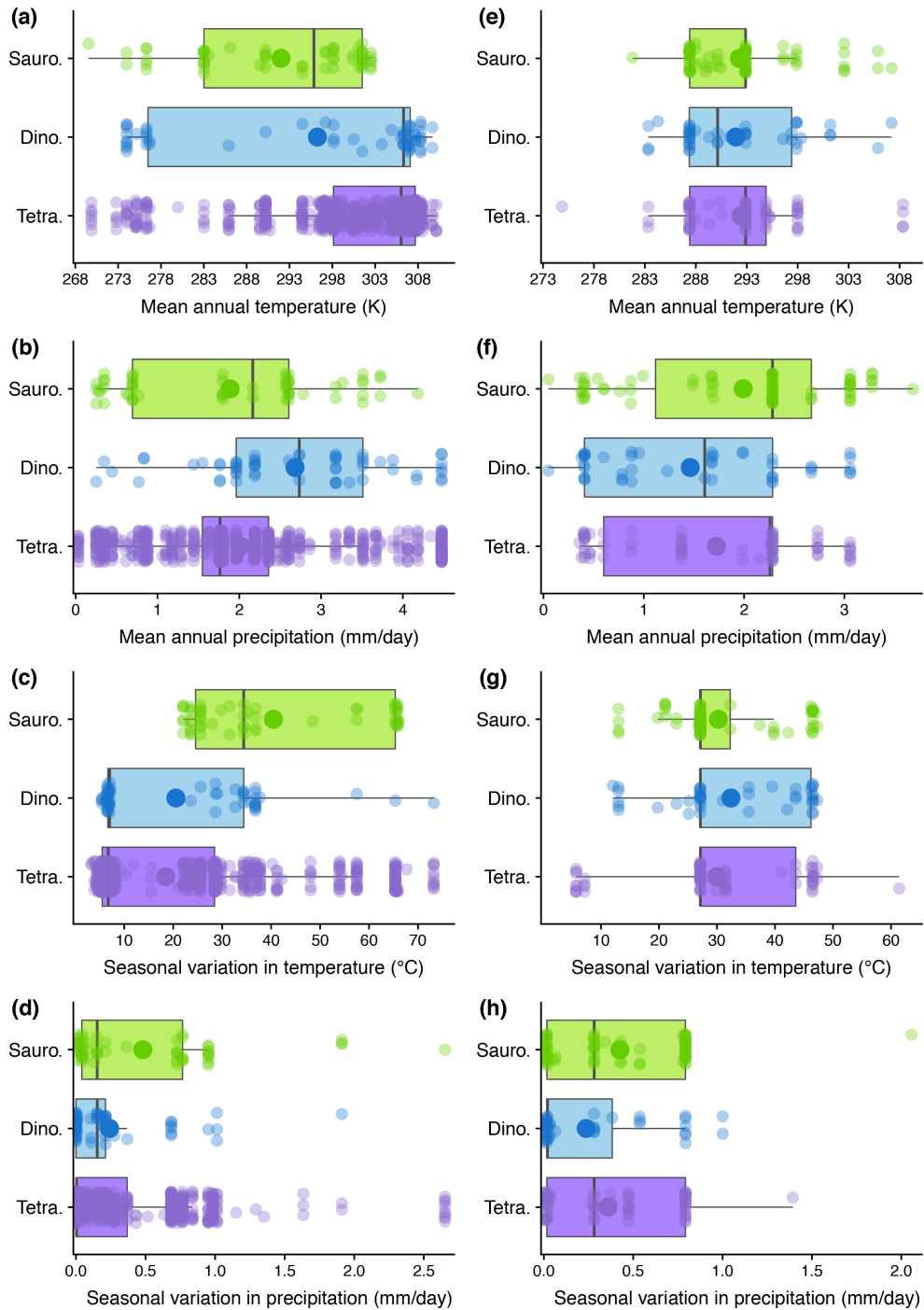


Figure 5.3: Visualisation of the palaeoclimatic conditions occupied by the three tetrapod/dinosaur groups in the Late Triassic (a–d) and Early Jurassic (e–h): sauropodomorphs (green), non-sauropodomorph dinosaurs and dinosauriforms (blue), and all other tetrapods (purple). Each point on the plots represents a single occurrence of a species (note, the vertical spacing of dots is random), and a single larger point for each group represents the mean value for each variable. Abbreviations: Sauro. = sauropodomorph dinosaurs, Dino. = non-sauropodomorph dinosaurs, Tetra. = all other tetrapods.

space than other dinosaurs and tetrapods, occupying cooler, drier areas with more seasonal variation in temperature (Figure 5.2a). However, the majority of sauropodomorph palaeoclimatic niche space still overlaps with that of other dinosaurs and tetrapods. Other dinosaur species occupied a noticeably wider palaeoclimatic niche space with very similar conditions to other tetrapods i.e. generally warm conditions with low seasonal variation. In the Early Jurassic the palaeoclimatic niches of all three groups are more similar (Figure 5.2b). Sauropodomorphs exhibit the greatest expansion in niche space from the Late Triassic, expanding into generally warmer, wetter conditions with less seasonal variation in temperature (Figure 5.2b).

These patterns are also evident from boxplots illustrating the variation in palaeoclimatic conditions occupied by each group in the Late Triassic and Early Jurassic (Figure 5.3). In the Late Triassic, sauropodomorphs occupied drier areas with more seasonal variation in temperature than other dinosauromorphs, and also displayed a more restricted range in mean annual temperatures (Figure 5.3a–d). However, in the Early Jurassic, the ranges in palaeoclimatic conditions they occupy align more closely with both other groups (Figure 5.3e–h). Pairwise comparisons (non-parametric Mann–Whitney–Wilcoxon tests) of the palaeoclimatic variables revealed that these differences in palaeoclimatic ranges during the Late Triassic between sauropodomorphs and other non-dinosauromorph tetrapods were statistically significant only for mean annual temperature and seasonal variation in temperature (Table D.2).

5.3.2 *Temporal variation in palaeoclimatic niche evolution*

Caution must be exercised when interpreting these phylogenies displaying reconstructed ancestral states, as unlike with morphological data, it is unclear what ancestral reconstructions of palaeoclimatic values actually represent. This would ideally be deciphered using ecological modelling techniques, but as this lies outside the scope of this chapter the ancestral states computed here are taken to represent the hypothetical palaeoclimatic niche space occupied by ancestral nodes on the phylogeny.

CHAPTER 5: EARLY DINOSAUR EVOLUTION & CLIMATE

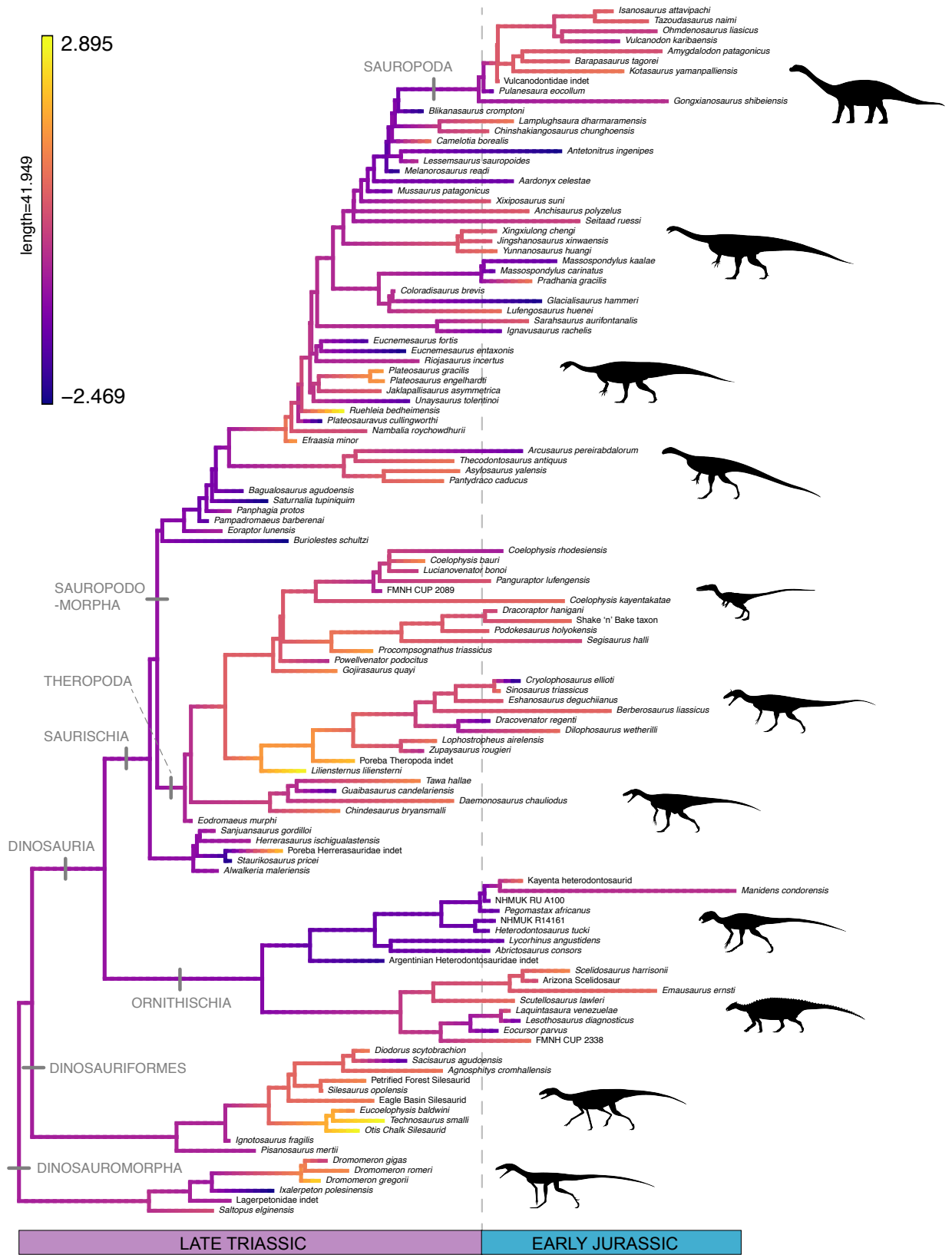


Figure 5.4: PC1 mapped onto dinosaur phylogeny (cont. on next page)

Figure 5.4: Dinosaur phylogeny displaying PC1 mapped as a continuous character. States at internal nodes of the tree were estimated using maximum likelihood (ML) and interpolating the states along each edge using equation [2] of Felsenstein (1985). Silhouettes of representative early dinosaur species (not to scale) from phylopic.org. Phylogenies mapped with 'raw palaeoclimatic variables can be found in Appendix E.

Palaeoclimatic niche disparity-through-time analyses show that there is a noticeable decrease in palaeoclimatic niche disparity across the interval from the Late Triassic to the Early Jurassic (note the non-overlap of confidence intervals) (Figure 5.5). This pattern is consistent across all time-calibrated trees (Appendix F). In general, analyses using more time intervals (either time bins or time slices) show more nuanced changes in disparity; however, using too many time intervals resulted in empty intervals that could not be utilised. Therefore, we present our results from analyses using 10 time intervals. The pattern of decreasing palaeoclimatic niche disparity-through-time is less pronounced in analyses that use ancestral states (Figure 5.5b–c). For some trees analysed using the time-slicing subsampling approach, the pattern recovered has large confidence intervals and, in some cases, palaeoclimatic disparity fluctuates widely. As noted above, ancestral states for palaeoclimatic variables should be treated with caution, as it is difficult to decipher what they truly represent. Focusing on analyses conducted using the time-binning subsampling method without ancestral states, palaeoclimatic niche disparity-through-time appears to increase at the beginning of the Late Triassic, then levels off, before decreasing across the Triassic–Jurassic boundary and once again levelling off towards the end of the Early Jurassic (Figure 5.6a, Appendix F). This pattern is also evident when sauropodomorphs and non-sauropodomorph dinosaurs are analysed separately (Figure 5.6, Appendix F).

5.3.3 *Spatial and temporal patterns in sampling and palaeoclimate*

For all tetrapods there is a greater amount of sampling in the Late Triassic than in the Early Jurassic (Figures 5.1, 5.7, and D.2). There are noticeably fewer collections at low palaeolatitudes in the Early Jurassic, particularly towards the end of this interval

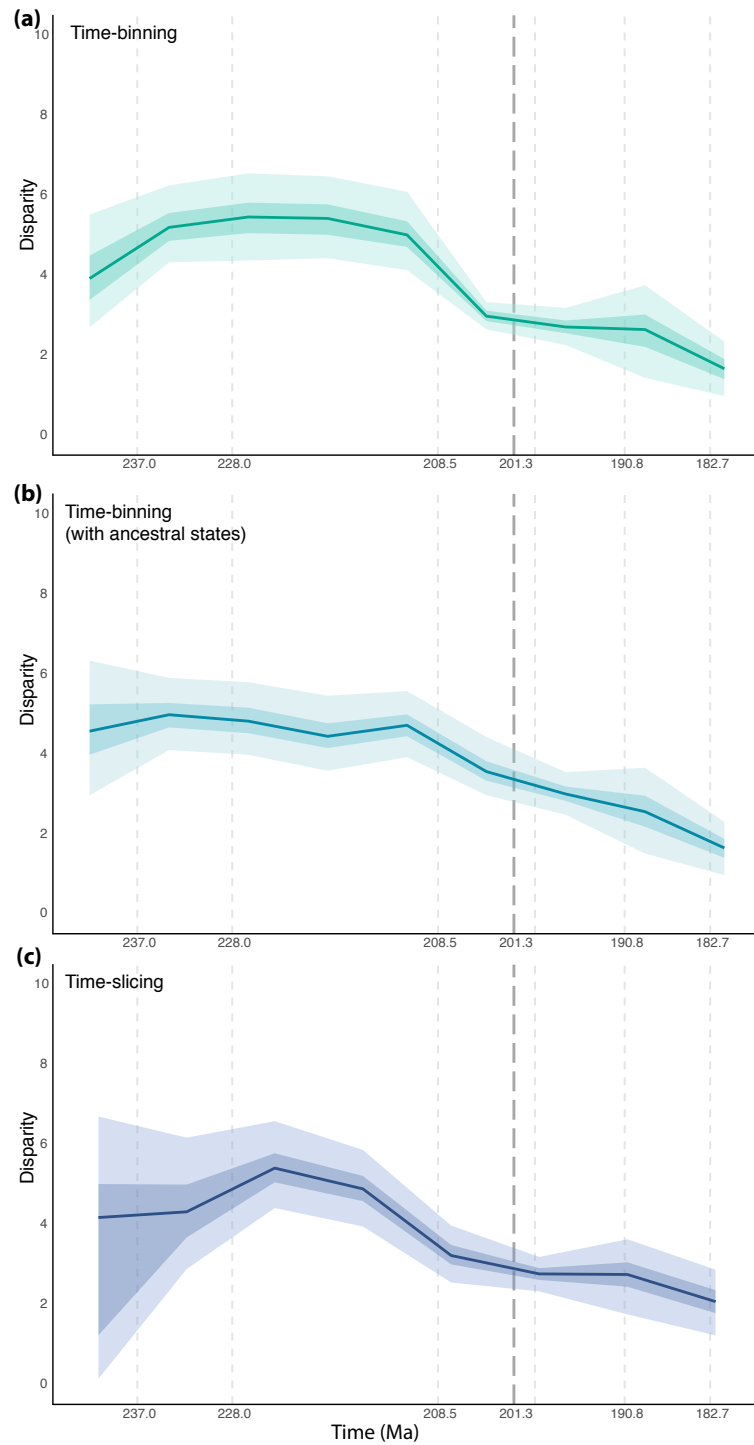


Figure 5.5: Representative palaeoclimatic niche disparity-through-time plots for tree 1 using (a) the time-binning approach, (b) time-binning with ancestral state reconstruction, and (c) time-slicing approach (which involves ancestral state reconstruction). The sum of variance is used as the disparity metric. Light and dark shaded areas of each plot represent, respectively, 75% and 97.5% confidence intervals from 1,000 bootstrapping replicates. The Triassic–Jurassic boundary is marked by a vertical dashed line. Trees 2–25 (for each of the three methods) can be found in Appendix F.

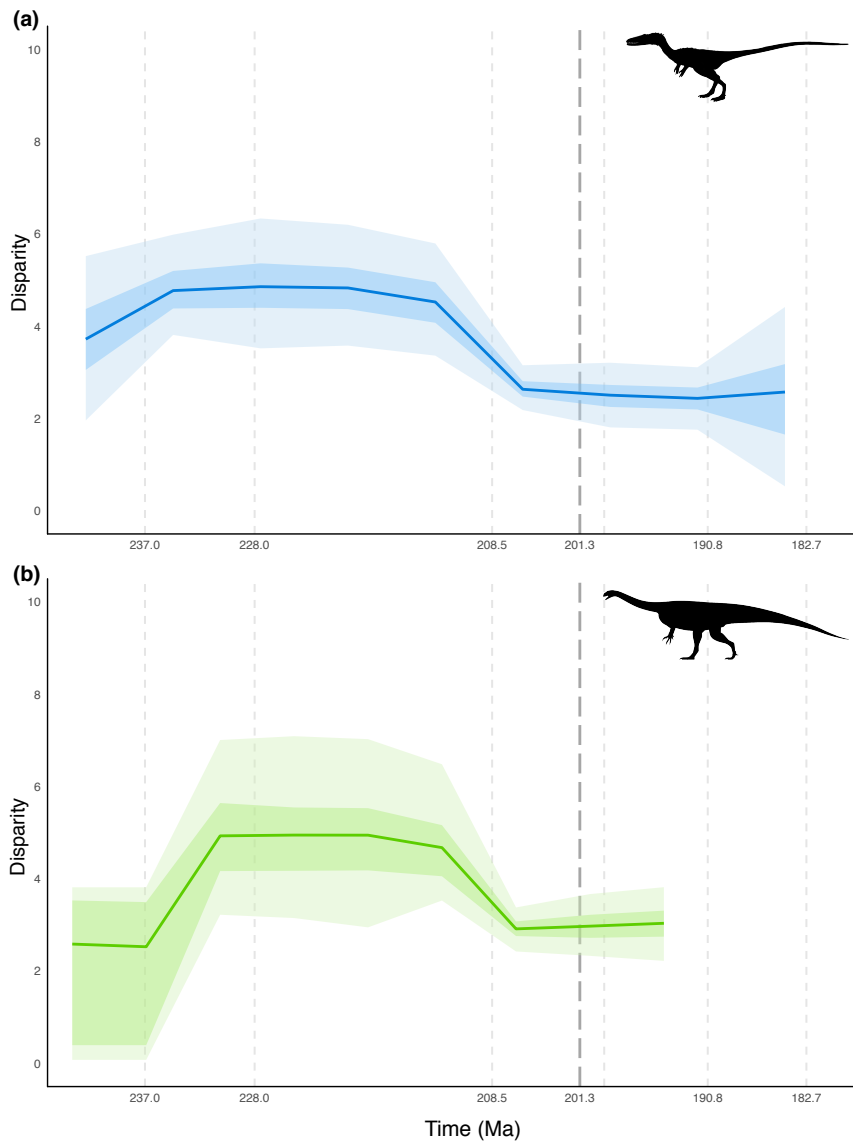


Figure 5.6: Representative palaeoclimatic niche disparity-through-time plots for tree 1 using the time-binning approach for (a) sauropodomorphs, and (b) non-sauropodomorph dinosaurs. The sum of variance is used as the disparity metric. Light and dark shaded areas of each plot represent, respectively, 75% and 97.5% confidence intervals from 1,000 bootstrapping replicates. The Triassic–Jurassic boundary is marked by a vertical dashed line. Trees 2–25 can be found in Appendix F.

(Figure D.2). This corresponds to an absence of localities with ‘extreme’ palaeoclimatic conditions, such as high temperatures and low precipitation (Figure 5.7). However, the correlation between palaeoclimatic variables and palaeolatitude for sampled localities does not differ markedly between the Late Triassic and Early Jurassic (Figure D.3, Table D4).

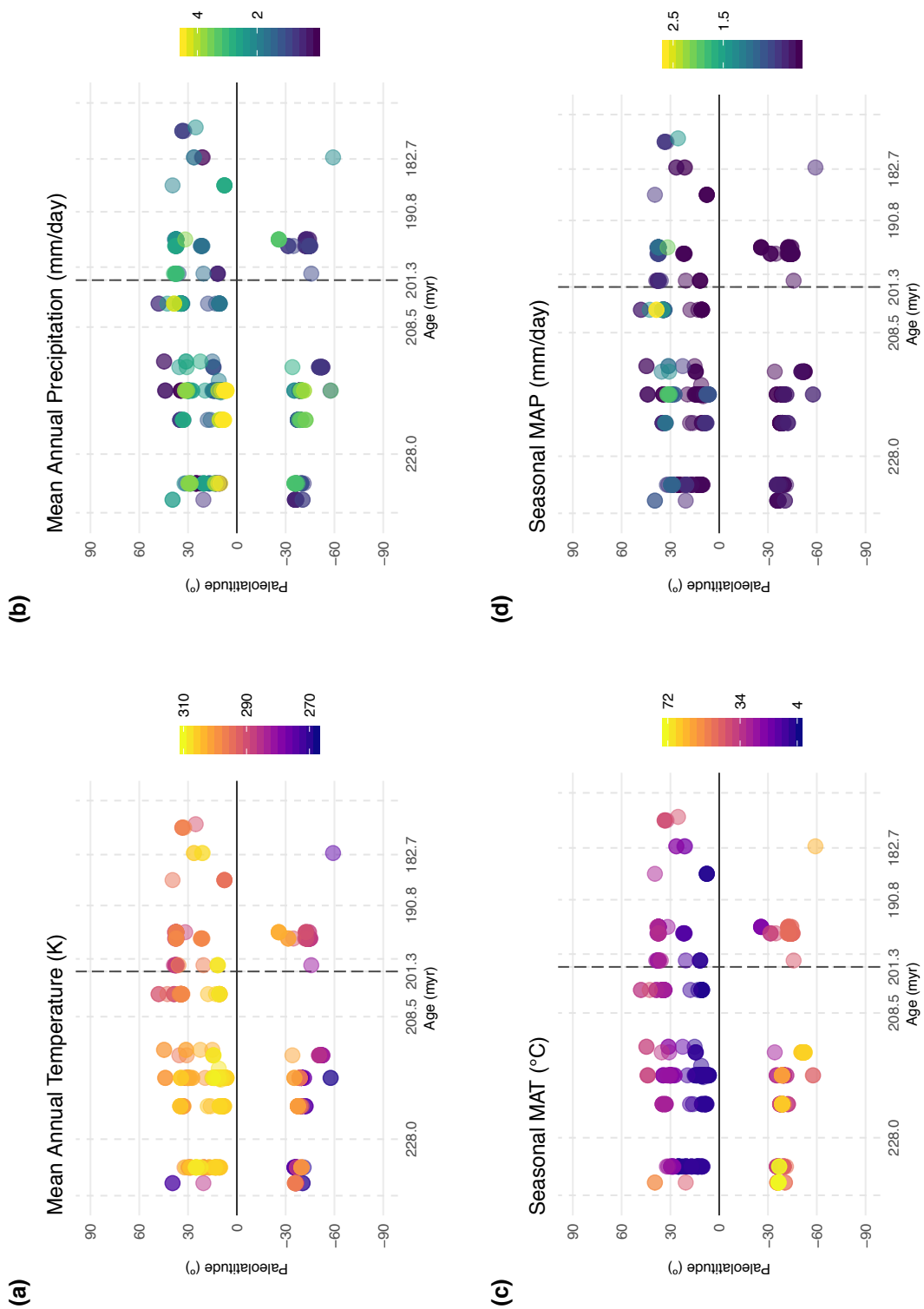


Figure 5.7: Variation in each palaeoclimatic variables across the the Late Triassic and Early Jurassic. Each point represents the condition at a single collection.

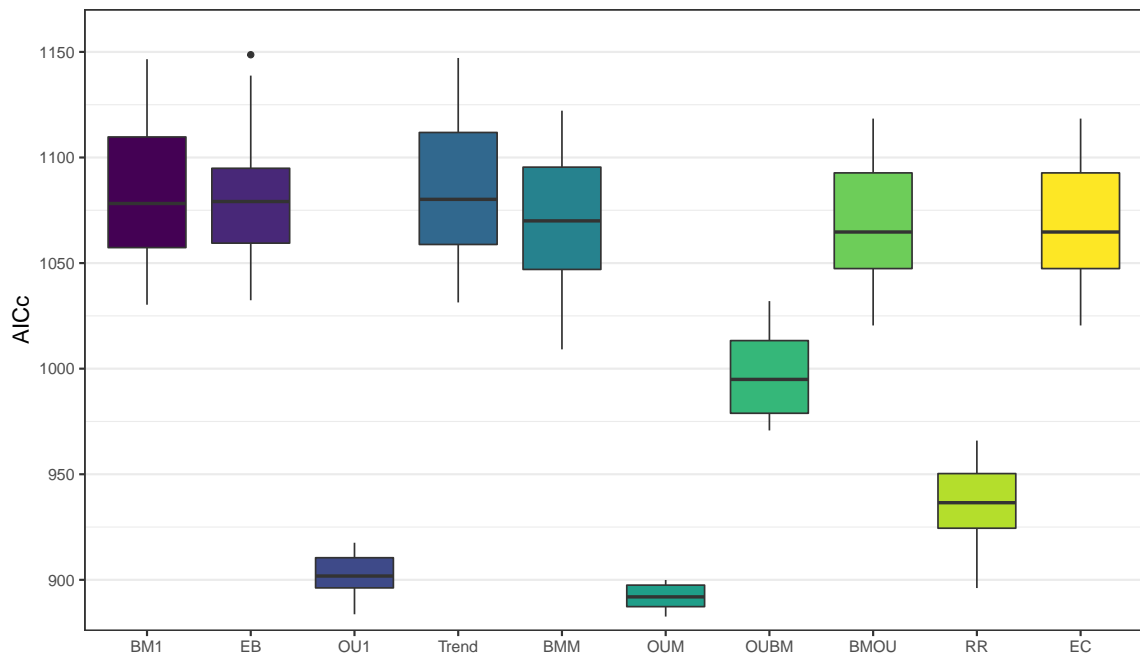


Figure 5.8: AICc scores of the evolutionary models fitted to the dinosaur phylogeny and palaeoclimate data. Lower AICc values indicate stronger support. Abbreviations: BM = Brownian motion, EB = Early Burst, OU1 = uniform OU model, Trend = Trend model, BMM = non-uniform BM model, OUM = non-uniform OU model, OUBM = OU to BM model, BMOU = BM to OU model, RR = “radiate and release” model, EC “constrained ecology” model.

5.3.4 Macroevolutionary models

Comparisons between the AICc scores for all the evolutionary models fitted to the dinosaur palaeoclimate niche space (Figure 5.8) show strongest support for models that involve an OU process (lower AICc values indicate stronger support). Generally, non-uniform models that have a regime shift at the Triassic–Jurassic boundary better fit the data, with the exception of the uniform OU model (OU1). All uniform models (BM1, EB, Trend) as well as the Brownian motion model with a regime shift (BMM), the non-uniform BM to OU model (BMOU) and the “constrained ecology” model (EC) all have similar AICc scores (Figure 5.8). The OU to BM model (OUBM) and the “release and radiate” model (RR) show marginally stronger support, but it is the two OU models, uniform (OU1) and non-uniform (OUM) that are most strongly supported (Figure 5.8). A t-test between these two models confirms that the non-uniform OU model is signif-

icantly different from the OU1 model, indicating that it is the model with the strongest support overall (t-test: $DF = 42.353$, $p = 0.0127$).

Theta values (the optimum values) for the OUM model were assessed for each of the traits (i.e. PC scores from the palaeoclimate data) and compared with the information for the PC axes. Together PC1 and PC2 account for over 80% of the variation in both intervals, so once again we focus on these two PC axes for the following interpretations. Generally, values of theta for PC1 increase across the regime shift at the Triassic–Jurassic boundary and decrease for PC2 (Table D5). As more negative values of PC1 are associated with greater seasonal variation in temperature (Figure 5.2), this change in theta values can be interpreted as a shift towards a lower degree of seasonal variation in temperature in the Early Jurassic. Likewise, as higher values of PC2 are associated with increased precipitation and greater seasonal variation in

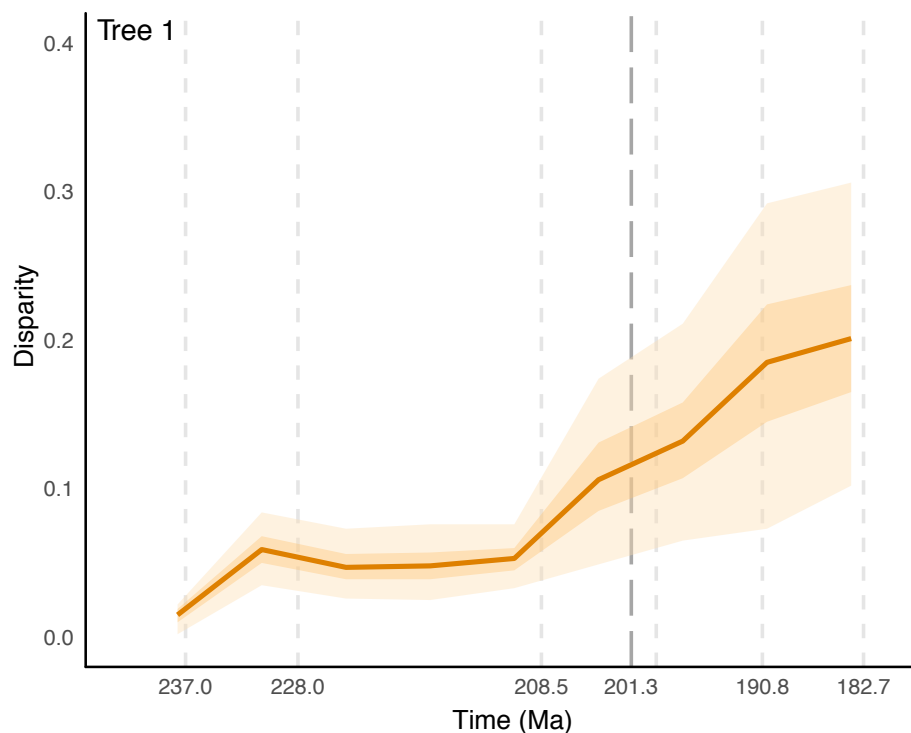


Figure 5.9: Sauropodomorph morphological disparity through time (using the time-binning approach). The sum of variance is used as the disparity metric. Light and dark shaded areas of each plot represent, respectively, 75% and 97.5% confidence intervals from 1,000 bootstrapping replicates. The Triassic–Jurassic boundary is marked by a vertical dashed line. Trees 2–25 can be found in Appendix G.

precipitation, the change from higher to lower values of theta can be interpreted as a switch towards drier and less seasonally variable conditions in the Early Jurassic.

5.3.5 *Sauropodomorph biology and palaeoclimate*

Across the sauropodomorph tree, phylogenetic signal was recovered for body mass (Pagel's $\lambda = 0.918$, $DF = 32$, $p = <0.001$), but not for any of the palaeoclimatic variables. Sauropodomorph body mass generally increased across the study time interval (Figure D.4), however, phylogenetic generalised least squares (PGLS) analysis indicated that there was no relationship between sauropodomorph body mass and palaeoclimate (Table 5.1). The null model was recovered as the best performing model, accounting for over one third of the AIC weight. Models that incorporated more than one variable received the lowest support, thus only models combining MAT with another variable are presented here. Morphological disparity-through-time analyses illustrated that there is a noticeable increase in sauropodomorph morphological disparity across the interval from the Late Triassic to the Early Jurassic (Figure 5.9) and this pattern is consistent across all time-calibrated trees (Appendix G).

Table 5.1: Summary of GLS model fits to sauropodomorph body mass, in order of AICc value. Abbreviations of climatic variables are as follows: MAT = mean annual temperature, MAP = mean annual precipitation, SVT = seasonal variation in temperature, SVP = seasonal variation in precipitation.

Regression model	R ₂	Log likelihood	AICc	AIC weight
TBCs	0.932	-3.09	24.179	0.990
TBCs + MAP	0.941	-2.457	34.915	0.005
TBCs + MAT	0.940	-2.519	35.038	0.004
MAT	0.63	-10.718	39.437	0.000
null model	0.165	-14.376	39.551	0.000
MAP	0.502	-12.048	42.096	0.000
MAT + MAP	0.833	-7.145	44.290	0.000
TBCs + MAT + MAP	0.954	-1.336	56.671	0.000

Table 5.2: Summary of explanatory variables within the PGLS multiple regression models for sauropodomorph body mass (indicated in Table 5.1). Abbreviations as in Table 5.1.

Regression model	MAT			MAP		
	slope	SE	p	slope	SE	p
null model	–	–	–	–	–	–
SVP	–	–	–	–	–	–
MAT	-1.21	8.055	0.882	–	–	–
MAP	–	–	–	–	–	–
SVT	–	–	–	–	–	–
MAT + SVP	1.069	8.516	0.901	–	–	–
MAT + MAP	-1.134	8.197	0.891	0.086	0.696	0.903
MAT + SVT	-1.833	10.529	0.863	–	–	–
Regression model	SVT			SVP		
	slope	SE	p	slope	SE	p
null model	–	–	–	–	–	–
SVP	–	–	–	-1.001	0.971	0.311
MAT	–	–	–	–	–	–
MAP	–	–	–	–	–	–
SVT	0.011	0.642	0.987	–	–	–
MAT + SVP	–	–	–	-1.045	1.043	0.324
MAT + MAP	–	–	–	–	–	–
MAT + SVT	-0.08	0.838	0.925	–	–	–

*p = <0.05, **p=<0.01, ***p=0.001

5.4 Discussion

The integration of ordination, disparity-through-time, and evolutionary rates analyses allowed us to provide a general scenario for the evolution of palaeoclimatic niche space in early dinosaurs. In the Late Triassic, non-sauropodomorph dinosaurs occupied similar palaeoclimatic niche space to other tetrapods, while sauropodomorphs occupied a more restricted palaeoclimatic niche space relative to the other groups (Figure 5.2). By contrast, in the Early Jurassic all groups occupy very similar palaeoclimatic niche spaces, with sauropodomorphs having expanded their range (Figure 5.2). This corresponds to a general shift towards slightly cooler conditions with less seasonal variation in temperature (Figure 5.3, Figure 5.4). The ordination analysis also indicated that the most important dimension of early dinosaur palaeoclimatic niche space in both intervals is dominated by measures of temperature (mean annual and seasonal variation in temperature) (Figure 5.2, Figure 5.4), suggesting that temperature was a key constraint on early dinosaur palaeoclimatic niche space.

The best supported evolutionary model in our analysis was the non-uniform (two-regime) OU model, closely followed by the uniform (single regime) OU model (Figure 5.8). This indicates that palaeoclimatic niche evolution was constrained before the Triassic-Jurassic boundary (201 Ma) and remained constrained after, but with a different adaptive optimum. However, with the uniform (single regime) OU model also being relatively strongly supported, this might mean that while the constraints on trait evolution before and after the boundary are different, this difference is relatively minor. This is further evidenced by the low support given to models that assume two very different scenarios before and after the boundary, such as the OU to BM model (Figure 5.8). Corroborating this idea of a regime shift at the Triassic–Jurassic boundary is the finding that palaeoclimatic niche disparity amongst dinosaur species decreased across the Triassic–Jurassic boundary (Figure 5.5, Figure 5.6). This pattern can be visualised when the PC scores have been mapped onto the dinosaur phylogeny; there appears

to be less variation in the Early Jurassic and palaeoclimatic conditions appear more homogeneous (Figure 5.4).

Previous studies have suggested that sauropodomorphs were absent from low latitude regions in the Late Triassic due to unstable conditions, such as fluctuating aridity and humidity, in equatorial regions (Whiteside *et al.*, 2015; Lindström *et al.*, 2016). This finding stemmed from an investigation into palaeoclimate proxy data (e.g. charcoal) and did not have the ability to examine climate on a global or temporal scale. Our results show that sauropodomorphs expanded both their geographical range (Figure 5.1) and palaeoclimatic niche space (Figure 5.2) in the Early Jurassic, alongside an increase in both morphological disparity (Figure 5.9) and body size (Benson *et al.*, 2014, 2018) (Figure D.4). However, this geographical and biological change appears to counter the finding that sauropodomorph palaeoclimatic niche disparity decreased across the Triassic–Jurassic boundary.

There is a distinct change in sampling regime from the Late Triassic to Early Jurassic (Figures 5.1 and D.2). In the Late Triassic, there is greater sampling evident in low latitude regions when compared with the Early Jurassic (Figure 5.7). These low latitude regions of the Late Triassic typically have more ‘extreme’ palaeoclimatic conditions e.g. high temperatures, low precipitation, and little seasonal variation in temperature (Figure 5.7a–c). With a different sampling regime in the Early Jurassic, there appears to be more homogeneity in the palaeoclimatic conditions at sampled sites. This implies that the changes in palaeoclimatic niche disparity-through-time may be due in part to temporal and spatial sampling patterns. However, while the correlation between palaeoclimate variables and palaeolatitude does not differ substantially between the two intervals (Figure 5.7, Table D4), there is evidence that the modelled palaeoclimatic conditions are also changing between the Late Triassic and Early Jurassic. The belt of warmer conditions that occurs close to the palaeoequator in the earlier Late Triassic appears to expand both northwards and southwards through into the Early Jurassic (Figure D.5). Many of the Early Jurassic dinosaur occurrences are located within this

expanding belt (Figure 5.1), which may provide a reason for the decrease in palaeoclimatic niche disparity, as there is less variation between climatic conditions of localities at similar absolute palaeolatitudes in the Early Jurassic when compared to the Late Triassic (Figures 5.7, D.3, and D.5).

The HadCM3L palaeoclimate model relies on changing palaeogeographies to inform palaeoclimate reconstructions, as CO₂ remains constant through time (Chapter 4, Section 4.2.3). While this is advantageous when looking across long temporal scales when compared with palaeoclimatic proxy data, it weakens the ability of studies such as this one to capture the nuances of climate change over relatively short timescales. To further test the influence of sampling on the patterns of palaeoclimatic niche evolution, it may be preferable to use a modelling approach, such as ecological niche modelling (e.g. Chiarenza *et al.*, 2019). Alternatively, or complementarily, the palaeoclimatic niche space could be subsampled in a way that is analogous to subsampled diversity estimates (see Chapter 1 and Chapter 3).

The most common explanation of how dinosaurs survived the Triassic–Jurassic extinction event to become more globally widespread in the Early Jurassic and begin over 100 million subsequent years of domination of terrestrial ecosystems involves their supposed competition with other taxa such as non-mammalian synapsids, non-crocodylomorph pseudosuchians and other archosauromorphs (e.g. rhynchosaurs and rauisuchians) (Tucker and Benton, 1982; Benton, 1983). Notions of the general “superiority” of dinosaurs, related to their metabolism and locomotory adaptations, such as a high body temperature and erect stance, have also long pervaded the literature (Bakker, 1972; Bonaparte, 1982). However, hypotheses of competition between major clades are often vague, prone to oversimplification, and difficult to test conclusively. We found that early dinosaur species (with the exception of sauropodomorphs in the Late Triassic) occupied the same range in palaeoclimatic niche space during both the Late Triassic and Early Jurassic as other tetrapods. This supports previous work that showed that during this interval, dinosaurs lived alongside and shared niches with

another major clade (Pseudosuchia) that occupied greater or similar levels of morphospace and evolved at indistinguishable rates (Brusatte *et al.* 2008a; Nesbitt *et al.*, 2017). These patterns are in stark contrast with the general views of dinosaurian “superiority” and the long-standing opinion that dinosaurs were preordained for success (Bakker, 1972; Bonaparte, 1982). It is possible that the shift in palaeoclimatic niche space and decrease in palaeoclimatic niche disparity evident between the Late Triassic and Early Jurassic represents dinosaurs adapting to new environments following the Triassic–Jurassic mass extinction. While it is not yet possible to say unequivocally what these adaptations were (Brusatte *et al.*, 2008a), our results suggest that for sauropodomorphs, this was linked to increasing body size and increased morphological disparity.

Our approach using palaeoclimatic reconstructions also offers a complementary way to explore hypotheses of biological interactions between dinosaurs and other terrestrial vertebrates. For example, in the case of sauropodomorphs, it would be possible to test the palaeoclimatic niche space of supposed competitors (i.e. other large herbivorous reptiles) to ascertain first whether they overlap with sauropodomorph palaeoclimatic niche space in the Late Triassic, and then if it was this palaeoclimatic niche space that sauropodomorphs expanded into during the Early Jurassic.

Until now, most studies of dinosaurs’ rise to ecological dominance have focused on biological interactions with other terrestrial vertebrates, or tentative links between patterns of dinosaur diversity and environmental conditions obtained from sedimentological data. This work provides the first quantitative investigation for the influence of climate on early dinosaur evolution, and our approach has enormous potential to uncover the climatic drivers behind macroevolutionary and macroecological patterns observed in the fossil record.

6 | CONCLUSIONS AND PERSPECTIVES

6.1 General conclusions and summary

This thesis employed advanced statistical, phylogenetic, and modelling approaches to quantitatively and comprehensively assess the patterns and drivers of tetrapod diversity during key intervals of the group's evolution during the late Palaeozoic and early Mesozoic.

Chapters 2 and 3 focused on early tetrapod diversity and biogeography during the Carboniferous and early Permian (358–272 million years ago), and how these patterns were impacted by the 'Carboniferous rainforest collapse' (CRC). Analyses of diversity using sampling standardisation revealed that species richness initially increased into the late Carboniferous, then decreased substantially across the Carboniferous/Permian boundary before slowly recovering in the early Permian. Our analysis of global phylogenetic biogeographic connectedness did not support the previous hypothesis that the CRC drove the development of endemism, and instead we found evidence for increased biogeographic connectedness amongst tetrapod communities (i.e. cosmopolitanism) in the early Permian following the CRC. This rejection of the previous endemism hypothesis (Sahney *et al.*, 2010) was supported by another study that suggested this increase in connectedness from our study reflected an increase in local-scale dispersal between tetrapod communities, rather than continental-scale dispersal (Brocklehurst *et al.*, 2018). The disappearance of the rainforests and opening of landscapes appears to have been favourable for amniotes, who, with their larger body sizes relative to earlier tetrapods, were free to disperse across the new landscapes and

diversify further.

Crucially, previous work on Carboniferous and early Permian tetrapod diversity failed to adequately account for spatial and temporal biases in sampling (Sahney *et al.*, 2010). Analyses of sampling and face-value diversity in Chapter 2 revealed a tight relationship between observed species richness and sampling. To further assess the impact of sampling on early tetrapod diversity estimates, in Chapter 3 a novel mechanistic ecological model, based on neutral theory, was used to simulate diversity patterns based on the sampling regime of the fossil record. The results demonstrated that the majority of the face-value diversity change can be explained by temporal variation in sampling, further highlighting the importance of accounting for sampling biases in analyses of palaeodiversity. The neutral simulations also detected a slight influence of the CRC from the face-value fossil data, as indicated by the simulations better fitting the empirical data when parameters were allowed to vary before and after the CRC. However, this does not mean that the fossil record can be taken at face-value, but rather that mechanistic models have great potential for addressing palaeoecological hypotheses.

Chapter 4 focused on the latitudinal patterns of tetrapod diversity during the Late Triassic. Sampling standardisation was again applied to examine whether a modern-type latitudinal biodiversity gradient (increasing diversity towards the equator) was present during this interval when the radiation of several modern lineages, such as mammaliamorphs and dinosaurs were underway. For most Late Triassic tetrapod groups, species richness was found to be highest at mid-latitudes. However, pseudosuchians (crocodylians and their relatives) exhibited a modern-type gradient in diversity, a pattern that is retained throughout the evolutionary history of crocodylians (Mannion *et al.*, 2015). Statistical analyses could not confirm a clear relationship between latitudinal species richness and palaeoclimatic conditions, informed by palaeoclimatic reconstructions from the general circulation model HadCM3L. Instead, sampling was determined to be the primary driver of the spatial (and latitudinal) distribution of Late

Triassic tetrapods, despite the Late Triassic being comparatively better sampled across latitudes than neighbouring intervals. However, there is still evidence to suggest that the palaeoclimatic ranges of certain tetrapod groups were constrained. The differences in palaeoclimatic ranges occupied by pseudosuchians and those of avemetarsalians (the lineage leading to dinosaurs), which had comparatively wider ranges, may be indicative of differences in thermal physiology between the two groups, in turn lending support to the hypothesis that early dinosaurs could have been mesothermic (Grady *et al.*, 2014; Eagle *et al.*, 2015).

Chapter 5 extended on the work from Chapter 4 by focusing on the influence of climate on early dinosaur diversity and global distribution. Previous work suggested that climate was a key driver of the early diversification of dinosaurs, as well as a constraint on the global distribution of sauropodomorphs (Whiteside *et al.*, 2011; Lindström *et al.*, 2016; Benton *et al.*, 2018; Bernardi *et al.*, 2018). Palaeoclimatic reconstructions from the general circulation model HadCM3L allowed us to explore early dinosaur palaeoclimate niche space across the Late Triassic and Early Jurassic. Further analysis using macroevolutionary models and disparity-through-time analyses, revealed that there was a shift in dinosaur palaeoclimate niche space across the Triassic–Jurassic boundary, with palaeoclimate niche disparity decreasing across the interval. This is in contrast with the finding that sauropodomorph morphological disparity and body mass increased across the same interval, alongside expanding both their global geographical range and palaeoclimate niche space. One explanation for these contrasting outcomes could be the difference in sampling regime between the Late Triassic and Early Jurassic, which might preclude an estimation of the full palaeoclimate niche space occupied by sauropodomorphs. However, this work supports the conclusions of other studies that showed that during this interval, dinosaurs lived alongside and shared niches with pseudosuchians, another major vertebrate clade that occupied greater or similar levels of morphospace and evolved at indistinguishable rates to early dinosaurs (Brusatte *et al.* 2008a; Nesbitt *et al.*, 2017). These patterns are in stark contrast with the general

views of dinosaurian “superiority” and the long-standing opinion that dinosaurs were preordained for success (Bakker, 1972; Bonaparte, 1982).

6.2 Future work and prospects

Chapters 2 and 3 represent the most comprehensive assessment of the influences of sampling biases on estimates of early tetrapod diversity. This work, alongside recent studies, has elucidated how environmental change impacted the diversification of the first vertebrates to live on land. However, it is clear that further investigation may be hindered by the inescapably incomplete nature of the early tetrapod occurrence data, despite recent concerted efforts to close the gaps in the early tetrapod fossil record (Clack *et al.*, 2016; Anderson *et al.*, 2015). One approach to mitigating this issue of data availability, used recently by Pardo *et al.* (2019) in their study on early tetrapods, is to incorporate museum record data with occurrence data from the Paleobiology Database. The PBDB data is restricted to only include fossil occurrences that have been published in the primary literature, but museum records may hold additional and complementary data that could help fill current gaps. Recent work by Marshall *et al.* (2018) suggests that museum data for western North American invertebrates represent 23 times the number of unique localities than are currently available in the PBDB. While extracting necessary data from museum collections would take considerable effort to compile, especially for tetrapods, it is a promising avenue of approach that I believe should be embraced.

Just as advances in technology and computing facilitated the first quantitative investigations of Phanerozoic diversity, current technological advances may develop the field even further. PaleoDeepDive is a long-awaited statistical machine-learning system built upon the DeepDive machine reading infrastructure, that will automatically locate and extract fossil occurrence data from published scientific papers, thus potentially revolutionising, and significantly speeding up, the process of data input into the Paleobiology Database (Peters *et al.*, 2014).

Combining fossil occurrence data with palaeoclimate reconstructions from a general circulation climate model, as in Chapters 4 and 5, is a novel approach that add increased rigour to estimations of the influence of climate on past diversity. Climate models such as HadCM3L allow investigations to be conducted across time intervals, which has not been taken advantage of in studies of terrestrial vertebrate diversity. This opens many possibilities for further research into other time intervals and using other fossil groups. Chapter 5 represents the first time palaeoclimate reconstructions from a general circulation model have been applied within a phylogenetic framework to answer questions about the mode and tempo of fossil species evolution. Again, this approach can be widely applied to other fossil groups. Approaches that do not rely on the face-value fossil record (i.e. modelling approaches using neutral theory and ecological niche modelling), as identified in this thesis, have enormous potential to test hypotheses concerning the impact of climate on fossil diversity (e.g. Chiarenza, *et al.*, 2019; Jones *et al.*, 2019; Saupe *et al.*, 2019).

While temporal and spatial sampling biases have, and will continue to have, an overwhelming influence on estimates of past diversity, there are several quantitative methods available to mitigate their effects. Advanced phylogenetic and modelling approaches can then illuminate patterns in diversity typically masked by sampling biases. As I mentioned in the introduction to this thesis, it is important to not regard acknowledgements of sampling biases as pessimism, but rather we should view our knowledge of the history of life on Earth as a work in progress.

REFERENCES

- AHLBERG, P. E. 1995. Elginerpeton pancheni and the earliest tetrapod clade. *Nature*, 373, 420–425.
- ALLISON, P. A. and BOTTJER, D. J. 2011. Taphonomy: Bias and Process Through Time. In ALLISON, P. A. and BRIGGS, D. E. G. (eds.) *Taphonomy Through Time*, Vol. 32. 1–17 pp.
- ALONSO, D., ETIENNE, R. S. and MCKANE, A. J. 2006. The merits of neutral theory. *Trends in Ecology and Evolution*, 21, 451–457.
- ALROY, J. 2010a. Geographical, environmental and intrinsic biotic controls on Phanerozoic marine diversification. *Palaeontology*, 53, 1211–1235.
- . 2010b. Fair Sampling of Taxonomic Richness and Unbiased Estimation of Origination and Extinction Rates. *Quantitative Methods in Paleobiology. Paleontological Society Short Course*, 16, 55–80.
- . 2010c. The Shifting Balance of Diversity Among Major Marine Animal Groups. *Science*, 329, 1191–1194.
- , MARSHALL, C. R., BAMBACH, R. K., BEZUSKO, K., FOOTE, M., FURSICH, F. T., HANSEN, T. A., HOLLAND, S. M., IVANY, L. C., JABLONSKI, D., JACOBS, D. K., JONES, D. C., KOSNIK, M. A., LIDGARD, S., LOW, S., MILLER, A. I., NOVACK-GOTTSHALL, P. M., OLSZEWSKI, T. D., PATZKOWSKY, M. E., RAUP, D. M., ROY, K., SEPKOSKI, J. J., SOMMERS, M. G., WAGNER, P. J. and WEBBER, A. 2001. Effects of sampling standardization on estimates of Phanerozoic marine diversification. *Proceedings of the National Academy of Sciences of the United States of America*, 98, 6261–6266.

- , ABERHAN, M., BOTTJER, D. J., FOOTE, M., FURSICH, F. T., HARRIES, P. J., HENDY, A. J. W., HOLLAND, S. M., IVANY, L. C., KIESSLING, W., KOSNIK, M. A., MARSHALL, C. R., MCGOWAN, A. J., MILLER, A. I., OLSZEWSKI, T. D., PATZKOWSKY, M. E., PETERS, S. E., VILLIER, L., WAGNER, P. J., BONUSO, N., BORKOW, P. S., BRENNEIS, B., CLAPHAM, M. E., FALL, L. M., FERGUSON, C. A., HANSON, V. L., KRUG, A. Z., LAYOU, K. M., LECKEY, E. H., NURNBERG, S., POWERS, C. M., SESSA, J. A., SIMPSON, C., TOMASOVYCH, A. and VISAGGI, C. C. 2008. Phanerozoic Trends in the Global Diversity of Marine Invertebrates. *Science*, 321, 97–100.
- ANDERSON, J. S. 2001. The phylogenetic trunk: maximal inclusion of taxa with missing data in an analysis of the Lepospondyli (Vertebrata, Tetrapoda). *Systematic Biology*, 50, 170–193.
- ANDERSON, J. S., SMITHSON, T., MANSKY, C. F., MEYER, T., CLACK, J. 2015. A diverse tetrapod fauna at the base of ‘Romer’s Gap’. *PLoS ONE* 10, e0125446.
- ARCHIBALD, S. B., BOSSERT, W. H., GREENWOOD, D. R., BRIAN, D., ARCHIBALD, S. B., BOSSERT, W. H., GREENWOOD, D. R. and FARRELL, B. D. 2010. Seasonality, the latitudinal gradient of diversity, and Eocene insects. *Paleobiology*, 36, 374–398.
- BAKKER, R. T. 1972. Anatomical and ecological evidence of endothermy in dinosaurs. *Nature*, 238, 81–85.
- BAMBACK, R. K. 1997. Species richness in marine benthic habitats through the Phanerozoic. *Paleobiology*, 3, 152–167.
- BAPST, D. W. 2012. Paleotree: An R package for paleontological and phylogenetic analyses of evolution. *Methods in Ecology and Evolution*, 3, 803–807.

- . 2013. A stochastic rate-calibrated method for time-scaling phylogenies of fossil taxa. *Methods in Ecology and Evolution*, 4, 724–733.
- . 2014. Assessing the effect of time-scaling methods on phylogeny-based analyses in the fossil record. *Paleobiology*, 40, 331–351.
- BARNES, R. 2018. dggridR: Discrete Global Grids. R package version 2.0.3.
- BARNOSKY, A. D., CARRASCO, M. A. and DAVIS, E. B. 2005. The Impact of the Species – Area Relationship on Estimates of Paleodiversity. *PLoS Biology*, 3, e266
- BARNOSKY, A. D., HADLY, E. A., GONZALEZ, P., HEAD, J., POLLY, P. D., LAWING, A. M., ERONEN, J. T., ACKERLY, D. D., ALEX, K., BIBER, E., BLOIS, J., BRASHARES, J., CEBALLOS, G., DAVIS, E., DIETL, G. P., DIRZO, R., DOREMUS, H., FORTELIUS, M., GREENE, H. W., HELLMANN, J., HICKLER, T., JACKSON, S. T., KEMP, M., KOCH, P. L., KREMEN, C., LINDSEY, E. L., LOOY, C., MARSHALL, C. R., MENDENHALL, C., MULCH, A., MYCHAJLIW, A. M., NOWAK, C., RAMAKRISHNAN, U., SCHNITZLER, J., DAS SHRESTHA, K., SOLARI, K., STEGNER, L., STEGNER, M. A., STENSETH, N. C., WAKE, M. H. and ZHANG, Z. 2017. Merging paleobiology with conservation biology to guide the future of terrestrial ecosystems. *Science*, 355.
- BARRETT, P. M., MCGOWAN, A. J. and PAGE, V. 2009. Dinosaur diversity and the rock record. *Proceedings of the Royal Society B: Biological Sciences*, 276, 2667–2674.
- BARTON, K. 2019. MuMIn: Multi-Model Inference. R package version 1.43.6
- BATH ENRIGHT, O. G., MINTER, N. J. and SUMNER, E. J. 2017. Palaeoecological implications of the preservation potential of soft-bodied organisms in sediment-density flows: Testing turbulent waters. *Royal Society Open Science*, 4, 170212

- BAUM BR 1992 Combining trees as a way of combining data sets for phylogenetic inference, and the desirability of combining gene trees. *Taxon* 41, 3–10.
- BENSON, R. B. J. 2018. Dinosaur Macroevolution and Macroecology. *Annual Review of Ecology, Evolution, and Systematics*, 49, 379–408.
- , BUTLER, R. J., LINDGREN, J. and SMITH, A. S. 2009. Mesozoic marine tetrapod diversity: mass extinctions and temporal heterogeneity in geological megabiases affecting vertebrates. *Proceedings of the Royal Society B: Biological Sciences*, 277, 829–834
- and BUTLER, R. J. 2011. Uncovering the diversification history of marine tetrapods: ecology influences the effect of geological sampling biases. *Geological Society, London, Special Publications*, 358, 191–208.
- and MANNION, P. D. 2012. Multi-variate models are essential for understanding vertebrate diversification in deep time. *Biology Letters*, 8, 127–130.
- , RICH, T. H., VICKERS-RICH, P. and HALL, M. 2012. Theropod fauna from Southern Australia indicates high polar diversity and climate-driven dinosaur provinciality. *PLoS ONE*, 7.
- and UPCHURCH, P. 2013. Diversity trends in the establishment of terrestrial vertebrate ecosystems: Interactions between spatial and temporal sampling biases. *Geology*, 41, 43–46.
- , CAMPIONE, N. E., CARRANO, M. T., MANNION, P. D., SULLIVAN, C., UPCHURCH, P. and EVANS, D. C. 2014. Rates of Dinosaur Body Mass Evolution Indicate 170 Million Years of Sustained Ecological Innovation on the Avian Stem Lineage. *PLoS Biology*, 12, e1001853

-
- , BUTLER, R. J., ALROY, J., MANNION, P. D., CARRANO, M. T. and LLOYD, G. T. 2016. Near-stasis in the long-term diversification of Mesozoic tetrapods. *PLoS Biology*, 14, 1–27.
- , HUNT, G., CARRANO, M. T. and CAMPIONE, N. 2018. Cope's rule and the adaptive landscape of dinosaur body size evolution. *Palaeontology*, 61, 13–48.
- BENTON, M. J. 1983. Dinosaur Success in the Triassic: A Noncompetitive Ecological Model. *The Quarterly Review of Biology*, 58, 29–51.
- . 1985. Mass extinction among non-marine tetrapods. *Nature*, 316, 811–814.
- . 1993. *The Fossil Record 2*. Chapman and Hall, London.
- . 1995. Diversification and Extinction in the History of Life. *Science*, 268, 52–58.
- . 2001. Biodiversity on land and in the sea. *Geological Journal*, 36, 211–230.
- . 2004. Origin and relationships of Dinosauria. In WEISHAMPEL, D. B., DODSON, P. and OSMOLSKA, H. (eds.) *The Dinosauria*, University of California Press, Berkeley, California, 7–19 pp.
- . 2010. The origins of modern biodiversity on land. *Philosophical Transactions of the Royal Society B: Biological Sciences*, 365, 3667–3679.
- , RUTA, M., DUNHILL, A. M. and SAKAMOTO, M. 2013. The first half of tetrapod evolution, sampling proxies, and fossil record quality. *Palaeogeography, Palaeoclimatology, Palaeoecology*, 372, 18–41.
- , DUNHILL, A. M., LLOYD, G. T. and MARX, F. G. 2011. Assessing the quality of the fossil record: insights from vertebrates. *Geological Society, London, Special Publications*, 358, 63–94.

- , BERNARDI, M. and KINSELLA, C. 2018. The Carnian Pluvial Episode and the origin of dinosaurs. *Journal of the Geological Society*, 175, 1019–1026.
- BERNARDI, M., GIANOLLA, P., PETTI, F. M., MIETTO, P. and BENTON, M. J. 2018. Dinosaur diversification linked with the Carnian Pluvial Episode. *Nature Communications*, 9, 1499.
- BLOMBERG, S. P., GARLAND, T. and IVES, A. R. 2003. Testing for phylogenetic signal in comparative data: Behavioral traits are more labile. *Evolution*, 57, 717–745.
- BONAPARTE, J. F. 1982. Faunal Replacement in the Triassic of South America. *Journal of Vertebrate Paleontology*, 2, 362–371.
- BONUSO, N. 2007. Shortening the Gap Between Modern Community Ecology and Evolutionary Paleoecology. *Palaios*, 22, 455–456.
- BRIGGS, D. E. G. 2003. The Role of Decay and Mineralization in the Preservation of Soft-Bodied Fossils. *Annual Review of Earth and Planetary Sciences*, 31, 275–301.
- BROCKLEHURST, N., UPCHURCH, P., MANNION, P. D. and O’CONNOR, J. 2012. The completeness of the fossil record of Mesozoic birds: Implications for early avian evolution. *PLoS ONE*, 7, e39056.
- , KAMMERER, C. F., FRÖBISCH, J. 2013. The early evolution of synapsids, and the influence of sampling on their fossil record. *Paleobiology* 39, 470–490.
- . 2015. A simulation-based examination of residual diversity estimates as a method of correcting for sampling bias. *Palaeontologia Electronica*, 18, 1–15.
- . 2015. The early evolution of synapsida (Vertebrata, Amniota) and the quality

- of their fossil record. Doctoral thesis. Humbolt University of Berlin.
- , RUTA, M., MÜLLER, J., FRÖBISCH, J. 2015. Elevated extinction rates as a trigger for diversification rate shifts: Early amniotes as a case study. *Scientific Reports*, 5, 17104
- , DAY, M. O., RUBIDGE, B. S. and FRÖBISCH, J. 2017. Olson's Extinction and the latitudinal biodiversity gradient of tetrapods in the Permian. *Proceedings of the Royal Society B: Biological Sciences*, 284, 20170231.
- , DUNNE, E. M., CASHMORE, D. D. and FRBISCH, J. 2018. Physical and environmental drivers of Paleozoic tetrapod dispersal across Pangaea. *Nature Communications*, 9, 5216
- BROWN, C. M., EVANS, D. C., CAMPIONE, N. E., O'BRIEN, L. J. and EBERTH, D. A. 2013. Evidence for taphonomic size bias in the Dinosaur Park Formation (Campa- nian, Alberta), a model Mesozoic terrestrial alluvial-paralic system. *Palaeogeog- raphy, Palaeoclimatology, Palaeoecology*, 372, 108–122.
- BRUSATTE, S. L., BENTON, M. J., RUTA, M. and LLOYD, G. T. 2008a. Superiority, competition, and opportunism in the evolutionary radiation of dinosaurs. *Science*, 321, 1485–1488.
- , BENTON, M. J., RUTA, M. and LLOYD, G. T. 2008b. The first 50 Myr of di- nosaur evolution: macroevolutionary pattern and morphological disparity. *Biology Letters*, 4, 733–736.
- , NESBITT, S. J., IRMIS, R. B., BUTLER, R. J., BENTON, M. J. and NORELL, M. A. 2010. The origin and early radiation of dinosaurs. *Earth-Science Reviews*, 101, 68–100.

- , NIEDŹWIEDZKI, G. and BUTLER, R. J. 2011. Footprints pull origin and diversification of dinosaur stem lineage deep into Early Triassic. *Proceedings of the Royal Society B: Biological Sciences*, 278, 1107–1113.
- BURNHAM, K. P. and ANDERSON, D. R. 2002. *Model Selection and Multimodel Inference*. Springer, New York.
- BUSH, A. M., MARKEY, M. J. and MARSHALL, C. R. 2004. Removing bias from diversity curves: the effects of spatially organized biodiversity on sampling-standardization. *Paleobiology*, 30, 666–686.
- BUTLER, M. A. and KING, A. A. 2004. Phylogenetic comparative analysis: A modeling approach for adaptive evolution. *American Naturalist*, 164, 683–695.
- BUTLER, R. J., BENSON, R. B. J., CARRANO, M. T., MANNION, P. D. and UPCHURCH, P. 2011a. Sea level, dinosaur diversity and sampling biases: investigating the ‘common cause’ hypothesis in the terrestrial realm. *Proceedings of the Royal Society B: Biological Sciences*, 278, 1165–1170.
- , BRUSATTE, S. L., REICH, M., NESBITT, S. J., SCHOCH, R. R. and HORNUNG, J. J. 2011b. The sail-backed reptile *Ctenosauriscus* from the latest Early Triassic of Germany and the timing and biogeography of the early archosaur radiation. *PLoS ONE*, 6, e25693.
- , BRUSATTE, S. L., ANDRES, B. and BENSON, R. B. J. 2012. How do geological sampling biases affect studies of morphological evolution in deep time? A case study of pterosaur (Reptilia: Archosauria) disparity. *Evolution*, 66, 147–162.
- , BENSON, R. B. J. and BARRETT, P. M. 2013. Pterosaur diversity: Untangling the influence of sampling biases, Lagerstätten, and genuine biodiversity signals. *Palaeogeography, Palaeoclimatology, Palaeoecology*, 372, 78–87.

- BUTTON, D. J., LLOYD, G. T., EZCURRA, M. D. and BUTLER, R. J. 2017. Mass extinctions drove increased global faunal cosmopolitanism on the supercontinent Pangaea. *Nature Communications*, 8, 733.
- CABREIRA, S. F., KELLNER, A. W. A., DIAS-DA-SILVA, S., ROBERTO DA SILVA, L., BRONZATI, M., MARSOLA, J. C. de A., MÜLLER, R. T., BITTENCOURT, J. de S., BATISTA, B. J. A., RAUGUST, T., CARRILHO, R., BRODT, A. and LANGER, M. C. 2016. A Unique Late Triassic Dinosauromorph Assemblage Reveals Dinosaur Ancestral Anatomy and Diet. *Current Biology*, 26, 3090–3095.
- CARRASCO, M. A. 2013. The impact of taxonomic bias when comparing past and present species diversity. *Palaeogeography, Palaeoclimatology, Palaeoecology*, 372, 130–137.
- CARVALHO, I. de S., DE GASPARINI, Z. B., SALGADO, L., DE VASCONCELLOS, F. M. and MARINHO, T. da S. 2010. Climate's role in the distribution of the Cretaceous terrestrial Crocodyliformes throughout Gondwana. *Palaeogeography, Palaeoclimatology, Palaeoecology*, 297, 252–262.
- CASCALES-MIÑANA B, CLEAL, C. J. DIEZ, J. B. 2013. What is the best way to measure extinction? A reflection from the palaeobotanical record. *Earth-Science Reviews*, 124, 126–147.
- , ———. 2014. The plant fossil record reflects just two great extinction events. *Terra Nova*, 26, 195–200.
- , DIEZ, J. B. GERRIENNE, P., CLEAL, C. J. 2016. A palaeobotanical perspective on the great end-Permian biotic crisis. *Historical Biology*, 28, 1066-1074.
- CELIS, A. de, NARVÁEZ, I. and ORTEGA, F. 2019. Spatiotemporal palaeodiversity patterns of modern crocodiles (Crocodyliformes: Eusuchia). *Zoological Journal of*

- the Linnean Society*, 1–22.
- CHAO, A. and JOST, L. 2012. Coverage-based rarefaction and extrapolation: Standardizing samples by completeness rather than size. *Ecology*, 93, 2533–2547.
- CHIARENZA, A. A., MANNION, P. D., LUNT, D. J., FARNSWORTH, A., JONES, L. A., KELLAND, S. J. and ALLISON, P. A. 2019. Ecological niche modelling does not support climatically-driven dinosaur diversity decline before the Cretaceous/Paleogene mass extinction. *Nature Communications*, 10.
- CHOWN, S. L. and GASTON, K. J. 2000. Areas, cradles and museums: the latitudinal gradient in species richness. *Trends in Ecology and Evolution*, 15, 311–315.
- CLACK, J. A. 2012. *Gaining ground: The origin and evolution of tetrapods* Second Edition. Indiana University Press, Indiana, USA.
- , BENNETT, C. E., CARPENTER, D. K., DAVIES, S. J., FRASER, N.C., KEARSEY, T. I., MARSHALL, J. E. A., MILLWARD, D., OTOO, B. K. A., REEVES, E. J., ROSS, A. J., RUTA, M., SMITHSON, K. Z., SMITHSON, T. R., WALSH, S. A. 2016. Phylogenetic and environmental context of a Tournaisian tetrapod fauna. *Nature Ecology and Evolution*, 1, 0001.
- CLAPHAM, M. E., KARR, J. A., NICHOLSON, D. B., ROSS, A. J., MAYHEW, P. J. 2016. Ancient origin of high taxonomic richness among insects. *Proceedings of the Royal Society B: Biological Sciences*, 283, 20152476.
- CLAVEL, J., ESCARGUEL, G. and MERCERON, G. 2015. mvMORPH: An R package for fitting multivariate evolutionary models to morphometric data. *Methods in Ecology and Evolution*, 6, 1311–1319.
- CLEAL, C. J. and THOMAS, B. A. 1999. Tectonics, tropical forest destruction and

- global warming in the Late Palaeozoic. *Acta Palaeobotanica*, 2, 17–19.
- and ———. 2005. Palaeozoic tropical rainforests and their effect on global climates: Is the past the key to the present? *Geobiology*, 3, 13–31.
- , OPLUSTIL, S, THOMAS, B. A, TENCHOV, Y. 2009. Pennsylvanian vegetation and climate in tropical Variscan Euramerica. *Episodes* 34, 3–12.
- , ———, ———, ———. 2009. Late Moscovian terrestrial biotas and palaeoenvironments of Variscan Euramerica. *Netherlands Journal of Geoscience*, 88, 181–278.
- , UHL, D., CASCALES-MIÑANA, B., THOMAS, B. A., BASHFORTH, A. R., KING, S. C. and ZODROW, E. L. 2012. Plant biodiversity changes in Carboniferous tropical wetlands. *Earth-Science Reviews*, 114, 124–155.
- CLEARY, T. J., MOON, B. C., DUNHILL, A. M. and BENTON, M. J. 2015. The fossil record of ichthyosaurs, completeness metrics and sampling biases. *Palaeontology*, 58, 521–536.
- , BENSON, R. B. J., EVANS, S. E. and BARRETT, P. M. 2018. Lepidosaurian diversity in the Mesozoic – Palaeogene: the potential roles of sampling biases and environmental drivers. *Royal Society Open Science*, 5, 171830.
- CLOSE, R. A., BENSON, R. B. J., UPCHURCH, P. and BUTLER, R. J. 2017. Controlling for the species-area effect supports constrained long-term Mesozoic terrestrial vertebrate diversification. *Nature Communications*, 8, 15381.
- , EVERS, S. W., ALROY, J. and BUTLER, R. J. 2018. How should we estimate diversity in the fossil record? Testing richness estimators using sampling-standardised discovery curves. *Methods in Ecology and Evolution*, 9, 1386–1400.

- , BENSON, R. B. J., ALROY, J., BEHRENSMEYER, A. K., BENITO, J., CARRANO, M. T., CLEARY, T. J., DUNNE, E. M., MANNION, P. D., UHEN, M. D. and BUTLER, R. J. 2019. Diversity dynamics of Phanerozoic terrestrial tetrapods at the local-community scale. *Nature Ecology and Evolution*, 3, 590–597.
- COATES, M. I., RUTA, M., FRIEDMAN, M. 2008. Ever since Owen: Changing perspectives on the early evolution of tetrapods. *Annual Review of Ecology, Evolution, and Systematics*, 39, 571–592.
- COOPER, N. and PURVIS, A. 2010. Body size evolution in mammals: complexity in tempo and mode. *The American Naturalist*, 175, 727–738.
- COPE ED. 1873. On some new Batrachia and fishes from the Coal Measures of Linton, Ohio. *Proceedings of the Academy of Natural Science of Philadelphia*, 340-343.
- COPE ED. 1874. Supplement to the extinct Batrachia and Reptilia of North America. I. Catalogue of the air-breathing Vertebrata from the Coal-measures of Linton, Ohio. *Transactions of the American Philosophical Society*, 15, 261-278.
- COPE ED. 1875. Supplement to the Extinct Batrachia and Reptilia of North America I. Catalogue of the Air Breathing Vertebrata from the Coal Measures of Linton, Ohio. *Transactions of the American Philosophical Society*, New Series 15, 261-278.
- COPE ED. 1882. Third contribution to the history of the Vertebrata of the Permian formation of Texas. *Proceedings of the American Philosophical Society*, 20, 447-461
- CRAMPTON, J. S., BEU, A. G., COOPER, R. A., JONES, C. M., MARSHALL, B. and MAXWELL, P. A. 2003. Estimating the rock volume bias in paleobiodiversity studies. *Science*, 301, 358–360.

- CUTBILL, J. L. and FUNNEL, B. M. 1967. Numerical analysis of the fossil record. In HARLAND, W. B., HOLAND, C. H., HOUSE, M. R., HUGHES, N. F., REYNOLDS, A. B., RUDWICK, M. J. S., SATTERTHWAITE, G. E., TARLO, B. H. and WILLEY, E. C. (eds.) *The Fossil Record*, Geological Society of London, London.
- DAL CORSO, J., RUFFELL, A. and PRETO, N. 2018. The Carnian Pluvial Episode (Late Triassic): New insights into this important time of global environmental and biological change. *Journal of the Geological Society*, 175, 986–988.
- DARWIN, C. 1859. *On the Origin of Species by Means of Natural Selection, or Preservation of Favoured Races in the Struggle for Life*. John Murray, London.
- DAY, M. O., RAJEZANI, J., BOWRING, S. A., SADLER, P. M., ERWIN, D. H., ABDALA, F., RUBRIDGE, B. S. 2015. When and how did the terrestrial mid-Permian mass extinction occur? Evidence from the tetrapod record of the Karoo Basin, South Africa. *Proceedings of the Royal Society B: Biological Sciences*, 282, 20150834.
- DEAN, C. D., MANNION, P. D. and BUTLER, R. J. 2016. Preservational bias controls the fossil record of pterosaurs. *Palaeontology*, 59, 225–247.
- DEBUYSSCHERE, M., GHEERBRANT, E. and ALLAIN, R. 2015. Earliest known European mammals: A review of the Morganucodonta from Saint-Nicolas-de-Port (Upper Triassic, France). *Journal of Systematic Palaeontology*, 13, 825–855.
- DRISCOLL, D. A., DUNHILL, A. M., STUBBS, T. L. and BENTON, M. J. 2019. The mosasaur fossil record through the lens of fossil completeness. *Palaeontology*, 62, 51–75.
- DUNHILL, A. M., HANNISDAL, B. and BENTON, M. J. 2014. Disentangling rock record bias and common-cause from redundancy in the British fossil record. *Nature Communications*, 5, 4818.

- , ———, BROCKLEHURST, N. and BENTON, M. J. 2018. On formation-based sampling proxies and why they should not be used to correct the fossil record. *Palaeontology*, 61, 119–132.
- DUNNE, E. M., CLOSE, R. A., BUTTON, D. J., BROCKLEHURST, N., CASHMORE, D. D., LLOYD, G. T. and BUTLER, R. J. 2018. Diversity change during the rise of tetrapods and the impact of the ‘Carboniferous rainforest collapse’. *Proceedings of the Royal Society B: Biological Sciences*, 285, 20172730.
- EAGLE, R. A., ENRIQUEZ, M., GRELLET-TINNER, G., PÉREZ-HUERTA, A., HU, D., TÜTKEN, T., MONTANARI, S., LOYD, S. J., RAMIREZ, P., TRIPATI, A. K., KOHN, M. J., CERLING, T. E., CHIAPPE, L. M. and EILER, J. M. 2015. Isotopic ordering in eggshells reflects body temperatures and suggests differing thermophysiology in two Cretaceous dinosaurs. *Nature Communications*, 6, 1–11.
- ERWIN, D. H. 2009. Climate as a Driver of Evolutionary Change. *Current Biology*, 19, R575–R583.
- EVANS, D. C., MADDIN, H. C., REISZ, R. R. 2009. A Re-Evaluation of Sphenacodontid Synapsid Material from the Lower Permian Fissure Fills near Richards Spur, Oklahoma. *Palaeontology* 52, 219-227.
- EZCURRA, M. D. 2016. The phylogenetic relationships of basal archosauromorphs, with an emphasis on the systematics of proterosuchian archosauriforms. *PeerJ*, 4, e1778.
- . 2017. A new early coelophysoid neotheropod from the late triassic of north-western Argentina. *Ameghiniana*, 54, 506–538.
- FARA, E. and BENTON, M. J. 2000. The Fossil Record of Cretaceous Tetrapods. *Palaios*, 15, 161–165.

- FARNSWORTH, A., LUNT, D. J. and VALDES, P. J. 2019. Past East Asian monsoon evolution controlled by palaeogeography, not CO₂. *Science Advances*, (in press).
- FASTOVSKY, D. E., HUANG, Y., HSU, J., MARTIN-MCNAUGHTON, J., SHEEHAN, P. M. and WEISHAMPEL, D. B. 2004. Shape of Mesozoic dinosaur richness. *Geology*, 32, 877–880.
- FELSENSTEIN, J. 1985. Phylogenies and the Comparative Method. *The American Naturalist*, 125, 1–15.
- FENTON, I. S., PEARSON, P. N., JONES, T. D., FARNSWORTH, A., LUNT, D. J., MARKWICK, P. and PURVIS, A. 2016. The impact of Cenozoic cooling on assemblage diversity in planktonic foraminifera. *Philosophical Transactions of the Royal Society B: Biological Sciences*, 371, 20150224.
- FOOTE, M. 1994. Temporal Variation in Extinction Risk and Temporal Scaling of Extinction Metrics. *Paleobiology*, 20, 424–444.
- FOSTER, G. L., ROYER, D. L. and LUNT, D. J. 2017. Future CO₂ and climate warming potentially unprecedented in 420 million years. *Nature Communications*, 8, 14845.
- FRASER, D. 2017. Can latitudinal richness gradients be measured in the terrestrial fossil record? *Paleobiology*, 43, 479–494.
- FRIEDMAN, M. and SALLAN, L. C. 2012. Five hundred million years of extinction and recovery: A phanerozoic survey of large-scale diversity patterns in fishes. *Palaeontology*, 55, 707–742.
- FRITSCH, A. 1875. Über die Fauna der Gaskohle des Pilsner und Rakonitzer Beckens. *Sitzungs-Berichte der königlichen böhmischen Gellschaft der Wissenschaften Prag*, 70-79.

- FRITSCH, A. 1876 Über die Fauna der Gaskohle des Pilsner und Rakonitzer Beckens. *Sitzungs-Berichte der königlichen böhmischen Gellschaft der Wissenschaften Prag*, 70-78.
- FRÖBISCH, J. 2008. Global taxonomic diversity of anomodonts (Tetrapoda, Therapsida) and the terrestrial rock record across the Permian-Triassic boundary. *PLoS ONE*, 3, e3733.
- . 2013. Vertebrate diversity across the end-Permian mass extinction — Separating biological and geological signals. *Palaeogeography, Palaeoclimatology, Palaeoecology*, 372, 50–61.
- GODOY, P. L., BENSON, R. B. J., BRONZATI, M. and BUTLER, R. J. 2019. The multi-peak adaptive landscape of crocodylomorph body size evolution. *BMC Evolutionary Biology*, 19, 167.
- GOLOBOFF, P. A, FARRIS, J. S., NIXON, K. C. 2008. TNT, a free program for phylogenetic analysis. *Cladistics*, 24, 774-786.
- GOOD, I. J. 1953. The population frequencies of species and the estimation of population. *Biometrika*, 40, 237–64.
- GOUGH, D. O. 1981. Solar interior structure and luminosity variations. *Solar Physics*, 74, 21–34.
- GRADY, J. M., ENQUIST, B., DETTWEILER-ROBINSON, E., WRIGHT, N. and SMITH, F. 2014. Evidence for mesothermy in dinosaurs. *Science*, 344, 1268–1272.
- GRIGG, G. and KIRSHNER, D. 2015. *Biology and Evolution of Crocodylians*. Ithaca and London, Cornell University Press (Comstock Publishing Associates and CSIRO Publications).

- GUILLERME, T. 2018. dispRity: A modular R package for measuring disparity. *Methods in Ecology and Evolution*, 9, 1755–1763.
- and COOPER, N. 2018. Time for a rethink: time sub-sampling methods in disparity-through-time analyses. *Palaeontology*, 61, 481–493.
- HANNISDAL, B. and PETERS, S. E. 2011. Phanerozoic Earth System Evolution and Marine Biodiversity. *Science*, 334, 1121–1124.
- HARMON, L. J., LOSOS, J. B., JONATHAN DAVIES, T., GILLESPIE, R. G., GITTLEMAN, J. L., BRYAN JENNINGS, W., KOZAK, K. H., MCPEEK, M. A., MORENO-ROARK, F., NEAR, T. J., PURVIS, A., RICKLEFS, R. E., SCHLUTER, D., SCHULTE, J. A., SEEHAUSEN, O., SIDLAUSKAS, B. L., TORRES-CARVAJAL, O., WEIR, J. T. and MOOERS, A. T. 2010. Early bursts of body size and shape evolution are rare in comparative data. *Evolution*, 64, 2385–2396.
- HILLEBRAND, H. 2004. On the Generality of the Latitudinal Diversity Gradient. *The American Naturalist*, 163, 192–211.
- HOLLAND, S. M. 2018. Diversity and tectonics: Predictions from neutral theory. *Paleobiology*, 44, 219–236.
- and SCLAFANI, J. A. 2015. Phanerozoic diversity and neutral theory. *Paleobiology*, 41, 369–376.
- HSIEH, T. C., MA, K. H. and CHAO, A. 2016. iNEXT: an R package for rarefaction and extrapolation of species diversity (Hill numbers). *Methods in Ecology and Evolution*, 7, 1451–1456.
- HUBBELL, S. P. 2001. *The Unified Neutral Theory of Biodiversity and Biogeography*. Princeton University Press.

- HUNT, G. 2012. Measuring rates of phenotypic evolution and the inseparability of tempo and mode. *Paleobiology*, 38, 351–373.
- HUNT, G. and CARRANO, M. T. 2010. Models and methods for analyzing phenotypic evolution in lineages and clades. In ALROY J, H. G. (ed.) *Quantitative Methods in Paleobiology*, The Paleontological Society Paper, New Haven.
- HUNT, G., CRONIN, T. M. and ROY, K. 2005. Species-energy relationship in the deep sea: A test using the Quaternary fossil record. *Ecology Letters*, 8, 739–747.
- HURVICH, C. M. and TSAI, C. L. 1989. Regression and time series model selection in small samples. *Biometrika*, 76, 297–307.
- IRMIS, R. B., NESBITT, S. J., PADIAN, K., SMITH, N. D., TURNER, A. H., WOODY, D. and DOWNS, A. 2007. A Late Triassic Dinosauriform Assemblage from New Mexico and the Rise of Dinosaurs. *Science*, 317, 358–362.
- . 2011. Evaluating hypotheses for the early diversification of dinosaurs. *Earth and Environmental Science Transactions of the Royal Society of Edinburgh*, 101, 397–426.
- , MUNDIL, R., MARTZ, J. W. and PARKER, W. G. 2011. High-resolution U-Pb ages from the Upper Triassic Chinle Formation (New Mexico, USA) support a diachronous rise of dinosaurs. *Earth and Planetary Science Letters*, 309, 258–267.
- JABLONSKI, D., ROY, K., VALENTINE, J. W., PRICE, R. M. and ANDERSON, P. S. 2003. The impact of the Pull of the Recent on the history of marine diversity. *Science*, 300, 1133–1135.
- JONES, L. A., MANNION, P. D., FARNSWORTH, A., VALDES, P. J., KELLAND, S. J. and ALLISON, P. A. 2019. Coupling of palaeontological and neontological

- reef coral data improves forecasts of biodiversity responses under global climatic change. *Royal Society Open Science*, 6, 182111.
- JORDAN, S. M. R., BARRACLOUGH, T. G. and ROSINDELL, J. 2016. Quantifying the effects of the break up of Pangaea on global terrestrial diversification with neutral theory. *Philosophical Transactions of the Royal Society B: Biological Sciences*, 371, 20150221.
- KNOLL, F. 2005. The tetrapod fauna of the Upper Elliot and Clarens formations in the main Karoo Basin (South Africa and Lesotho). *Bulletin de la Societe Geologique de France*, 176, 81–91.
- KRÖGER, B. 2017. Changes in Latitudinal Diversity Gradient during the Great Ordovician Biodiversification Event. *Geology*, 46, 1–10.
- LANE, A., JANIS, C. M. and SEPKOSKI, J. J. 2005. Estimating paleodiversities: a test of the taxic and phylogenetic methods. *Paleobiology*, 31, 21–34.
- LANGER, M. C., RAMEZANI, J. and DA ROSA, Á. A. S. 2018. U-Pb age constraints on dinosaur rise from south Brazil. *Gondwana Research*, 57, 133–140.
- LANGER, M. C., EZCURRA, M. D., BITTENCOURT, J. S. and NOVAS, F. E. 2010. The origin and early evolution of dinosaurs. *Biological Reviews*, 85, 55–110.
- LEGENDRE, L. J., GUCROSSED D SIGNNARD, G., BOTHA-BRINK, J. and CUBO, J. 2016. Palaeohistological Evidence for Ancestral High Metabolic Rate in Archosaurs. *Systematic Biology*, 65, 989–996.
- LINDSTRÖM, S., IRMIS, R. B., WHITESIDE, J. H., SMITH, N. D., NESBITT, S. J. and TURNER, A. H. 2016. Palynology of the upper Chinle Formation in northern New Mexico, U.S.A.: Implications for biostratigraphy and terrestrial ecosystem change

- during the Late Triassic (Norian-Rhaetian). *Review of Palaeobotany and Palynology*, 225, 106–131.
- LLOYD, G. T. 2012. A refined modelling approach to assess the influence of sampling on palaeobiodiversity curves: new support for declining Cretaceous dinosaur richness. *Biology Letters*, 8, 123–126.
- . 2016. Estimating morphological diversity and tempo with discrete character-taxon matrices: implementation, challenges, progress, and future directions. *Biological Journal of the Linnean Society*, 118, 131–151.
- , BAPST, D. W., FRIEDMAN, M., DAVIS, K. E. 2016. Probabilistic divergence time estimation without branch lengths: dating the origins of dinosaurs, avian flight, and crown birds. *Biology Letters*, 12, 20160609.
- LONG, R. A. and MURRY, P. A. 1995. Late Triassic (Carnian and Norian) tetrapods from the southwestern United States. *New Mexico Museum of Natural History and Science Bulletin*, 4, 1–254.
- LUNT, D. J., FARNSWORTH, A., LOPTSON, C., L FOSTER, G., MARKWICK, P., O'BRIEN, C. L., PANCOST, R. D., ROBINSON, S. A. and WROBEL, N. 2015. Palaeogeographic controls on climate and proxy interpretation. *Climate of the Past*, 12, 1181–1198.
- MACARTHUR, R. H., WILSON, E. O. 1967. *The Theory of Island Biogeography*. Princeton NJ: Princeton University Press.
- MANNION, P. D., UPCHURCH, P., CARRANO, M. T. and BARRETT, P. M. 2011. Testing the effect of the rock record on diversity: A multidisciplinary approach to elucidating the generic richness of sauropodomorph dinosaurs through time. *Biological Reviews*, 86, 157–181.

- , BENSON, R. B. J., UPCHURCH, P., BUTLER, R. J., CARRANO, M. T. and BARRETT, P. M. 2012. A temperate palaeodiversity peak in Mesozoic dinosaurs and evidence for Late Cretaceous geographical partitioning. *Global Ecology and Biogeography*, 21, 898–908.
- , UPCHURCH, P., BENSON, R. B. J. and GOSWAMI, A. 2014. The latitudinal biodiversity gradient through deep time. *Trends in Ecology and Evolution*, 29, 42–50.
- , BENSON, R. B. J., CARRANO, M. T., TENNANT, J. P., JUDD, J. and BUTLER, R. J. 2015. Climate constrains the evolutionary history and biodiversity of crocodylians. *Nature Communications*, 6, 8438.
- MARCOT, J. D., FOX, D. L. and NIEBUHR, S. R. 2016. Late Cenozoic onset of the latitudinal diversity gradient of North American mammals. *Proceedings of the National Academy of Sciences*, 113, 7189–7194.
- MARKWICK, P. J. 1998. Paleontological Society Crocodylian Diversity in Space and Time: The Role of Climate in Paleoecology and its Implication for Understanding K / T Extinctions. *Paleobiology*, 24, 470–497.
- MARSH, A. D. and ROWE, T. B. 2018. Anatomy and systematics of the sauropodomorph *Sarhsaurus aurifontanalis* from the Early Jurassic Kayenta Formation. *PLoS ONE*, 13, e0204007
- MARTIN, J. E., AMIOT, R., LÉCUYER, C. and BENTON, M. J. 2014. Sea surface temperature contributes to marine crocodylomorph evolution. *Nature Communications*, 5, 1–7. MARTÍNEZ, R. N., APALDETTI, C., ALCOBER, O. A., COLOMBI, C. E., SERENO, P. C., FERNANDEZ, E., MALNIS, P. S., CORREA, G. A. and ABELIN, D. 2012. Vertebrate succession in the ischigualasto formation. *Journal*

- of Vertebrate Paleontology*, 32, 10–30.
- MARTÍNEZ, R. N. and APALDETTI, C. 2017. A late norian-rhaetian coelophysid neotheropod (dinosauria, saurischia) from the quebrada del barro formation, Northwestern Argentina. *Ameghiniana*, 54, 488–505.
- MATZKE, N. J. and WRIGHT, A. 2016. Inferring node dates from tip dates in fossil Canidae: The importance of tree priors. *Biology Letters*, 12.
- MAYHEW, P. J., JENKINS, G. B. and BENTON, T. G. 2008. A long-term association between global temperature and biodiversity, origination and extinction in the fossil record. *Proceedings of the Royal Society B: Biological Sciences*, 275, 47–53.
- MCALLISTER REES, P., NOTO, C. R., PARRISH, J. M. and PARRISH, J. T. 2004. Late Jurassic climates, vegetation, and dinosaur distributions. *Journal of Geology*, 112, 643–653.
- MCKAY, M. D., BECKMAN, R. J. and CONOVER, W. J. 1979. Comparison of Three Methods for Selecting Values of Input Variables in the Analysis of Output from a Computer Code. *Technometrics*, 21, 239–245.
- MCPHEE, B. W. and CHOINIERE, J. N. 2018. The osteology of *Pulanesaura eocollum*: Implications for the inclusivity of Sauropoda (Dinosauria). *Zoological Journal of the Linnean Society*, 182, 830–861.
- , BENSON, R. B. J., BOTHA-BRINK, J., BORDY, E. M. and CHOINIERE, J. N. 2018. A Giant Dinosaur from the Earliest Jurassic of South Africa and the Transition to Quadrupedality in Early Sauropodomorphs. *Current Biology*, 28, 3143–3151.
- MILLER, A. I. and FOOTE, M. 1996. Calibrating the Ordovician radiation of marine life:

- Implications for Phanerozoic diversity trends. *Paleobiology*, 22, 304–309.
- . 2000. Conversations about Phanerozoic global diversity. *Paleobiology*, 26, 53–73.
- MITTELBACH, G. G., SCHEMSKE, D. W., CORNELL, H. V., ALLEN, A. P., BROWN, J. M., BUSH, M. B., HARRISON, S. P., HURLBERT, A. H., KNOWLTON, N., LESSIOS, H. A., MCCAIN, C. M., MCCUNE, A. R., MCDADE, L. A., MCPEEK, M. A., NEAR, T. J., PRICE, T. D., RICKLEFS, R. E., ROY, K., SAX, D. F., SCHLUTER, D., SOBEL, J. M. and TURELLI, M. 2007. Evolution and the latitudinal diversity gradient: Speciation, extinction and biogeography. *Ecology Letters*, 10, 315–331.
- MÜLLER, R. T., DA ROSA, Á. A. S., ROBERTO DA SILVA, L., AIRES, A. S. S., PACHECO, C. P., PAVANATTO, A. E. B. and DIAS-DA-SILVA, S. 2015. Wachholz, a new exquisite dinosaur-bearing fossiliferous site from the Upper Triassic of southern Brazil. *Journal of South American Earth Sciences*, 61, 120–128.
- MÜLLER, R. T., LANGER, M. C. and DIAS-DA-SILVA, S. 2018. An exceptionally preserved association of complete dinosaur skeletons reveals the oldest long-necked sauropodomorphs. *Biology Letters*, 14, 20180633.
- MUSCENTE, A. D., SCHIFFBAUER, J. D., BROCE, J., LAFLAMME, M., O'DONNELL, K., BOAG, T. H., MEYER, M., HAWKINS, A. D., HUNTLEY, J. W., MCNAMARA, M., MACKENZIE, L. A., STANLEY, G. D., HINMAN, N. W., HOFMANN, M. H. and XIAO, S. 2017. Exceptionally preserved fossil assemblages through geologic time and space. *Gondwana Research*, 48, 164–188.
- NESBITT, S. J., SMITH, N. D., IRMIS, R. B., TURNER, A. H., DOWNS, A. and NORELL, M. A. 2009. A complete skeleton of a Late triassic Saurischian and the early evolution of dinosaurs. *Science*, 326, 1530–1533.

- , BARRETT, P. M., WERNING, S., SIDOR, C. A. and CHARIG, A. J. 2013. The oldest dinosaur? A Middle Triassic dinosauriform from Tanzania. *Biology Letters*, 9, 20120949.
- , BUTLER, R. J., EZCURRA, M. D., BARRETT, P. M., STOCKER, M. R., ANGIELCZYK, K. D., SMITH, R. M. H., SIDOR, C. A., NIEDŹWIEDZKI, G., SENNIKOV, A. G. and CHARIG, A. J. 2017. The earliest bird-line archosaurs and the assembly of the dinosaur body plan. *Nature*, 544, 484–487.
- NORELL, M. A. and NOVACEK, M. J. 1992. Congruence Between Superpositional and Phylogenetic Patterns: Comparing Cladistic Patterns With Fossil Records. *Cladistics*, 8, 319–337.
- NOTO, C. R. and GROSSMAN, A. 2010. Broad-scale patterns of late jurassic dinosaur paleoecology. *PLoS ONE*, 5, 1–11.
- OLSEN, P. E., KENT, D. V, SUES, H., KOEBERL, C. and HUBER, H. 2002. Ascent of Dinosaurs Linked to an Iridium Anomaly at the Triassic-Jurassic Boundary. *Science*, 296, 1305–1307.
- ORME, D., FRECKLETON, R., THOMAS, G., PETZOLDT, T., FRITZ, S., ISAAC, N. and PEARSE, W. 2018. caper: Comparative Analyses of Phylogenetics and Evolution in R. R package version 1.0.1.
- PARDO, J. D., SZOSTAKIWSKYJ, M., AHLBERG, P. E., ANDERSON, J. S. 2017. Hidden morphological diversity among early tetrapods. *Nature*, 546, 642-645.
- , SMALL, B. J., MILNER, A. R. and HUTTENLOCKER, A. K. 2019. Carboniferous–Permian climate change constrained early land vertebrate radiations. *Nature Ecology and Evolution*, 3, 200–206.

- PEARSON, M. R., BENSON, R. B. J., UPCHURCH, P., FRÖBISCH, J. and KAMMERER, C. F. 2013. Reconstructing the diversity of early terrestrial herbivorous tetrapods. *Palaeogeography, Palaeoclimatology, Palaeoecology*, 372, 42–49.
- PETERS, S. E., FOOTE, M. 2001. Biodiversity in the Phanerozoic: a reinterpretation. *Paleobiology*, 27, 583–601.
- . 2005. Geologic constraints on the macroevolutionary history of marine animals. *Proceedings of the National Academy of Sciences of the United States of America*, 102, 12326–31.
- and HEIM, N. a. 2010. The geological completeness of paleontological sampling in North America. *Paleobiology*, 36, 61–79.
- and HEIM, N. A. 2011. Macrostratigraphy and macroevolution in marine environments: testing the common-cause hypothesis. *Geological Society, London, Special Publications*, 358, 95–104.
- , ZHANG, C., LIVNY, M., RE, C. 2014. A machine reading system for assembling synthetic paleontological databases. *PLoS ONE*, 9, 1–22.
- and MCCLENNEN, M. 2015. The Paleobiology Database application programming interface. *Paleobiology*, 42, 1–7.
- PHILLIPS, J. 1860. *Life on the earth: its origin and succession*. Macmillan, Cambridge, England.
- PIE, M. R., CAMPOS, L. L. F., MEYER, A. L. S. and DURAN, A. 2017. The evolution of climatic niches in squamate reptiles. *Proceedings of the Royal Society B: Biological Sciences*, 284, 20170268.

- PINHEIRO, J., BATES, D., DEBROY, S. and R CORE TEAM. 2019. nlme: Linear and Nonlinear Mixed Effects Models. R package version 3.1-141. POWELL, M. G. 2007. Latitudinal diversity gradients for brachiopod genera during late Palaeozoic time: Links between climate, biogeography and evolutionary rates. *Global Ecology and Biogeography*, 16, 519–528.
- PRESTON, F. W. 1962. The canonical distribution of commonness and rarity: Part I. *Ecology*, 43, 185–215 and 410–432.
- PRETTO, F. A., LANGER, M. C. and SCHULTZ, C. L. 2019. A new dinosaur (Saurischia: Sauropodomorpha) from the Late Triassic of Brazil provides insights on the evolution of sauropodomorph body plan. *Zoological Journal of the Linnean Society*, 185, 388–416.
- PURNELL, M. A., DONOGHUE, P. J. C., GABBOTT, S. E., MCNAMARA, M. E., MURDOCK, D. J. E. and SANSOM, R. S. 2018. Experimental analysis of soft-tissue fossilization: opening the black box. *Palaeontology*, 61, 317–323.
- R CORE TEAM. 2017. R: A Language and Environment for Statistical Computing. Vienna, Austria. <https://www.r-project.org/>
- . 2018. R: A Language and Environment for Statistical Computing. Vienna, Austria. <https://www.r-project.org/>
- RAGAN, M. 1992 Phylogenetic inference based on matrix representation of trees. *Molecular Phylogenetics and Evolution*, 1, 113-126.
- RAHBEK, C., GOTELLI, N. J., COLWELL, R. K., ENTSMINGER, G. L., RANGEL, T. F. L. V. B. and GRAVES, G. R. 2007. Predicting continental-scale patterns of bird species richness with spatially explicit models. *Proceedings of the Royal Society B: Biological Sciences*, 274, 165–174.

- RAUP, D. M. 1972. Taxonomic Diversity during the Phanerozoic. *Science*, 177, 1065–1071.
- . 1976. Species Diversity in the Phanerozoic: An Interpretation Species diversity in the Phanerozoic: an interpretation. *Paleobiology*, 2, 289–297.
- . and SEPKOSKI, J. J. 1982. Mass Extinctions in the Marine Fossil Record. *Science*, 215, 10–12.
- REVELL, L. J. 2012. phytools: An R package for phylogenetic comparative biology (and other things). *Methods in Ecology and Evolution*, 3, 217–223.
- ROMER, A. S. 1928 Vertebrate faunal horizons in the Texas Permo-Carboniferous red beds. *University of Texas Bulletin*, 2801, 67-108.
- RONQUIST, F., KLOPFSTEIN, S., VILHELMSSEN, L., SCHULMEISTER, S., MURRAY, D. L. and RASNITSYN, A. P. 2012a. A total-evidence approach to dating with fossils, applied to the early radiation of the hymenoptera. *Systematic Biology*, 61, 973–999.
- , TESLENKO, M., VAN DER MARK, P., AYRES, D. L., DARLING, A., HÖHNA, S., LARGET, B., LIU, L., SUCHARD, M. A. and HUELSENBECK, J. P. 2012b. Mrbayes 3.2: Efficient Bayesian phylogenetic inference and model choice across a large model space. *Systematic Biology*, 61, 539–542.
- ROSE, P. J., FOX, D. L., MARCOT, J. and BADGLEY, C. 2011. Flat latitudinal gradient in Paleocene mammal richness suggests decoupling of climate and biodiversity. *Geology*, 39, 163–166.
- ROSENZWEIG, M. L. 1995. *Species diversity in space and time*. Cambridge University Press, New York.

- ROSINDELL, J. and CORNELL, S. J. 2007. Species-area relationships from a spatially explicit neutral model in an infinite landscape. *Ecology Letters*, 10, 586–595.
- , WONG, Y. and ETIENNE, R. S. 2008. A coalescence approach to spatial neutral ecology. *Ecological Informatics*, 3, 259–271.
- ROWE, T. B., SUES, H. D. and REISZ, R. R. 2011. Dispersal and diversity in the earliest North American sauropodomorph dinosaurs, with a description of a new Taxon. *Proceedings of the Royal Society B: Biological Sciences*, 278, 1044–1053.
- RUTA, M., PISANI, D., LLYOD, G. T., BENTON, M. J. 2007. A supertree of Temnospondyli: cladogenetic patterns in the most species-rich group of early tetrapods. *Proceedings of the Royal Society B: Biological Sciences*, 274, 3087–3095.
- , COATES, M. I. 2007. Dates, nodes and character conflict: Addressing the Lissamphibian origin problem. *Journal of Systematic Palaeontology*, 5, 69–122.
- , BENTON, M. J. 2008. Calibrated diversity, tree topology and the mother of mass extinctions: the lesson of temnospondyls. *Palaeontology*, 51, 1261–1288.
- , BOTHA-BRINK, J., MITCHELL, S. A. and BENTON, M. J. 2013. The radiation of cynodonts and the ground plan of mammalian morphological diversity. *Proceedings of the Royal Society B: Biological Sciences*, 280, 20131865
- SAHNEY, S. and BENTON, M. J. 2008. Recovery from the most profound mass extinction of all time. *Proceedings of the Royal Society B: Biological Sciences*, 275, 759–765.
- and ———. 2017. The impact of the pull of the Recent on the fossil record of tetrapods. *Evolutionary Ecology Research*, 18, 7–23.

- , ——— and FALCON-LANG, H. J. 2010. Rainforest collapse triggered Carboniferous tetrapod diversification in Euramerica. *Geology*, 38, 1079–1082.
- SAKAMOTO, M., VENDITTI, C. and BENTON, M. J. 2016. ‘Residual diversity estimates’ do not correct for sampling bias in palaeodiversity data. *Methods in Ecology and Evolution*, 2, 1–7.
- SANDER, P. M., CHRISTIAN, A., CLAUSS, M., FECHNER, R., GEE, C. T., GRIEBELER, E. M., GUNGA, H. C., HUMMEL, J., MALLISON, H., PERRY, S. F., PREUSCHOFT, H., RAUHUT, O. W. M., REMES, K., TÜTKEN, T., WINGS, O. and WITZEL, U. 2011. Biology of the sauropod dinosaurs: The evolution of gigantism. *Biological Reviews*, 86, 117–155.
- SANDERS, H. L. 1968. Marine Benthic Diversity: A Comparative Study. *The American Naturalist*, 102, 243–282.
- SAUPE, E. E., FARNSWORTH, A., LUNT, D. J., SAGOO, N., PHAM, K. V. and FIELD, D. J. 2019. Climatic shifts drove major contractions in avian latitudinal distributions throughout the Cenozoic. *Proceedings of the National Academy of Sciences*, 116, 12895–12900.
- SEPKOSKI, J. J., BAMBACH, R. K., RAUP, D. M. and VALENTINE, J. W. 1981. Phanerozoic marine diversity and the fossil record. *Nature*, 293, 435–437.
- SERTICH, J. J. W. and LOEWEN, M. A. 2010. A new basal sauropodomorph dinosaur from the lower Jurassic Navajo sandstone of southern Utah. *PLoS ONE*, 5, e9789.
- SETON, M., MÜLLER, R. D., ZAHIROVIC, S., GAINA, C., TORSVIK, T., SHEPHARD, G., TALSMA, A., GURNIS, M., TURNER, M., MAUS, S. and CHANDLER, M. 2012. Global continental and ocean basin reconstructions since 200Ma. *Earth-Science Reviews*, 113, 212–270.

- SEYMOUR, R. S., BENNETT-STAMPER, C. L., JOHNSTON, S. D., CARRIER, D. R. and GRIGG, G. C. 2004. Evidence for endothermic ancestors of crocodiles at the stem of archosaur evolution. *Physiological and Biochemical Zoology*, 77, 1051–1067.
- SHIRLEY, M. H. and AUSTIN, J. D. 2017. Did Late Pleistocene climate change result in parallel genetic structure and demographic bottlenecks in sympatric Central African crocodiles, *Mecistops* and *Osteolaemus*? *Molecular Ecology*, 26, 6463–6477.
- SHUBIN, N. H. and SUES, H. 1991. Biogeography of Early Mesozoic Continental Tetrapods: Patterns and Implications. *Paleobiology*, 17, 214–230.
- SIDOR, C. A., VILHENA, D. A., ANGIELCZYK, K. D., HUTTENLOCKER, A. K., NESBITT, S. J., PEECOOK, B. R., STEYER, J. S., SMITH, R. M. H., TSUJI, L. A. 2013. Provincialization of terrestrial faunas following the end-Permian mass extinction. *Proceedings of the National Academy of Sciences*, 110, 8129–8133.
- SIGNOR, P. W. and LIPPS, J. H. 1982. Sampling bias, gradual extinction patterns and catastrophes in the fossil record. *Geological Society of America Special Publication*, 190, 291–296.
- SLATER, G. J. 2013. Phylogenetic evidence for a shift in the mode of mammalian body size evolution at the Cretaceous-Palaeogene boundary. *Methods in Ecology and Evolution*, 4, 734–744.
- SMITH, A. B. 2001. Large-scale heterogeneity of the fossil record: implications for Phanerozoic biodiversity studies. *Philosophical Transactions of the Royal Society B: Biological Sciences*, 356, 351–367.
- and MCGOWAN, A. J. 2007. The shape of the Phanerozoic marine palaeodiversity curve: How much can be predicted from the sedimentary rock record of

- Western Europe? *Palaeontology*, 50, 765–774.
- , LLOYD, G. T. and MCGOWAN, A. J. 2012. Phanerozoic marine diversity: rock record modelling provides an independent test of large-scale trends. *Proceedings of the Royal Society B: Biological Sciences*, 279, 4489–4495.
- SMITH, F. A., BOYER, A. G., BROWN, J. H., COSTA, D. P., DAYAN, T., ERNEST, S. K. M., EVANS, A. R., FORTELIUS, M., GITTLEMAN, J. L., HAMILTON, M. J., HARDING, L. E., LINTULAAKSO, K., LYONS, S. K., MCCAIN, C., OKIE, J. G., SAARINEN, J. J., SIBLY, R. M., STEPHENS, P. R., THEODOR, J. and UHEN, M. D. 2010. The evolution of maximum body size of terrestrial mammals. *Science*, 330, 1216–1219.
- STADLER, T. 2010. Sampling-through-time in birth-death trees. *Journal of Theoretical Biology*, 267, 396–404.
- STARRFELT, J. and LIOW, L. H. 2016. How many dinosaur species were there? Fossil bias and true richness estimated using a poisson sampling model. *Philosophical Transactions of the Royal Society B: Biological Sciences*, 371, 20150219.
- TENNANT, J. P., CHIARENZA, A. A. and BARON, M. 2018. How has our knowledge of dinosaur diversity through geologic time changed through research history? *PeerJ*, 2018, 1–42.
- THOMPSON, S. E. D. 2019. Theory and models of biodiversity in fragmented landscapes. Imperial College London and National University of Singapore.
- TUCKER, M. E. and BENTON, M. J. 1982. Triassic environments, climates and reptile evolution. *Palaeogeography, Palaeoclimatology, Palaeoecology*, 40, 361–379.
- UHL, D. and CLEAL, C. J. 2010. Late Carboniferous vegetation change in lowland and intramontane basins in Germany. *International Journal of Coal Geology*, 83,

318–328.

- UPCHURCH, P., MANNION, P. D., BENSON, R. B. J., BUTLER, R. J. and CARRANO, M. T. 2011. Geological and anthropogenic controls on the sampling of the terrestrial fossil record: A case study from the dinosauria. *Geological Society Special Publication*, 358, 209–240.
- UYEDA, J. C., CAETANO, D. S. and PENNELL, M. W. 2015. Comparative Analysis of Principal Components Can be Misleading. *Systematic Biology*, 64, 677–689.
- VALDES, P. J., ARMSTRONG, E., BADGER, M. P. S., BRADSHAW, C. D., BRAGG, F., CRUCIFIX, M., DAVIES-BARNARD, T., DAY, J., FARNSWORTH, A., GORDON, C., HOPCROFT, P. O., KENNEDY, A. T., LORD, N. S., LUNT, D. J., MARZOCCHI, A., PARRY, L. M., POPE, V., ROBERTS, W. H. G., STONE, E. J., TOURTE, G. J. L. and WILLIAMS, J. H. T. 2017. The BRIDGE HadCM3 family of climate models: HadCM3@Bristol v1.0. *Geoscientific Model Development*, 10, 3715–3743.
- VALENTINE, J. W. 1969. Patterns of taxonomic and ecological structure of the shelf benthos during Phanerozoic time. *Palaeontology*, 12, 684–709.
- VERGNON, R., DULVY, N. K. and FRECKLETON, R. P. 2009. Niches versus neutrality: Uncovering the drivers of diversity in a species-rich community. *Ecology Letters*, 12, 1079–1090.
- VILHENA, D. A. and SMITH, A. B. 2013. Spatial Bias in the Marine Fossil Record. *PLoS ONE*, 8, e74470.
- WALKER, F. M., DUNHILL, A. M., WOODS, M. A., NEWELL, A. J. and BENTON, M. J. 2017. Assessing sampling of the fossil record in a geographically and stratigraphically constrained dataset: The chalk group of Hampshire, southern UK. *Journal of the Geological Society*, 174, 509–521.

- WALL, P. D., IVANY, L. C. and WILKINSON, B. H. 2009. Revisiting Raup: exploring the influence of outcrop area on diversity in light of modern sample-standardization techniques. *Paleobiology*, 35, 146–167.
- WANG, Y. M., YOU, H. L. and WANG, T. 2017. A new basal sauropodiform dinosaur from the Lower Jurassic of Yunnan Province, China. *Scientific Reports*, 7, 1–11.
- WHITESIDE, J. H., GROGAN, D. S., OLSEN, P. E. and KENT, D. V. 2011. Climatically driven biogeographic provinces of Late Triassic tropical Pangea. *Proceedings of the National Academy of Sciences of the United States of America*, 108, 8972–8977.
- , LINDSTRÖM, S., IRMIS, R. B., GLASSPOOL, I. J., SCHALLER, M. F., DUNLAVEY, M., NESBITT, S. J., SMITH, N. D. and TURNER, A. H. 2015. Extreme ecosystem instability suppressed tropical dinosaur dominance for 30 million years. *Proceedings of the National Academy of Sciences of the United States of America*, 112, 7909–7913.
- WILLIG, M. R., KAUFMAN, D. M. and STEVENS, R. D. 2003a. Latitudinal Gradients of Biodiversity: Pattern, Process, Scale, and Synthesis. *Annual Review of Ecology, Evolution, and Systematics*, 34, 273–309.
- WILLIG, M. R., KAUFMAN, D. M. and STEVENS, R. D. 2003b. Latitudinal Gradients of Biodiversity: Pattern, Process, Scale, and Synthesis. *Annual Review of Ecology, Evolution, and Systematics*, 34, 273–309.
- WILLIS, K. J. and BIRKS, H. J. B. 2006. What is natural? The need for a long-term perspective in biodiversity conservation. *Science*, 314, 1261–1265.
- WRIGHT, D. F. 2017. Bayesian estimation of fossil phylogenies and the evolution of early to middle Paleozoic crinoids (Echinodermata). *Journal of Paleontology*, 91,

799–814.

- ZHANG, C., STADLER, T., KLOPFSTEIN, S., HEATH, T. A. and RONQUIST, F. 2016. Total-Evidence Dating under the Fossilized Birth-Death Process. *Systematic Biology*, 65, 228–249.
- ZHANG, Q. N., YOU, H. L., WANG, T. and CHATTERJEE, S. 2018. A new sauropodiform dinosaur with a 'sauropodan' skull from the Lower Jurassic Lufeng Formation of Yunnan Province, China. *Scientific Reports*, 8, 13464.

Appendices

A | Early tetrapod diversity

The material below is the supplementary information that accompanied the publication "Diversity change during the rise of tetrapods and the impact of the 'Carboniferous rain-forest collapse", the main text of which is Chapter 2 of this thesis. The full text and supplementary files can be found at: <https://royalsocietypublishing.org/doi/full/10.1098/rspb.2017.2730>

A.1 Implementing SQS through iNEXT

We standardised our diversity samples using Shareholder Quorum Subsampling (SQS; Alroy 2010a; 2010b; 2010c, 2014), a method also known in the ecological literature as 'coverage-based rarefaction' (Chao and Jost, 2012). SQS standardises diversity samples to equal coverage of the underlying frequency distribution. Coverage is a measure of sample completeness that can be estimated using Good's u (Good, 1953), and corresponds to the fraction of individuals in the underlying sampling pool that are made up of the species present in the sample. Standardising your diversity data to a coverage (or "quorum" level) of 0.5 will therefore tell you how many species you would expect to find, on average, in a sample of 50% of the individuals drawn at random from the underlying sampling pool or assemblage.

We implemented SQS using the R package iNEXT (Hsieh *et al.*, 2016). iNEXT im-

plements SQS using the multinomial probability formulae derived by Chao and Jost (2012), rather than the exact algorithm described by Alroy (2014). These two approaches yield identical results when subsampling or 'interpolating' (drawing down) the data. However, iNEXT also allows extrapolating the data to equal coverage using the well-known Chao1/2 formulae (Chao, 1984; see Chao and Jost, 2012 for further details). This allows interpolated, observed and extrapolated estimates to be seamlessly united into a single coverage-based rarefaction curve (Figure 3A). Following the recommendation of Hsieh *et al.* (2016), we only used extrapolated estimates based on extrapolated sample sizes that were less than twice as large as the true sample size.

Coverage-based rarefaction curves, in which standardised diversity is plotted as a function of coverage, show how among-assembly differences in the shape of the abundance distribution affect relative richness at different levels of coverage. For example, a very uneven assembly might be less diverse than a more even assembly at low levels of coverage, but more diverse at higher levels of coverage (because most of the individuals in the uneven assembly are made up of the most common species). Therefore, coverage-based rarefaction curves, like sizebased rarefaction curves, can cross a number of times depending on how abundance distributions differ in shape. However, coverage-based rarefaction curves require smaller sample sizes to identify when crossing points occur (Chao and Jost, 2012). Combining interpolated, observed and extrapolated estimates allows us to generate diversity curves at higher levels of coverage, which makes maximal use of the available data and avoids discarding information from better-sampled assemblages (Chao and Jost, 2012).

A.2 Carboniferous and early Permian sampling

Sampling throughout this interval is uneven both temporally and spatially. In addition to the patterns discussed in the main text we also assessed correlation between species

Table A.1: The most speciose collections (=fossil localities) in the Paleobiology Database from the Tournaisian to Kungurian, and the method of sampling associated with each site. The total number of species per collection is shown alongside the proportion of the interval's total diversity each collection represents.

Collection	Interval	Formation	Total spp.	% of total interval richness	Sampling method
Coffee Creek, TX	Kungurian	Arroyo	36	34.90%	Multiple expeditions
Craddock Bonebed, TX	Kungurian	Arroyo	18	17.40%	Quarrying
Richard's Spur, OK	Kungurian	Garber	23	22.30%	Quarrying
Archer City Bonebed 1, TX	Artinskian	Putnam/ Archer	16	17.80%	Multiple expeditions
El Cobre Canyon, NM	Gzhelian	Cutler	15	25.40%	Multiple expeditions
Nyraňy, Czech Republic	Moscovian	Kladno	24	26.90%	Coal mine
Linton, OH	Moscovian	Upper Freeport	33	37.10%	Coal mine

Table A.2: Pearson's product moment correlation co-efficient (i.e. Pearson's r) showing the strength and direction of association between raw species richness and proxies for sampling (number of fossiliferous formations, number of collections [=fossil localities], and number of occupied equal-area 50 km² grid cells)

	No. species	Formations	Collections	Grid cells
No. species	-	0.518	0.764**	0.630
Formations	0.518	-	0.735*	0.696***
Collections	0.764**	0.735*	-	0.849*
Grid cells	0.630	0.696***	0.849*	-

* $p < 0.05$, ** $p < 0.01$, *** $p = 0.001$

richness and proxies for sampling. There is a weak correlation between species richness and the number of fossiliferous formations in each interval from the Tournaisian–Kungurian ($R_2 = 0.1251$, $p = 0.166$; Pearson's $r = 0.5183$) (Figure A1C). However, this result may be due to a small number of intervals (namely, the Moscovian, Artinskian, and Kungurian) where species richness is high relative to sampling. Exceptionally well-sampled sites contribute greatly to the total diversity in each of these intervals (Table A1).

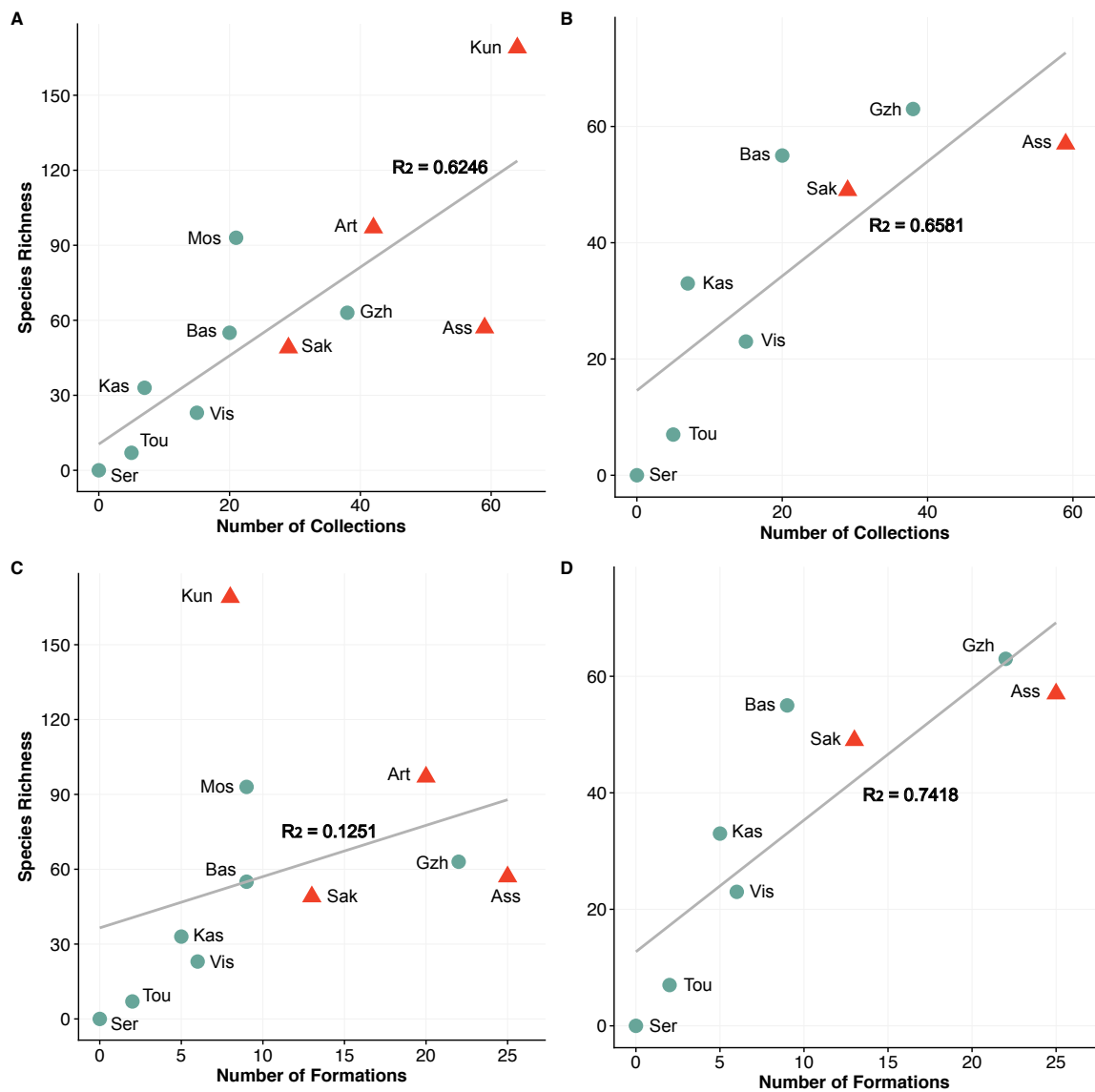


Figure A.1: Correlation between species richness and total collection counts (A-B) and total formation count (C-D) per interval, when all intervals are included (A and C) and when the three most well-sampled intervals (Moscovian, Artinskian, and Kungurian) are removed (B and D). Abbreviations of interval names: Tou-Tournaisian; Vis-Visean; -Ser-Serpukhovian; Bas-Bashkirian; Mos-Moscovian; Kas-Kasimovian; Gzh-Gzhelian; Ass-Asselian; Sak-Sakmarian; Art-Artinskian; Kun-Kungurian.

A.3 Phylogenetic Biogeographic Connectedness

We used the method of Button *et al.* (2017), which uses both geographic and phylogenetic information to quantify phylogenetic biogeographic connectedness (pBC) between regions containing tetrapod fauna (see Figure A2). We followed the procedure detailed in Button *et al.* and outline the details of our specific analyses below. Example code for these analyses can be found in the supplementary data files of the Button *et al.* paper.

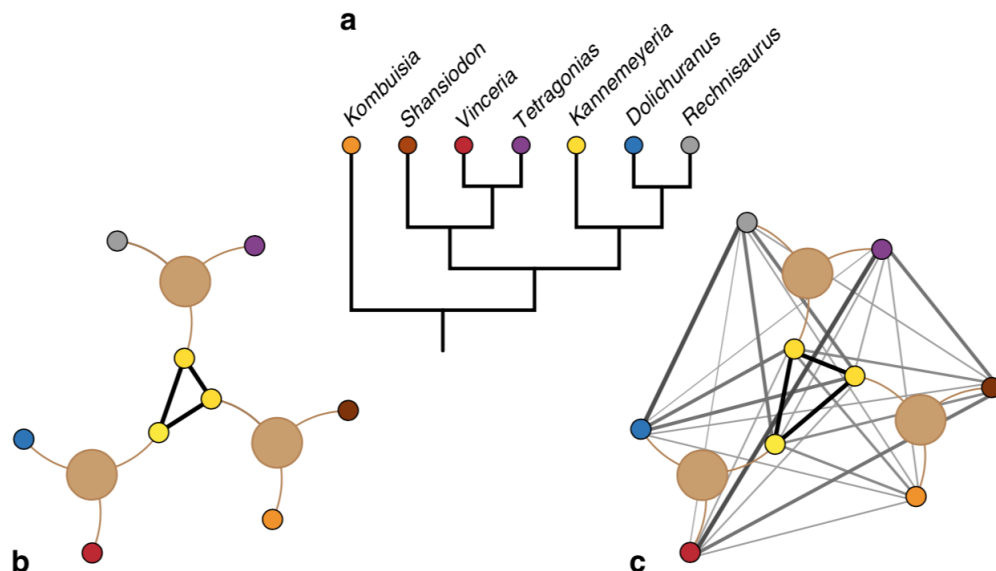


Figure A.2: Schematic illustration of network biogeography methods, reproduced with permission from Button *et al.* (2017). **a** Simplified phylogeny of Dicynodontia. **b, c** Taxon-locality networks. Localities are indicated by the large, pale brown circles, taxa are coloured as in **a**. Taxa are connected by brown lines to the locality at which they occur. **b** Rescaled non-phylogenetic biogeographic connectedness (BC) of Sidor *et al.* (2013). A single taxon, *Kannemeyeria* (yellow), is present at all three localities, resulting in a link of value = 1 (solid black line) between each locality. **c** Phylogenetic biogeographic connectedness (pBC), as proposed here. Links (grey lines) between taxa from different localities are weighted inversely to their phylogenetic relatedness. Line thickness and shade is proportional to the strength of the link (and thus inversely proportional to phylogenetic distance between the two taxa)

A.3.1 *Palaeogeographical regions*

As noted from our analyses of diversity and sampling through time, global sampling during this interval from the Carboniferous to early Permian is uneven, both temporally and spatially. However, with the inclusion of phylogenetic information, and the use of relatively broad geographical regions, interpretations made based upon these analyses quantifying biogeographic connectedness are less vulnerable to variations in sampling than those of previous workers (e.g. Sahney *et al.* 2010). The addition of geographical regions (originating in the countries India, Russia, and Brazil) in the early Permian that are not present in the Carboniferous, should logically increase the tendency towards a pattern of endemism. However, we see the opposite pattern in the early Permian where there is a trend towards cosmopolitanism. Additionally, we performed a sensitivity analysis by combining certain geographical regions (for example, B and C in the early Permian [Table A3]). In each case, the number of regions did not change our results.

A.3.2 *Early tetrapod supertree*

A time-calibrated informal species-level early tetrapod supertree was constructed by hand based on the most up-to-date phylogenetic analyses available for Carboniferous and early Permian terrestrial tetrapods (see online supplementary material). This supertree includes 325 taxa within the interval from the Tournaisian to Kungurian. This topology was used to produce 100 time-calibrated trees, in which polytomies were randomly resolved, using the *timePaleoPhy()* function of the *paleotree* package in R (Bapst, 2012). Trees were dated according to first occurrence dates with a minimum branch-length of 1 Myr. The phylogenetic biogeographic analyses were performed across all of these trees, in order to account for phylogenetic uncertainty.

Table A.3: Geographic clusters (A-G) as defined by k-means clustering of palaeocoordinates for all tetrapod occurrences from the Carboniferous (Tournaisian–Gzhelian) and early Permian (Asselian–Kungurian). Each cluster has been assigned a name in accordance with the approximate location on a modern map. Colours simply simply represent the different clusters and have no meaning beyond this.

	Carboniferous		Permian	
A	Eastern USA	West Virginia (in part), Alabama, Iowa	Mid USA	New Mexico, Colorado, Utah
B	Southern USA	Texas, New Mexico, Colorado, Oklahoma (in part), Kansas (in part)	Southern USA 1	Texas and Oklahoma: e.g. Garber, Belle Plains, and Admiral formations
C	Mid USA	Kansas (in part), West Virginia (in part), Illinois, Ohio, Pennsylvania, Oklahoma (in part)	Southern USA 2	Texas and Oklahoma: e.g. Arroyo, Vale, and Hennessey formations
D	Nova Scotia and Scotland	e.g. Joggins, East Kirkton	Eastern USA and Brazil	Including Ohio and West Virginia
E	Mainland Europe	France, Germany, Czech Republic	Europe	Czech Republic, Germany, Britain, France
F	British Isles	Ireland, England, Scotland (in part), and some localities in Nova Scotia (e.g. Point Edward)	India	Kashmir
G	Australia	(single locality)	Russia	

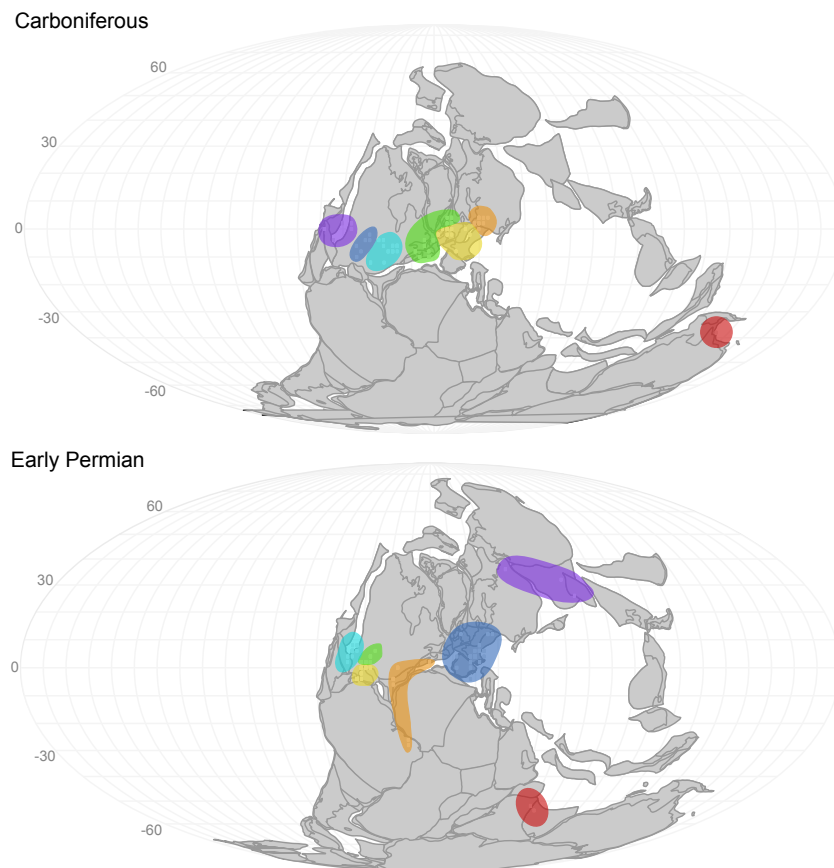


Figure A.3: Palaeomaps illustrating the locations of the geographic regions defined by cluster analysis in both the Carboniferous and early Permian for the biogeographic analyses of all tetrapod species.

The overall topology of the informal early tetrapod supertree follows that of Ruta *et al.* (2007) and Pardo *et al.* (2017). The phylogenetic tree of Anderson (2001) was used to place additional species of Lepospondyli on the supertree. Brocklehurst *et al.* (2015) provided a phylogenetic tree for amniotes (pelycosaur, parareptiles, eu-reptiles, and therapsids) and diadectamorphs. The temnospondyl portion of the tree came from a novel “metatree” (sensu Lloyd *et al.* 2016) of temnospondyls that extends a previous formal supertree (Ruta *et al.* 2007) for Temnospondyli as a whole. Here 102 published cladistic matrices were reanalysed under a parsimony optimality criterion and all possible most parsimonious solutions encoded as matrices using Baum and Ragan (Baum, 1992; Ragan, 1992) Matrix Representation with Parsimony (MRP). (These are available along with the original matrices and other metadata at [154](http://graemetl-</p></div><div data-bbox=)

loyd.com/matramph.html.) Taxa were reconciled against a master list of valid species (including some as yet unnamed OTUs), with supraspecific taxa being replaced by the valid constituent species that were also present as OTUs in other source matrices. The source matrices were combined with a taxonomic hierarchy to generate a single MRP matrix, with each source matrix weighted on their dependence and publication year (see Lloyd *et al.* 2016). After searching for the optimal topologies with TNT (Goloboff *et al.* 2008) 5,248 equally parsimonious trees were returned and a strict consensus produced. This tree was subsequently pruned of younger taxa not relevant to the current analyses.

B | Early tetrapods & neutral theory

These figures are supplementary to Chapter 3, "Tetrapod diversification and the 'Carboniferous rainforest collapse' under neutral theory".

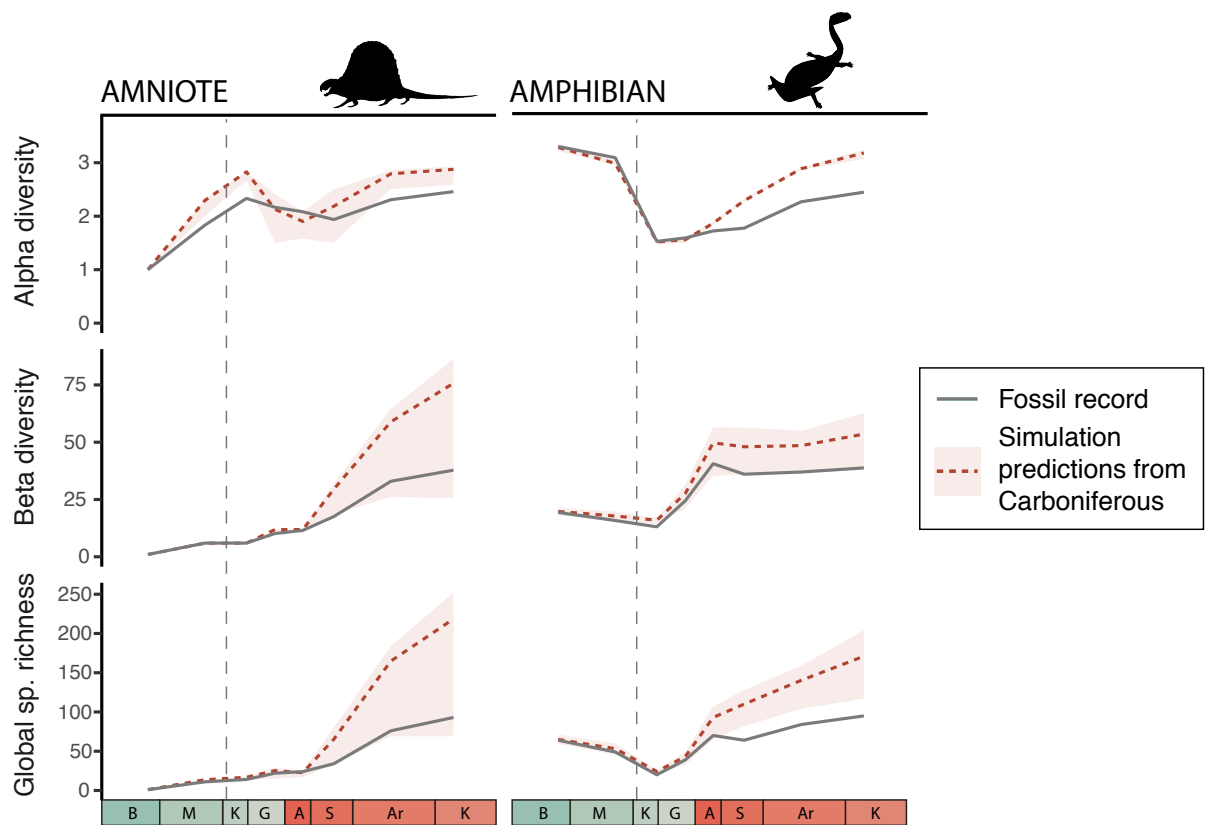


Figure B.1: Predictions of tetrapod diversity from a neutral model parameterised for Carboniferous diversity. Simulations were parameterised based solely on the Carboniferous. In this scenario there was no habitat loss due to the CRC. Three metrics of biodiversity are shown for both amphibians and amniotes from the Bashkirian to Kungurian from either simulated communities (red dashed line) or from empirical data (solid grey line). The shaded area represents the variation in the five best fitting simulations. The following abbreviations are used for intervals: "B" = Bashkirian, "M" = Moscovian, "K" = Kasimovian, "G" = Gzhelian, "A" = Asselian, "S" = Sakmarian, "Ar" = Artinskian and "K" = Kungurian.

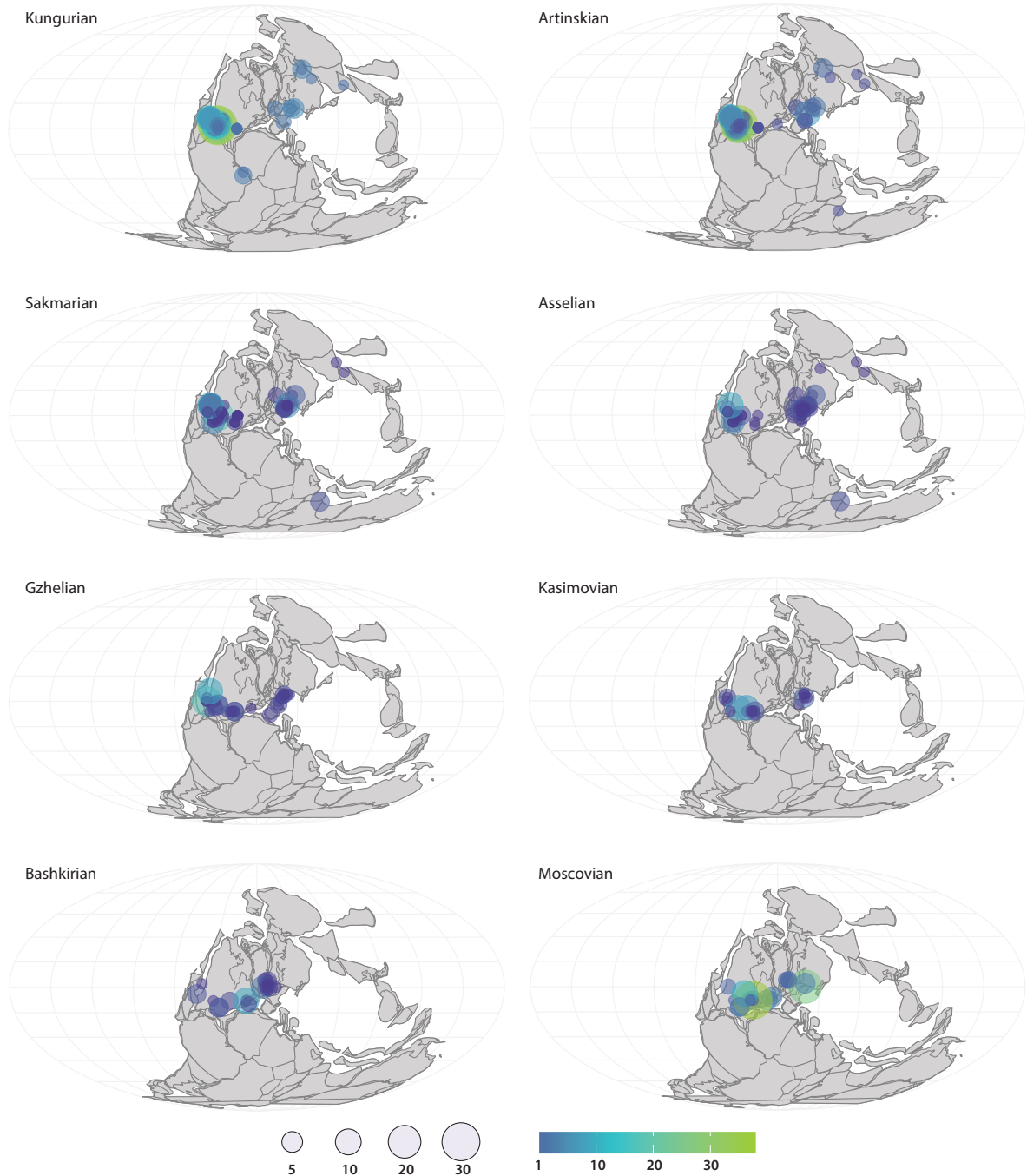


Figure B.2: Global palaeogeographical maps showing the localities of fossil sites in each stage of the late Carboniferous and early Permian. The size of each circle corresponds to the number of species found at each site (see size and colour legends).

C | Late Triassic latitudinal diversity

These figures and tables are supplementary to Chapter 4, "Latitudinal patterns of Late Triassic tetrapod diversity and climate"

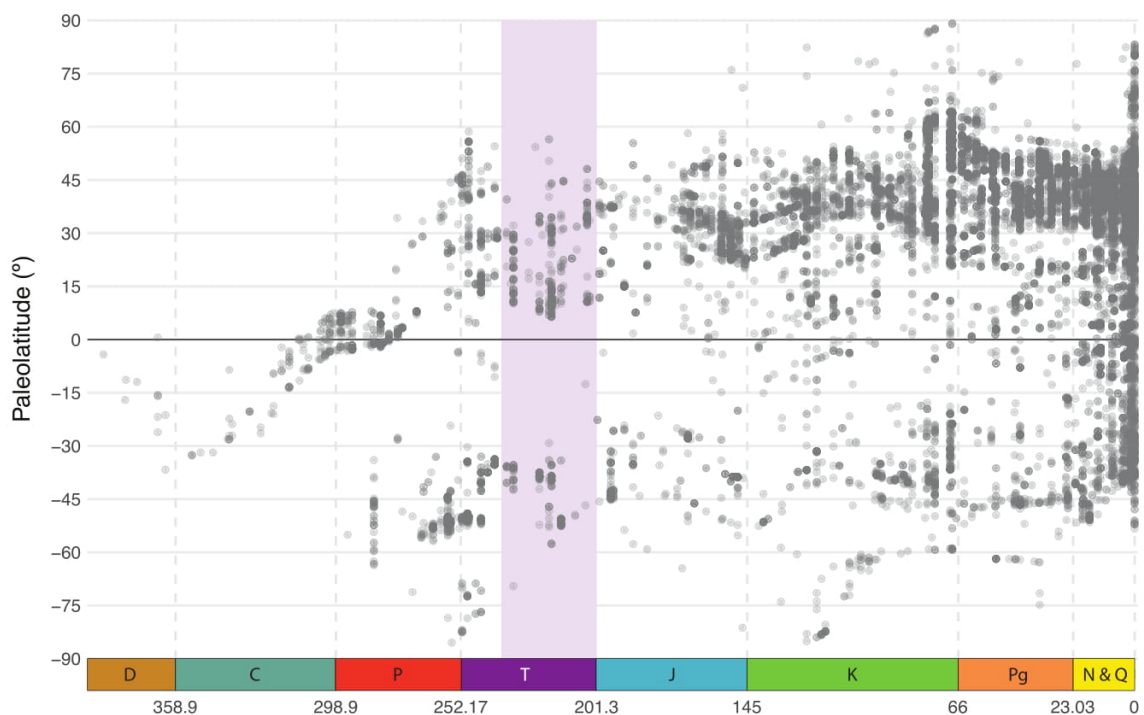


Figure C.1: Palaeolatitudinal positions of sampled tetrapod localities from the Devonian to the present day, with a shaded area highlighting the Late Triassic

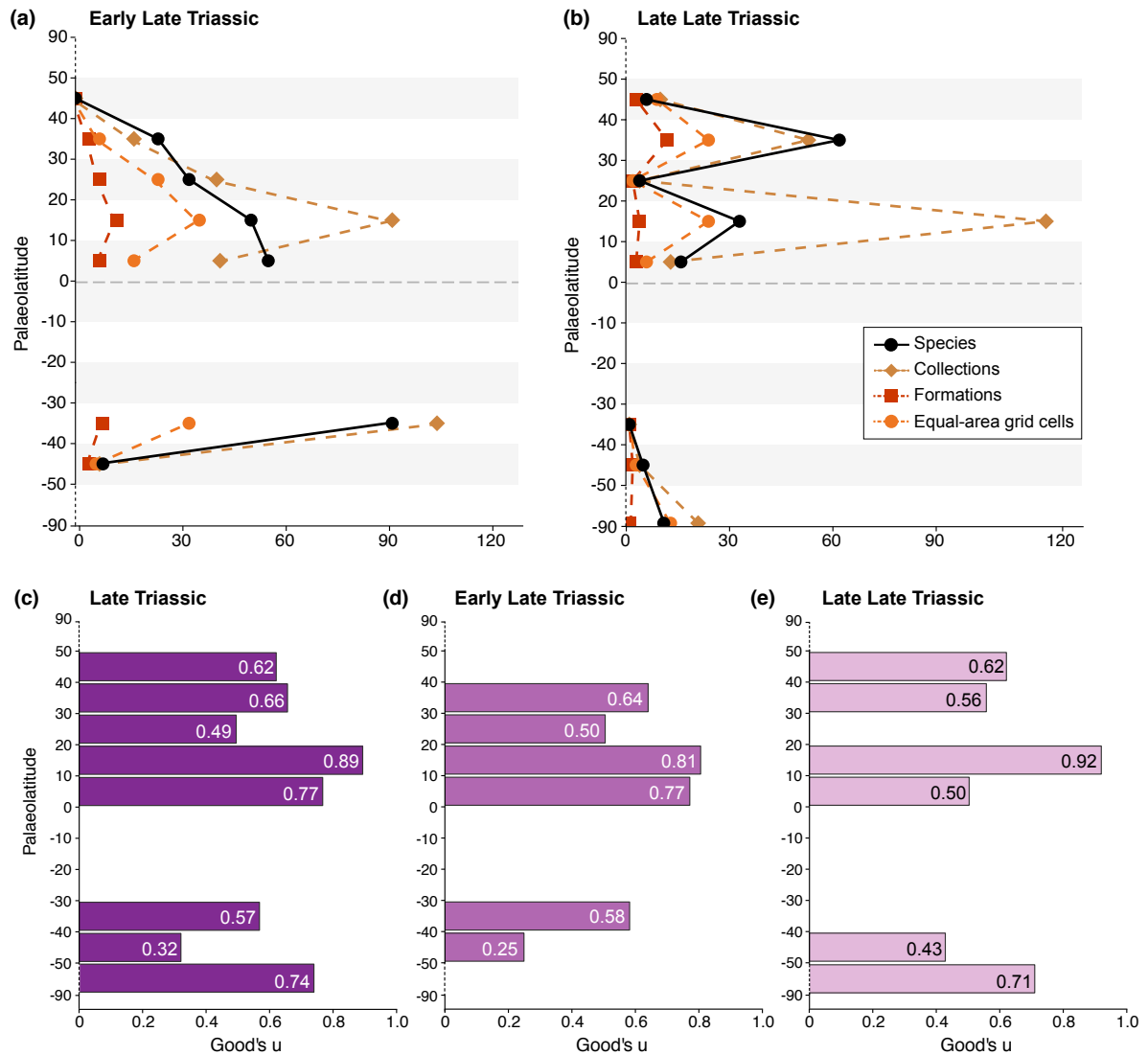


Figure C.2: Patterns of raw species richness and sampling during the (a) early Late Triassic and (b) late Late Triassic. Good's u (a measure of 'coverage') values for each palaeolatitude bin during (c) all stages of the Late Triassic, (d) the early Late Triassic and (e) the late Late Triassic.

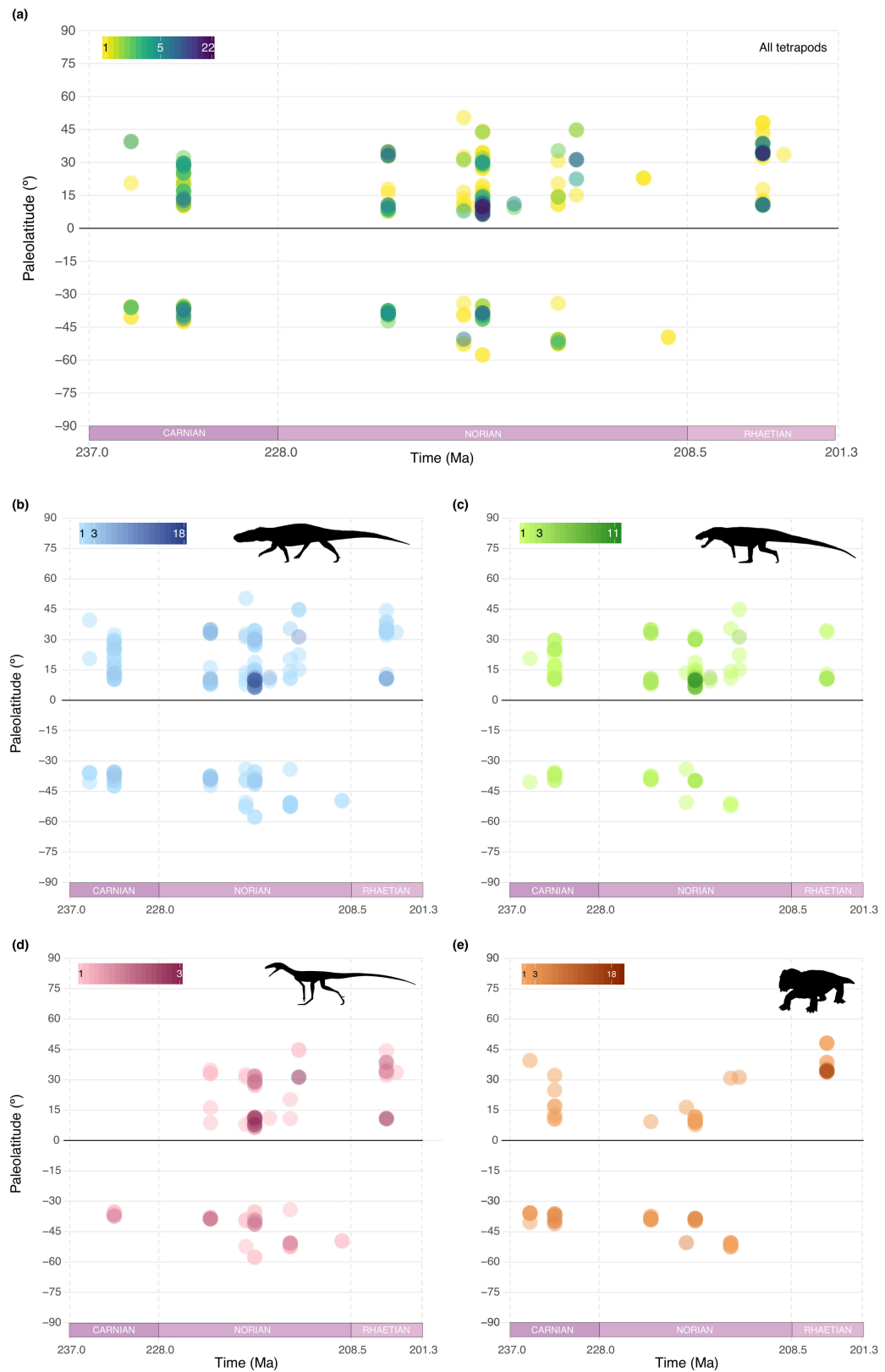


Figure C.3: Local richness (alpha diversity) across latitudes throughout the Late Triassic for (a) all tetrapods, (b) Archosauromorpha, (c) Pseudosuchia, (d) Avemetatarsalia, and (e) Synapsida. Images: phylopic.org.

Table C.1: Details of the occurrences contained within each of the richest collections (=fossil localities) during the Late Triassic

Collection	Location	Interval	Palaeo-latitude	Tetrapod richness*	Details of sampling
Saint Nicolas de Port	France	Rhaetian	34.2 N	22	This site has yielded the most abundant and diverse mammalian assemblage known from the Late Triassic (Debuysschere et al. 2015)
Placerias Quarry	AZ, USA	Norian	9.8 N	22	This site, which is part of the Chinle Formation, was discovered in 1930 by Charles Camp (UCMP) and has been extensively sampled ever since
Otis Chalk Quarry 3	TX USA	Norian	6.5 N	14	This is one of several quarries in the Otis Chalk, which is part of the Dockum formation. Fossils were first discovered here in the 1920s
Miller's Ranch Quarry	TX USA	Norian	7.8 N	12	This site was discovered by local residents and first excavated in 1977 by a group from Dallas Museum
Downs Quarry	AZ, USA	Norian	9.9 N	11	This quarry, discovered in 1980, lies close to Placerias quarry (approx. 72m east and 3m above)
Stinking Springs	AZ, USA	Norian	10.1 N	11	This is the richest of five sites from the region. It lies approximately 50km from Placerias quarry
Ghost Ranch Quarry	NM, USA	Rhaetian	10.8 N	10	Known for concentration of Coelophysis fossils, fossils from this site were first published on by Edwin Colbert in 1947
Faxinal do Soturno, Linha Sao Luiz	Brazil	Norian	-38.5 S	10	Most of the excavations on this site, located within the Caturrita Formation, have taken place in the last two decades

Table C.2: Correlation between palaeolatitude and four variables from the palaeoclimate model HadCM3L, namely mean annual surface temperature (MAT), mean annual precipitation (MAP), seasonal variation in temperature (SVT) and seasonal variation in precipitation (SVP), during the Late Triassic.

Climate variable	R ₂	t	p
MAT	0.785	1059.72	<0.001
MAP	0.028	31.701	<0.001
SVT	0.799	5.302	<0.001
SVP	0.064	4.66	<0.001

Table C.3: Likelihood ratio test results (test performed in R by running an ANOVA on GLS model outputs) for the top two best models of the GLS analysis

Regression model	df	AIC	BIC	Log Likelihood	p value
TBCs	4	48.208	54.964	-20.104	-
TBCs + MAT	5	50.204	58.648	-20.102	0.946

D | Early dinosaur evolution & climate I

The figures and tables on the following pages are supplementary to Chapter 5: "The role of climate in the early evolution of dinosaurs".

Table D.1: List of species and specimens (in alphabetical order) included in the informal dinosauriform supertree

Aardonyx celestae
Abrictosaurus consors
Agnosphitys cromhallensis
Alwalkeria maleriensis
Amygdalodon patagonicus
Anchisaurus polyzelus
Antetonitrus ingenipes
Arcusaurus pereirabdalorum
 Argentinian Heterodontosauridae indet.
 Arizona Scelidosaur
Asylosaurus yalensis
Bagualosaurus agudoensis
Barapasaurus tagorei
Berberosaurus liassicus
Blikanasaurus cromptoni
Buriolestes schultzi
Camelotia borealis
Chindesaurus bryansmalli
Chinshakiangosaurus chunghoensis
Coelophysis bauri
Coelophysis kayentakatae
Coelophysis rhodesiensis
Coloradisaurus brevis
Cryolophosaurus ellioti
Daemonosaurus chauliodus
Dilophosaurus wetherilli
Diodorus scytobrachion
Dracoraptor hanigani
Dracovenator regenti
Dromomeron gigas
Dromomeron gregorii
Dromomeron romeri
 Eagle Basin Silesaurid
Efraasia minor
Emausaurus ernsti
Eocursor parvus
Eodromaeus murphi
Eoraptor lunensis
Eshanosaurus deguchiianus
Eucnemesaurus entaxonis
Eucnemesaurus fortis
Eucoelophysis baldwini
 FMNH CUP 2089

FMNH CUP 2338
Glacialisaurus hammeri
Gojirasaurus quayi
Gongxianosaurus shibeiensis
Guaibasaurus candelariensis
Herrerasaurus ischigualastensis
Heterodontosaurus tucki
Ignavusaurus rachelis
Ignotosaurus fragilis
Isanosaurus attavipachi
Ixalerpeton polesinensis
Jaklapallisaurus asymmetrica
Jingshanosaurus xinwaensis
Kayenta heterodontosaurid
Kotasaurus yamanpalliensis
Lagerpetonidae indet.
Lamplughsaura dharmaramensis
Laquintasaura venezuelae
Lesothosaurus diagnosticus
Lessemsaurus sauropoides
Liliensternus liliensterni
Lophostropheus airelensis
Lucianovenator bonoi
Lufengosaurus huenei
Lycorhinus angustidens
Manidens condorensis
Massospondylus carinatus
Massospondylus kaalae
Melanorosaurus readi
Mussaurus patagonicus
Nambalia roychowdhurii
NHMUK R14161
NHMUK RU A100
Ohmdenosaurus liasicus
Otis Chalk Silesaurid
Pampadromaeus barberenai
Panguraptor lufengensis
Panphagia protos
Pantydraco caducus
Pegomastax africanus
Petrified Forest Silesaurid
Pisanosaurus mertii
Plateosauravus cullingworthi
Plateosaurus engelhardti
Plateosaurus gracilis
Podokesaurus holyokensis

Poreba Herrerasauridae indet.
Poreba Theropoda indet.
Powellvenator podocitus
Pradhania gracilis
Procompsognathus triassicus
Pulanesaura eocollum
Riojasaurus incertus
Ruehleia bedheimensis
Sacisaurus agudoensis
Saltopus elginensis
Sanjuansaurus gordilloi
Sarhsaurus aurifontanalisis
Saturnalia tupiniquim
Scelidosaurus harrisonii
Scutellosaurus lawleri
Segisaurus halli
Seitaad ruessi
Shake 'n' Bake taxon
Silesaurus opolensis
Sinosaurus triassicus
Staurikosaurus pricei
Tawa hallae
Tazoudasaurus naimi
Technosaurus smalli
Thecodontosaurus antiquus
Unaysaurus tolentinoi
Vulcanodon karibaensis
Vulcanodontidae indet.
Xingxiulong chengi
Xixiposaurus suni
Yunnanosaurus huangi
Zupaysaurus rougieri

Table D.2: Recently-described (2017–2019) dinosaur species added to the Button *et al.* (2017) supertree of amniote species. The species' positions within the tree were based on the approximate phylogenetic positions outlined in the original publications listed here.

Species	Reference	Age	Clade
<i>Ixalerpeton polesinensis</i>	Cabreira et al. (2016)	Carnian/Norian	Lagerpetidae
<i>Lucianovenator bonoi</i>	Martinez & Apaldetti (2017)	Norian	Coelophysidae
<i>Powellvenator podocitus</i>	Ezcurra (2017)	Norian	Coelophysidae
<i>Buriolestes schultzi</i>	Cabreira et al. (2016)	Carnian/Norian	Sauropodomorpha
<i>Xingxiulong chengi</i>	Wang et al. (2017)	Hettangian	Sauropodiformes
<i>Yizhousaurus sunae</i>	Zhang et al. (2018)	Hettangian	Sauropodomorpha
<i>Macrocollum itaquii</i>	Muller et al. (2018)	Norian	Sauropodomorpha
<i>Ledumahadi mafube</i>	McPhee et al. (2018)	Hettangian – Sinemurian	Sauropodomorpha
<i>Ingentia prima</i>	Apaldetti et al. (2018)	Norian-Rhaetian	Sauropodomorpha
<i>Bagualosaurus agudoensis</i>	Pretto et al. (2018)	Carnian/Norian	Sauropodomorpha

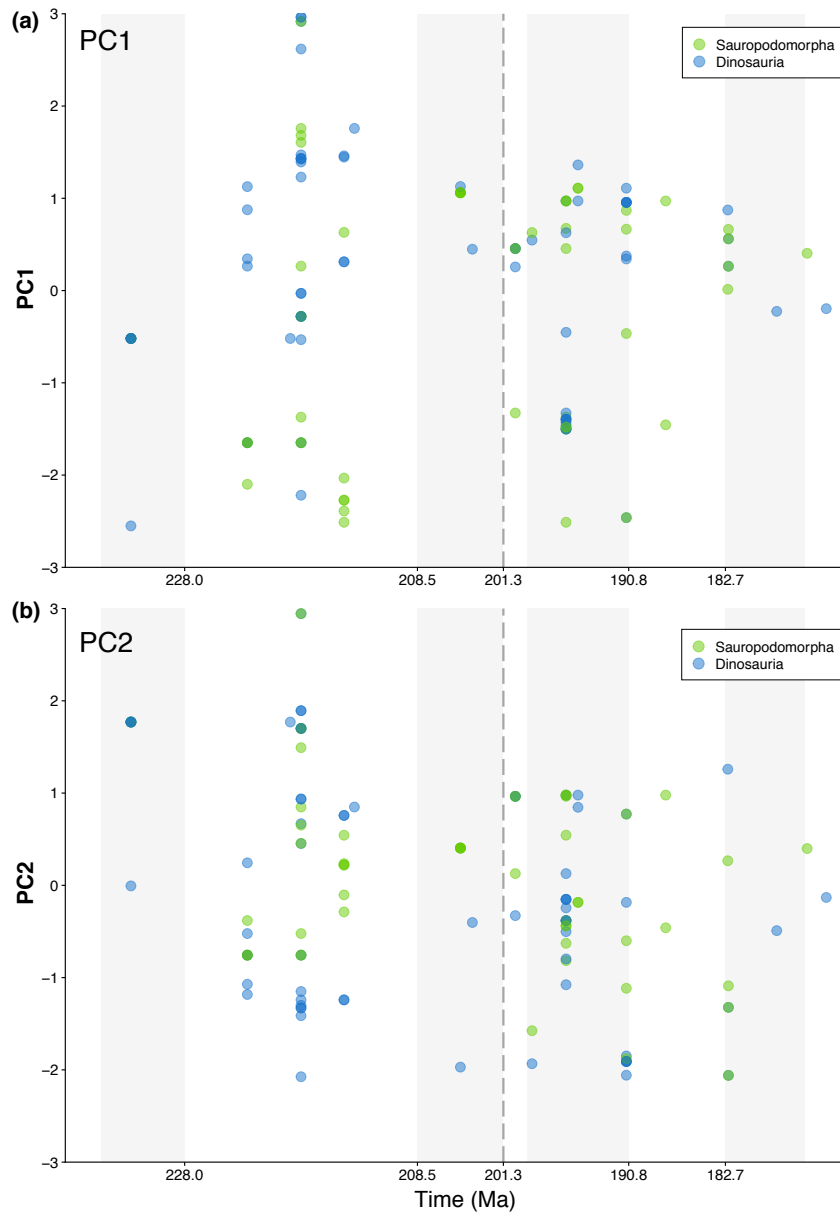


Figure D.1: Scatterplot displaying PC1 values from the ordination analysis of palaeoclimatic niche space

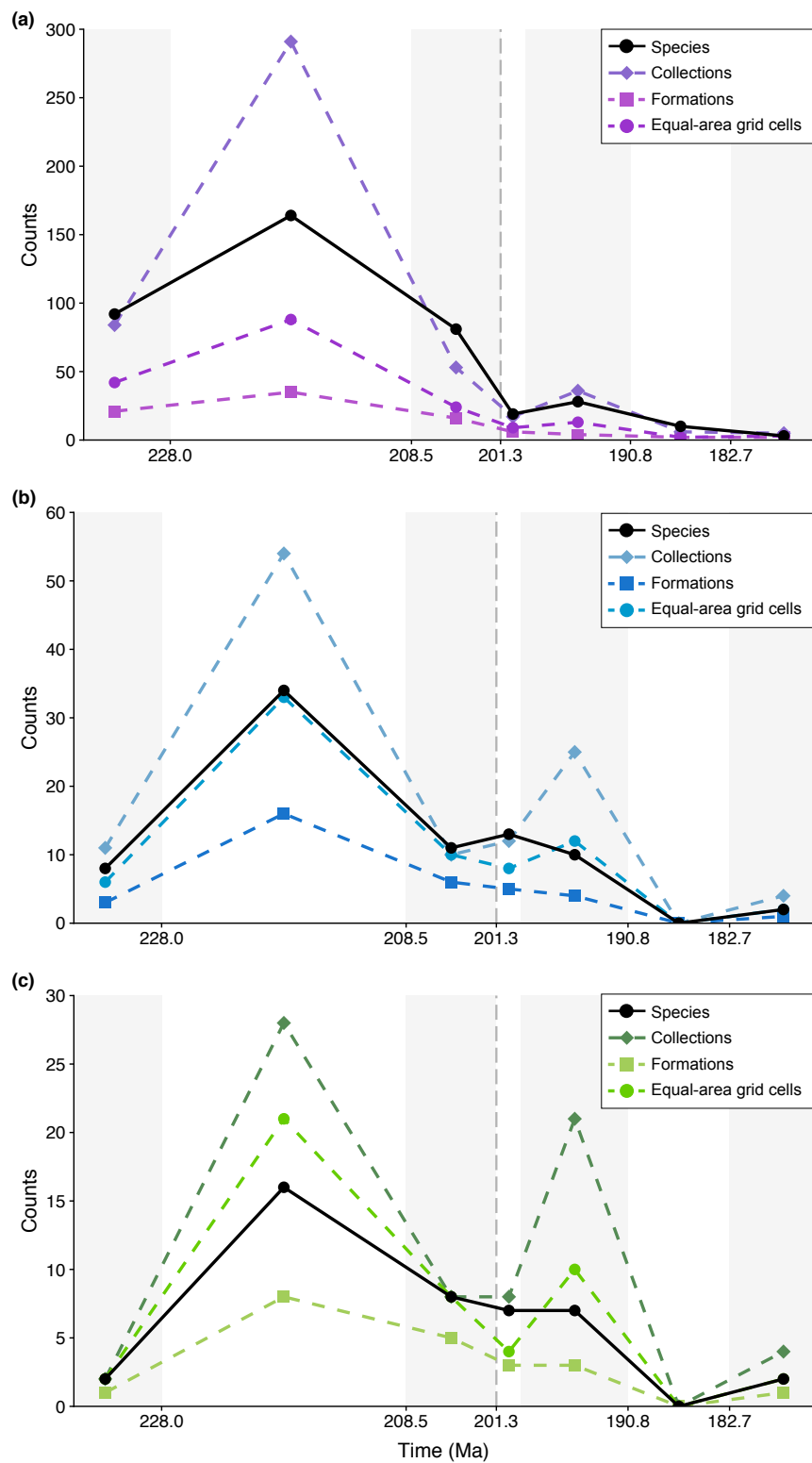


Figure D.2: Temporal sampling patterns for (a) all tetrapods, including dinosaurs, (b) dinosaurs, and (c) sauropodomorphs.

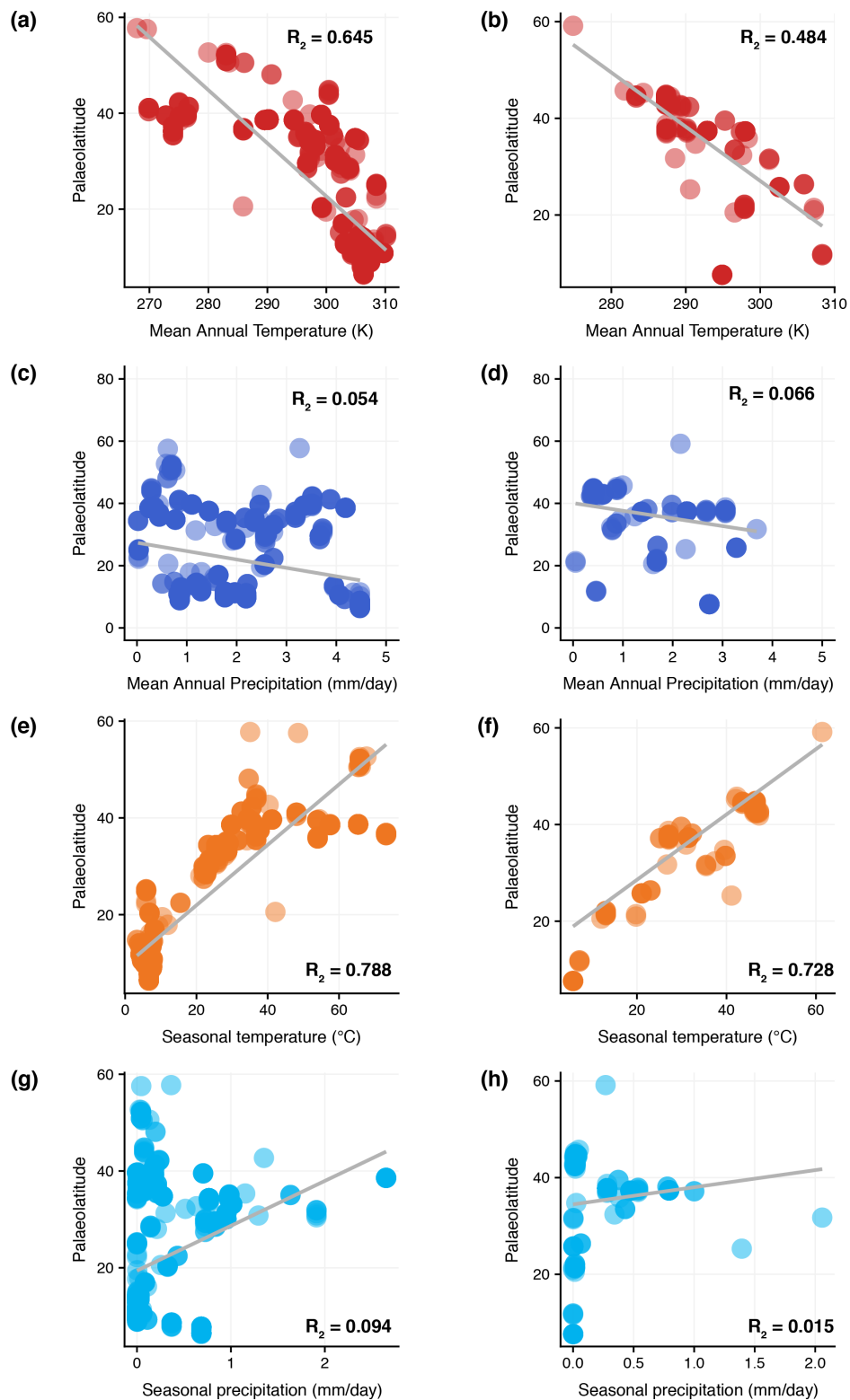


Figure D.3: Correlation between each palaeoclimatic variable and palaeolatitude in the Late Triassic (left) and Early Jurassic (right). Further details of the regression analyses are given in Table D4.

Table D.3: Pairwise comparisons (Mann–Whitney–Wilcoxon) of values for each climatic variable between the three tetrapod/dinosaur groups in both the Late Triassic and Early Jurassic. Abbreviations: Tetrapods = non-dinosaur tetrapods, Dinosaurs = non-sauropodomorph dinosaurs, Sauros = sauropodomorphs. Abbreviations for palaeoclimatic variables: MAT = mean annual temperature, MAP = mean annual precipitation, SVT = seasonal variation in temperature, SVP = seasonal variation in precipitation.

Late Triassic	Group 1	Group 2	p	W
MAT	Tetrapods	Dinosaurs	0.485	6073
	Tetrapods	Sauros	<0.001***	6246
	Dinosaurs	Sauros	0.148	611
MAP	Tetrapods	Dinosaurs	0.199	4930
	Tetrapods	Sauros	0.371	4860
	Dinosaurs	Sauros	0.07	638
SVT	Tetrapods	Dinosaurs	0.486	5268
	Tetrapods	Sauros	<0.001***	4860
	Dinosaurs	Sauros	0.0114*	317
SVP	Tetrapods	Dinosaurs	0.642	5938
	Tetrapods	Sauros	0.352	3942
	Dinosaurs	Sauros	0.546	459
Early Jurassic	Group 1	Group 2	p	W
MAT	Tetrapods	Dinosaurs	0.24	733
	Tetrapods	Sauros	0.52	589
	Dinosaurs	Sauros	0.901	392
MAP	Tetrapods	Dinosaurs	0.006**	1173
	Tetrapods	Sauros	0.371	733
	Dinosaurs	Sauros	0.253	315
SVT	Tetrapods	Dinosaurs	0.979	861
	Tetrapods	Sauros	0.978	645
	Dinosaurs	Sauros	0.753	365
SVP	Tetrapods	Dinosaurs	0.046*	1087
	Tetrapods	Sauros	0.182	771
	Dinosaurs	Sauros	0.518	345

*p = <0.05, **p=<0.01, ***p=0.001

Table D.4: Correlation between palaeolatitude and four variables from the palaeoclimate model HadCM3L for both the late Triassic and Early Jurassic. Abbreviations as in Table D3.

Climate variable	R₂	t	p
<i>Late Triassic</i>			
MAT	0.645	-42.96	<0.001
MAP	0.054	-7.693	<0.001
SVT	0.788	61.39	<0.001
SVP	0.094	10.302	<0.001
<i>Early Jurassic</i>			
MAT	0.486	-13.62	<0.001
MAP	0.066	-3.868	<0.001
SVT	0.728	22.961	<0.001
SVP	0.015	2.014	0.045

Table D.5: Theta values (the optimum value) from the non-uniform OU model (OUM) for the first 10 time-calibrated trees. These values represent those seen across all trees. In the column labelled “Shift”, 1 = before the change in model parameters i.e. before the Triassic-Jurassic boundary at 201.3 Ma, and 2 = after the shift, i.e. after 201.3 Ma

Tree	Shift	PC1	PC2
1	1	-0.128	0.284
	2	0.138	-0.328
2	1	0.012	0.31
	2	0.416	-0.522
3	1	0.213	0.059
	2	0.226	-0.371
4	1	-0.027	0.303
	2	0.319	-0.421
5	1	-0.12	0.306
	2	0.359	-0.469
6	1	-0.122	0.34
	2	0.36	-0.444
7	1	0.028	0.093
	2	0.334	-0.468
8	1	0.192	0.197
	2	0.564	-0.531
9	1	-0.12	0.308
	2	0.204	-0.295
10	1	-0.125	0.294
	2	0.282	-0.413

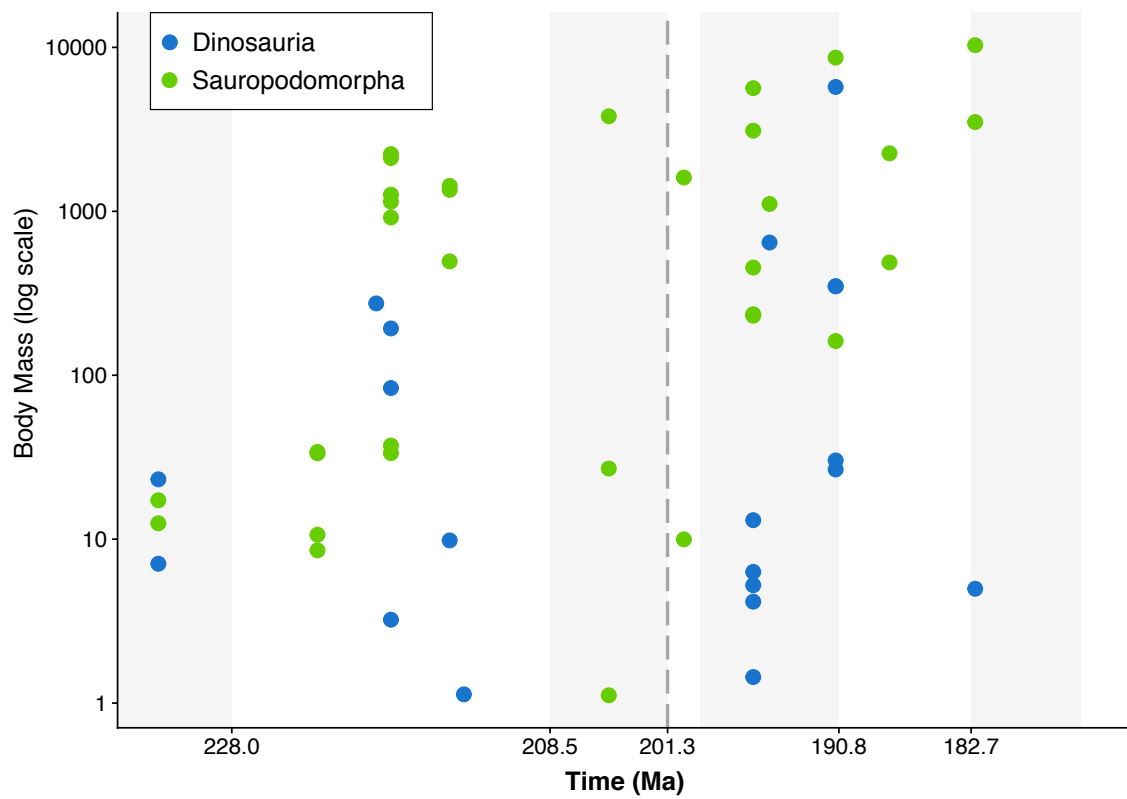


Figure D.4: Body mass estimates (log transformations) for sauropodomorphs (green) and non-sauropodomorph dinosaurs (blue) across the Late Triassic and Early Jurassic

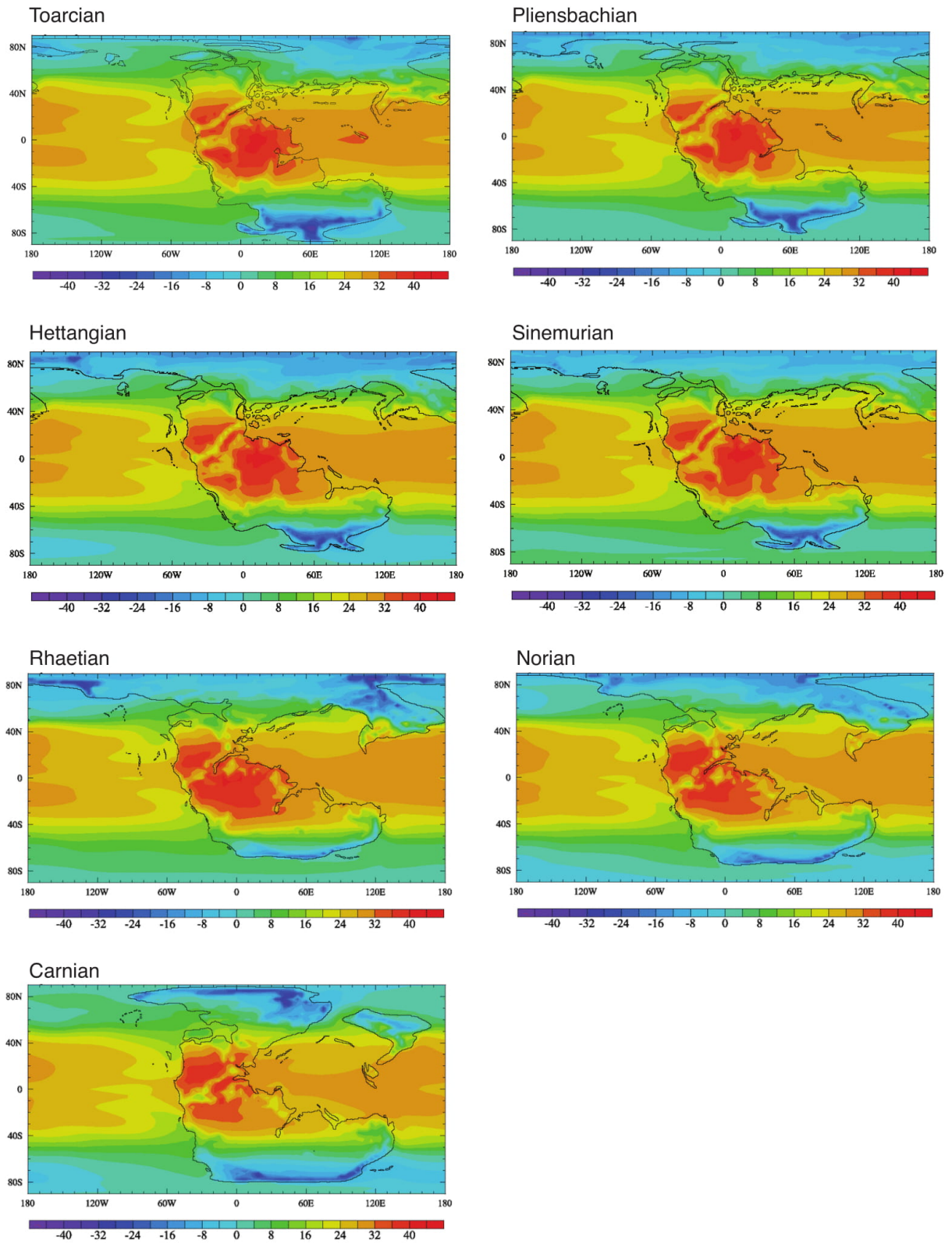
Modelled Surface Air Temperature (°C)

Figure D.5: Modelled surface air temperature (°C) during the Late Triassic and Early Jurassic from the model HadCM3L

E | Early dinosaur evolution & climate II

The following figures are supplementary to Chapter 5, "The role of climate in the early evolution of dinosaurs"

They, along with Figure 5.4, display the dinosaur phylogeny where either PC scores or palaeoclimatic variables have been mapped on as continuous characters using the *contMap* function in the R package *phytools*. For further information see sections 5.2.5 and 5.3.2. For details of the major dinosaur clades represented on the tree, see Figure 5.4.

Abbreviations for the palaeoclimatic variables are as follows: MAT = Mean annual temperature, MAP = Mean annual precipitation, SVT = Seasonal variation in temperature, SVP = Seasonal variation in precipitation.

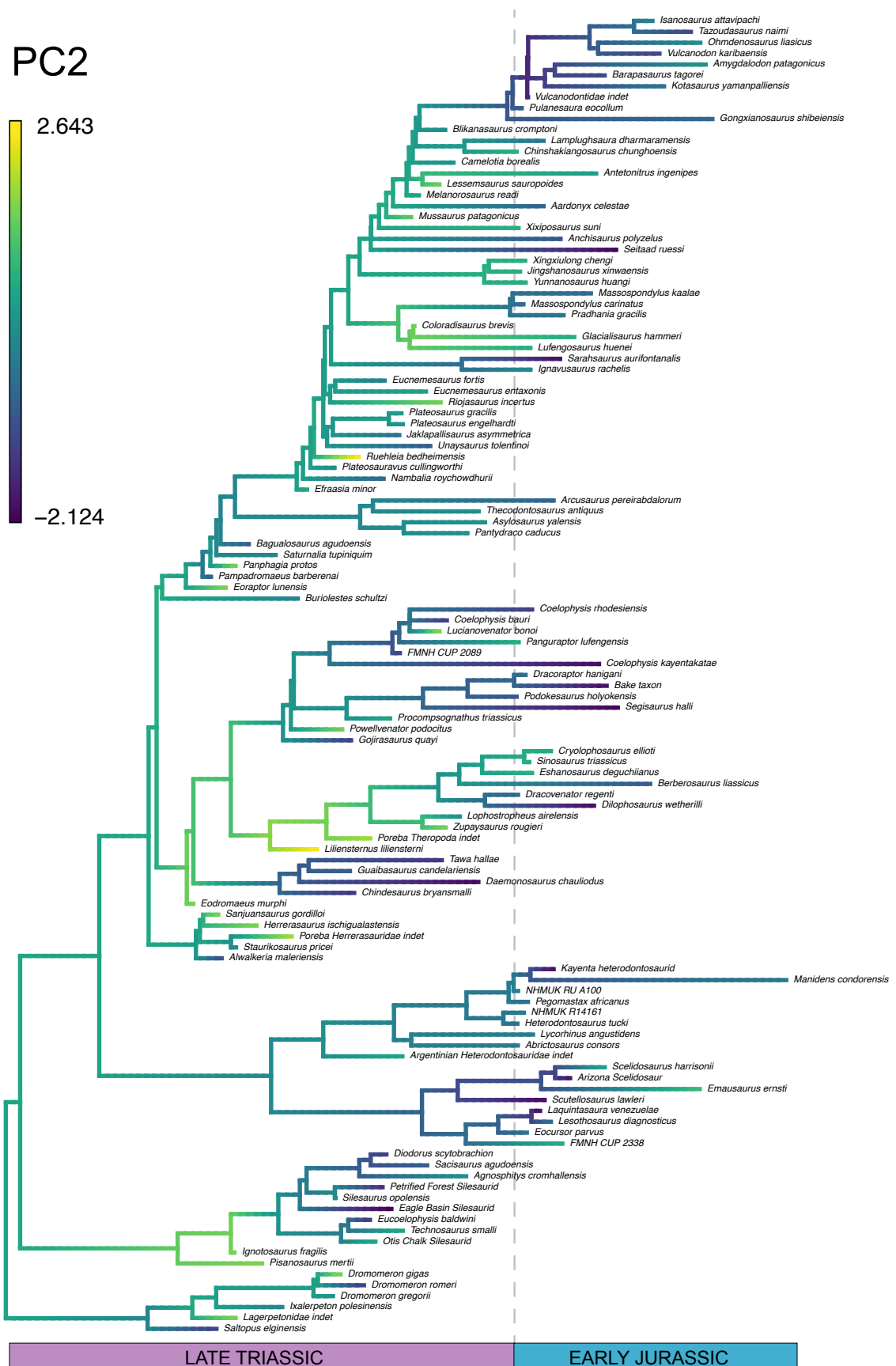


Figure E.1: PC2 mapped onto dinosaur phylogeny

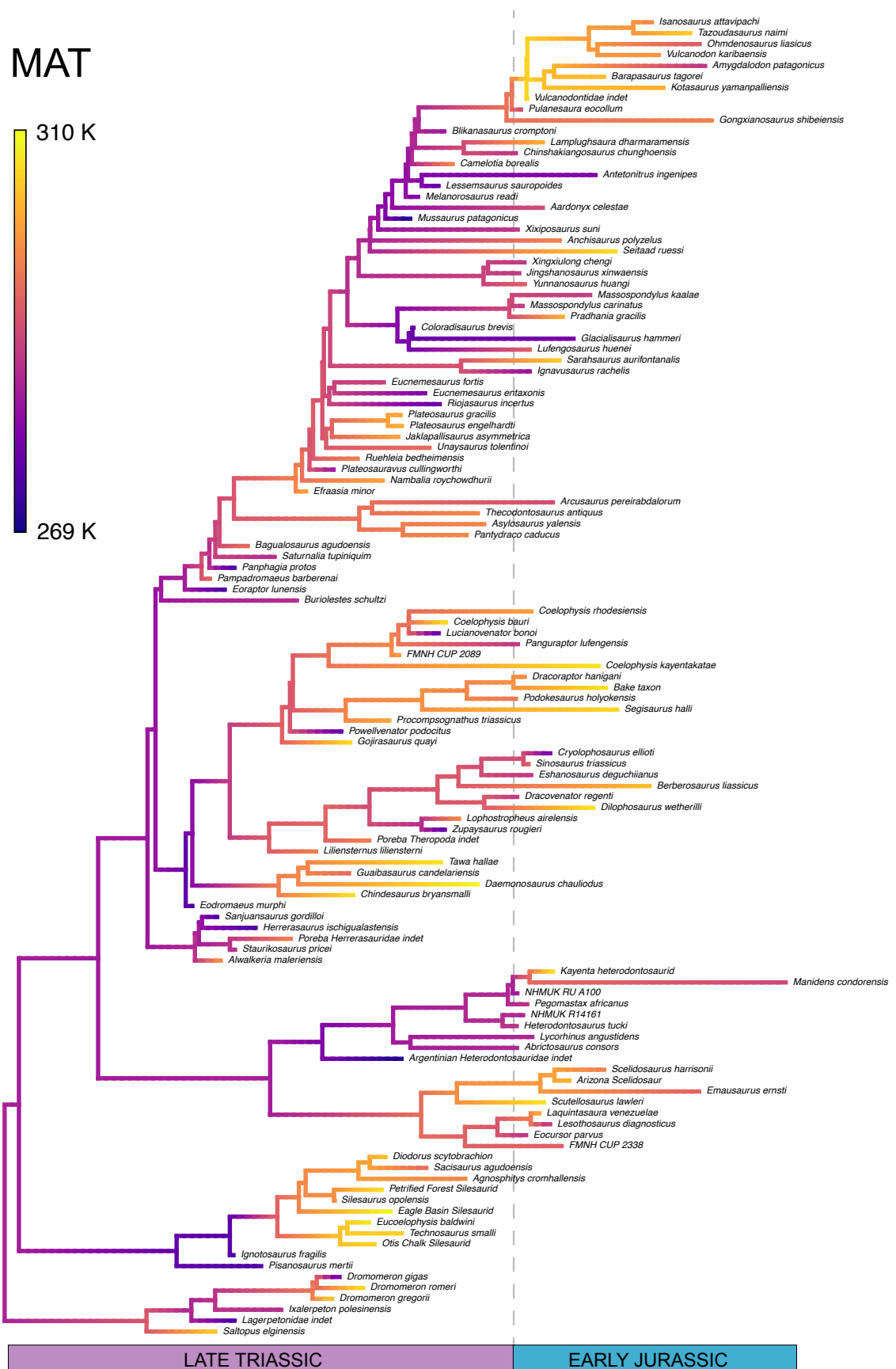


Figure E.2: MAT mapped onto dinosaur phylogeny

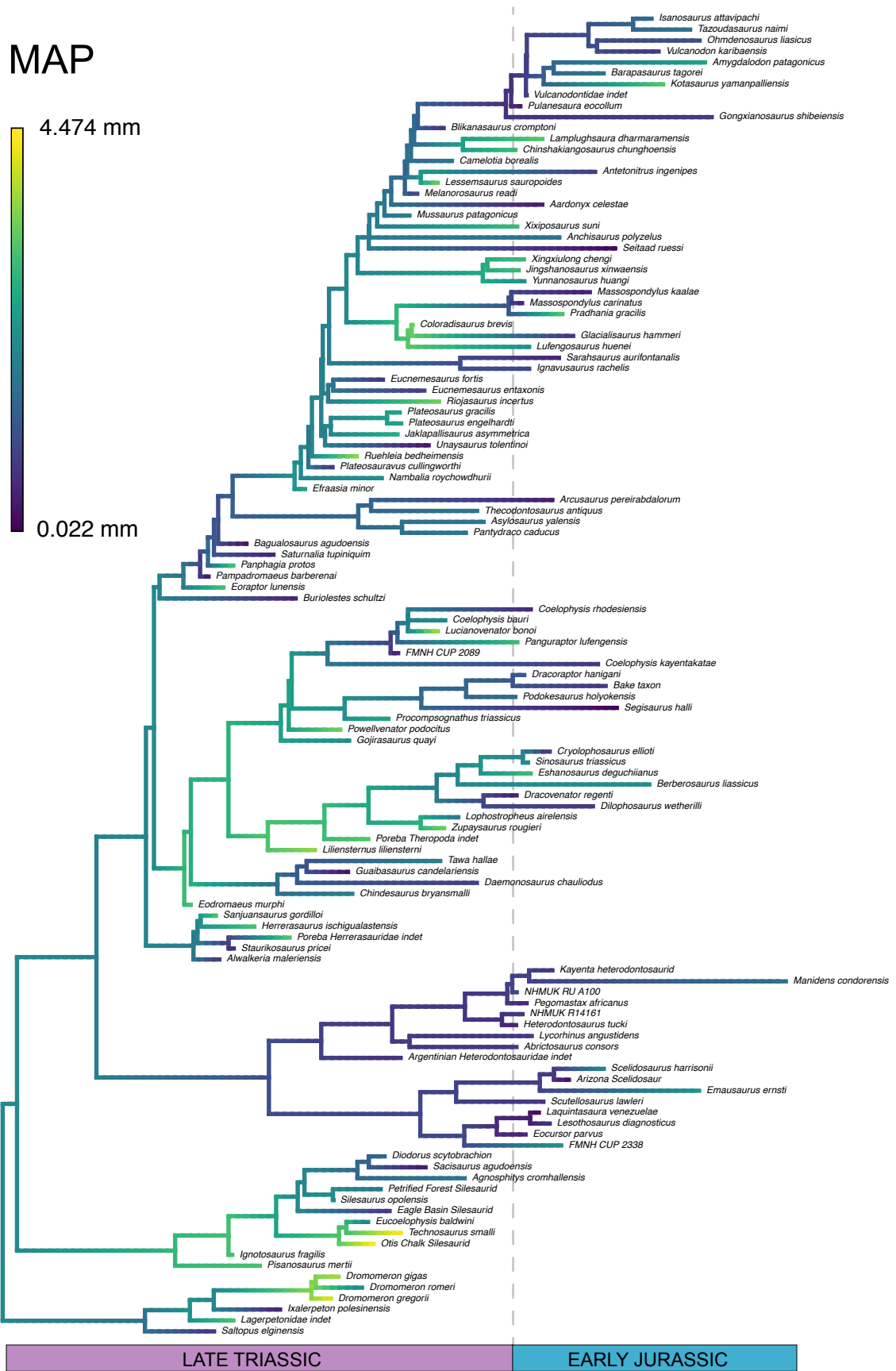


Figure E.3: MAP mapped onto dinosaur phylogeny

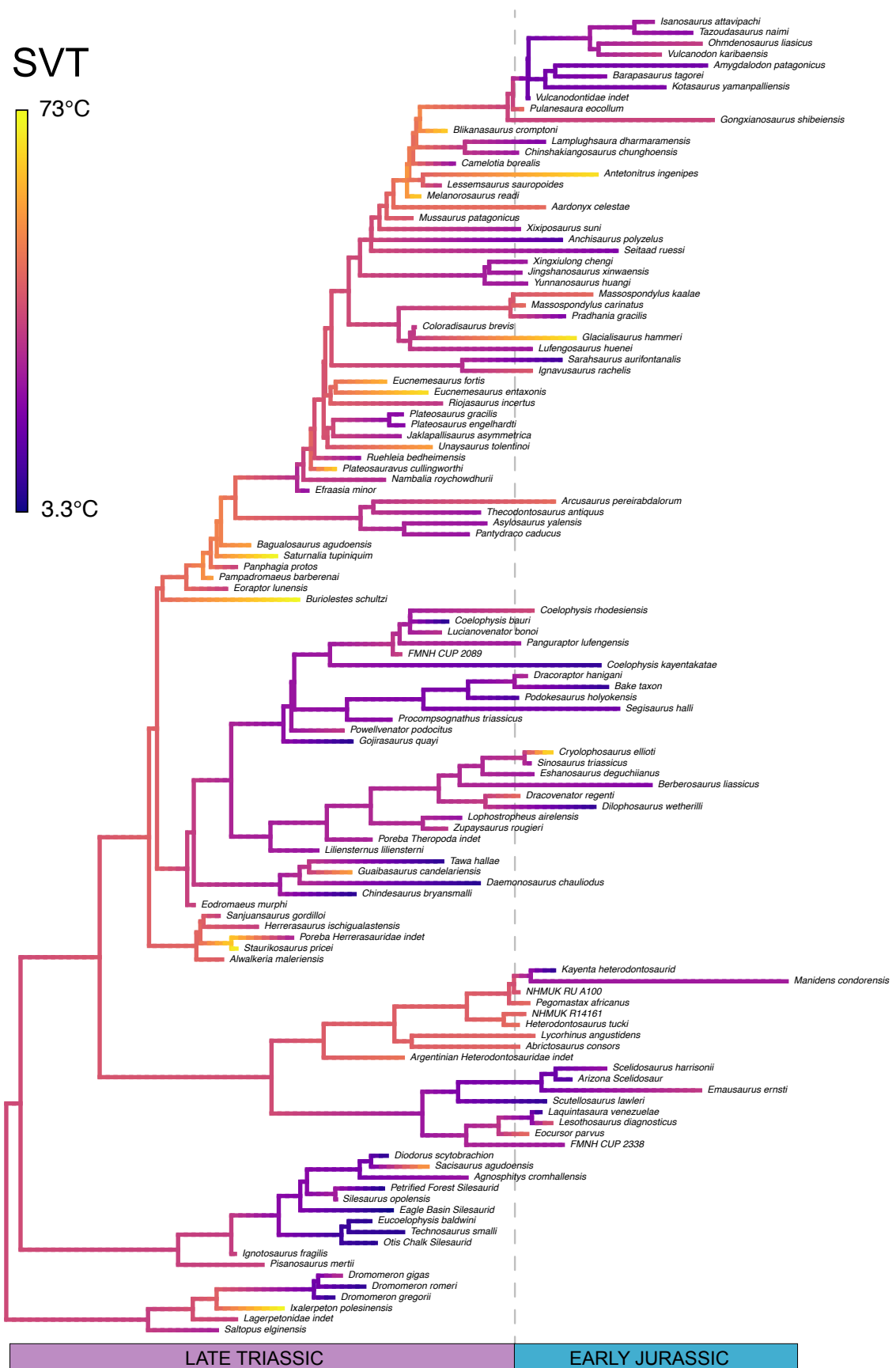


Figure E.4: SVT mapped onto dinosaur phylogeny

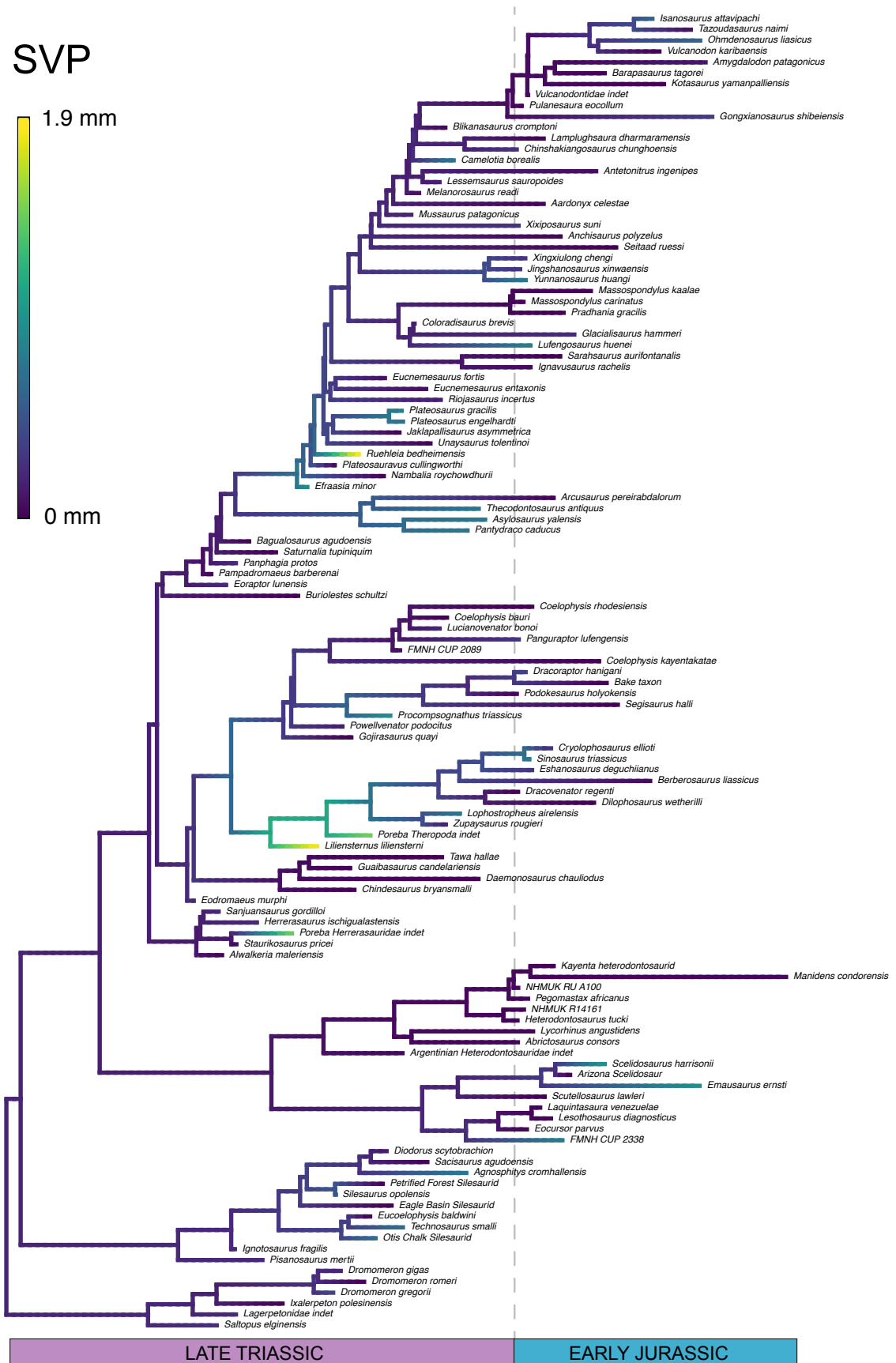


Figure E.5: SVP mapped onto dinosaur phylogeny

F | Early dinosaur evolution & climate III

The following figures are supplementary to Chapter 5, "The role of climate in the early evolution of dinosaurs".

They, along with Figure 5.5, illustrate dinosaur palaeoclimatic niche disparity-through-time. For further information see sections 5.2.5 and 5.3.2. The subsampling method used to is displayed above the plot panels, and, if applicable, the dinosaur sub-group can be found in the figure caption.

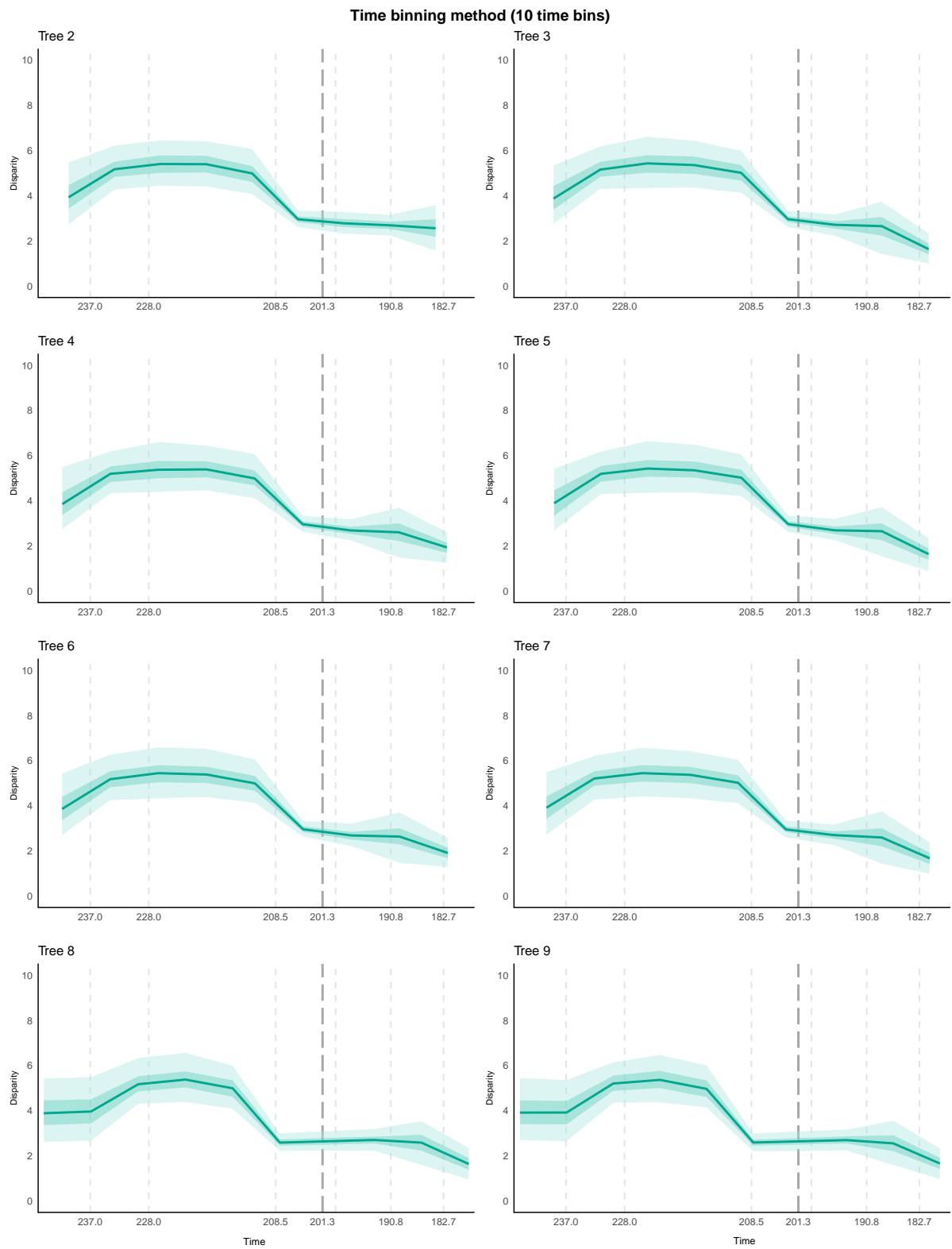


Figure F.1: Dinosaur palaeoclimatic niche disparity-through-time

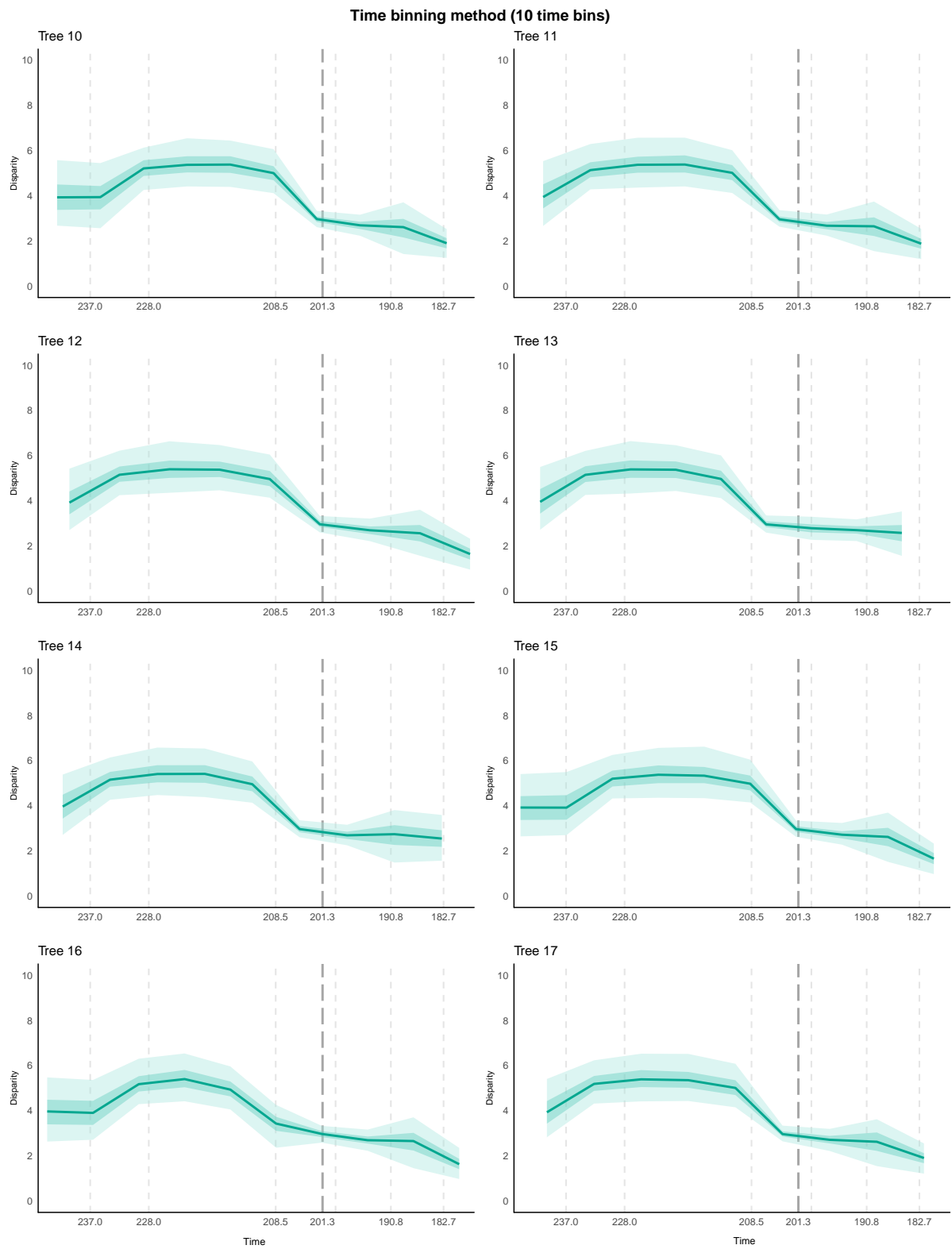


Figure F.2: Dinosaur palaeoclimatic niche disparity-through-time

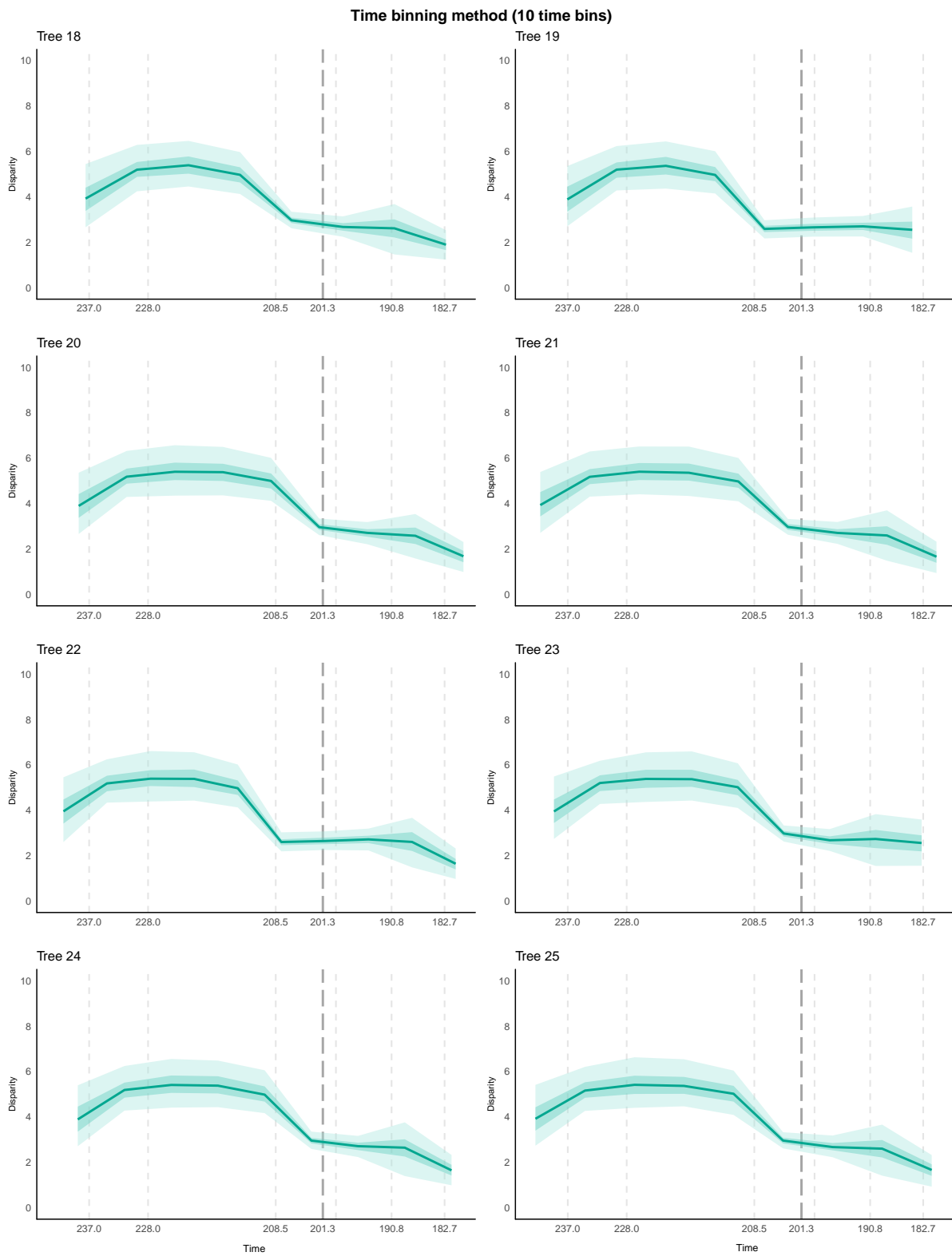


Figure F.3: Dinosaur palaeoclimatic niche disparity-through-time

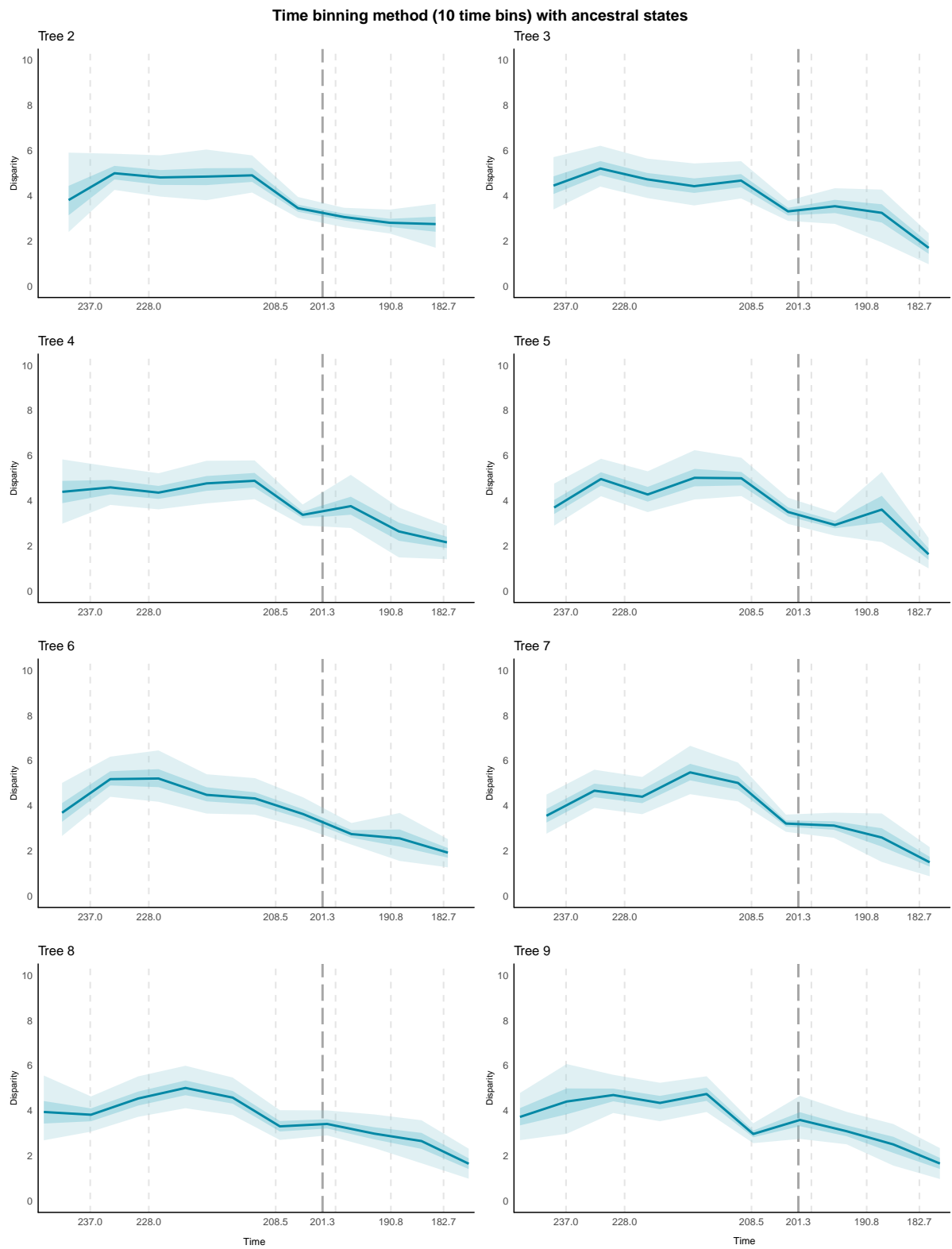


Figure F.4: Dinosaur palaeoclimatic niche disparity-through-time

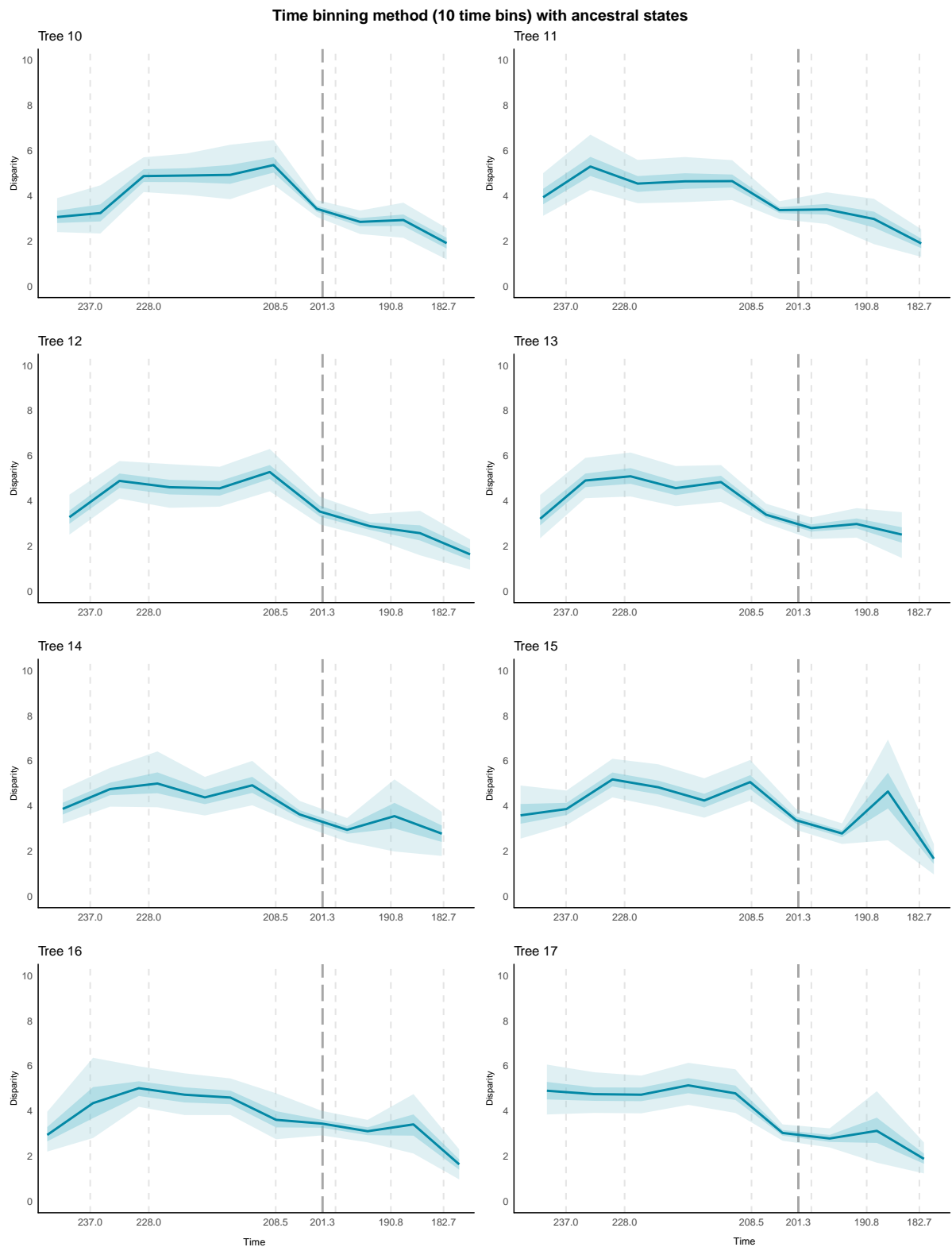


Figure F.5: Dinosaur palaeoclimatic niche disparity-through-time

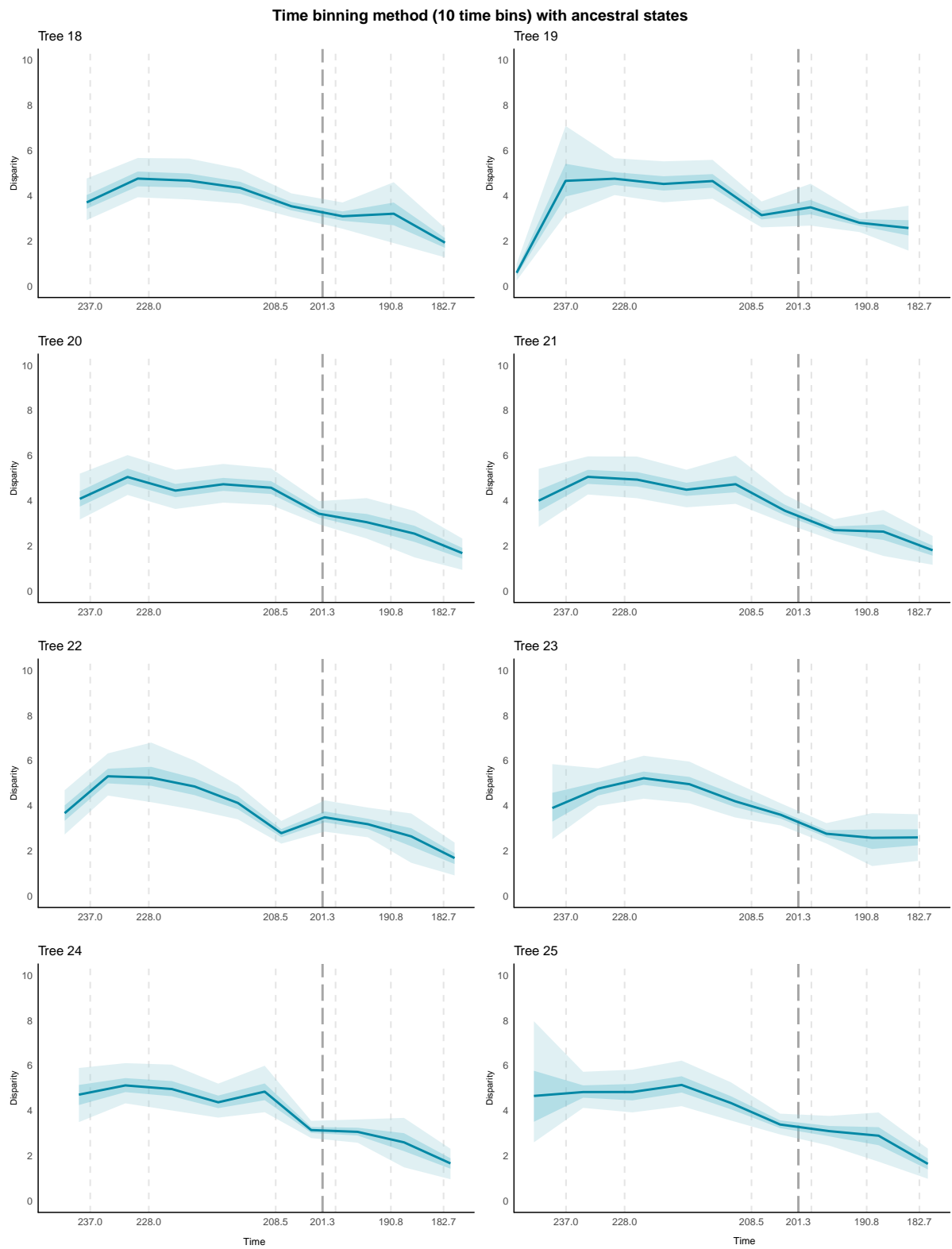


Figure F.6: Dinosaur palaeoclimatic niche disparity-through-time

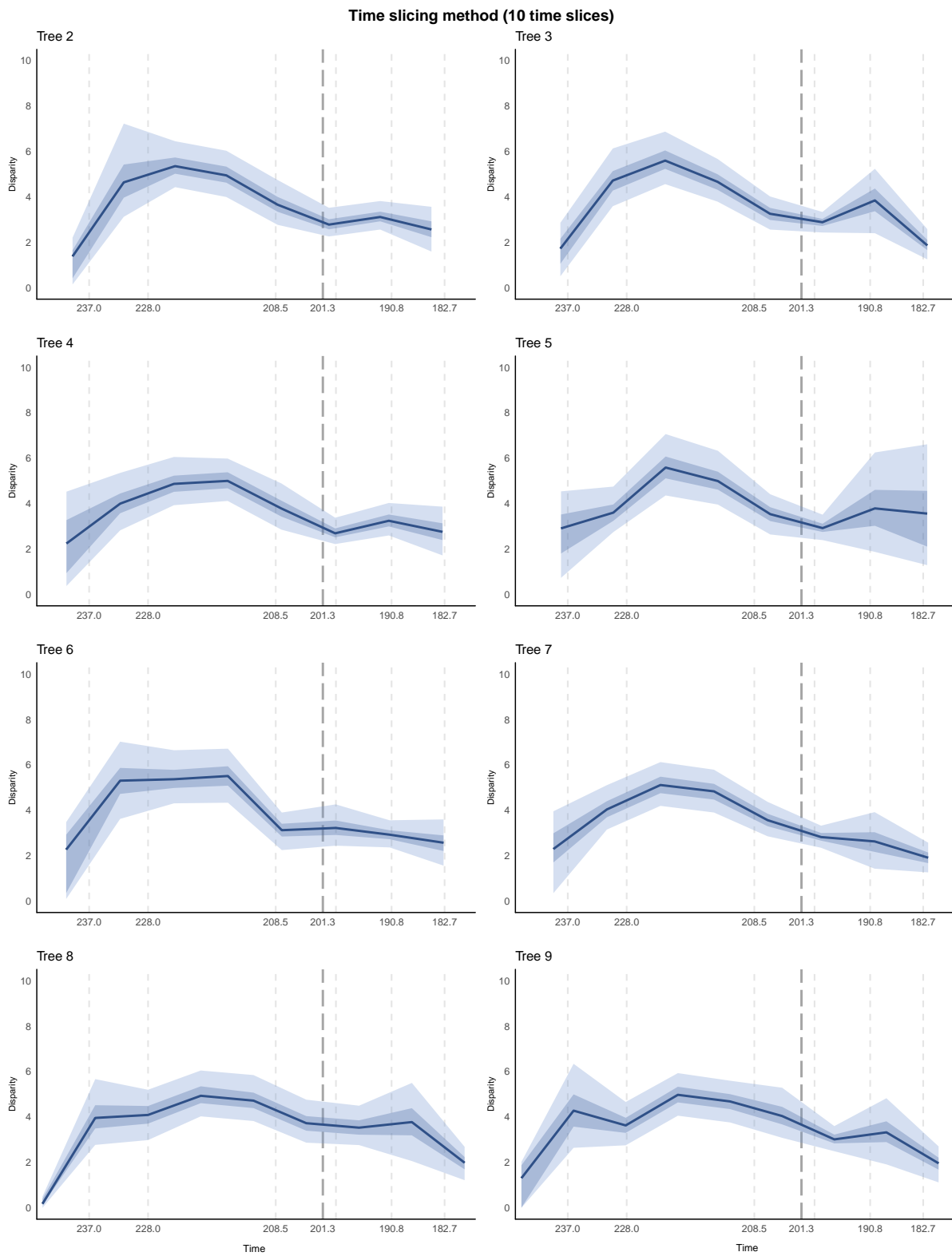


Figure F.7: Dinosaur palaeoclimatic niche disparity-through-time

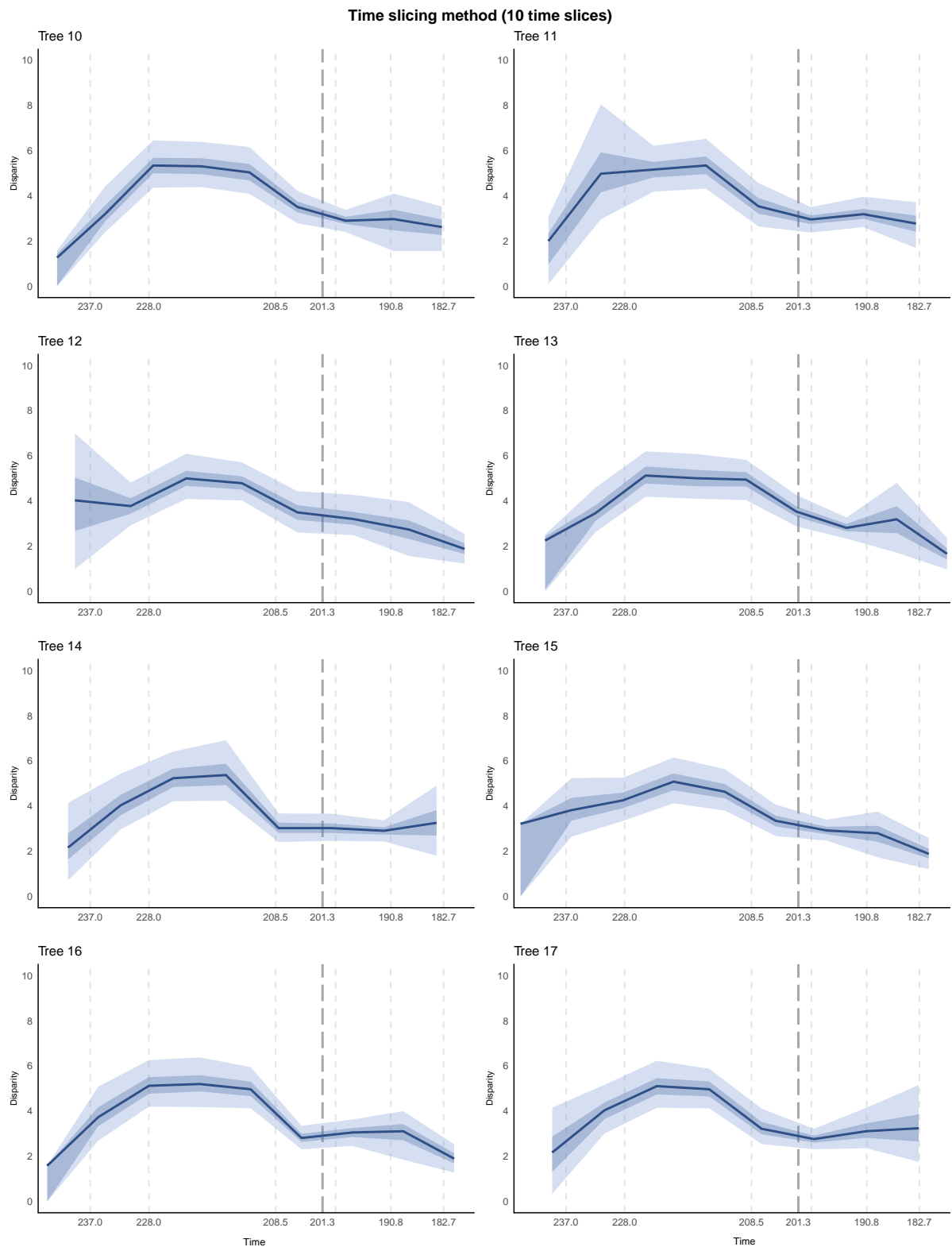


Figure F.8: Dinosaur palaeoclimatic niche disparity-through-time

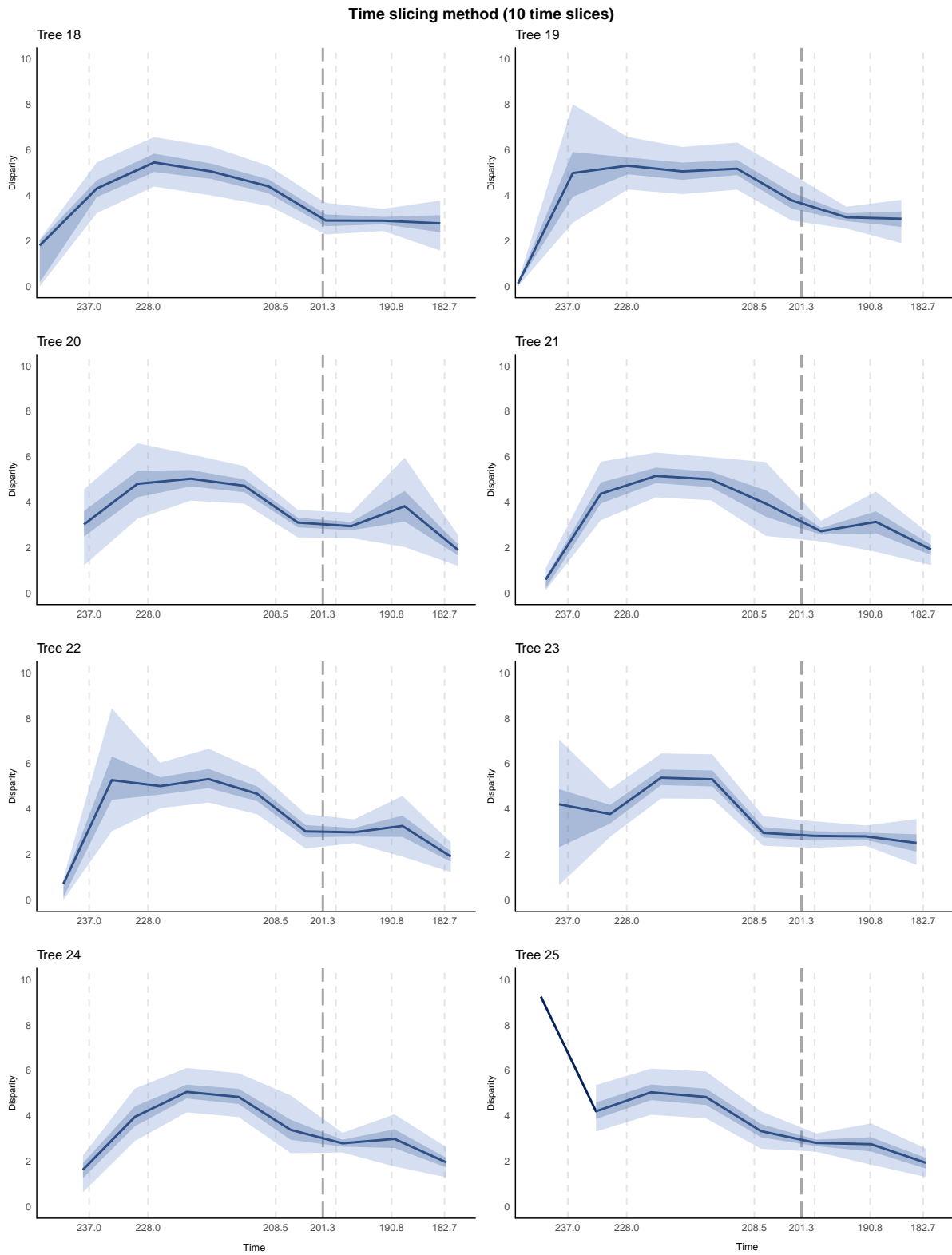


Figure F.9: Dinosaur palaeoclimatic niche disparity-through-time

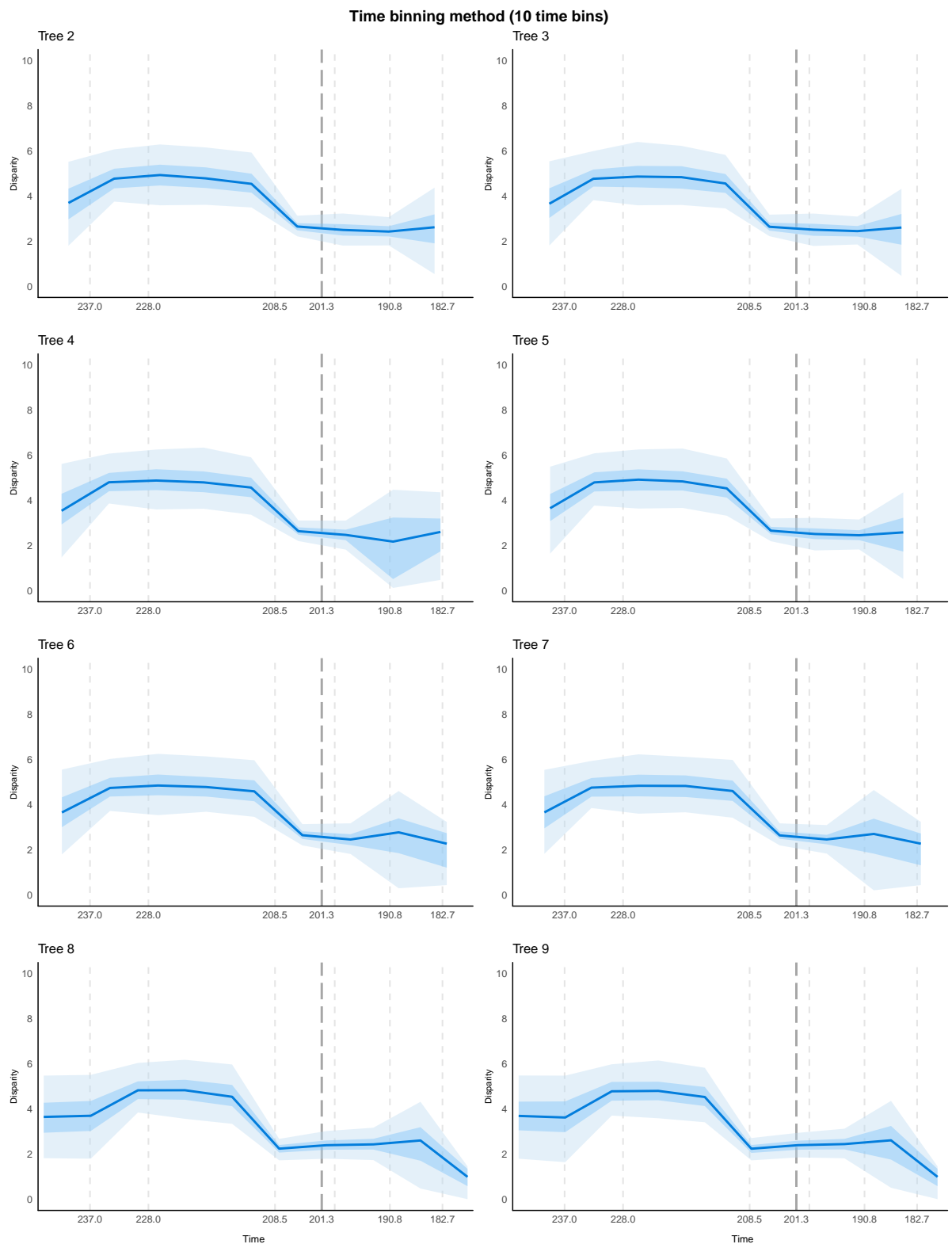


Figure F.10: Non-sauropodomorph dinosaur palaeoclimatic niche disparity-through-time

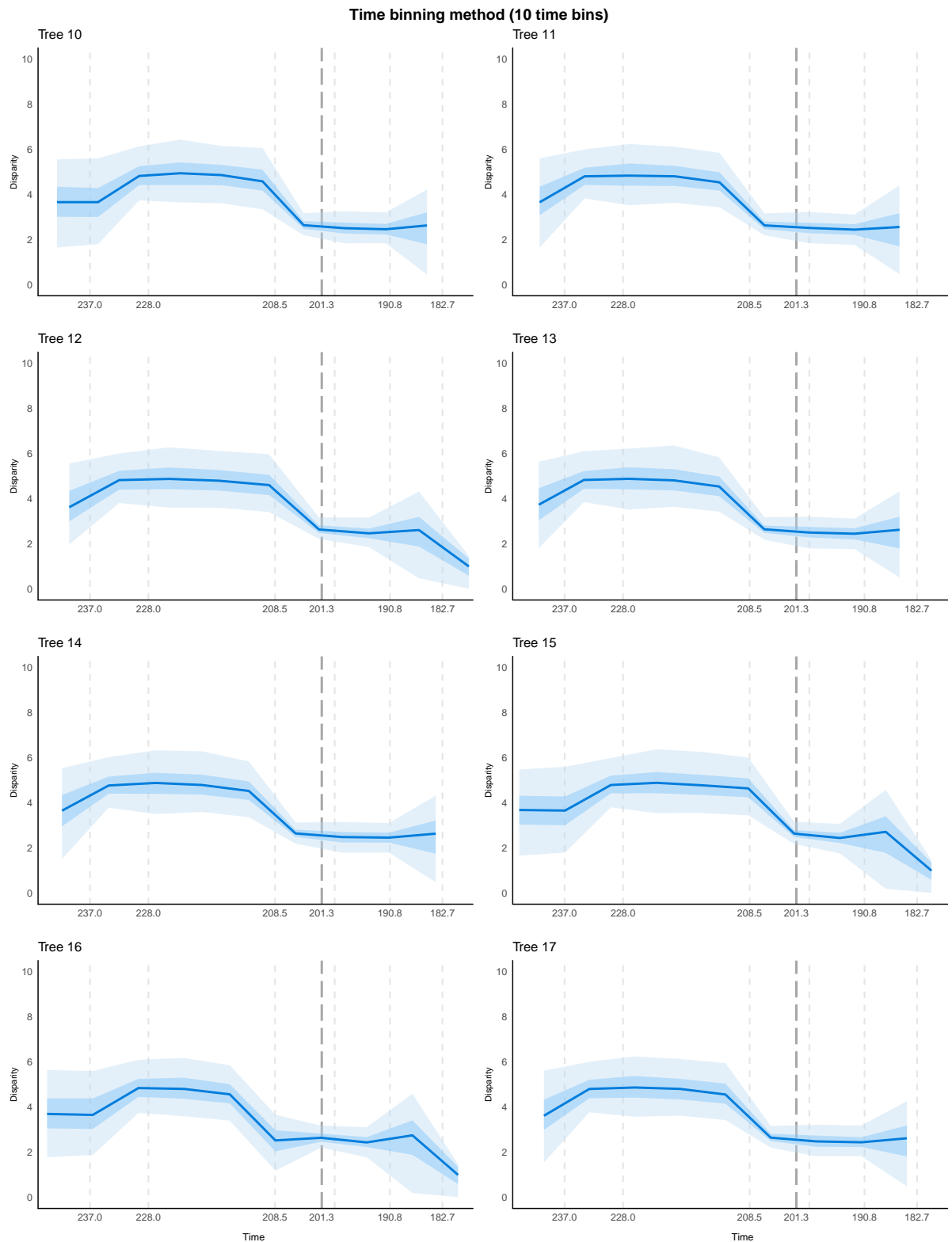


Figure F.11: Non-sauropodomorph dinosaur palaeoclimatic niche disparity-through-time

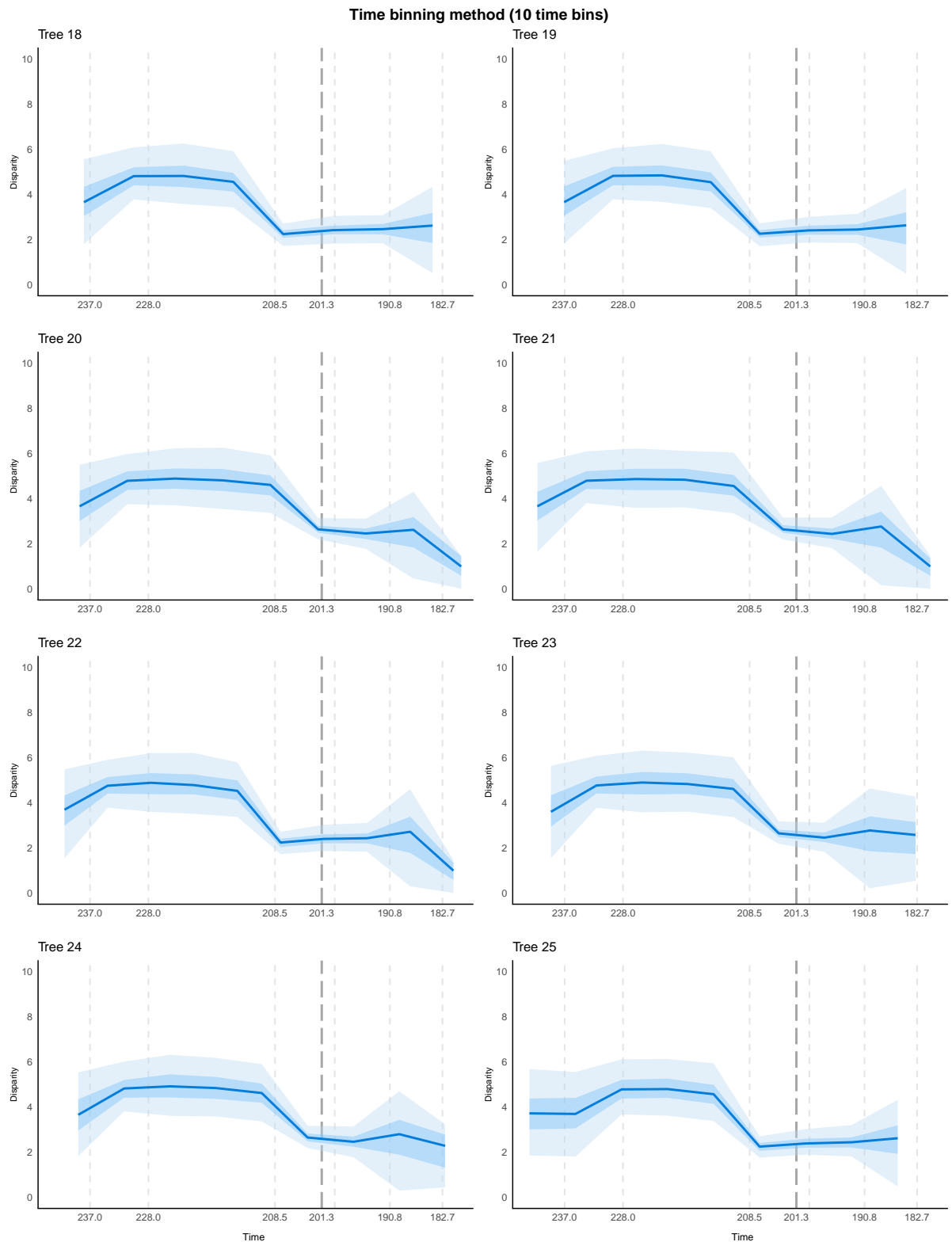


Figure F.12: Non-sauropodomorph dinosaur palaeoclimatic niche disparity-through-time

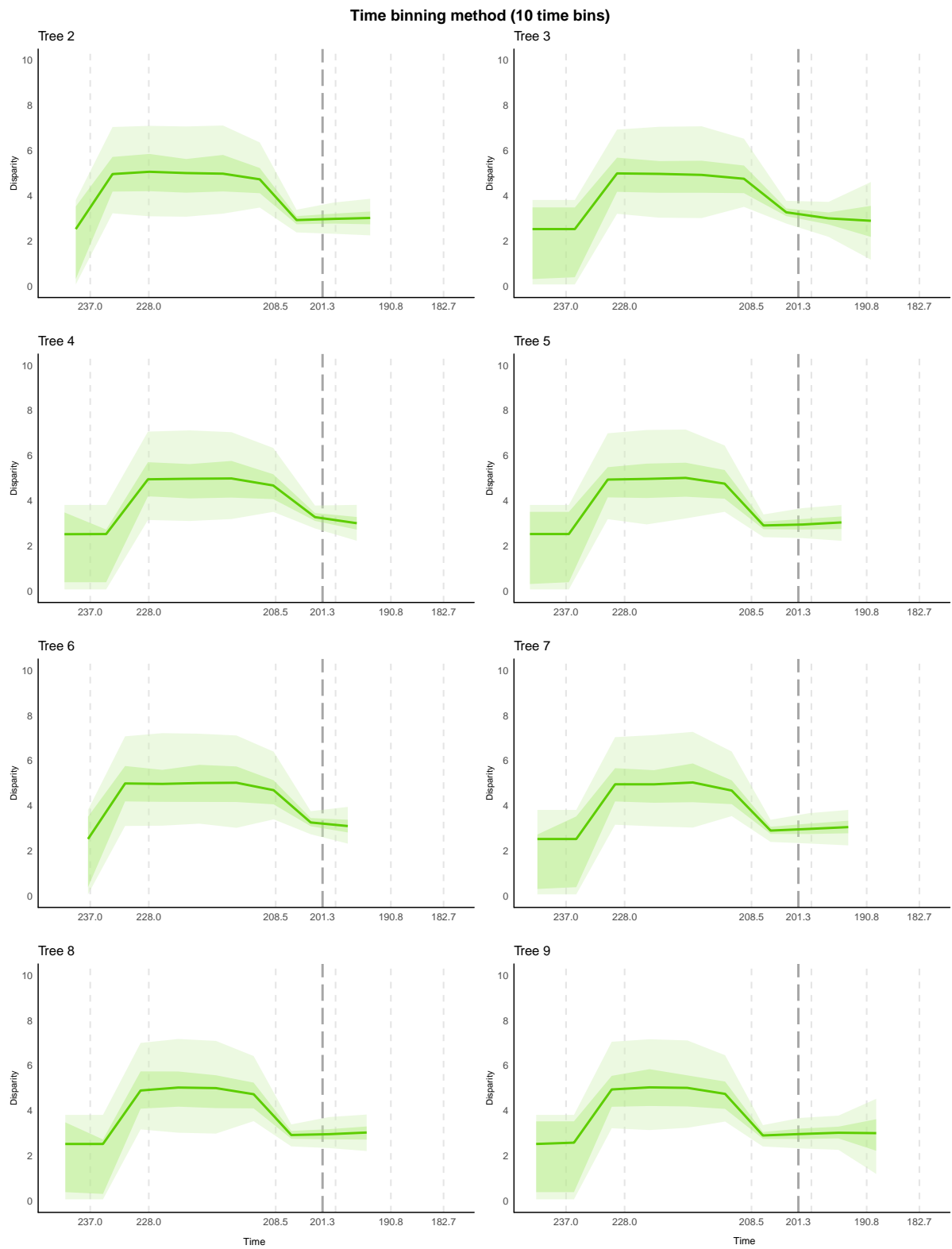


Figure F.13: Sauropodomorph palaeoclimatic niche disparity-through-time

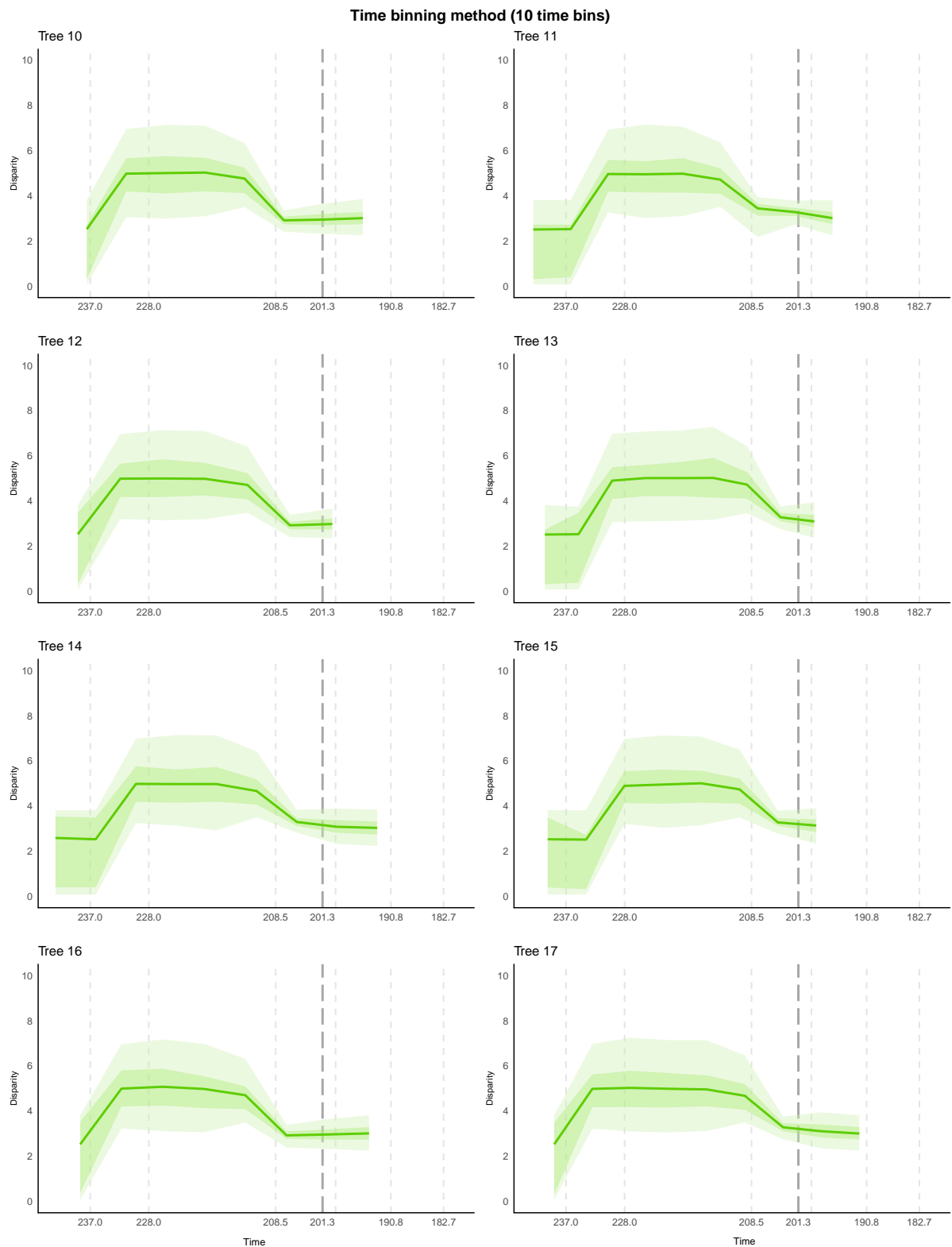


Figure F.14: Sauropodomorph palaeoclimatic niche disparity-through-time

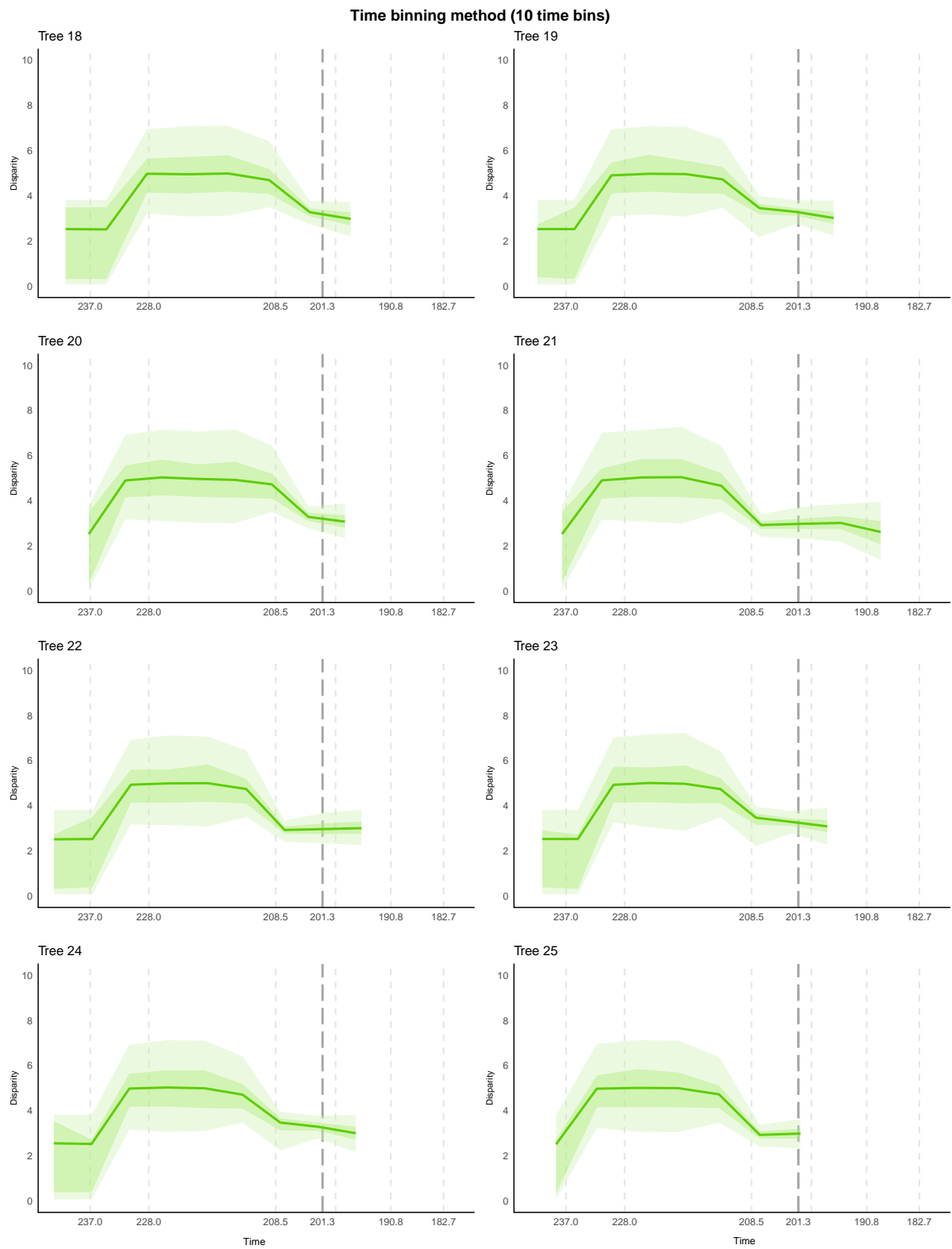


Figure F.15: Saurodomorph palaeoclimatic niche disparity-through-time

G | Early dinosaur evolution & climate IV

The following figures are supplementary to Chapter 5, "The role of climate in the early evolution of dinosaurs"

They, along with Figure 5.6, illustrate sauropodomorph morphological disparity-through-time. For further information see sections 5.2.7 and 5.3.5.

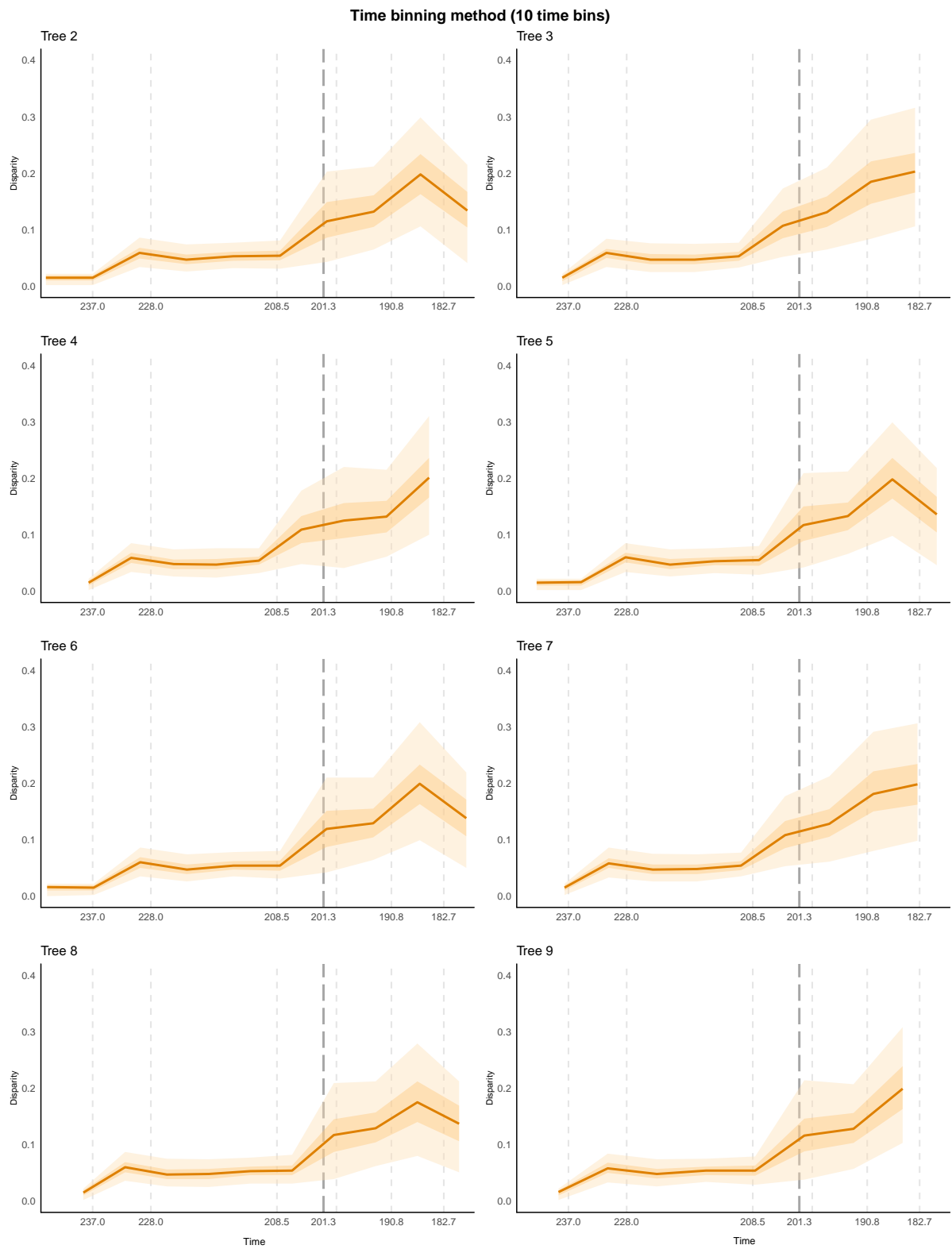


Figure G.1: Sauropodomorph morphological disparity-through-time

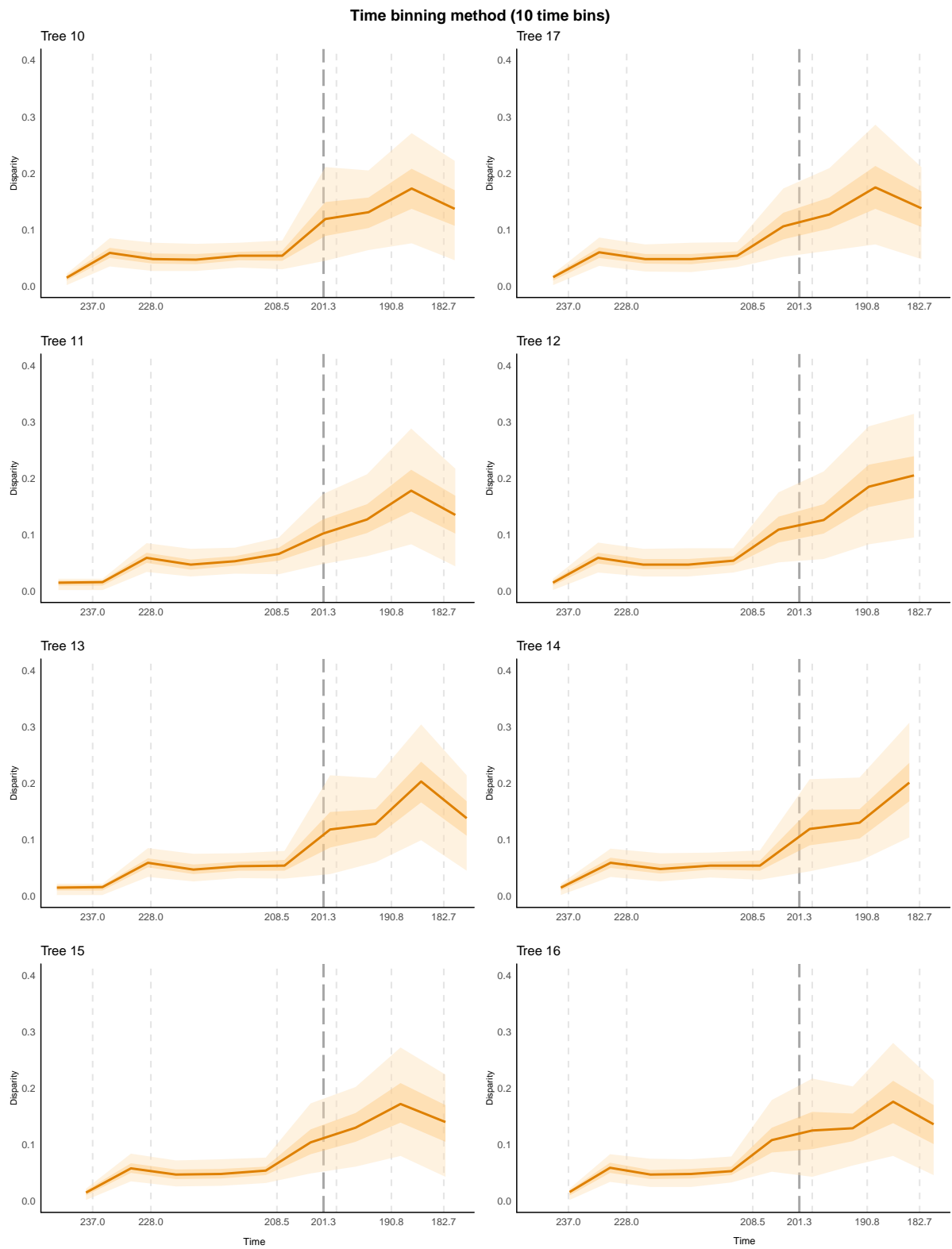


Figure G.2: Sauropodomorph morphological disparity-through-time

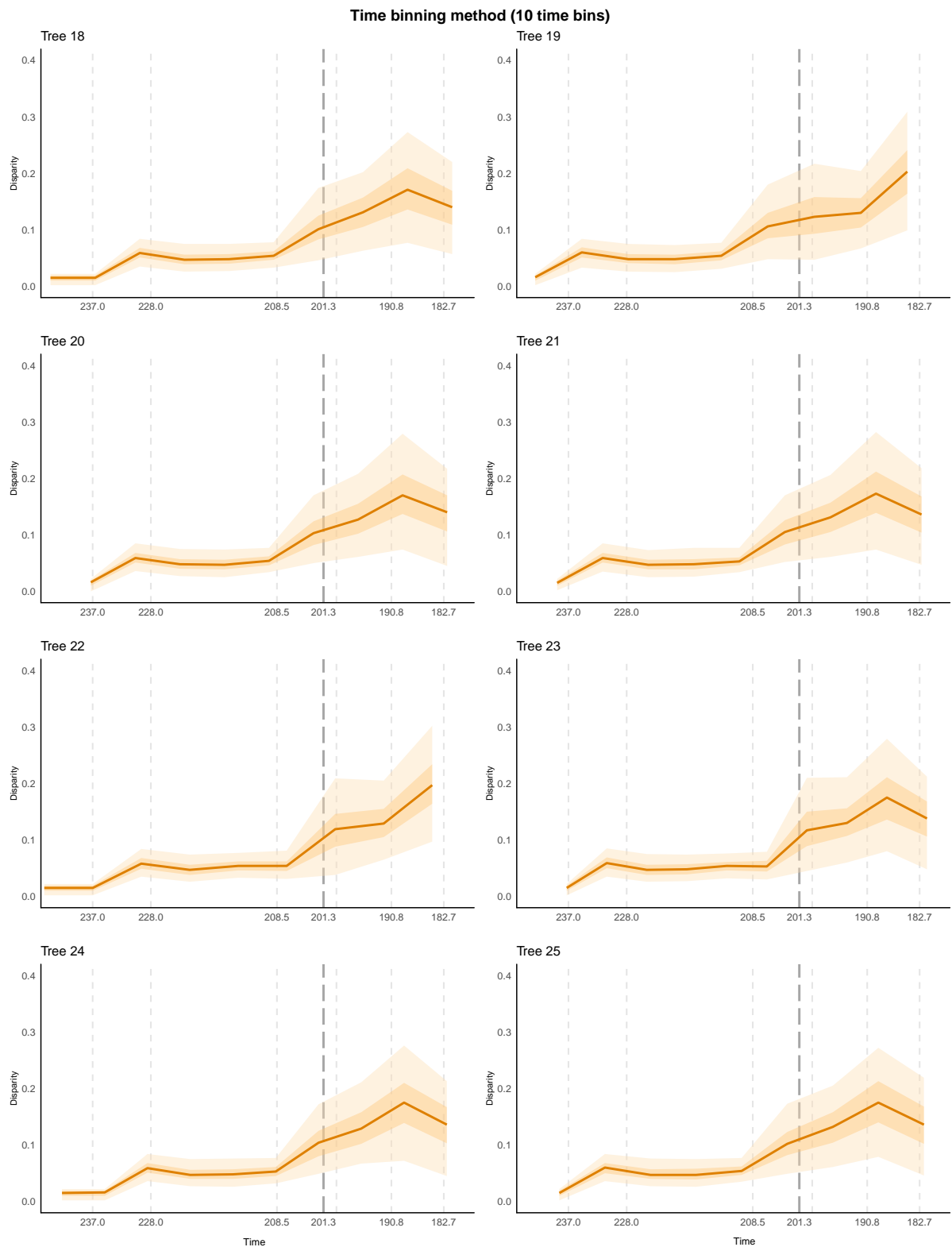


Figure G.3: Sauropodomorph morphological disparity-through-time